ISSN 0915-6364

NATIONAL INSTITUTE FOR FUSION SCIENCE

Cross Sections for Electron-Impact Induced Transitions Between Excited States in He: n, n'=2, 3 and 4

V.P. Shevelko and H. Tawara

(Received - Aug. 9, 1995)

NIFS-DATA-28 Aug.1995

RESEARCH REPORT
NIFS-DATA Series

This report was prepared as a preprint of compilation of evaluated atomic, molecular, plasma-wall interaction, or nuclear data for fusion research, performed as a collaboration research of the Data and Planning Center, the National Institute for Fusion Science (NIFS) of Japan. This document is intended for future publication in a journal or data book after some rearrangements of its contents.

NAGOYA, JAPAN

CROSS SECTIONS FOR ELECTRON-IMPACT INDUCED TRANSITIONS BETWEEN EXCITED STATES IN He: n, n′ = 2, 3 AND 4

V.P.Shevelko and H.Tawara

(Received August 9, 1995)

CROSS SECTIONS FOR ELECTRON-IMPACT INDUCED TRANSITIONS BETWEEN EXCITED STATES IN He: n, n′ = 2, 3 AND 4

V.P.Shevelko[1)] and H.Tawara[2)]

[1)] P.N.Lebedev Physics Institute, Russian Academy of Sciences, 117927 Moscow, Russia
[2)] National Institute for Fusion Science, Nagoya 464-01, Japan

Abstract

Cross sections σ and corresponding maxwellian rate coefficients <vσ> have been calculated for all 153 spin-allowed and spin-forbidden transitions between excited states in He with the principal quantum numbers n, n′ = 2, 3 and 4 induced by electron impact. Calculations have been performed using Coulomb-Born approximation with exchange (CBE) in the partial wave representation with orthogonalized wavefunctions of the initial and final states in the incident electron energy range from threshold up to 2000 eV for spin-allowed transitions ($\Delta S=0$) and up to 200 eV for spin-forbidden (intercombination, $\Delta S=1$) transitions where the corresponding excitation cross sections are still relatively large. The fitting parameters for σ and <vσ> of spin-allowed transitions have been obtained. The results are compared with experimental data and other calculations.

[keywords: excitation, electron scattering, partial wave method, model potential, cross section, rate coefficient]

Contents

1. Introduction

A knowledge of excitation cross sections and rate coefficients of He atoms from the ground and excited states is required for many physical applications: gaseous discharges, rare-gas lasers[1), fusion[2) and astrophysical[3,4) plasmas, diagnostics and heating of plasma by neutral He beams[5), etc. While the information about excitation in He from the ground state is quite essential (see, e.g., refs.[5-8)), relatively little is known about excitation from excited states with the principal quantum numbers n≥2 , especially regarding experimental data. In this respect theoretical calculations are of a special interest.

Our aim in this work is to perform calculations of the excitation cross sections and the corresponding rate coefficients between excited (n, n′ = 2, 3 and 4) states in He in a wide electron-impact energy range: from threshold up to 2000 eV for spin-allowed transitions (ΔS=0) and up to 200 eV for spin-forbidden (intercombination, ΔS=1) transitions.

2. Theoretical approaches

a) Born approximation

In the Born approximation the wavefunctions of the incident and scattered electrons are described by the plane waves exp(-**ikr**) and the excitation cross section for transition 0 - 1 is given by the Fourier components of the electron-atom interaction potential $V_k(r)$[9) *) :

$$\sigma^B = \sum_\kappa Q_\kappa(0-1)\sigma_\kappa^B(l_0,l_1) \tag{1}$$

$$\sigma_\kappa^B(l_0,l_1) = \frac{8}{(2l_0+1)k_0^2}\int_{k_0-k_1}^{k_0+k_1} |R^B(q)|^2 \frac{dq}{q^3}[\pi a_0^2] \tag{2}$$

$$R_\kappa^B(q) = [(2\kappa+1)\ (2l_0+1)\ (2l_1+1)]^{1/2}\begin{pmatrix} l_0 l_1 \kappa \\ 000 \end{pmatrix}\int_0^\infty P_0(r)P_1(r)\left[j_\kappa(qr)-\delta_{\kappa 0}\right]dr$$

$$= q^2\int_0^\infty V_\kappa(r)j_\kappa(qr)r^2dr \tag{3}$$

$$\kappa = \kappa_{\min},\ \kappa_{\min}+2,\ldots,\ l_0+l_1;\quad \kappa_{\min} = |l_0-l_1|, \tag{4}$$

---

*) Atomic units are used: e=m=ħ=1.

where P(r) is the radial wavefunction of the bound electron, Q_κ is the angular coefficient, V_κ is the interaction matrix element, q is the momentum transfer $\mathbf{q}=\mathbf{k}_0 - \mathbf{k}_1$, $j_\kappa(x)$ is the spherical Bessel function. From the energy concervation law one has

$$E - E' \equiv \frac{k_0^2}{2} - \frac{k_1^2}{2} = \Delta E, \qquad k_0 \pm k_1 = \sqrt{2E}(1 \pm \sqrt{1 - \Delta E / E}),$$

(5)

where $\Delta E = E_0 - E_1$ is the transition energy, E_0 and E_1 being the binding energies of the initial and final states. E and E′ are the energies of the incident and scattered electron, respectively.

The accurate calculations of the Born cross sections in He are given in refs.[10,11].

b) Bethe formula

For dipole (optically allowed) transitions with $\kappa = 1, \Delta l = \pm 1, \Delta S = 0$ induced by electron impact, an approximate formula for the excitation cross section can be obtained from (3) using the expansion:

$$j_\kappa(qr) \approx \frac{q^\kappa}{(2\kappa+1)!!} r^\kappa, \qquad qr \ll 1$$

(6)

The result is known as the Bethe formula

$$\sigma = \frac{8f}{E\Delta E} \ln \frac{q_0}{k_0 - k_1} \; [\pi a_0^2],$$

(7)

where f is the oscillator strength of the transition 0 - 1 and q_0 is the cutting-off parameter. The reasonable estimation for q_0 is given by [12]:

$$q_0 = \min(k_0 + k_1, \sqrt{2E_0})$$

(8)

The Bethe formula and its modifications are often used for estimation of the dipole excitation cross sections because of its simplicity, but the accuracy of the Bethe formula is less than that of the Born approximation.

c) Model potential

If the interaction matrix element $V_\kappa(r)$ in (3) is known one can calculate the Born cross sections without knowing the radial wavefunctions P(r). In ref.[13] a model potential V^M (r) was suggested in the form:

$$V_\kappa^M(r) = \frac{\lambda_\kappa r^\kappa}{\left(r^2 + r_0^2\right)^{\kappa+1/2}}, \qquad \kappa \neq 0,$$

(9)

where r_0 is the cutting-off (effective) radius and λ_κ is the interaction constant. The model potential (9) has the correct asymptotics at $r \to 0$ and $r \to \infty$. For dipole transitions (κ=1) one has

$$V_1^M(r) = \frac{\lambda_1 r}{(r^2 + r_0^2)^{3/2}}, \qquad \lambda_1 = \left(\frac{3(2l_0+1)}{Q_1} \frac{f}{2\Delta E} \right)^{1/2}, \tag{10}$$

where ΔE is the transition energy.

The sophisticated numerical calculations of the excitation cross sections showed that a reasonable fit of the model potential to the exact one can be achieved if one puts[14)]

$$r_0 = \frac{n_0^* n_1^*}{z(\Delta + 0.5)}, \qquad \Delta = n_1^* - n_0^*, \tag{11}$$

$$n^* = n - \Delta = z(E_{nl} / Ry)^{-1/2}, \tag{12}$$

where E_{nl} is the energy level counted from the ionization limit, n^* is the effective quantum number and Δ is the quantum defect. Here z is the spectroscopic symbol: for neutrals $z = 1$, for positive ions $z > 1$.

With the model potential $V_1^M(r)$ the expression for the Born dipole cross section can be written in a closed analytical form:

$$\sigma = \frac{8f}{E\Delta E}\left[\Phi(x_{min}) - \Phi(x_{max})\right]\left[\pi a_0^2\right], \quad \Phi(x) = (x^2/2)\left[K_0(x)K_2(x) - K_1^2(x)\right] \tag{13}$$

$$x_{max,min} = r_0\left(k_0 \pm k_1\right), \tag{14}$$

where K(x) is the MacDonald function, $k_0 \pm k_1$ are given in (5) and f is the oscillator strength. The function Φ(x) to within 1.5% is fitted by the formula

$$\Phi(x) \approx e^{-2x} \ln\left(2.193 + 0.681\frac{1 + \ln(1 + 0.8\sqrt{x})}{x}\right) \tag{15}$$

At high electron-impact energies E » ΔE, Eq.(13) gives for the cross section:

$$\sigma = \frac{8f}{E\,\Delta E}\ln\frac{1.36\,E^{1/2}}{r_0\,\Delta E}[\pi a_0^2], \qquad E >> \Delta E, \tag{16}$$

that corresponds to the excitation rate coefficient

$$< v\sigma >= 1.74\frac{f\,\beta^{1/2}}{z\Delta}e^{-\Delta E/T}\ln\frac{1.26z}{\Delta E\, r_0 \beta^{1/2}}[10^{-7}\,cm^3\,s^{-1}], \quad \beta = z^2 Ry / T << 1 \tag{17}$$

For transitions n_0 - n_1, i.e. averaged over the quantum numbers l and m, one can use in (13, 16, 17) the corresponding oscillator strength. In the case of high n-values the Kramers formula is used:

$$f(n_0 - n_1) = \frac{2C}{n_0^2}\left(\frac{n_0 n_1}{\Delta n(n_0 + n_1)}\right)^3, \quad \Delta n = n_1 - n_0, \quad C = 16/3\sqrt{3}\pi \approx 1 \tag{18}$$

d) Ochkur approximation

For spin-forbidden transitions with ΔS=1 the Ochkur approximation [15] is used which is similar to the Born approximation:

$$\sigma^O = \sum_\kappa \frac{2S_1 + 1}{2(2S_p + 1)} Q_\kappa(0-1)\sigma_\kappa^O(l_0, l_1) \tag{19}$$

$$\sigma_\kappa^O(l_0, l_1) = \frac{8\pi}{(2l_0 + 1)k_0^2} \int_{k_0-k_1}^{k_0+k_1} |R_\kappa^O(q)|^2 \frac{dq}{q^3} \; [\pi a_0^2] \tag{20}$$

$$R_\kappa^O(q) = [(2\kappa + 1)\ (2l_0 + 1)\ (2l_1 + 1)]^{1/2} \begin{pmatrix} l_0 l_1 \kappa \\ 000 \end{pmatrix} \frac{q^2}{k_0^2} \int_0^\infty P_0(r)P_1(r)j_\kappa(qr)dr \tag{21}$$

$$\kappa = \kappa_{\min}, \quad \kappa_{\min} + 2, \ldots, \quad l_0 + l_1; \qquad \kappa_{\min} = |l_0 - l_1|, \tag{22}$$

where S_1 is the spin of an atom in the final state, S_p is the spin of the parent ion. As seen from (21) the integral $R_\kappa^O(q)$ does not contain a term with δ-function which describes the interaction of the incident electron with a target nucleus and is of the order of k_0^{-2}. Due to the additional factor q^2/k_0^2 the exchange cross section decreases at large E as

$$\sigma_\kappa^O \propto E^{-3}, \quad E \to \infty, \quad \Delta S = 1. \tag{23}$$

We note that the q-representation of the excitation cross section for forbidden transitions in the Born approximation is only possible in the Ochkur approach. In the general case it is necessary to use the expansion of the wavefunctions on the partial waves of the incident and scattered electrons.

e) Partial wave method

For transitions with a change of spin $\Delta S \neq 0$ it is necessary to take into account the electron exchange effect. The inclusion of this effect in the framework of the Born approximation (Ochkur approach) is applicable only for neutral atoms. Moreover, in many cases it is often reqiured to perform the procedure of unitarization (normalization) of the Born cross sections which is especially important for the intermediate and low energies.

All these effects are included in the so-called generalized Born approximation[12] using the partial wave representation. Let us consider the excitation of an atom or ion by electron impact:

$$X_z(a_0) + e(E,\lambda_0) \rightarrow X_z^* + e(E_1,\lambda_1), \tag{24}$$

where λ denotes the orbital momenta of the incident and scattered electrons (partial waves). In the first order of the perturbation theory the excitation cross section can be written in the form:

$$\sigma = \sum_{\kappa} Q'_{\kappa}(0-1)\sigma'_{\kappa}(l_0,l_1) + \sum_{\kappa} Q_{\kappa}(0-1)\sigma''_{\kappa}(l_0,l_1) \tag{25}$$

The first sum in (25) describes the contribution of direct and interference terms for which the angular parts Q are exactly the same, while the second sum is connected with exchange excitation. The angular coefficients Q depend only on all angular (orbital and spin) momenta of an atom or ion and a type of the coupling scheme (see ref.[12]). The cross sections σ_κ are the one-electron cross sections depending only on the quantum numbers *nl* of the bound electron and the incident electron energy E. In the case of intercombination transitions with ΔS=1 the first sum in (25) equals to zero, so the transitions take place mainly due to the electron exchange effects.

The cross sections σ_κ can be written in the form:

$$\sigma'_{\kappa}(l_0,l_1) = \frac{4}{(2l_0+1)(2\kappa+1)k_0^2} \sum_{\lambda_0\lambda_1} R^d_{\kappa}(R^d_{\kappa} - R''_{\kappa})[\pi a_0^2] \tag{26}$$

$$\sigma''_{\kappa}(l_0,l_1) = \frac{4}{(2l_0+1)(2\kappa+1)k_0^2} \sum_{\lambda_0\lambda_1} (R''_{\kappa})^2\,[\pi a_0^2] \tag{27}$$

$$R''_{\kappa} = \sum_{\kappa''} (-1)^{l_0+l_1+\kappa''}(2\kappa+1)\begin{Bmatrix} \kappa l_0 l_1 \\ \kappa'' \lambda_0 \lambda_1 \end{Bmatrix} \tag{28}$$

$$R^d_\kappa = [(2l_0+1)(2l_1+1)(2\lambda_0+1)(2\lambda_1+1)]^{1/2}\begin{pmatrix} l_0 l_1 \kappa \\ 000 \end{pmatrix}\begin{pmatrix} \lambda_0 \lambda_1 \kappa \\ 000 \end{pmatrix}$$

$$\times 2\iint F_{k_0\lambda_0}(r'')F_{k_1\lambda_1}(r'')\frac{r_<^\kappa}{r_>^{\kappa+1}}P_0(r')P_1(r')dr'dr''$$

(29)

$$R^e_{\kappa''} = [(2l_0+1)(2l_1+1)(2\lambda_0+1)(2\lambda_1+1)]^{1/2}\begin{pmatrix} l_0 \lambda_1 \kappa'' \\ 000 \end{pmatrix}\begin{pmatrix} \lambda_0 l_1 \kappa'' \\ 000 \end{pmatrix}$$

$$\times 2\iint F_{k_0\lambda_0}(r'')F_{k_1\lambda_1}(r'')\frac{r_<^\kappa}{r_>^{\kappa+1}}P_0(r')P_1(r')dr'dr''$$

(30)

Here P(r) are the radial wavefunctions of the bound electron, F(r) are the radial wavefunctions of the incident and scattered electrons; values of k_0 and k_1 satisfy Eq. (5). The indexes κ and κ″ are changed in the limits given by the properties of 3j- and 6j-symbols :

$$\kappa_{\min} \le \kappa \le \kappa_{\max}, \qquad \kappa''_{\min} \le \kappa'' \le \kappa''_{\max}$$

(31)

$$\kappa_{\min} = \max(|l_0 - l_1|, |\lambda_0 - \lambda_1|), \quad \kappa_{\max} = \min(l_0 + l_1, \lambda_0 + \lambda_1),$$

(32)

$$\kappa''_{\min} = \max(|\lambda - l_0|, |l_1 - \lambda_0|), \ \kappa''_{\max} = \min(l_0 + \lambda_1, l_1 + \lambda_0).$$

(33)

Eqs. (25-33) represent the Coulomb-Born approximation if the wavefunctions of the incident and scattered electrons are the Coulomb functions, the radial parts $F_{k\lambda}(r)$ of which satisfy the equations:

$$\left[\frac{d^2}{dr^2} - \frac{\lambda(\lambda+1)}{r^2} + \frac{z-1}{r} + k^2\right]F_{k\lambda}(r) = 0,$$

$$F_{k\lambda}(r) = 0, \quad r \to 0,$$

$$F_{k\lambda}(r) \approx k^{-1/2}\sin\left(kr + \frac{z-1}{k}\ln(2kr) - \frac{\pi\lambda}{2} + \delta_\lambda\right), \ r \to \infty$$

(34)

where δ_λ is the phase shift. For neutral tergets (z=1) the function $F_{k\lambda}(r)$ becomes the component $j_\lambda(kr)$ of the plane wave and the CB approximation becomes the Born approach in the partial wave representation.

At threshold energy $E=E_{th}=\Delta E$, the cross sections (25-33) are zero, $\sigma_{th}=0$, for neutral atoms, and σ_{th}=constant for ions. CBE method provides the following asymptotics for excitation cross sections at $E \to \infty$:

$$\sigma \propto \begin{cases} (\ln E)/E, & \Delta S = 0, \ \Delta l = \pm 1 \\ E^{-1}, & \Delta S = 0, \ \Delta l \ne \pm 1 \\ E^{-3}, & \Delta S = 1. \end{cases}$$

(35)

In general, the total wavefunctions of the system electron+ion in the initial and final states are not orthogonal because the bound P(r) and continuous F(r) wavefunctions correspond to the different potentials of z/r and (z-1)/r types. This disadvantage can be removed by introducing the orthogonalized wavefunctions $\Phi_{k\lambda}(r)$ (see ref.[15]):

$$\Phi_{k_0\lambda_0}(r) = F_{k_0\lambda_0}(r) - < F_{k_0\lambda_0}(r)|P_1 > P_1\delta_{l_1\lambda_0}$$

$$\Phi_{k_1\lambda_1}(r) = F_{k_1\lambda_1}(r) - < F_{k_1\lambda_1}(r)|P_0 > P_0\delta_{l_0\lambda_1} \tag{36}$$

Therefore, we will call CBE approximation the first order the approach (25-34) with the Coulomb functions (34) for the direct part R^d and with the orthogonilized functions (36) for the exchange part R^e. The CBE method defined this way provides for intercombination transitions (ΔS=1) the same accuracy as the Born approximation for spin-allowed transitions (ΔS=0). For multicharged ions (z>>1) the functions F and Φ practically coincide because

$$< F_{k\lambda}|P_{nl} > \propto z^{-1}$$

3. Comparison with experiment and other calculations

In this work calculations of the excitation cross sections between excited states in He have been performed by the ATOM code using CBE approximation (25-34) in the partial wave representation (see ref.[9] in detail). The results are shown in Figs. 1-153 in comparison with available experimental data and calculations.

In this work the calculated CBE excitation cross sections σ and corresponding rate coefficients $<v\sigma>$ for spin-allowed transitions ($\Delta S = 0$) are fitted by approximation formulae:

$$\sigma = \frac{\pi a_0^2}{2l_0+1}\left(\frac{Ry}{DE}\right)^2\left(\frac{E_1}{E_0}\right)^{3/2}\frac{C}{u+\varphi}\left(\frac{u}{u+\alpha}\right)^{1/2} \tag{37}$$

$$< v\sigma >= \frac{10^{-8}cm^3s^{-1}}{2l_0+1}\left(\frac{RyE_1}{DE\,E_0}\right)^{3/2} e^{-\Delta E/T}\frac{A\beta^{1/2}(\beta+1)(\alpha\beta+1)^{-1/2}}{\beta+\chi} \tag{38}$$

$$\alpha = \Delta E / DE, \quad u = (E-\Delta E)/DE, \quad \beta = DE/T, \tag{39}$$

where C, φ, A and χ are the fitting parameters, E_0 and E_1 are the atomic energy levels of the initial and final states counted from the ionization limit, ΔE is the excitation energy. In this work a scaling value DE=5Ry is used. The reduced electron energy u and the temperature β are changed in the limits:

$$0.02 \le u \le 16.0, \qquad 0.25 \le \beta \le 8.0, \qquad E_{max} = 2000 \text{ eV}. \tag{40}$$

The fiting parameters C, φ, A and χ for triplet-triplet transitions and singlet-singlet transitions are given in Tables 1 and 2, respectively. The oscillator strengths f also calculated by the

ATOM code are given in the Tables. Errors (in %) of fittings by Eqs. (37) and (38) are presented in the 6th and 9th columns, respectively.

The present results are compared with the following data:

Flannery et al. (1975) - a ten-channel eikonal approximation,
Fon et al. (1981) - the five-state R-matrix calculations,
Badnell (1984) - Hartree-Fock approximation with orthogonalized wavefunctions of the core and valence electron,
Berrington et al. (1985) - an R-matrix calculation with eleven lowest target states included,
Mathur et al. (1987) - a distorted wave approximation (DWA),
Kingston (1992) - an R-matrix calculation,
Bray et al. (1993) - DWA,
de Heer et al. (1995) - preferred data obtained from compilation;
Rall et al., (1989) - experiment.

As seen from the Figures, some dipole cross sections have the double-peak structure (e.g., 2^1S-3^1P, 2^1S-4^1P, 2^1P-4^1S, 3^3P-3^3D, 3^3P-4^3D, 4^3S-4^3P transitions). Our calculations show that the additional maximum at low electron energy is connected with the strong influence of the exchange effect which is very important for He-like systems. In Figs. 154-159 the contribution of the pure exchange part in (25) (with zero direct and interference parts $\sigma_\kappa' = 0$) is shown together with the total excitation cross sections and the model cross sections (13,14) also calculated by the ATOM code.

In Figs. 160-170 a comparison of CBE results with Ochkur approximation is given for some intercombination transitions ($\Delta S=1$). It is seen that the pure Ochkur approximation Eqs. (19-22) can be used at relatively high (as compared to ΔE) incident electron energies $E > 10$-20 eV where the intercombination cross sections have the asymptotic $\sigma \propto E^{-3}$.

4. Conclusion

A comparison of the calculated excitation cross sections for He performed in this work by the CBE method using orthogonalized wavefunctions showed that at electron energies $E > 20$ eV our results are close to recommended data and sophisticated calculations. At low energies $E < 20$ eV our cross sections are relatively high as compared to the other calculations. However, to make some definite decision the further experiments have to be carried out for transitions between excited states in He.

Table 1. Transition energies ΔE (eV), oscillator strengths f, fitting parameters, Eqs.(37-40), and effective radius r_0, Eq.(11), for triplet-triplet transitions in He.

Transit.	ΔE (eV)	f	C	φ	Err.(%)	A	χ	Err.(%)	$r_0(a_0)$
2s-2p	1.14	0.539	1.46×10^3	0.224	12	1.13×10^3	0.24	6	4.36
3s	2.89		54.2	0.0532	19	87.0	0.624	5	
3p	3.19	0.0636	78.8	0.0702	50	57.8	0.0983	13	2.84
3d	3.25		143	0.0337	25	258	0.712	2	
4s	3.77		25.5	0.0264	35	48.8	0.726	2	
4p	3.89	0.0253	59.5	0.0596	70	45.7	0.106	11	2.42
4d	3.91		79.5	0.0182	30	169	0.869	3	
4f	3.92		12.3	3.59×10^{-3}	25	38.1	1.50	12	
2p-3s	1.75	0.069	482	0.475	12	260	0.125	20	4.15
3p	2.04		259	0.0575	20	385	0.572	7	
3d	2.11	0.61	4.85×10^3	0.391	25	2.77×10^3	0.120	20	3.72
4s	2.63	0.0105	105	0.181	40	76.4	0.171	15	3.17
4p	2.74		119	0.0256	20	230	0.801	1	
4d	2.77	0.123	1.59×10^3	0.157	40	1.28×10^3	0.206	10	3.02
4f	2.77		119	8.38×10^{-3}	40	249	0.786	1	
3s-3p	0.288	0.89	9.11×10^3	0.162	30	7.93×10^3	0.285	15	10.7
3d	0.355		343	0.011	2	638	0.793	3	
4s	0.875		202	0.0416	2	320	0.657	10	
4p	0.989	0.050	176	0.0312	60	180	0.252	10	6.11
4d	1.02		160	0.0223	20	285	0.716	5	
4f	1.02		203	4.54×10^{-3}	20	43	0.919	1	
3p-3d	0.0664	0.112	1.59×10^4	5.44×10^{-2}	30	1.89×10^4	0.441	10	15.6
4s	0.587	0.145	2.44×10^3	0.269	26	1.62×10^3	0.181	18	8.58
4p	0.700		909	0.0527	3	1.30×10^3	0.556	9	
4d	0.729	0.48	7.86×10^3	0.313	17	4.80×10^3	0.147	20	7.50
4f	0.730		1.78×10^3	0.0269	10	3.10×10^3	0.748	5	
3d-4s	0.520		84.8	6.69×10^{-3}	12	172	0.890	1	
4p	0.634	0.022	516	0.0465	60	498	0.252	12	8.22
4d	0.662		1.25×10^3	0.0698	7	1.58×10^3	0.453	12	
4f	0.663	1.01	3.52×10^4	0.502	18	1.96×10^4	0.121	25	7.98
4s-4p	0.114	1.21	2.90×10^4	0.108	25	3.09×10^4	0.356	12	19.9
4d	0.142		1.31×10^3	8.86×10^{-3}	2	2.49×10^3	0.822	4	
4f	0.143		211	2.46×10^{-3}	7	439	0.916	1	
4p-4d	0.0281	0.20	6.65×10^4	0.0286	18	8.79×10^4	0.494	8	27.8
4f	0.0292		1.17×10^3	5.80×10^{-3}	4	2.26×10^3	0.842	3	
4d-4f	0.00105	3.88×10^{-3}	8.51×10^4	5.74×10^{-3}	17	1.44×10^5	0.670	4	31.8

Table 2. Transition energies ΔE (eV), oscillator strengths *f*, fitting parameters Eqs.(37-40) and effective radius r_0, Eq. (11), for singlet-singlet transitions in He.

Transit.	ΔE(eV)	f	C	φ	Err.(%)	A	χ	Err.(%)	$r_0(a_0)$
2s-2p	0.565	0.346	$1.79x10^3$	0.141	13	$1.61x10^3$	0.302	14	4.36
3s	2.30		70.7	0.0690	25	105	0.571	8	
3p	2.46	0.167	309	0.579	60	144	0.0214	30	2.84
3d	2.46		209	0.0656	30	322	0.572	10	
4s	3.05		30.6	0.0387	50	52.6	0.602	7	
4p	3.12	0.0526	160	0.393	70	88.9	0.0320	30	2.42
4d	3.12		76.7	0.0250	70	141	0.603	7	
4f	3.12		21.7	0.0254	60	41.9	0.676	5	
2p-3s	1.74	0.044	340	0.690	20	156	0.0835	25	4.26
3p	1.89		299	0.0996	25	397	0.523	10	
3d	1.89	0.695	$6.32x10^3$	0.598	25	$3.26x10^3$	0.111	20	4.04
4s	2.49	$7.90x10^{-3}$	82.7	0.286	50	50.7	0.0971	20	3.30
4p	2.56		139	0.0741	25	218	0.662	5	
4d	2.56	0.121	$1.96x10^3$	0.356	15	$1.30x10^3$	0.195	15	3.23
4f	2.56		172	0.0528	35	273	0.591	7	
3s-3p	0.154	0.571	$1.10x10^4$	0.106	20	$1.11x10^4$	0.359	12	13.3.
3d	0.154		291	0.011	5	531	0.772	4	
4s	0.752		238	0.0512	40	375	0.650	7	
4p	0.816	0.165	775	0.447	40	413	0.0976	25	6.96
4d	0.816		341	0.0443	60	583	0.712	6	
4f	0.816		262	0.0305	20	462	0.770	5	
3p-4s	0.60	0.0943	$1.50x10^3$	0.332	60	977	0.154	20	8.00
4p	0.66		989	0.0655	2	$1.37x10^3$	0.546	10	
4d	0.66	0.62	$1.09x10^4$	0.344	40	$6.87x10^3$	0.159	20	8.00
4f	0.66		$1.94x10^3$	0.0391	20	$3.22x10^3$	0.722	6	
3d-3p	$1.97x10^{-4}$	$1.95x10^{-4}$	$3.00x10^4$	$4.52x10^{-3}$	20	$5.06x10^4$	0.683	3	18.0
4s	0.599		51.1	0.0256	10	88.6	0.742	5	
4p	0.66	0.011	306	0.0455	40	326	0.323	10	8.00
4d	0.66		$1.28x10^3$	0.0856	1	$1.56x10^3$	0.441	13	
4f	0.66	1.014	$3.46x10^4$	0.506	30	$1.96x10^4$	0.120	25	8.01
4s-4p	0.0627	0.783	$3.59x10^4$	0.0620	40	$4.20x10^4$	0.428	5	24.0
4d	0.0627		$1.21x10^3$	$7.76x10^{-3}$	6	$2.30x10^3$	0.821	4	
4f	0.0636		168	$5.31x10^{-3}$	4	332	0.865	3	
4d-4p	$9.93x10^{-6}$	$4.20x10^{-5}$	$7.85x10^5$	0.0418	100	$2.65x10^5$	0.162	10	31.8
4f	$8.51x10^{-4}$	$3.16x10^{-3}$	$8.73x10^4$	$5.48x10^{-3}$	17	$1.48x10^5$	0.676	3	32.0
4f-4p	$8.18x10^{-4}$		$1.03x10^3$	$6.64x10^{-3}$	1	$1.98x10^3$	0.870	3	

Aknowledgements

The authors are grateful to F.J. de Heer and L.A.Vainshtein for valuable remarks and to I.Yu.Tolstikhina for her help in computer work.

REFERENCES

1) F.R Flannery, W.R. Morrison, B.L. Richmond, J. Appl. Phys., **46** (1975) 1186
2) H.P. Summers, Adv. At. Mol. Opt. Phys., **33** (1994) 275
3) J.A. Tully, H.P. Summers, Astrophys. J., **229** (1979) L113
4) Y. Itikawa, J. Phys., **B 33** (1994) 253
5) F.J., de Heer, R. T. Hoekstra, A.E. Kingston, H.P. Summers, Atomic and Plasma-Material Interaction Data for Fusion (Suppl. Journ. Nuclear Fusion), Vol. **3** (1992) 19 (IAEA, Vienna)
6) T. Kato, R.K Janev, Atomic and Plasma-Material Interaction Data for Fusion (Suppl. Journ. Nuclear Fusion), Vol. **3** (1992) 33 (IAEA, Vienna)
7) T.Kato, Y. Itikawa, K. Sakimoto, **NIFS-DATA-15**, National Institute for Fusion Science, Japan (1992)
8) K.A., Berrington, P.M.J. Sawey, At. Data and Nucl. Data Tables, **55** (1993) 81
9) V.P. Shevelko, L.A. Vainshtein, Atomic Physics for Hot Plasmas , IOP Publishing, Bristol (1993)
10) Y.K.Kim, M.Inokuti, Phys. Rev. **181** (1969) 205
11) D. Ton-That, S.T.Manson, M.R.Flannery, J. Phys. **B 10** (1977) 621
12) L.A. Vainshtein, I.I.Sobelman, E.A.Yukov, Excitation of Atoms and Broadening of Spectral Lines, Springer, Berlin (1995) (2nd edition)
13) I.L. Beigman, A.M.Urnov, V.P.Shevelko, J. Phys. **B 9** (1976) 2859
14) V.P. Shevelko, Phys. Scripta, **43** (1991) 266
15) V.I. Ochkur, JETP **18** (1964) 503
16) M.R. Flannery, K.J. McCann, Phys. Rev. **A 12** (1975) 846
17) W.C. Fon, K.A. Berrington, P.G. Burke, A.E. Kingston, J. Phys., **B 14** (1981) 2921
18) N.R. Badnell, J. Phys., **B 17** (1984) 4013
19) K.A. Berrington, P.G. Burke, L.C.G. Freitag, A.E. Kingston, J. Phys., **B 18** (1985) 4135
20) K.C. Mathur, R.P. McEachran, L.A. Parcell, A.D. Steuffer, J. Phys., **B 20** (1987) 1599
21) A.E. Kingston, (1992), private communiation (unpublished).
22) I. Bray, I.E. McCarthy, Phys. Rev. **A 47** (1993) 317
23) F.J. de Heer, H.O. Folkerts, F.W. Bliek, R. Hoekstra, T. Kato, A.E. Kingston, K.A. Berrington, H.P. Summers, Atomic and Plasma-Material Interaction Data for Fusion (Suppl. Journ. Nuclear Fusion), Vol. **6** , IAEA, Vienna (1995) (in preparation).
24) D.L.A. Rall, F.A. Sharpton, M.B. Chulman, L.W. Anderson, J.E. Lawler, C.C. Lin, Phys. Rev. Lett., **62** (1989) 2253

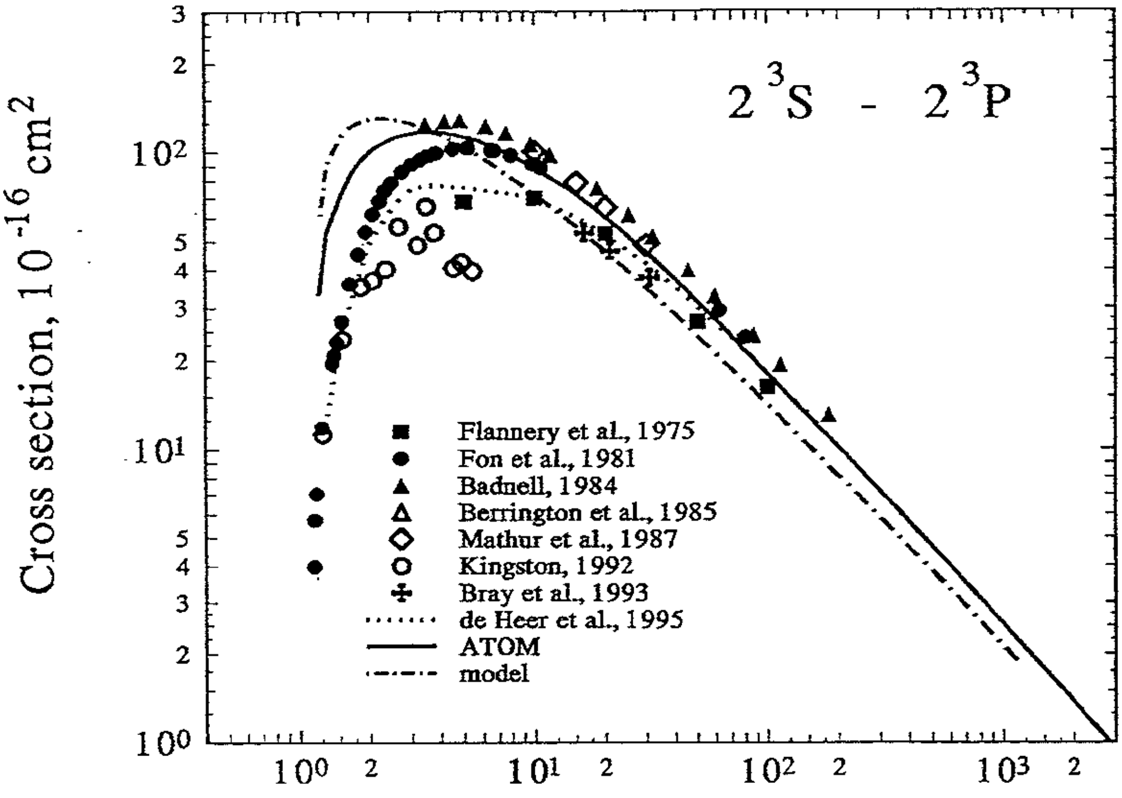

Fig.1 Electron energy, eV

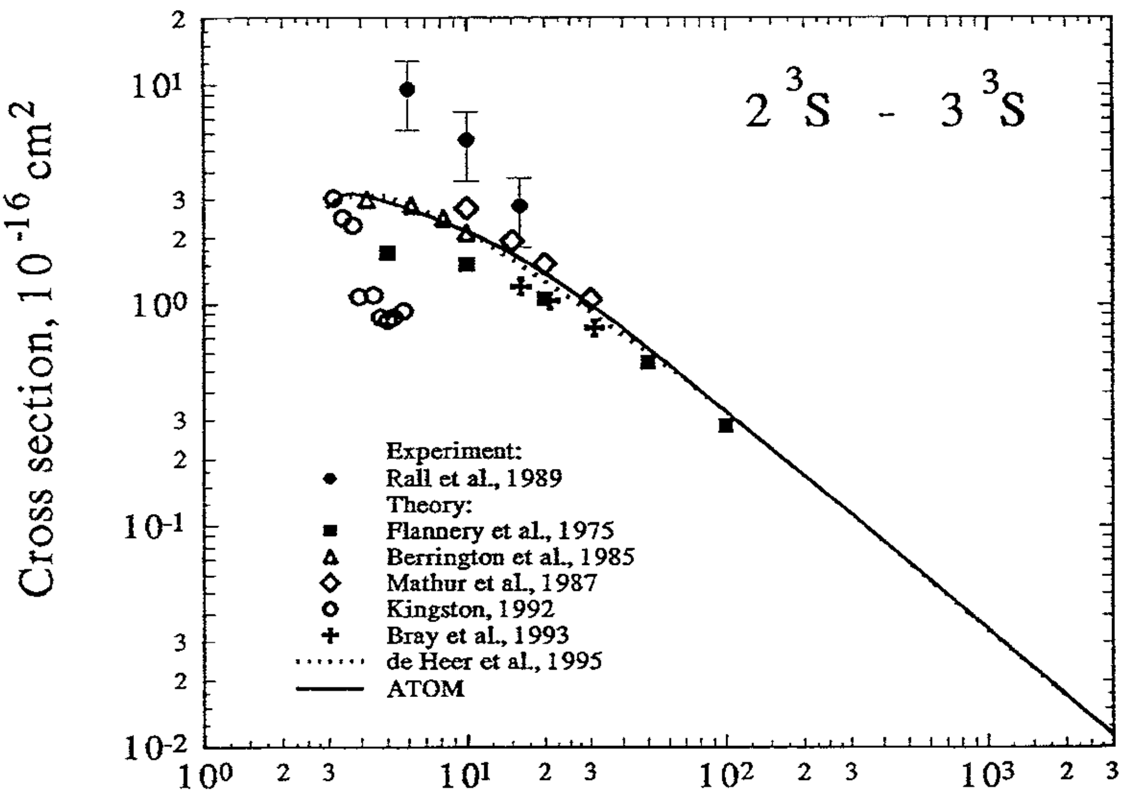

Fig.2 Electron energy, eV

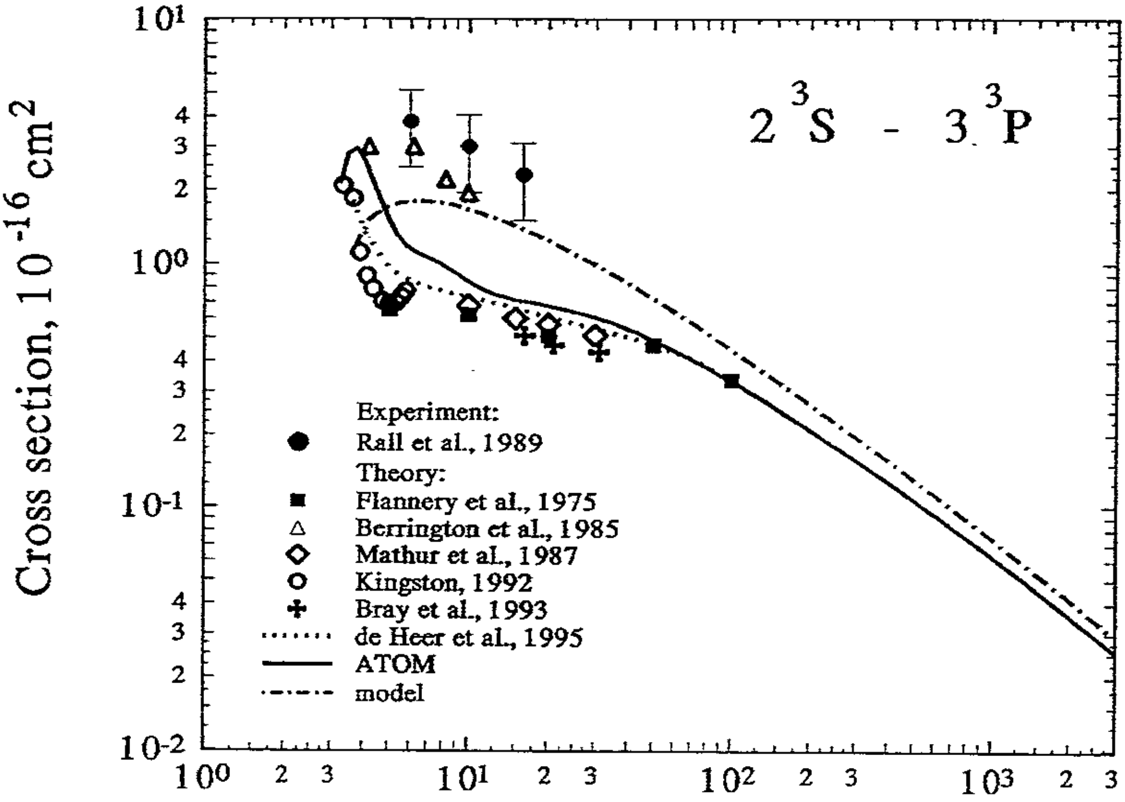

Fig.3 Electron energy, eV

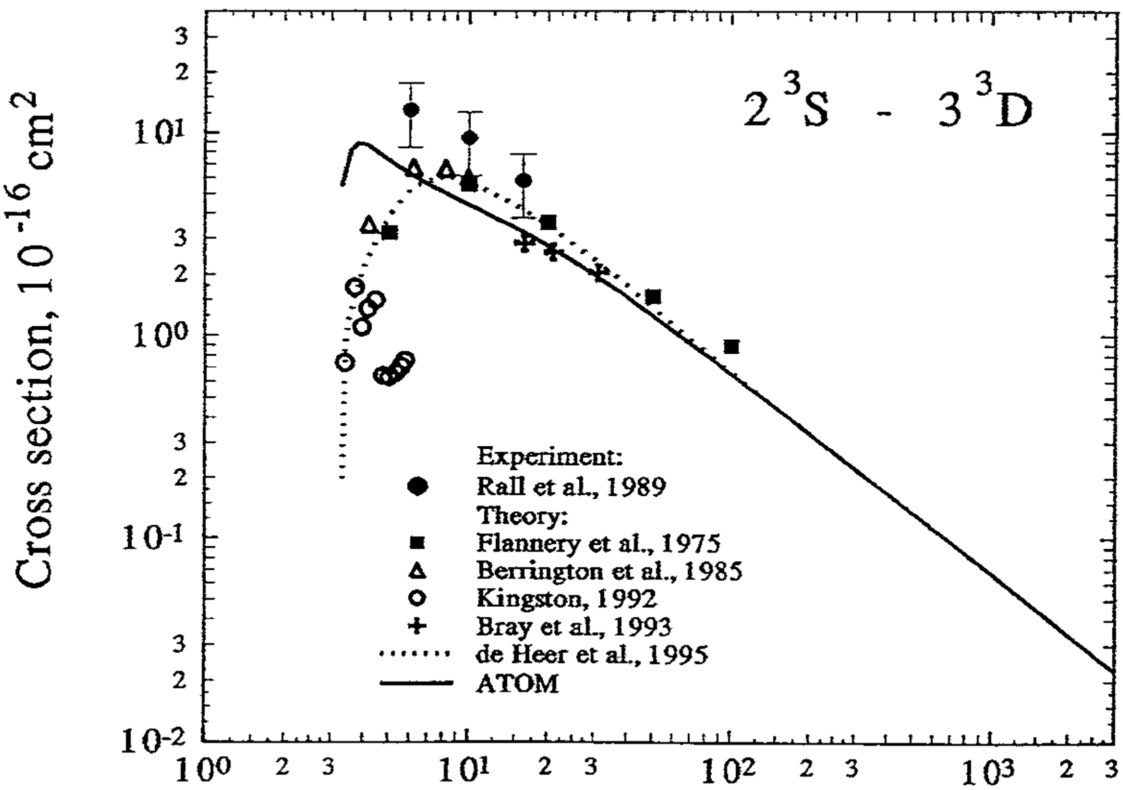

Fig.4 Electron energy, eV

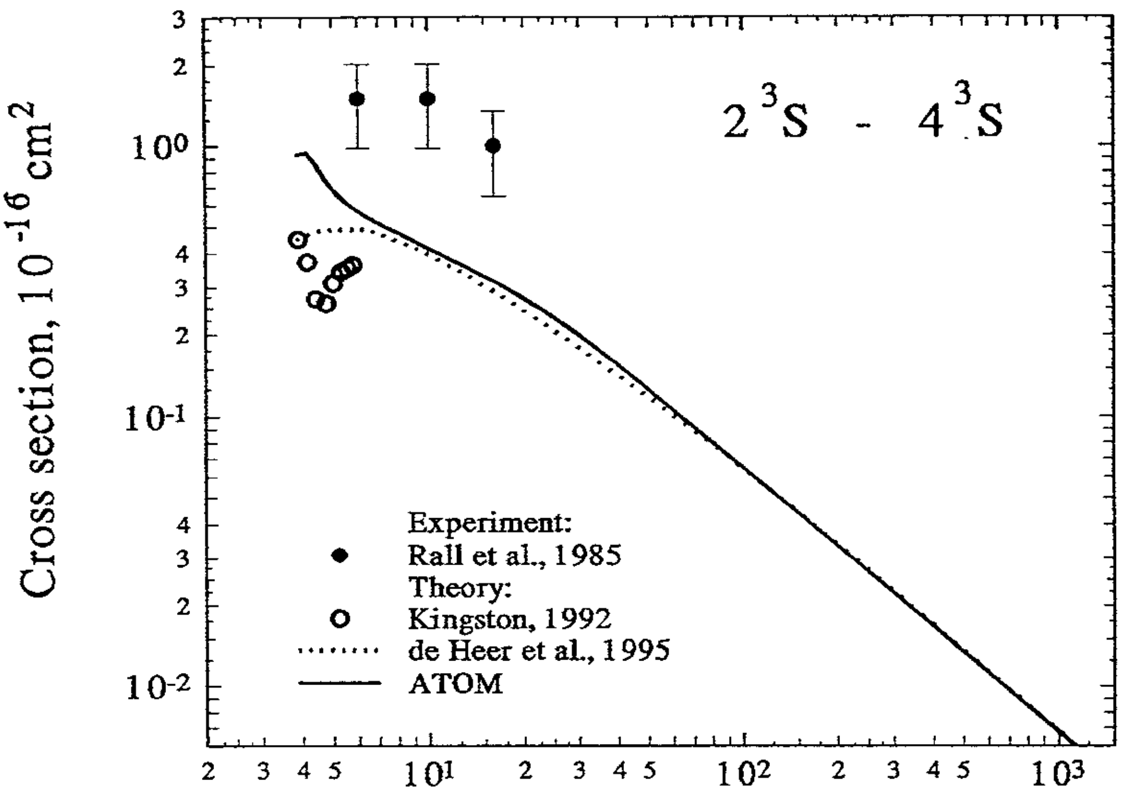

Fig.5 Electron energy, eV

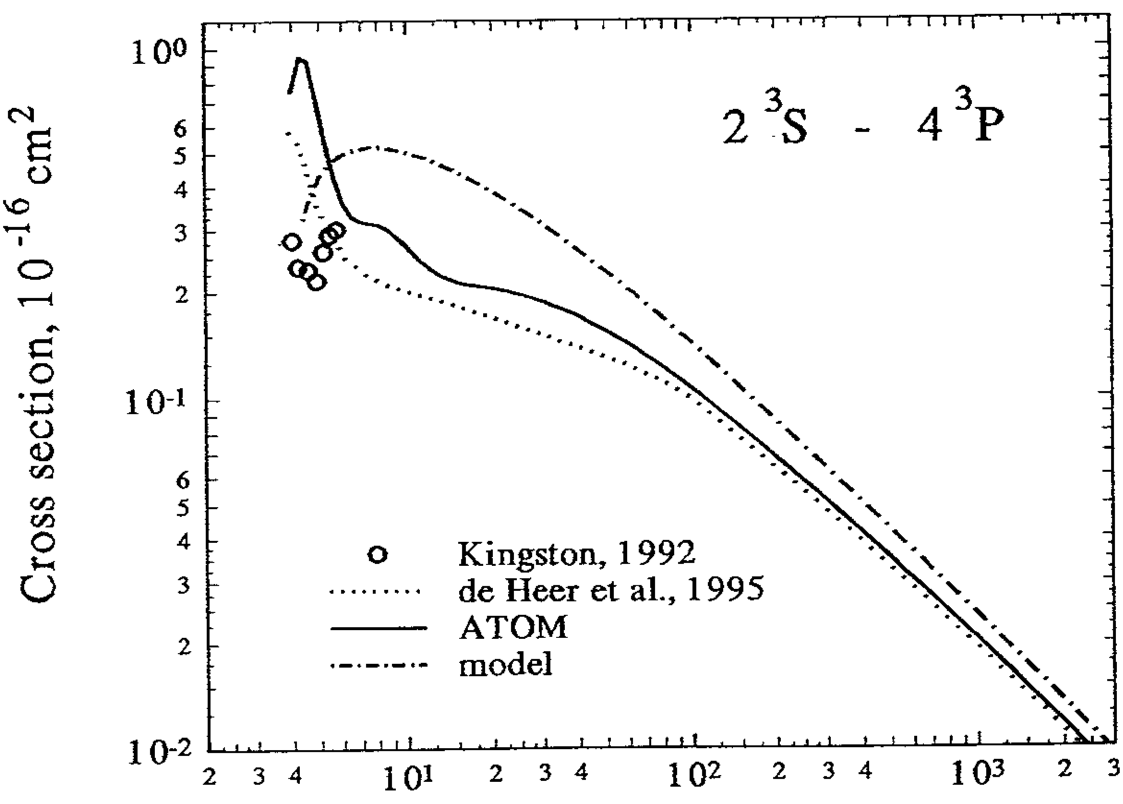

Fig.6 Electron energy, eV

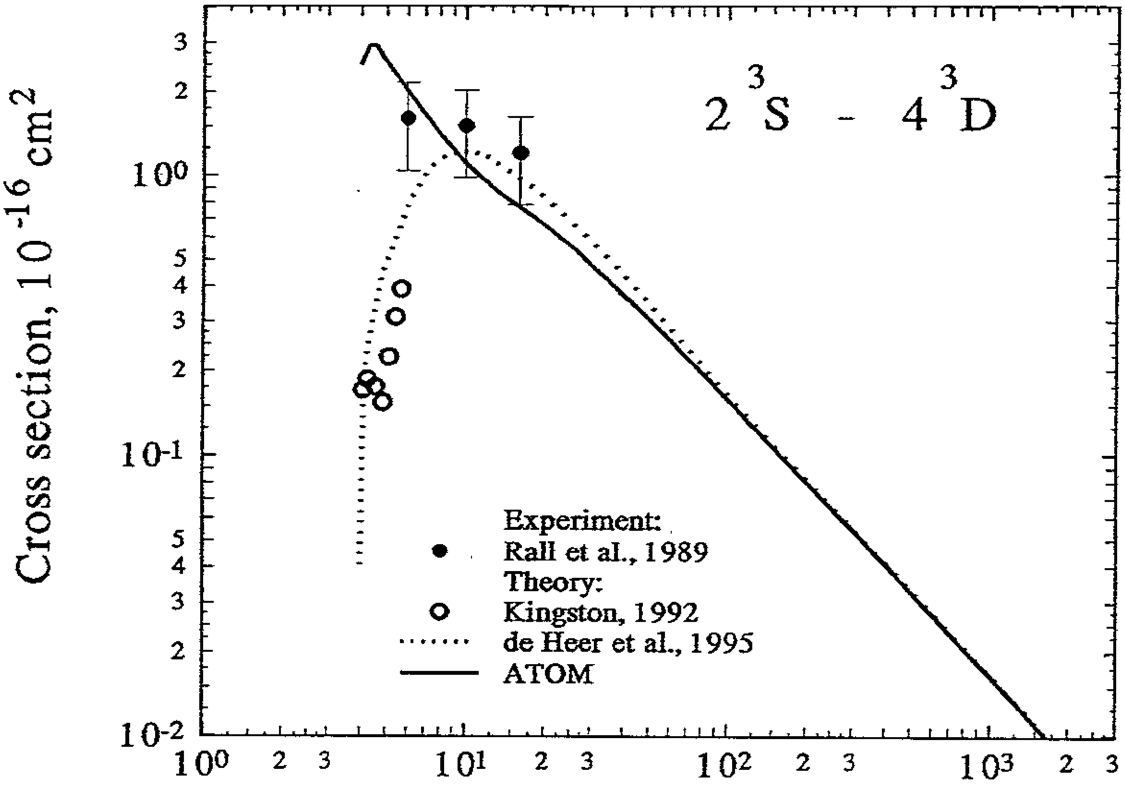

Fig.7 Electron energy, eV

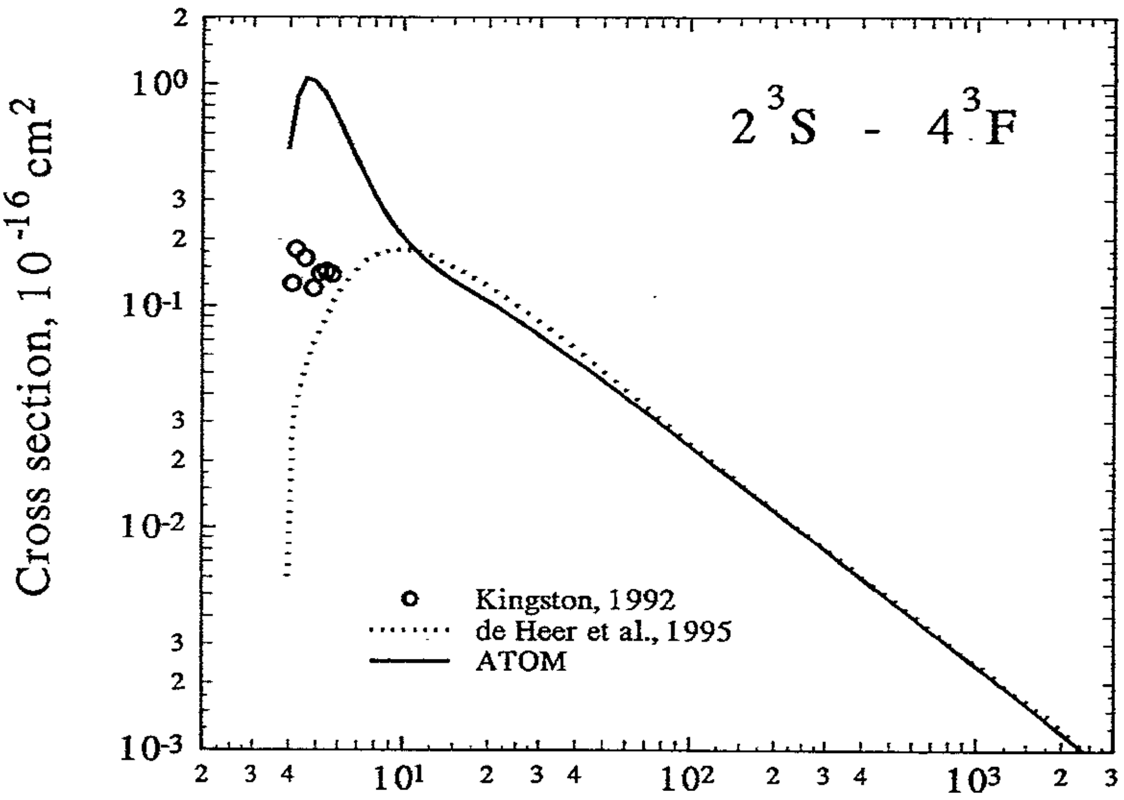

Fig.8 Electron energy, eV

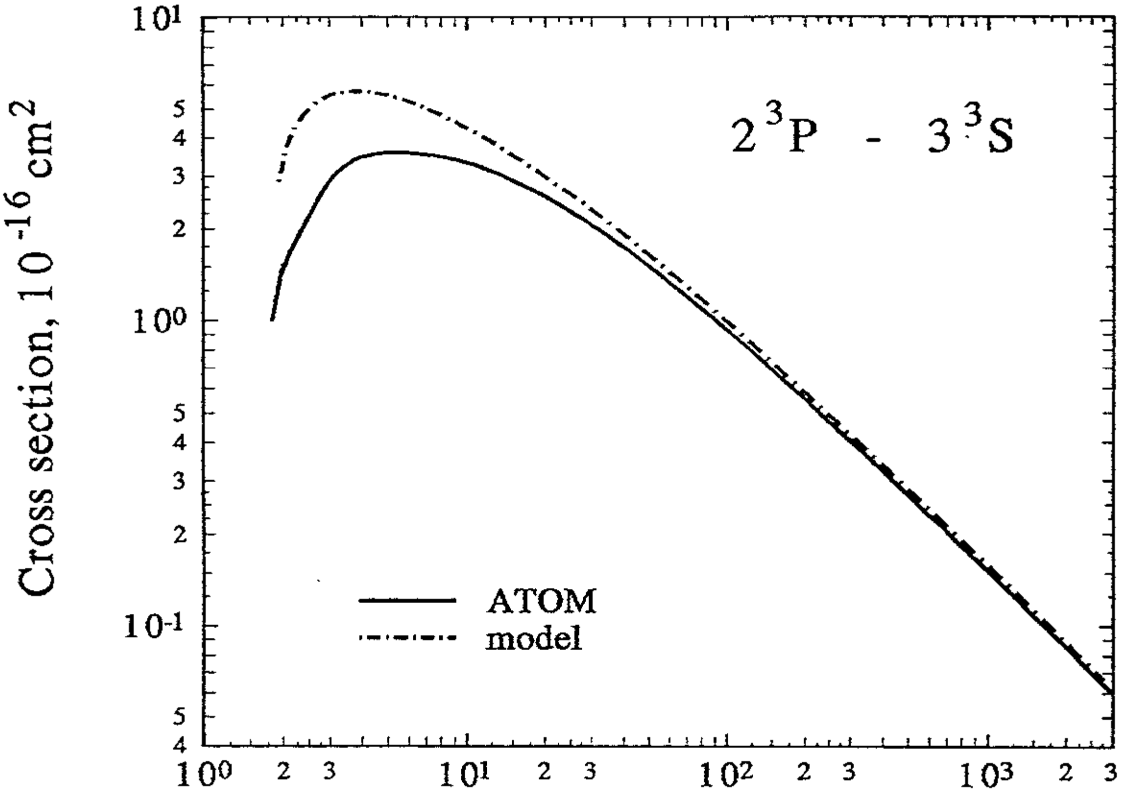

Fig.9 Electron energy, eV

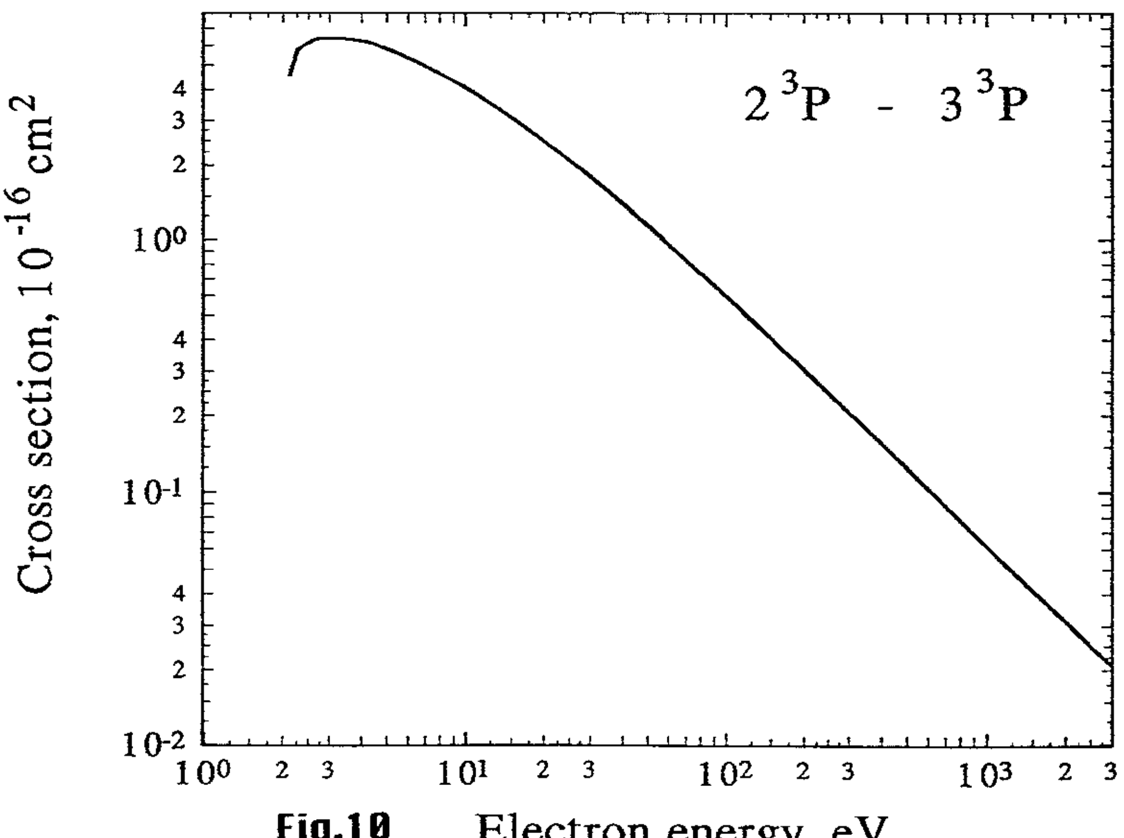

Fig.10 Electron energy, eV

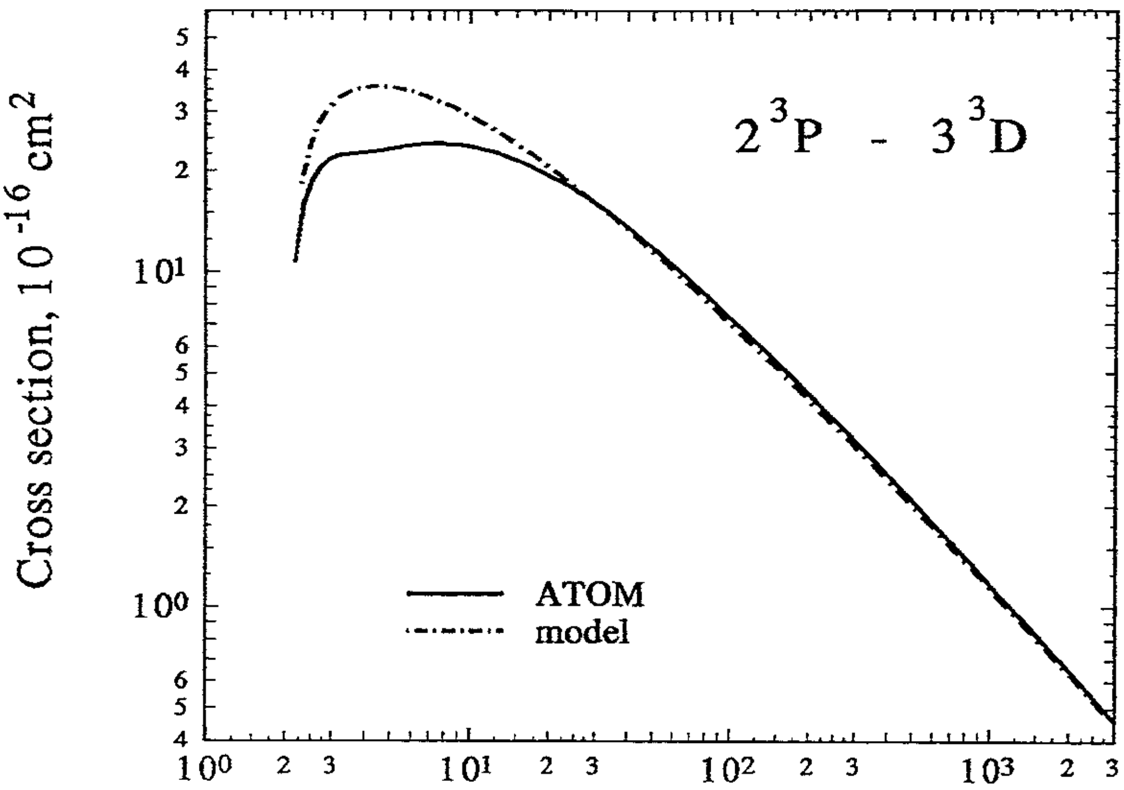

Fig.11 Electron energy, eV

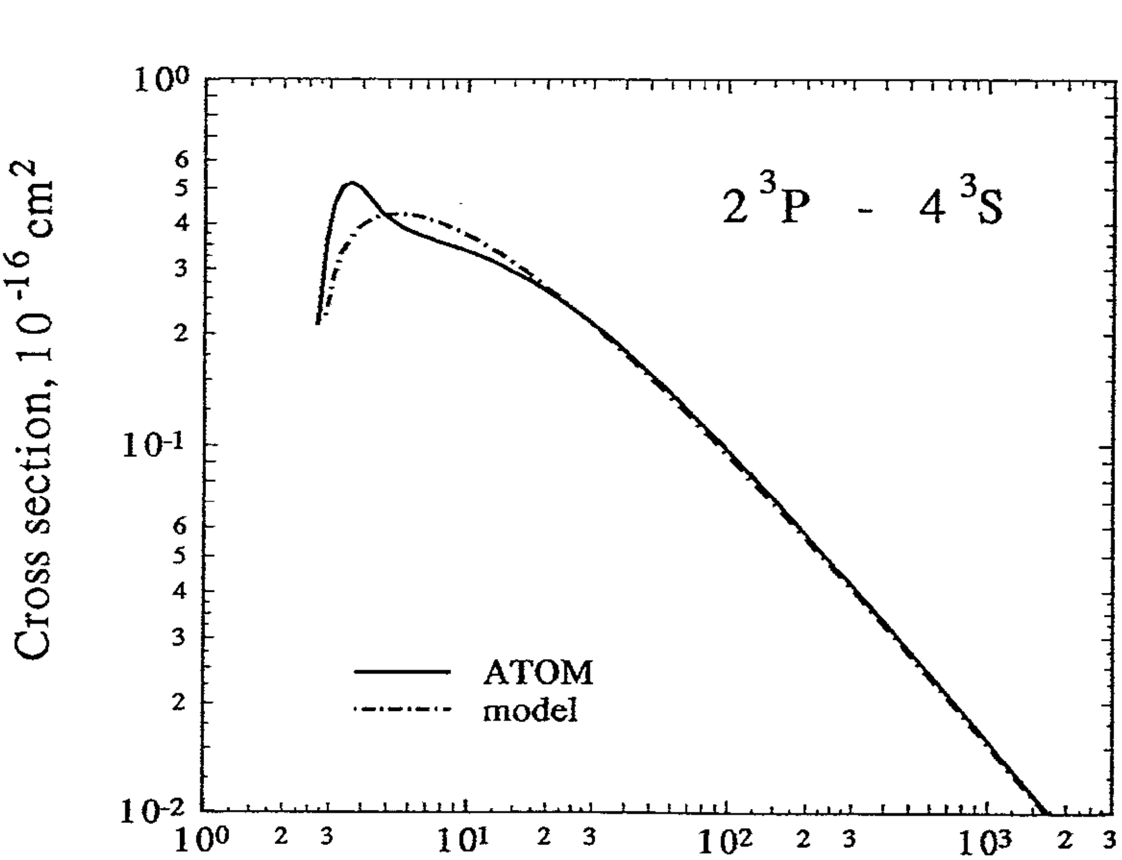

Fig.12 Electron energy, eV

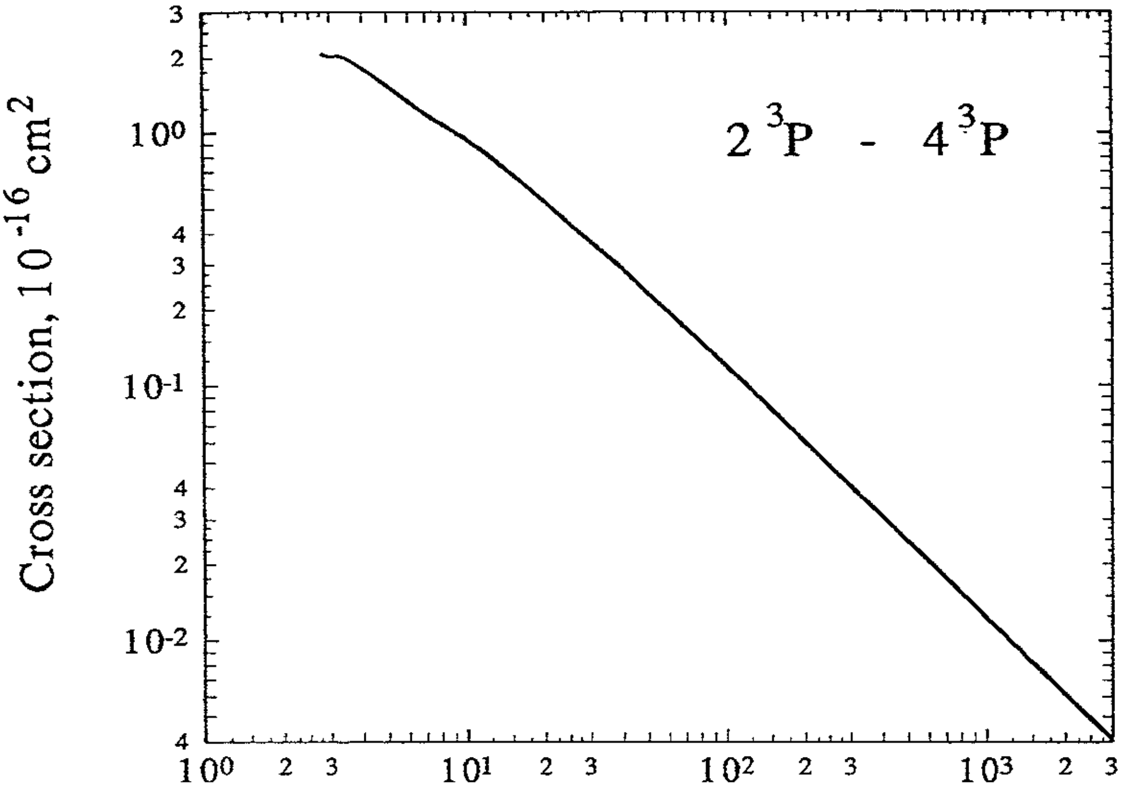

Fig.13 Electron energy, eV

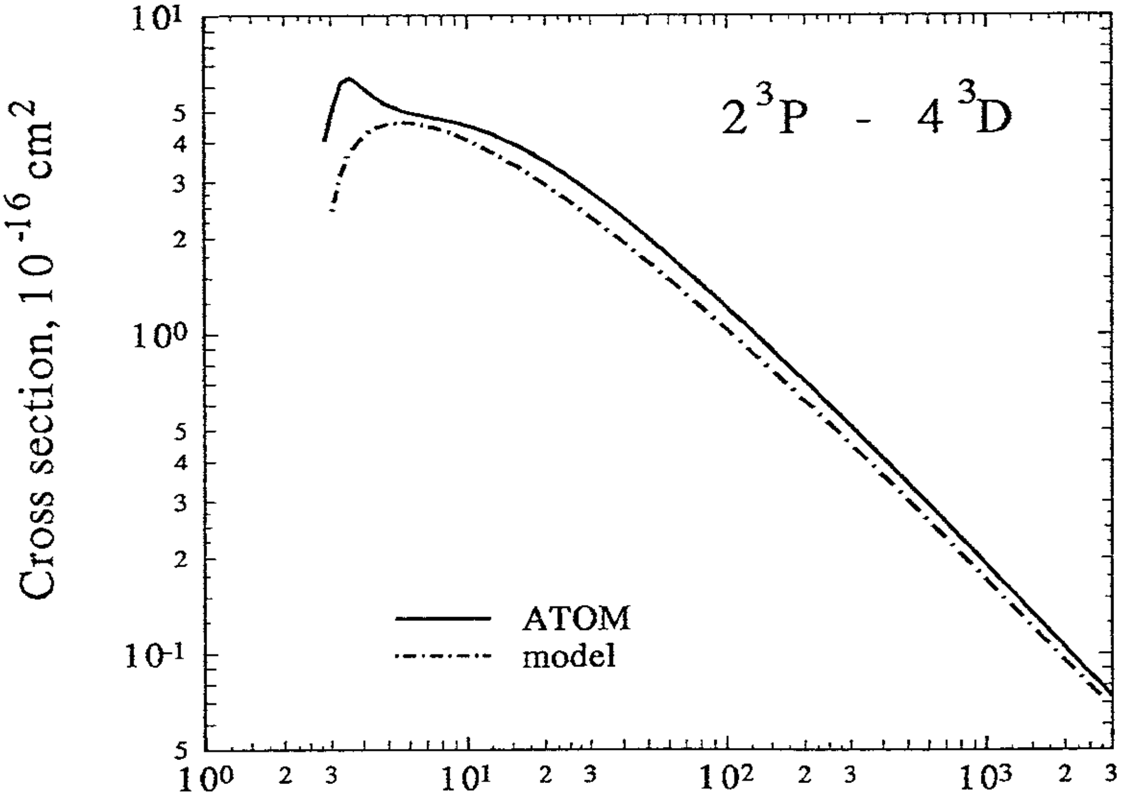

Fig.14 Electron energy, eV

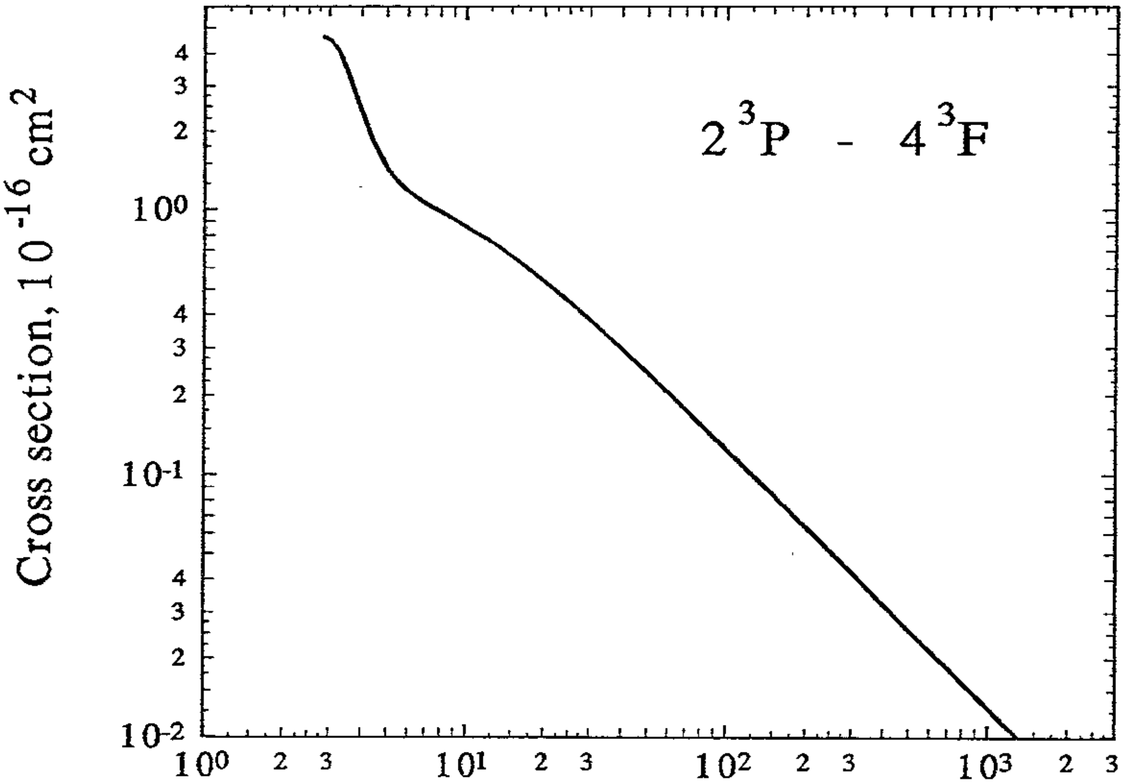

Fig.15 Electron energy, eV

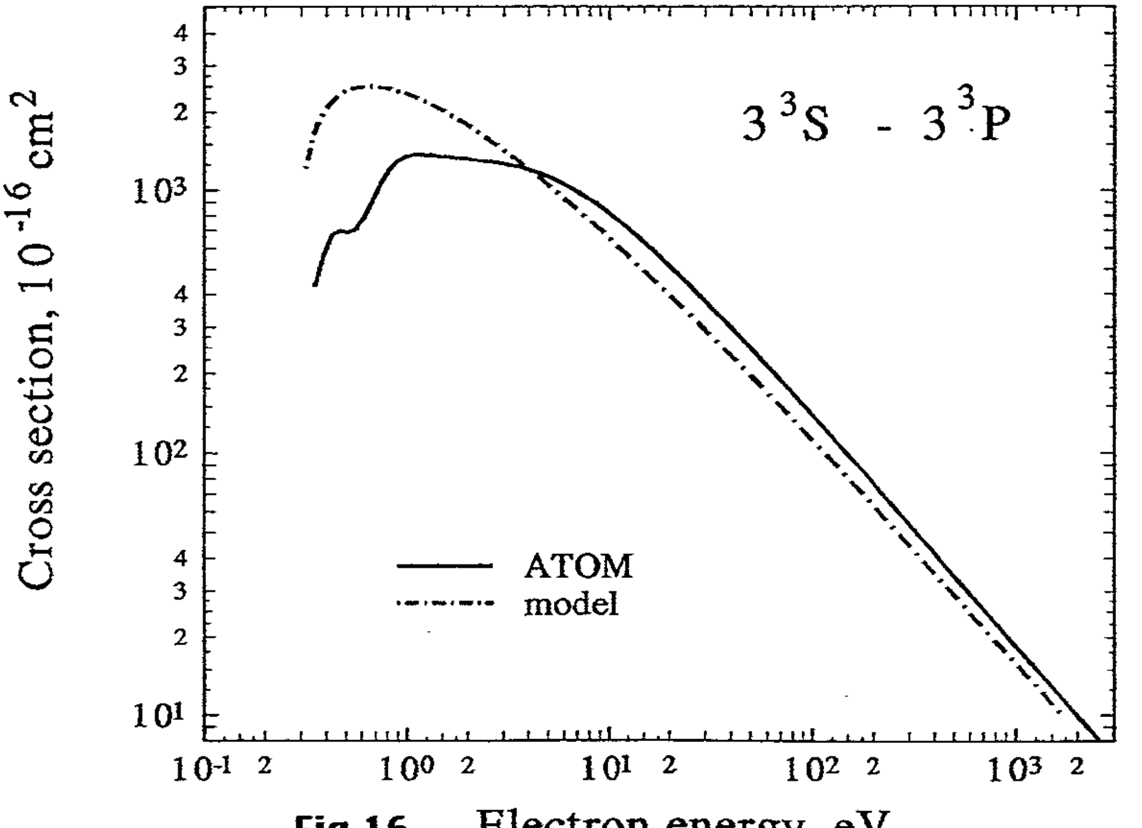

Fig.16 Electron energy, eV

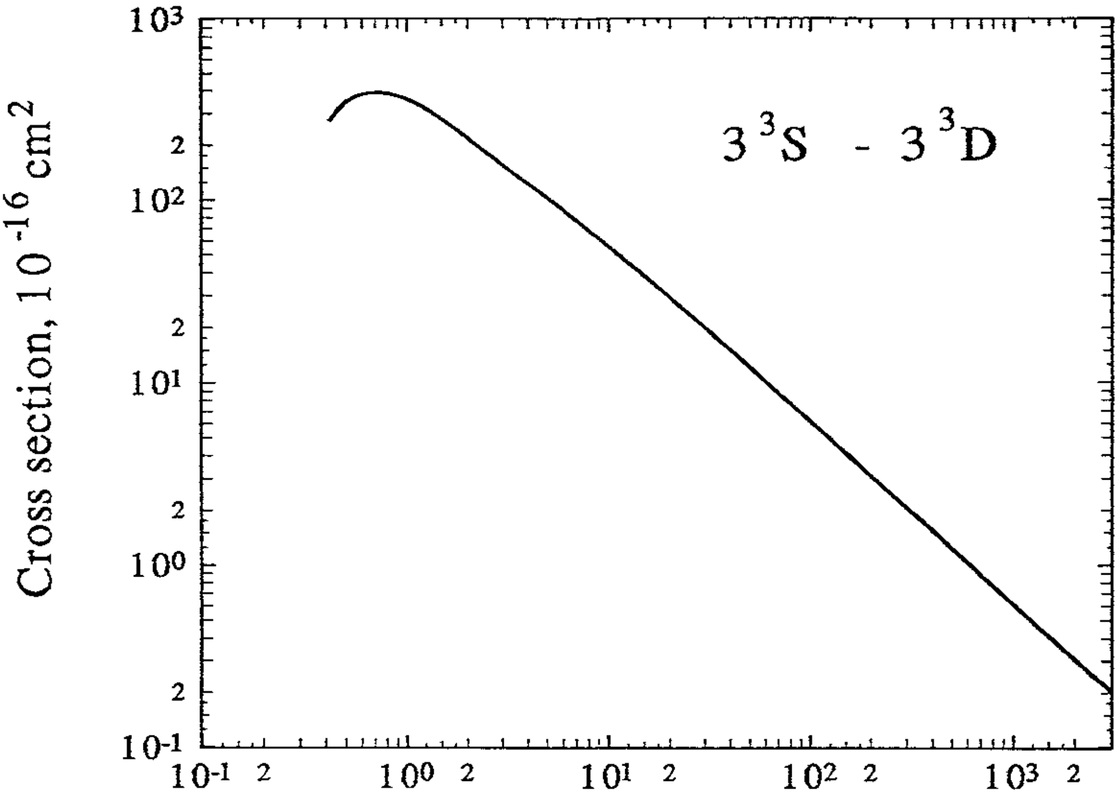

Fig.17 Electron energy, eV

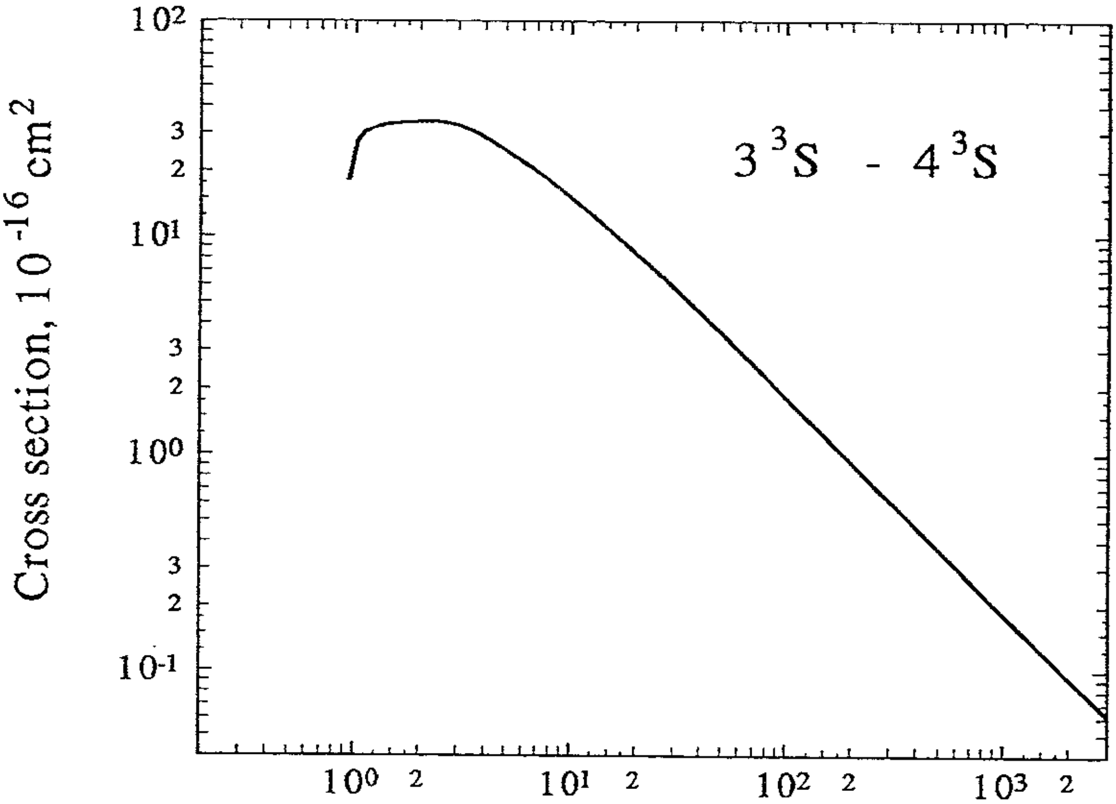

Fig.18 Electron energy, eV

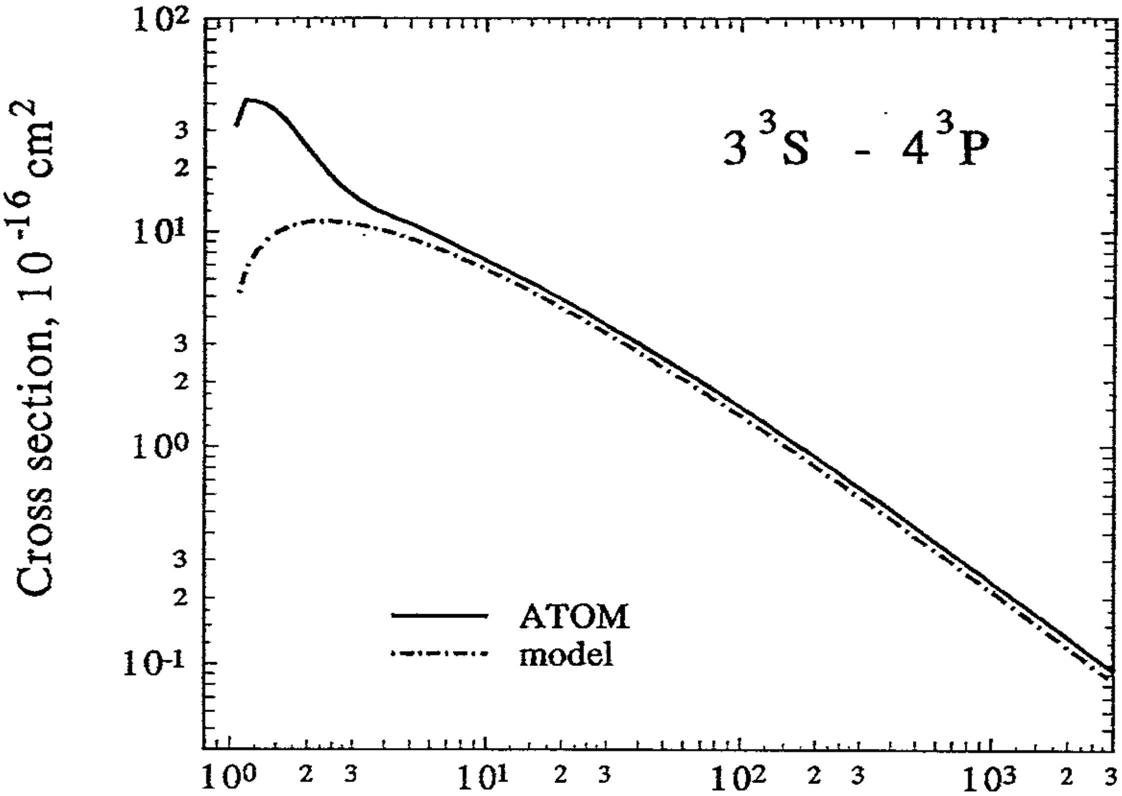

Fig.19 Electron energy, eV

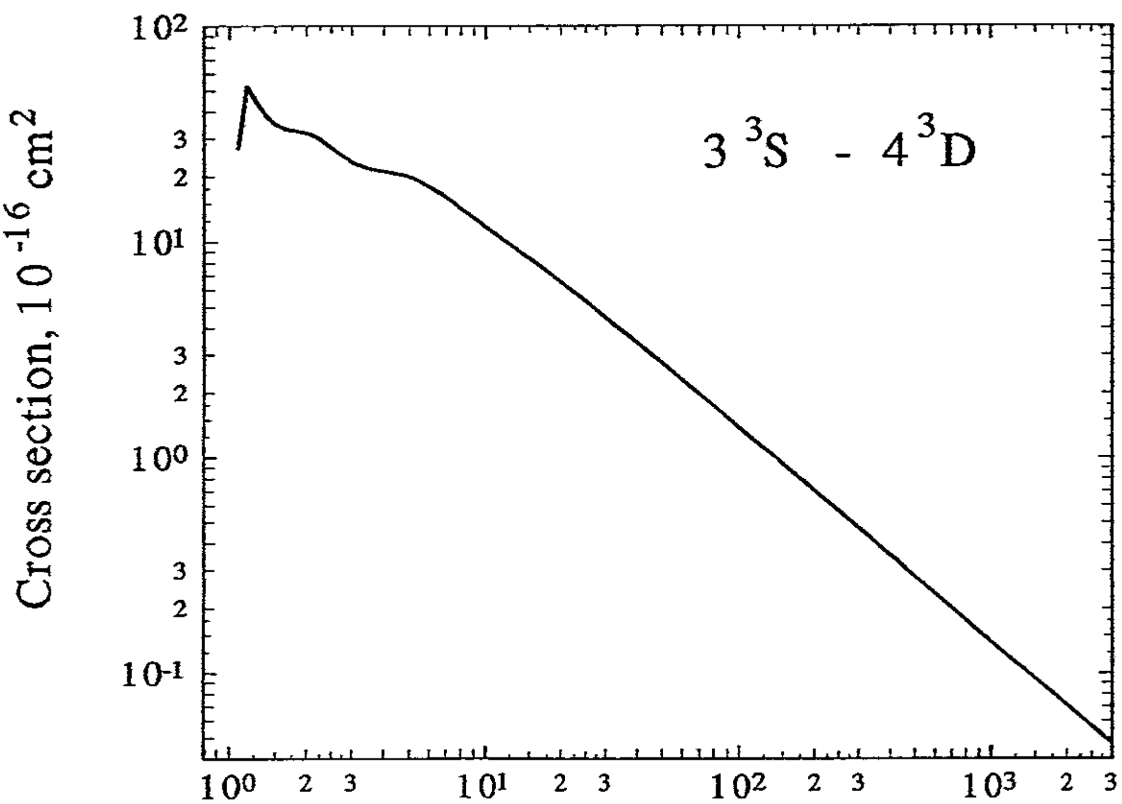

Fig.20 Electron energy, eV

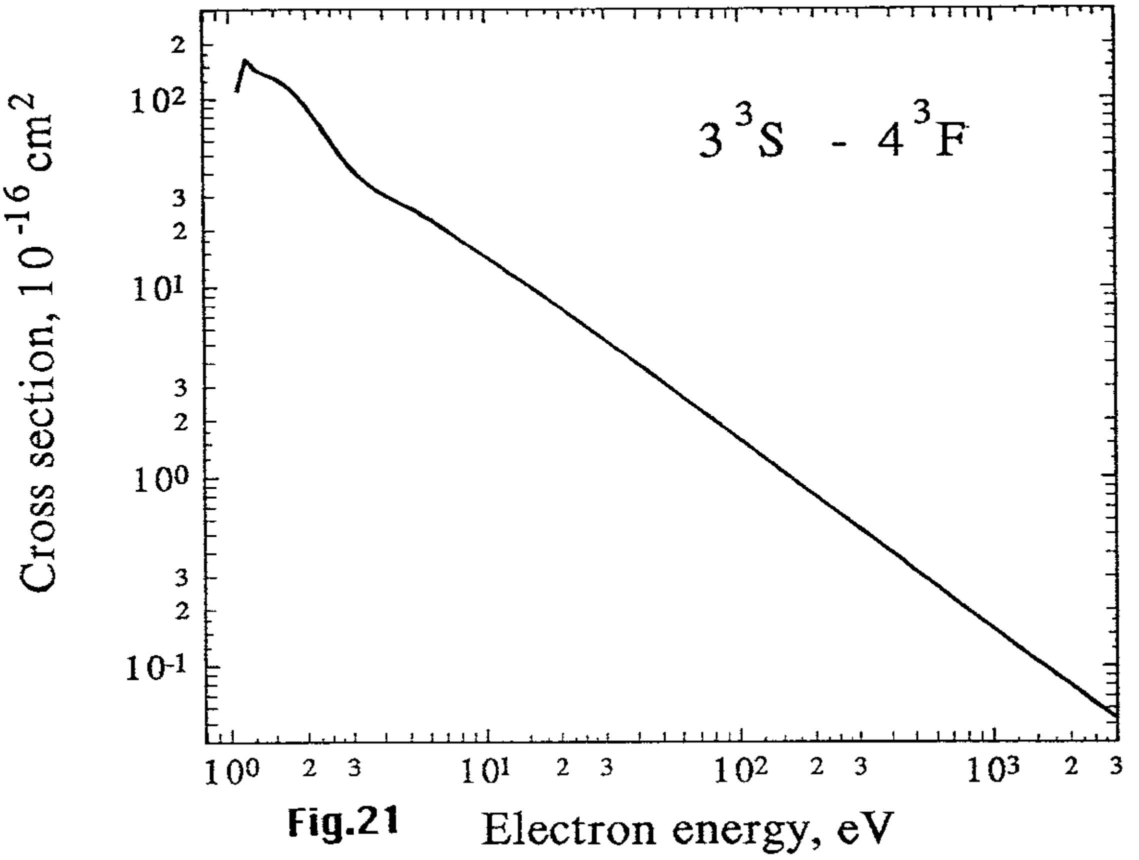

Cross section, 10^{-16} cm^2
$3\,^3S$ - $4\,^3F$
Electron energy, eV

Fig.21

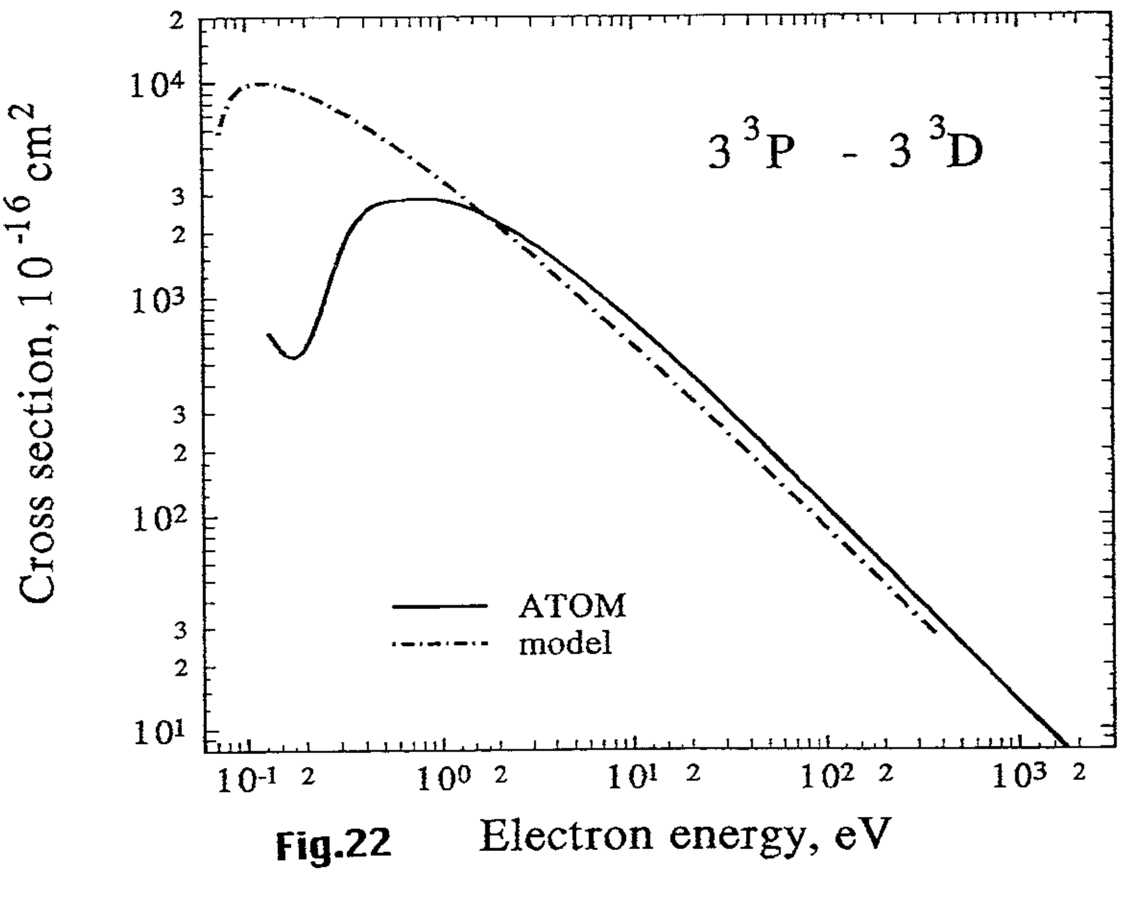

Cross section, 10^{-16} cm^2
$3\,^3P$ - $3\,^3D$
ATOM
model
Electron energy, eV

Fig.22

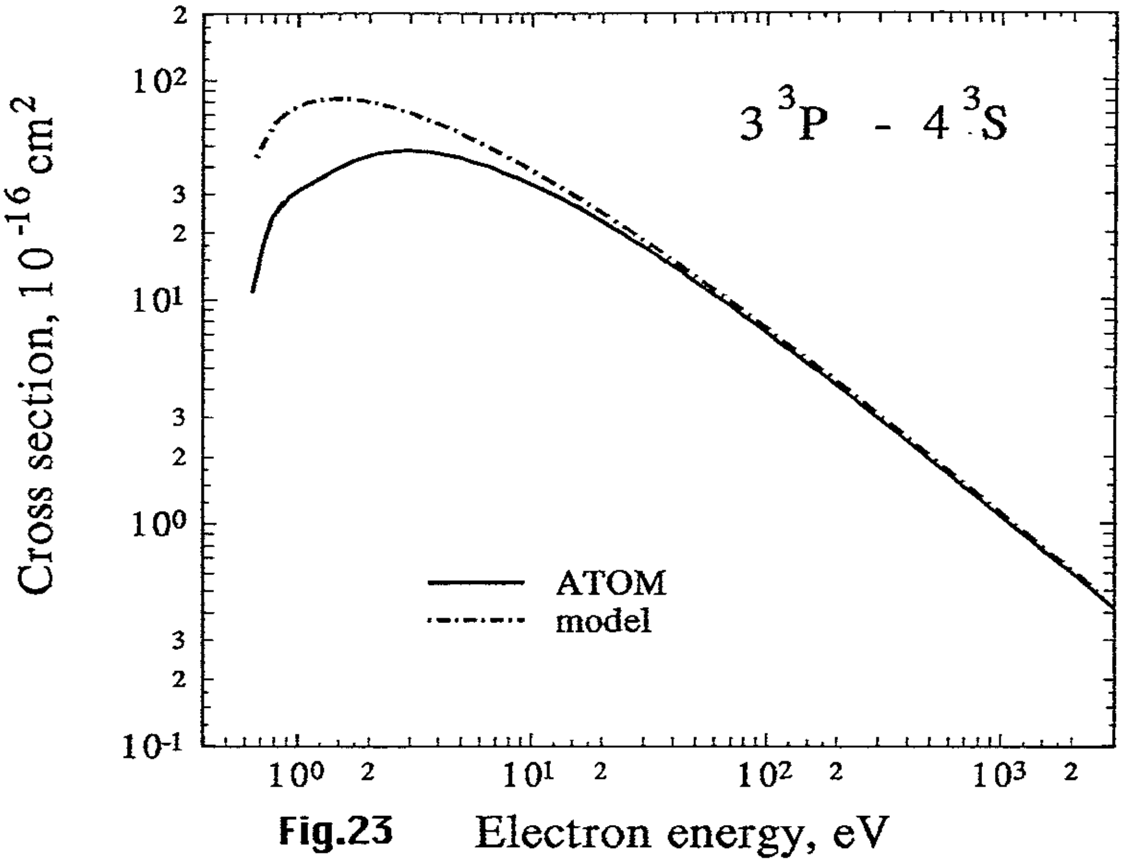

Cross section, 10^-16 cm^2
$3\,^3P - 4\,^3S$
ATOM
model
Electron energy, eV

Fig.23

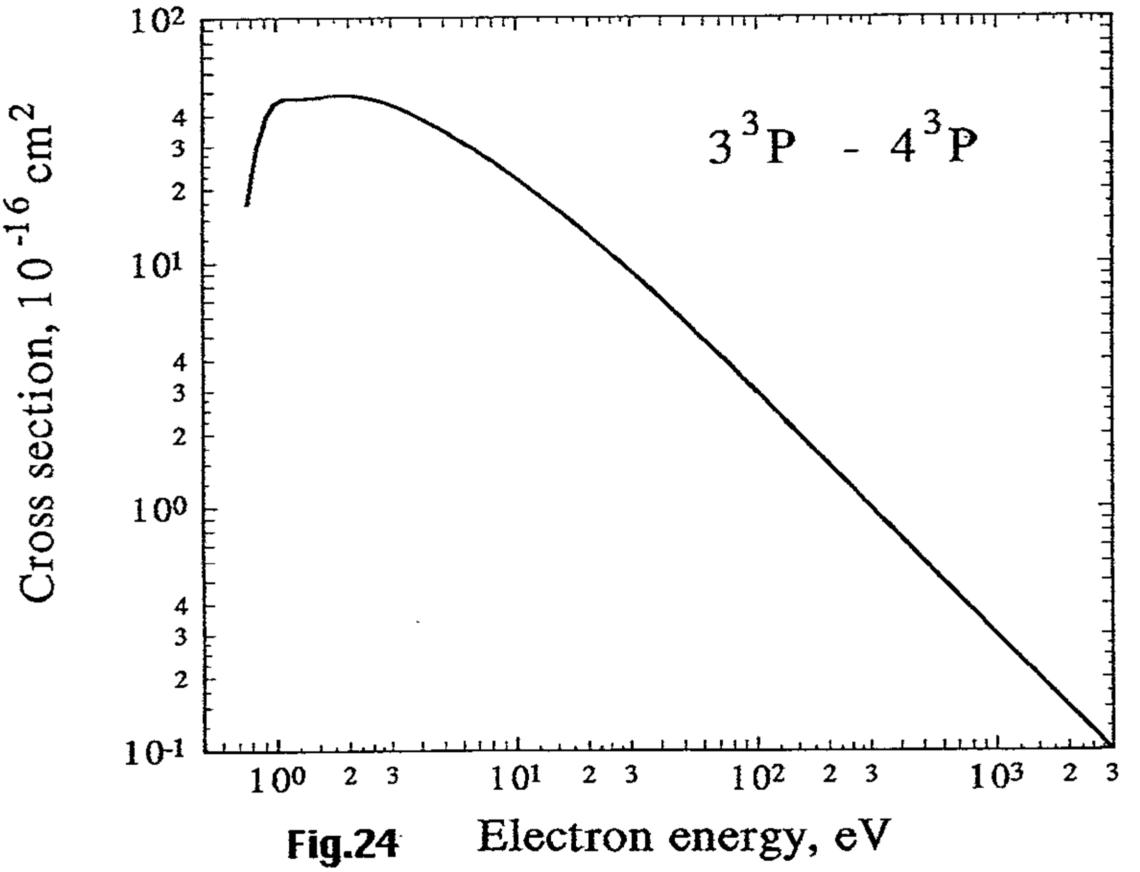

Cross section, 10^-16 cm^2
$3\,^3P - 4\,^3P$
Electron energy, eV

Fig.24

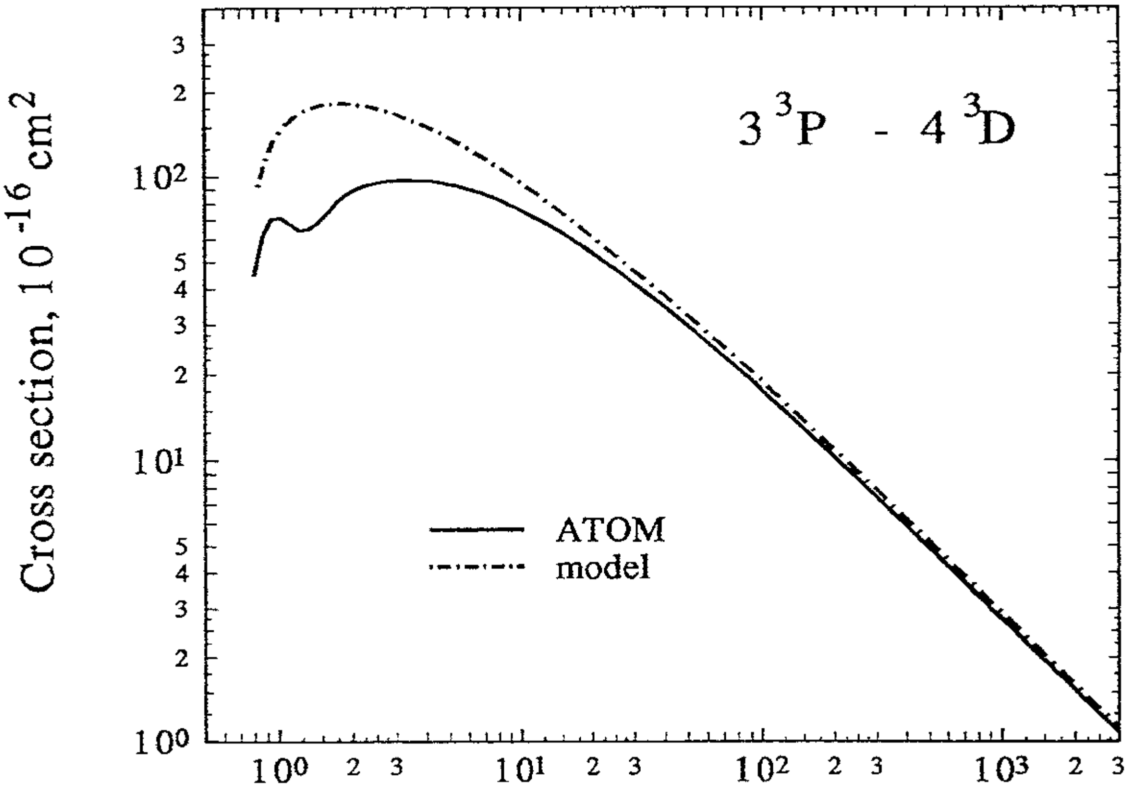

Fig.25 Electron energy, eV

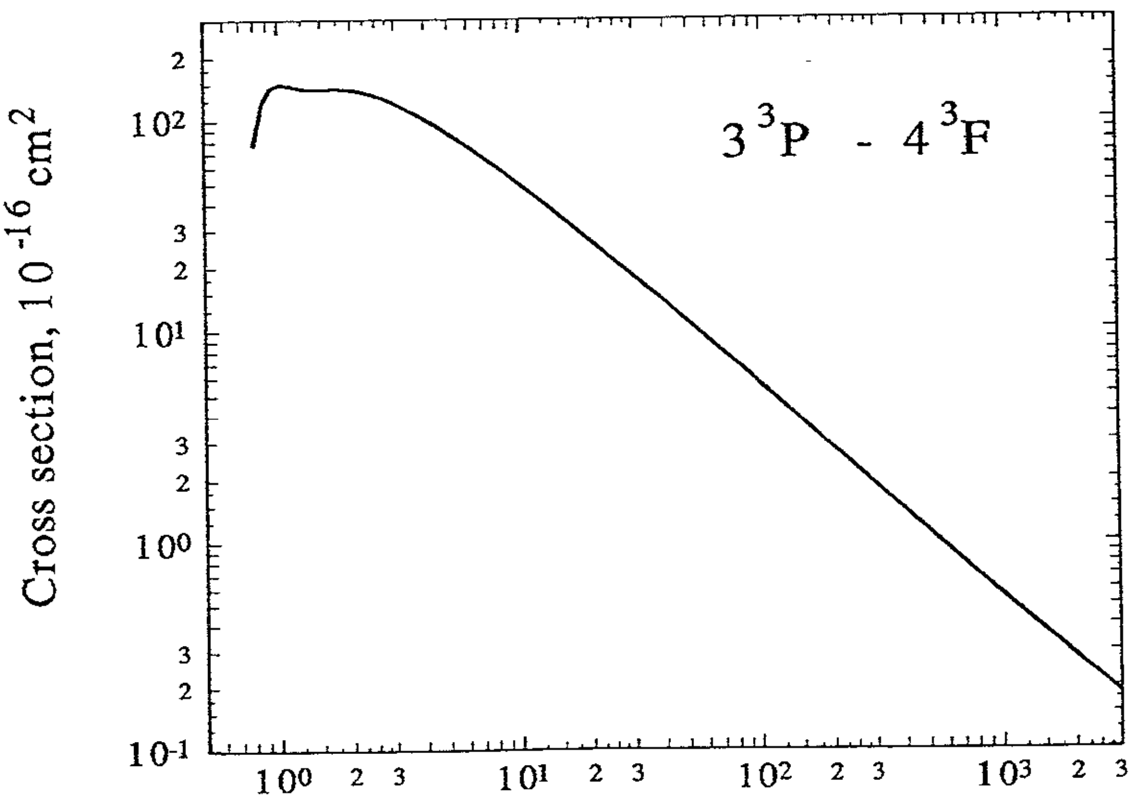

Fig.26 Electron energy, eV

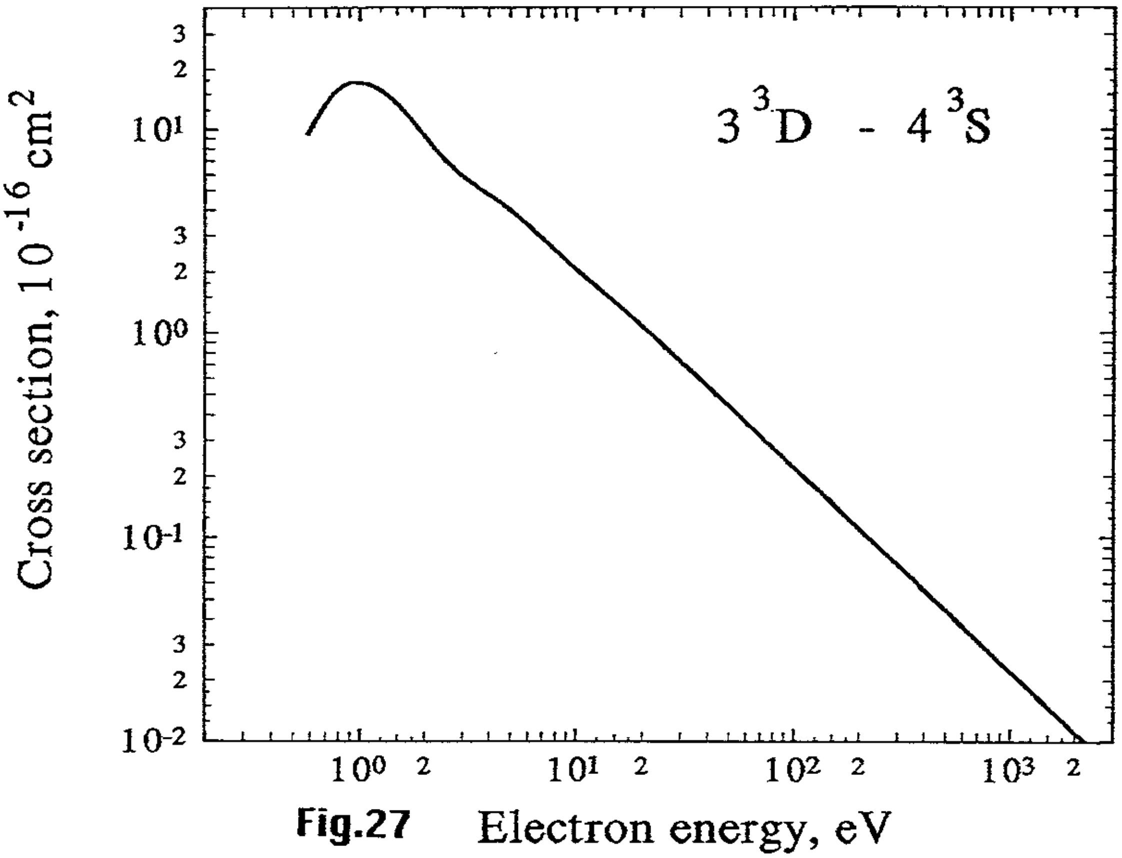

Cross section, 10 -16 cm2
3 3D - 4 3S
10-2
100
101
102
103
Electron energy, eV

Fig.27

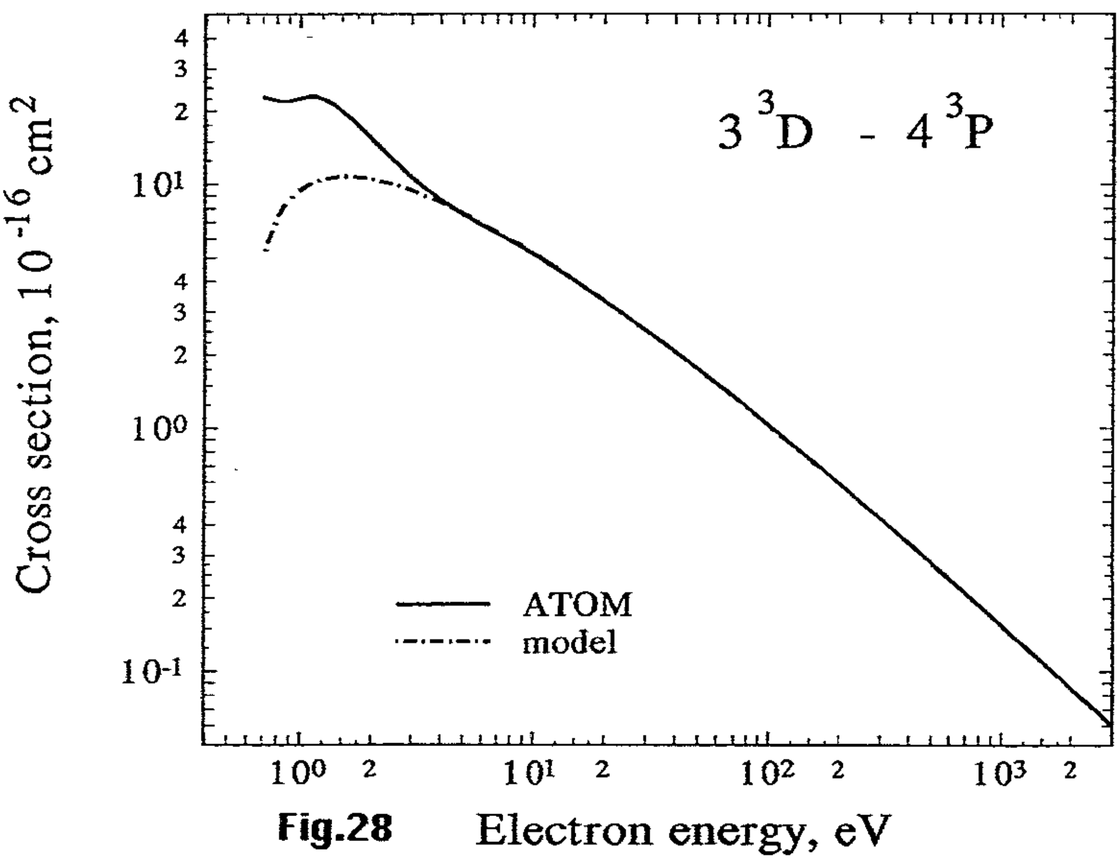

Cross section, 10 -16 cm2
3 3D - 4 3P
ATOM
model
10-1
100
101
102
103
Electron energy, eV

Fig.28

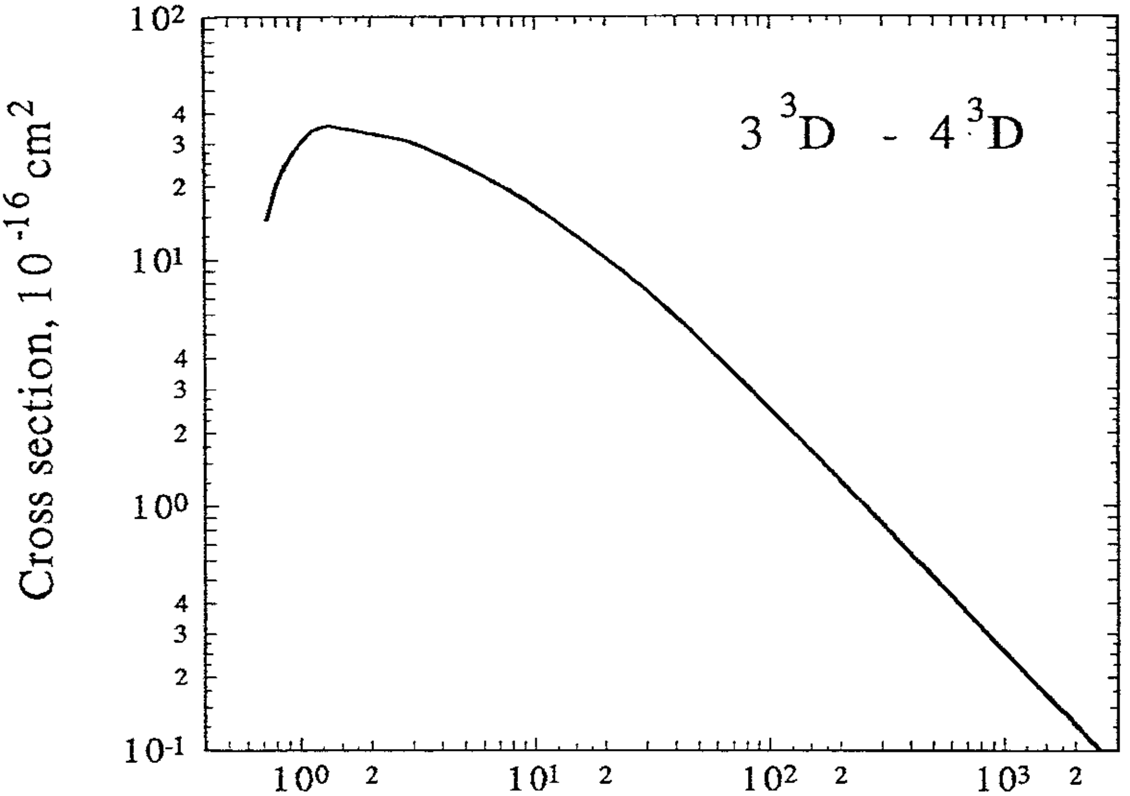
3 ³D - 4 ³D
Cross section, 10⁻¹⁶cm²
Electron energy, eV

Fig.29

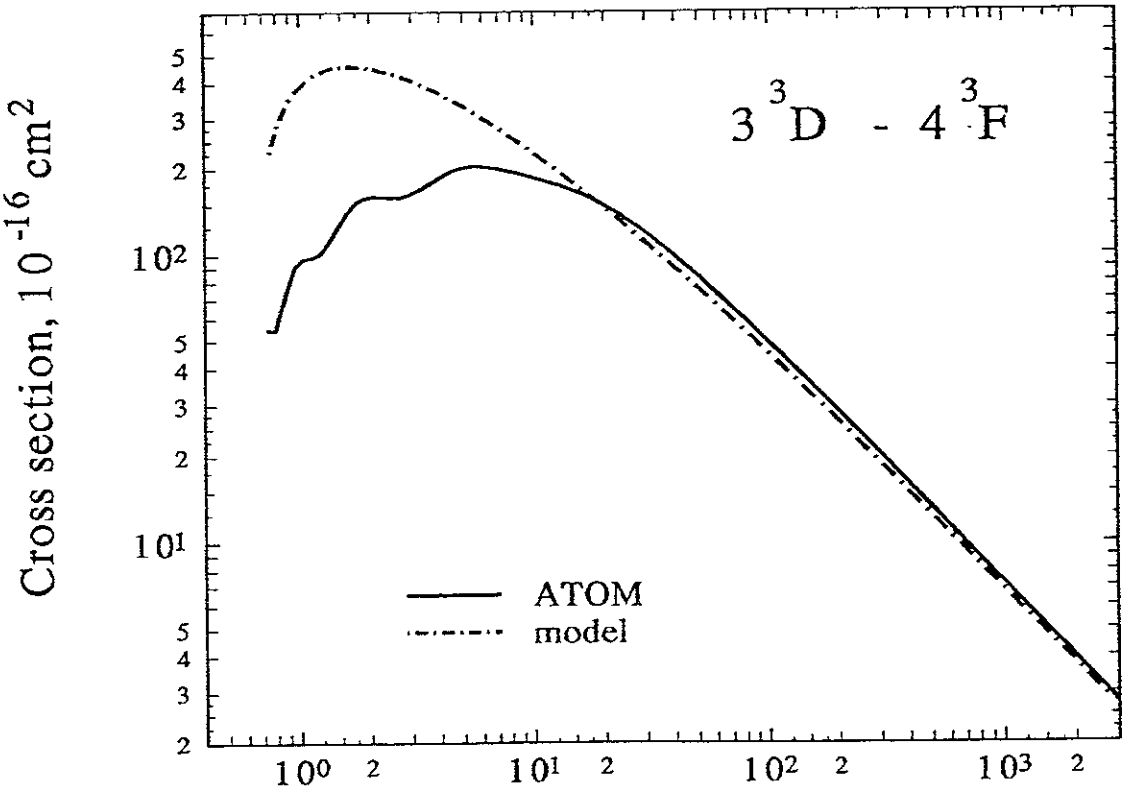
3 ³D - 4 ³F
ATOM
model
Cross section, 10⁻¹⁶cm²
Electron energy, eV

Fig.30

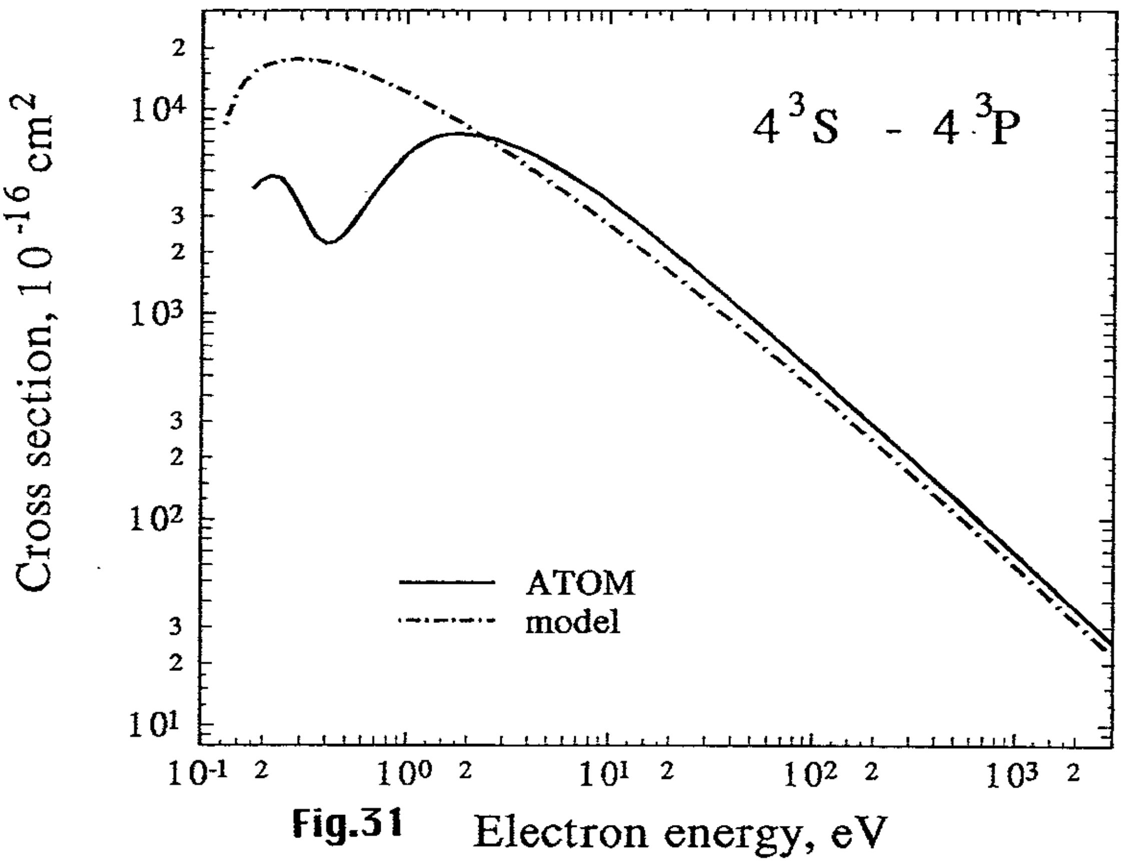

Cross section, 10 -16 cm2
2
104
3
2
103
3
2
102
3
2
101
10-1 2 100 2 101 2 102 2 103 2
4 3S - 4 3P
ATOM
model
Electron energy, eV

Fig.31

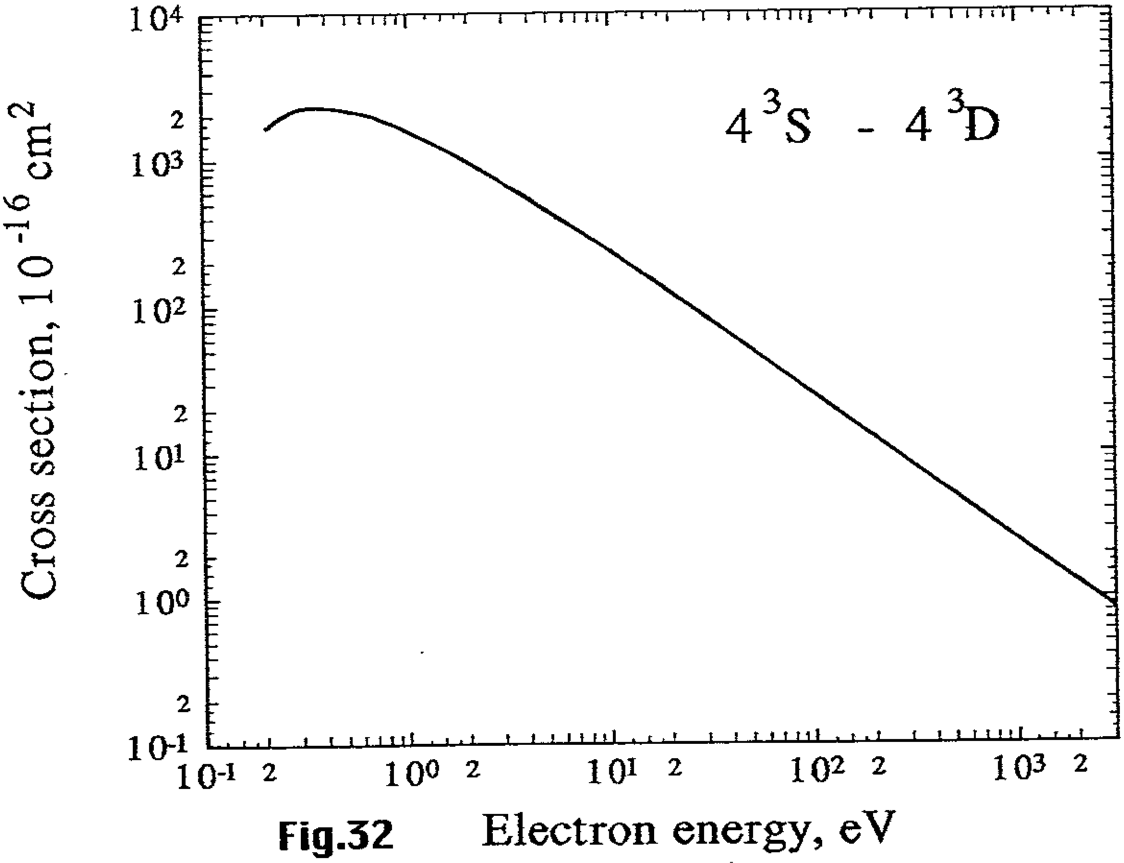

Cross section, 10 -16 cm2
104
2
103
2
102
2
101
2
100
2
10-1
10-1 2 100 2 101 2 102 2 103 2
4 3S - 4 3D
Electron energy, eV

Fig.32

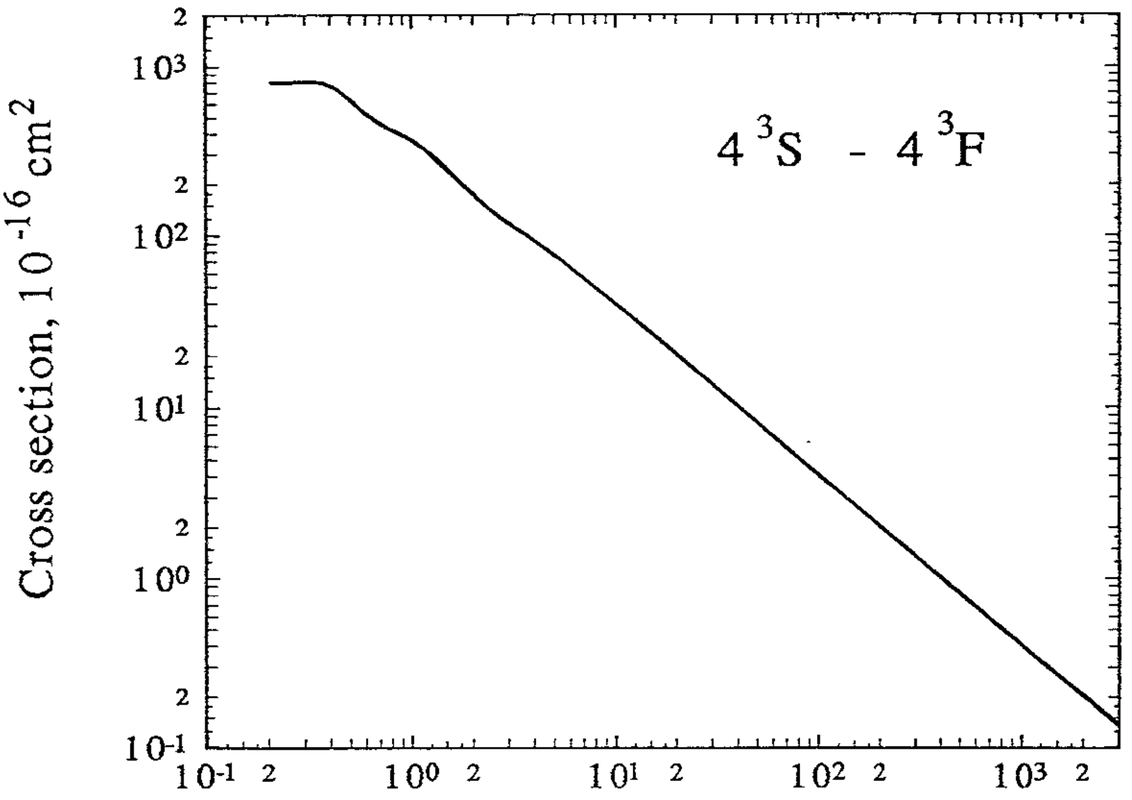

4 ³S - 4 ³F
Cross section, 10⁻¹⁶ cm²
Electron energy, eV

Fig.33

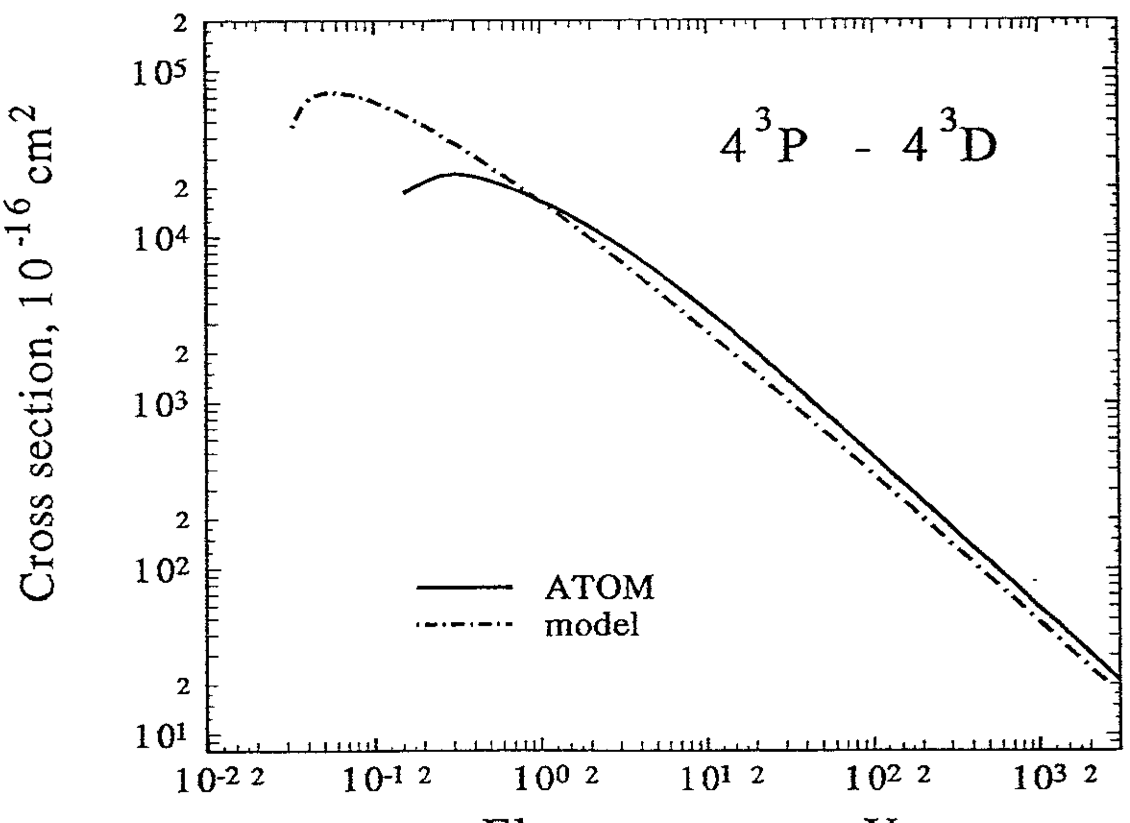

4 ³P - 4 ³D
ATOM
model
Cross section, 10⁻¹⁶ cm²
Electron energy, eV

Fig.34

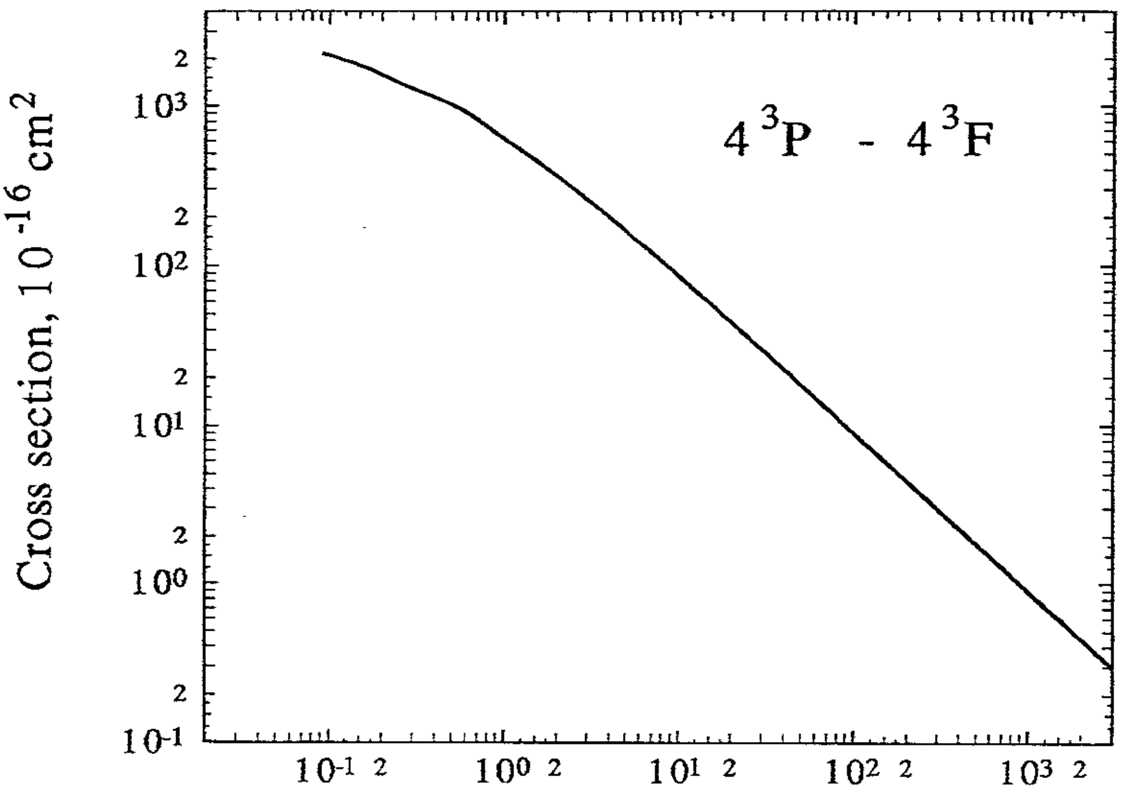

Cross section, 10^{-16} cm^2
$4\,^3P - 4\,^3F$
Electron energy, eV

Fig.35

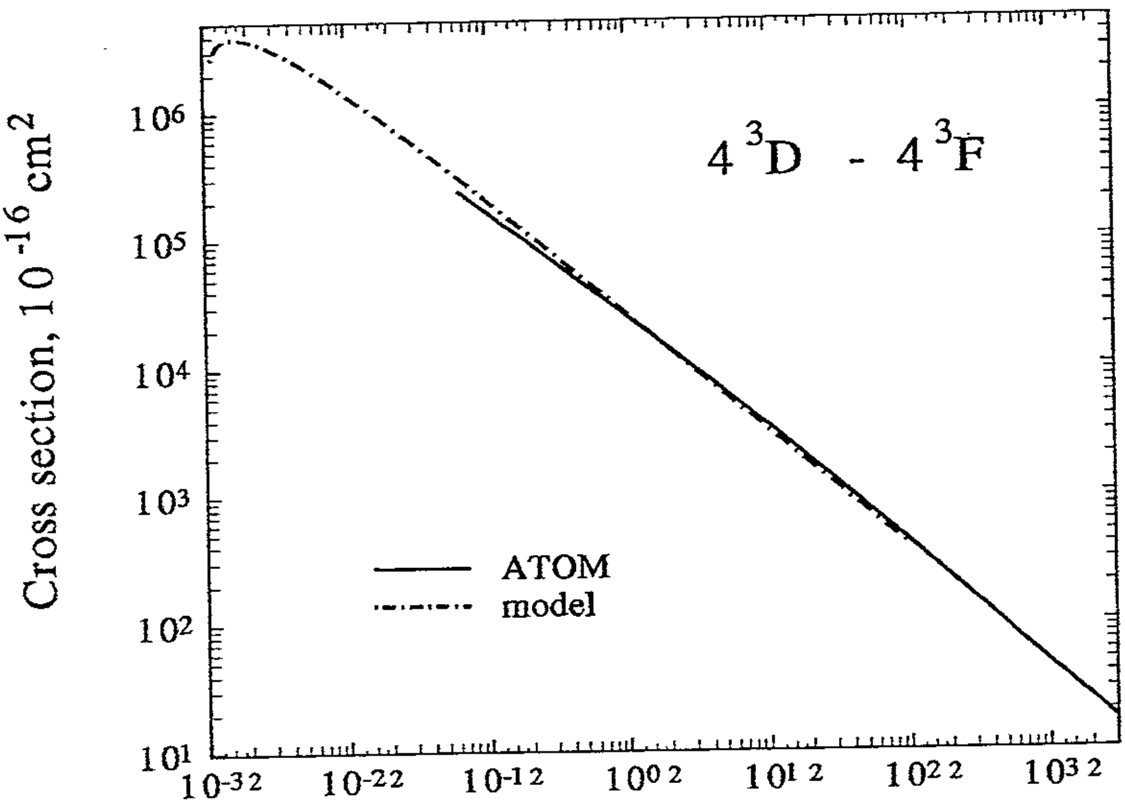

Cross section, 10^{-16} cm^2
$4\,^3D - 4\,^3F$
ATOM
model
Electron energy, eV

Fig.36

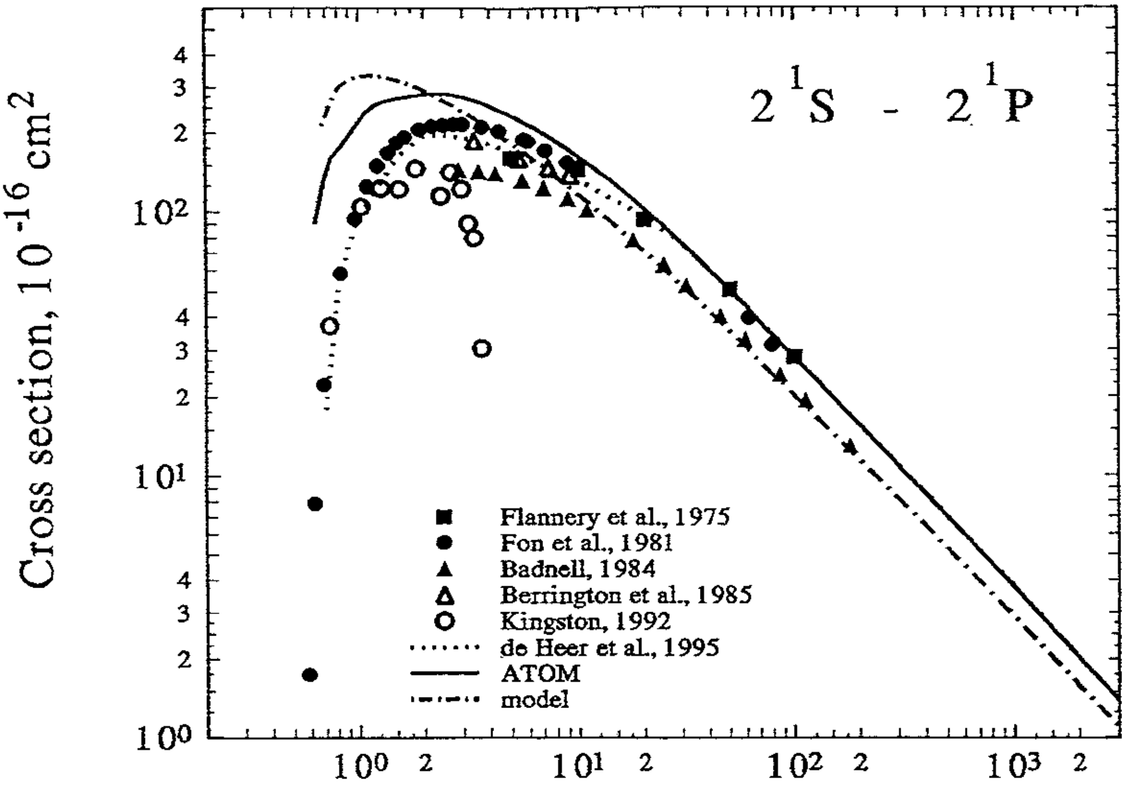

Cross section, 10^{-16} cm^2
$2\,^1S - 2\,^1P$
Flannery et al., 1975
Fon et al., 1981
Badnell, 1984
Berrington et al., 1985
Kingston, 1992
de Heer et al., 1995
ATOM
model
Electron energy, eV

Fig.37

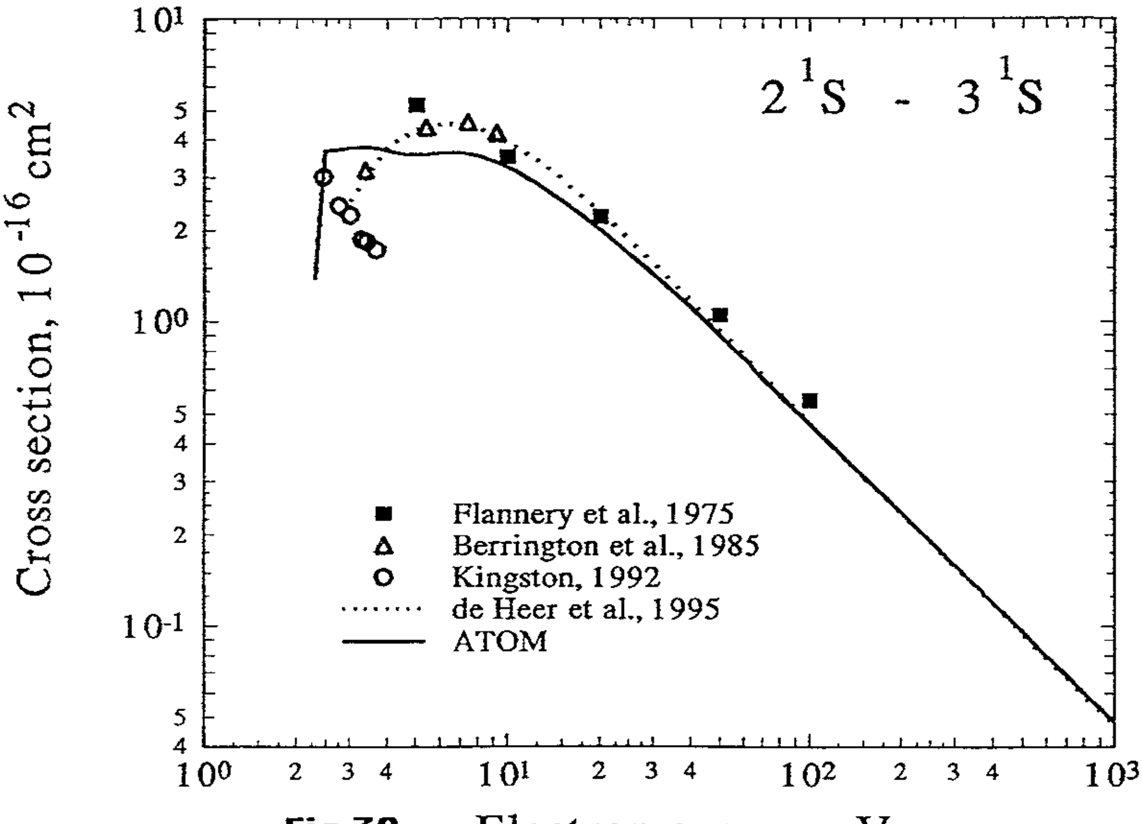

Cross section, 10^{-16} cm^2
$2\,^1S - 3\,^1S$
Flannery et al., 1975
Berrington et al., 1985
Kingston, 1992
de Heer et al., 1995
ATOM
Electron energy, eV

Fig.38

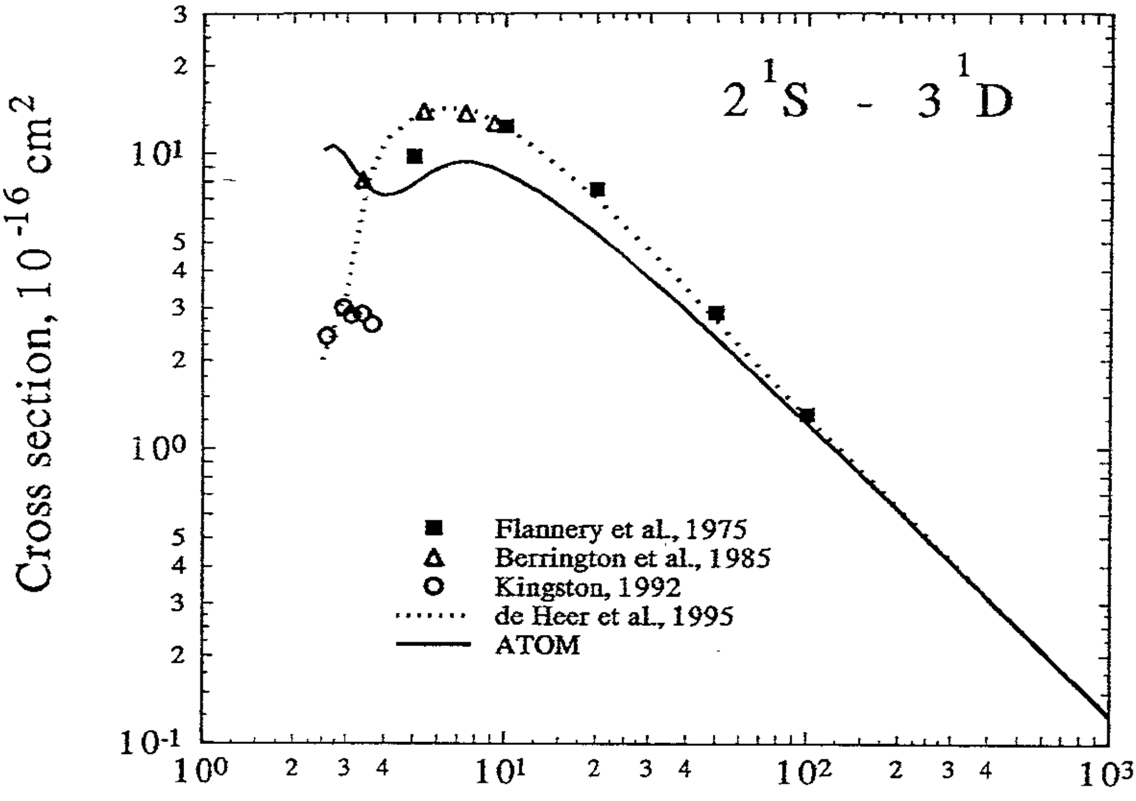

Fig.39 Electron energy, eV

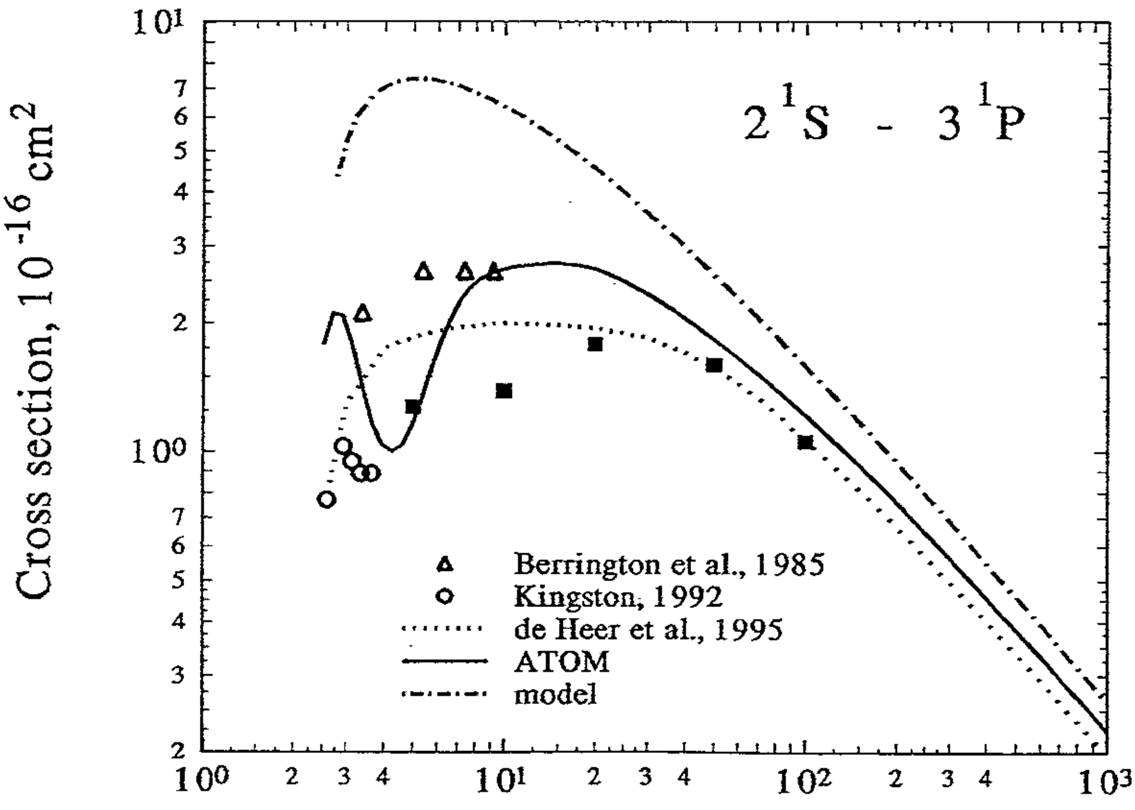

Fig.40 Electron energy, eV

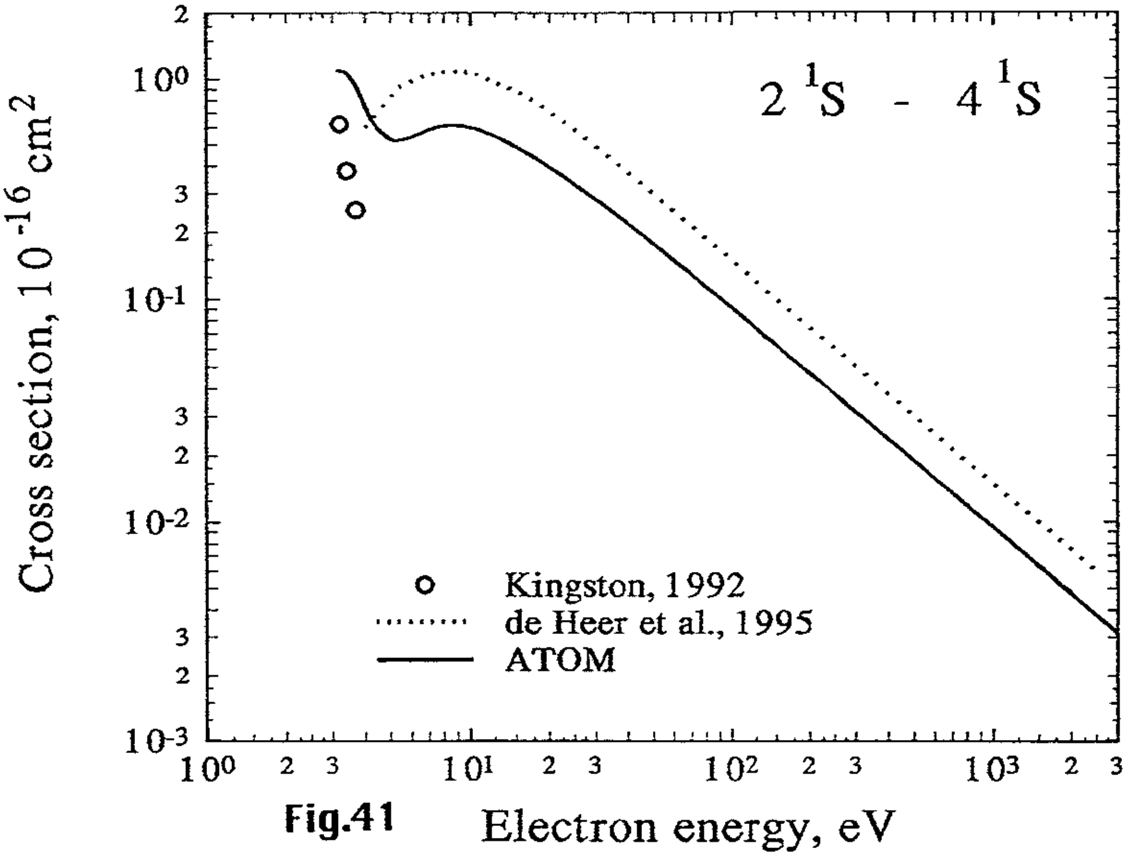
2 ¹S - 4 ¹S
Kingston, 1992
de Heer et al., 1995
ATOM
Cross section, 10⁻¹⁶ cm²
Electron energy, eV

Fig.41

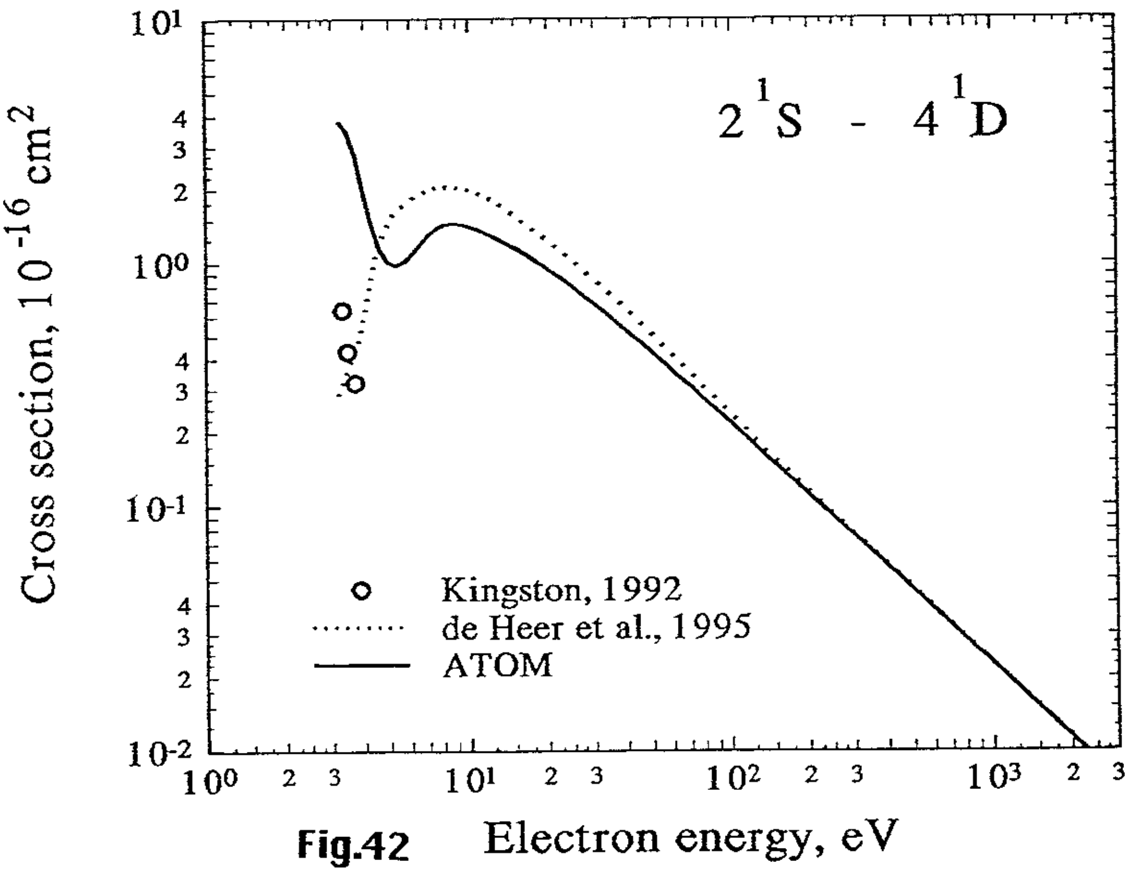
2 ¹S - 4 ¹D
Kingston, 1992
de Heer et al., 1995
ATOM
Cross section, 10⁻¹⁶ cm²
Electron energy, eV

Fig.42

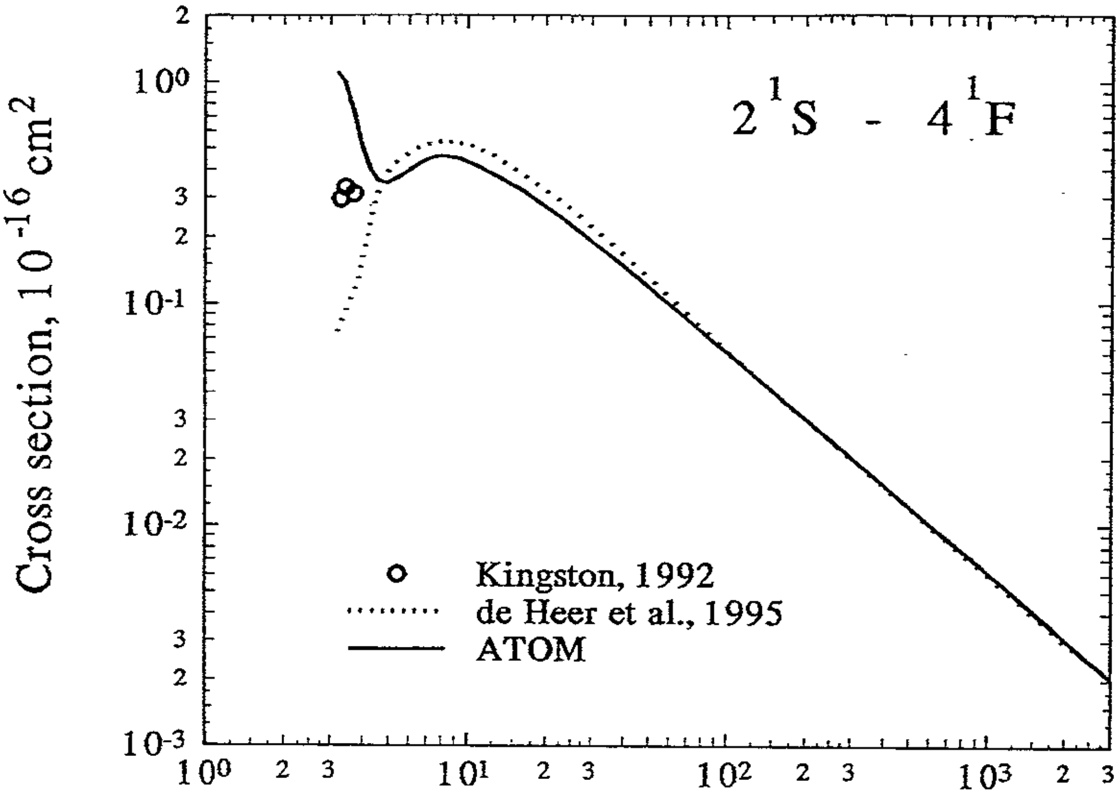

Fig.43 Electron energy, eV

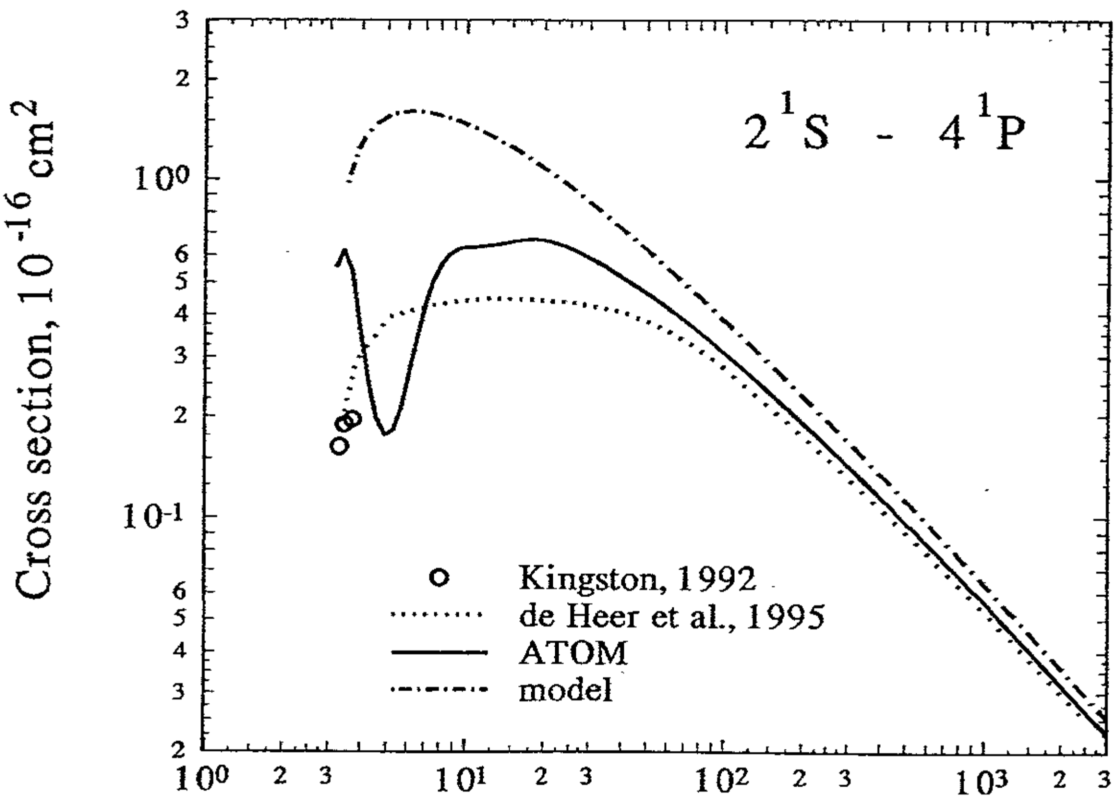

Fig.44 Electron energy, eV

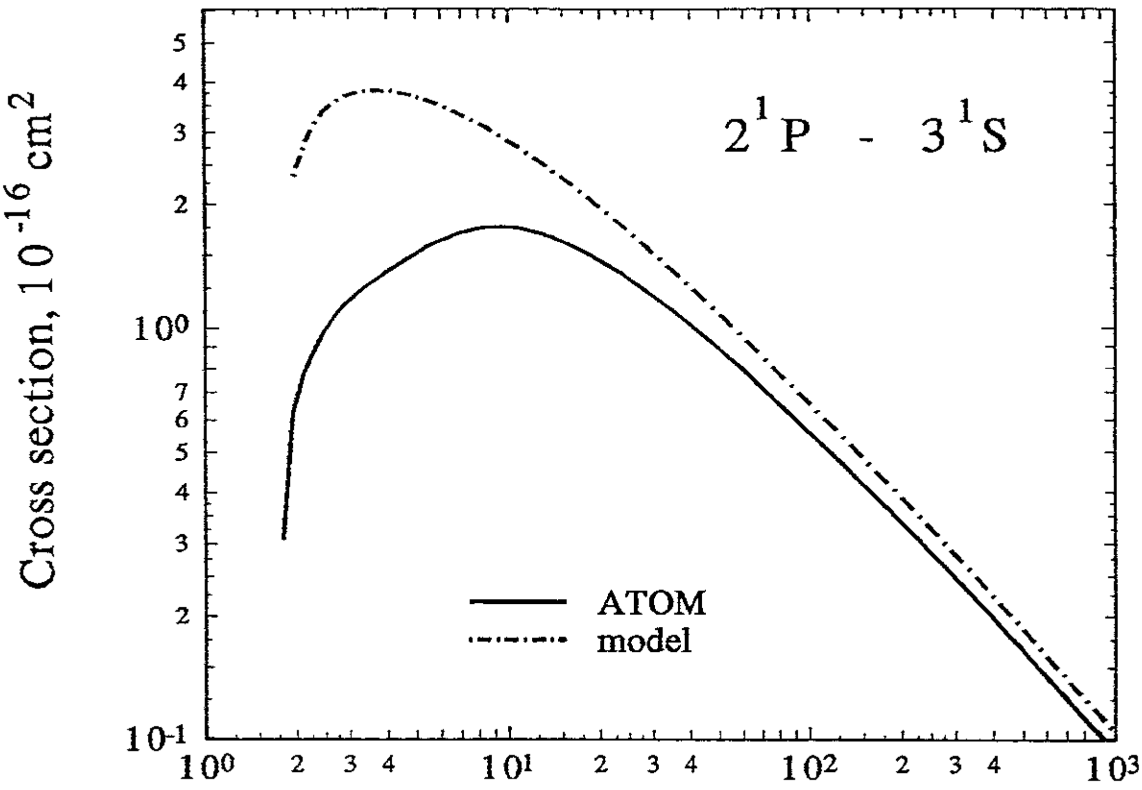

Fig.45 Electron energy, eV

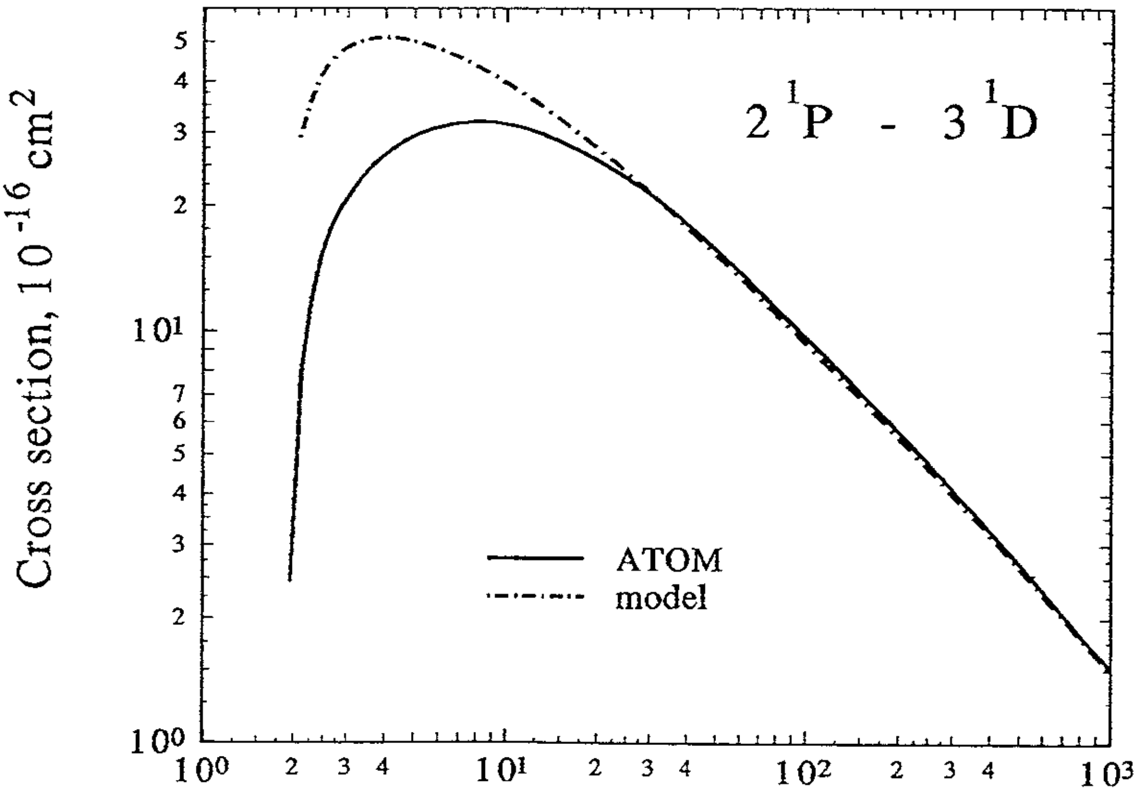

Fig.46 Electron energy, eV

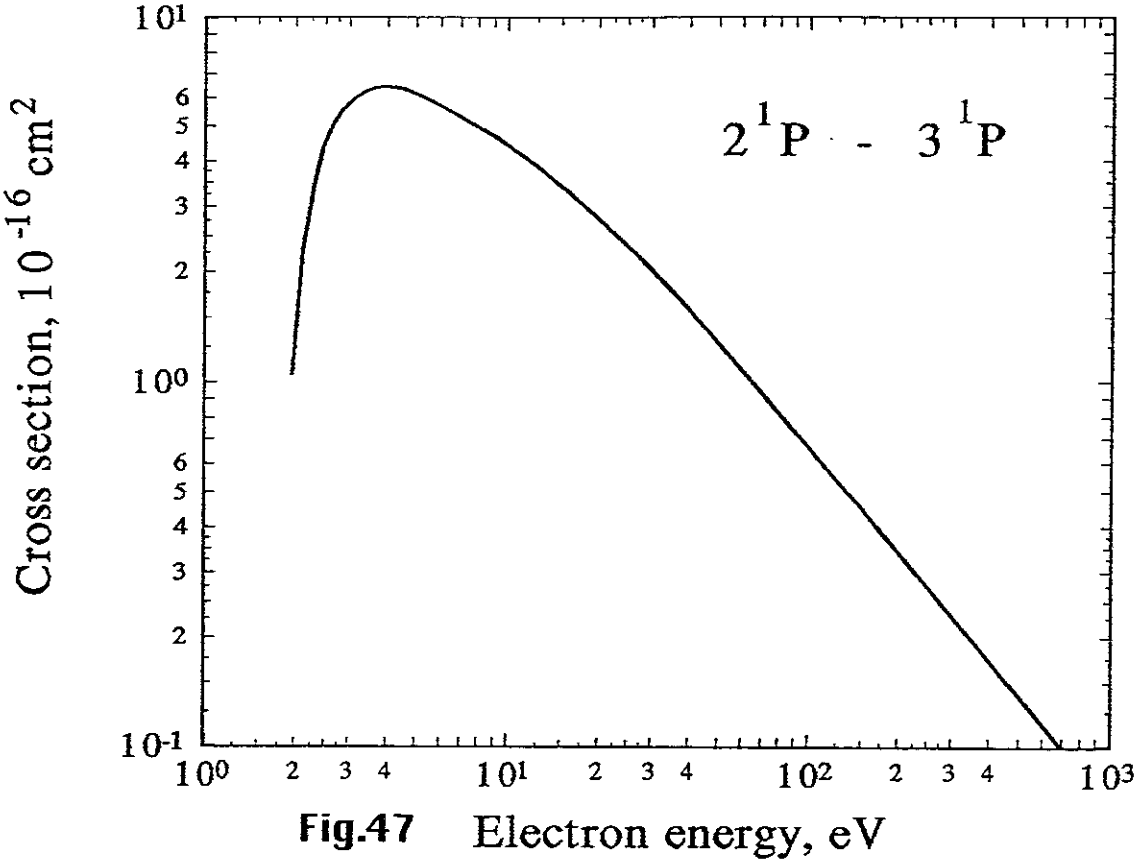

Cross section, 10 -16 cm2
2 1P - 3 1P
Electron energy, eV

Fig.47

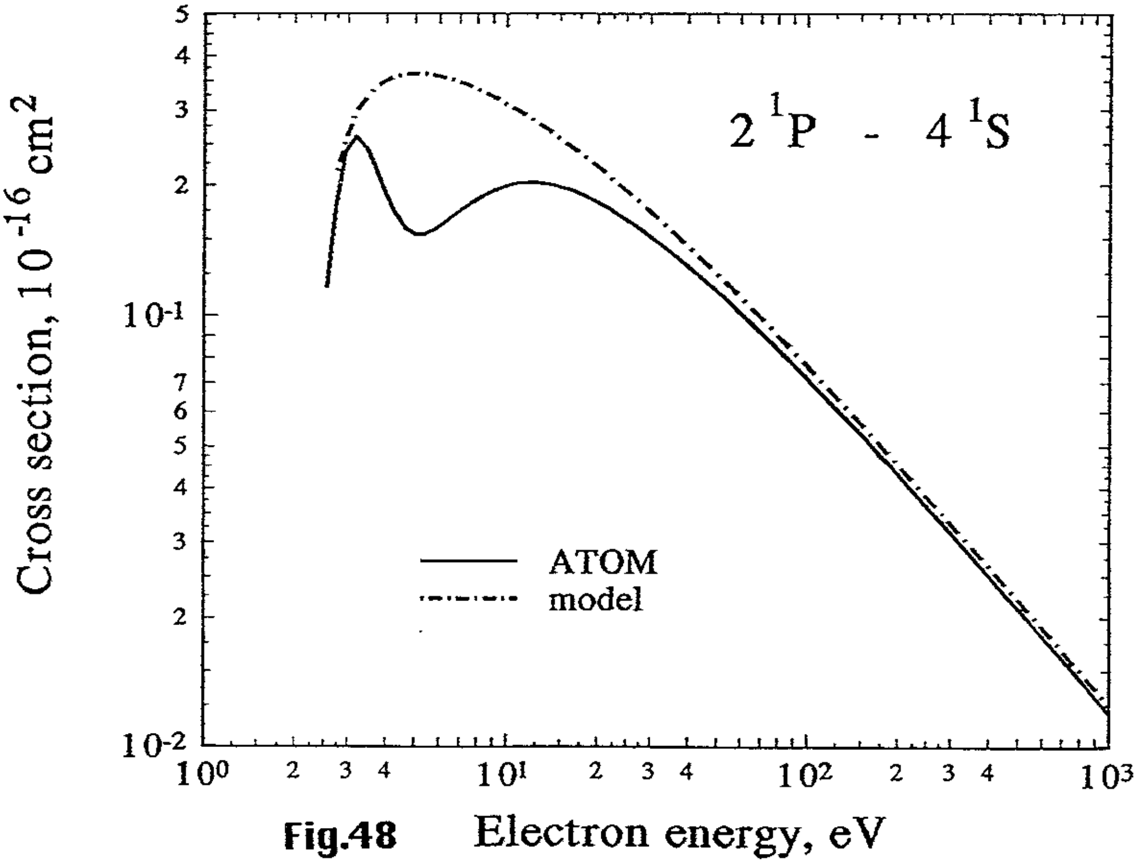

Cross section, 10 -16 cm2
2 1P - 4 1S
ATOM
model
Electron energy, eV

Fig.48

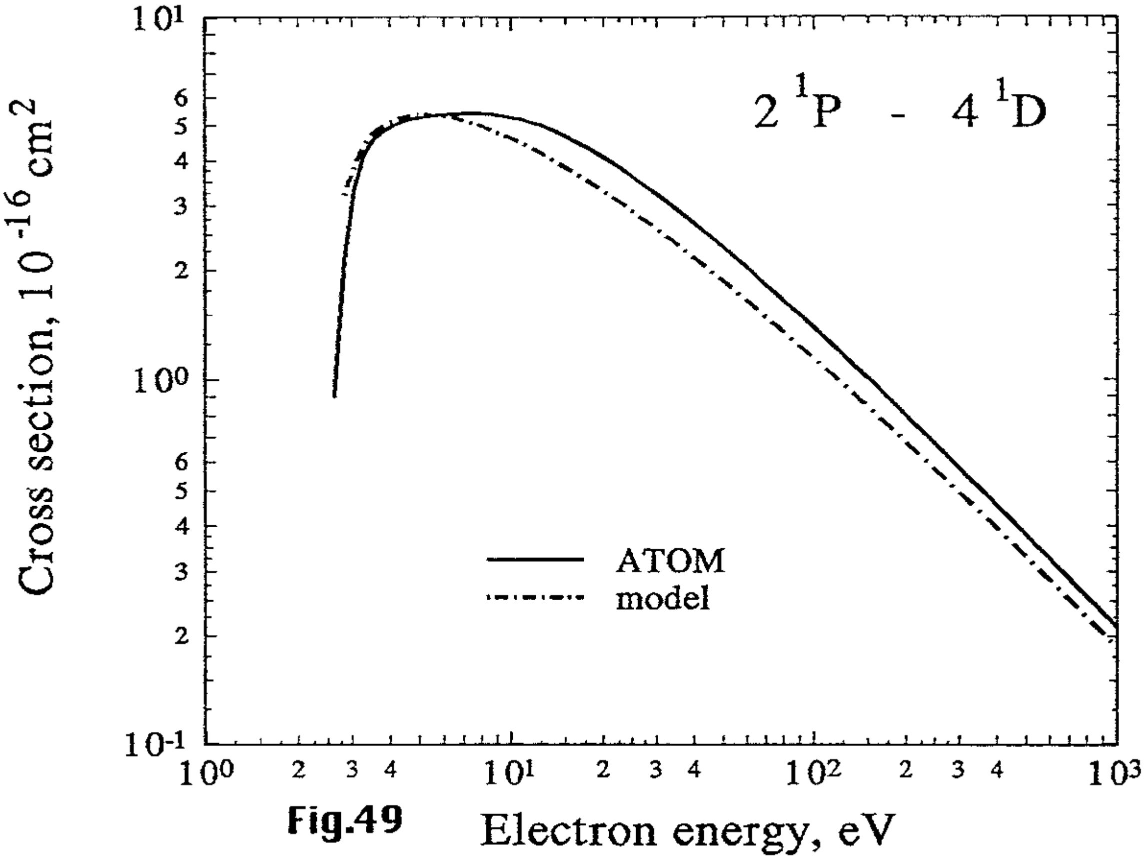

Cross section, 10^-16 cm^2
2 ¹P - 4 ¹D
ATOM
model
Electron energy, eV

Fig.49

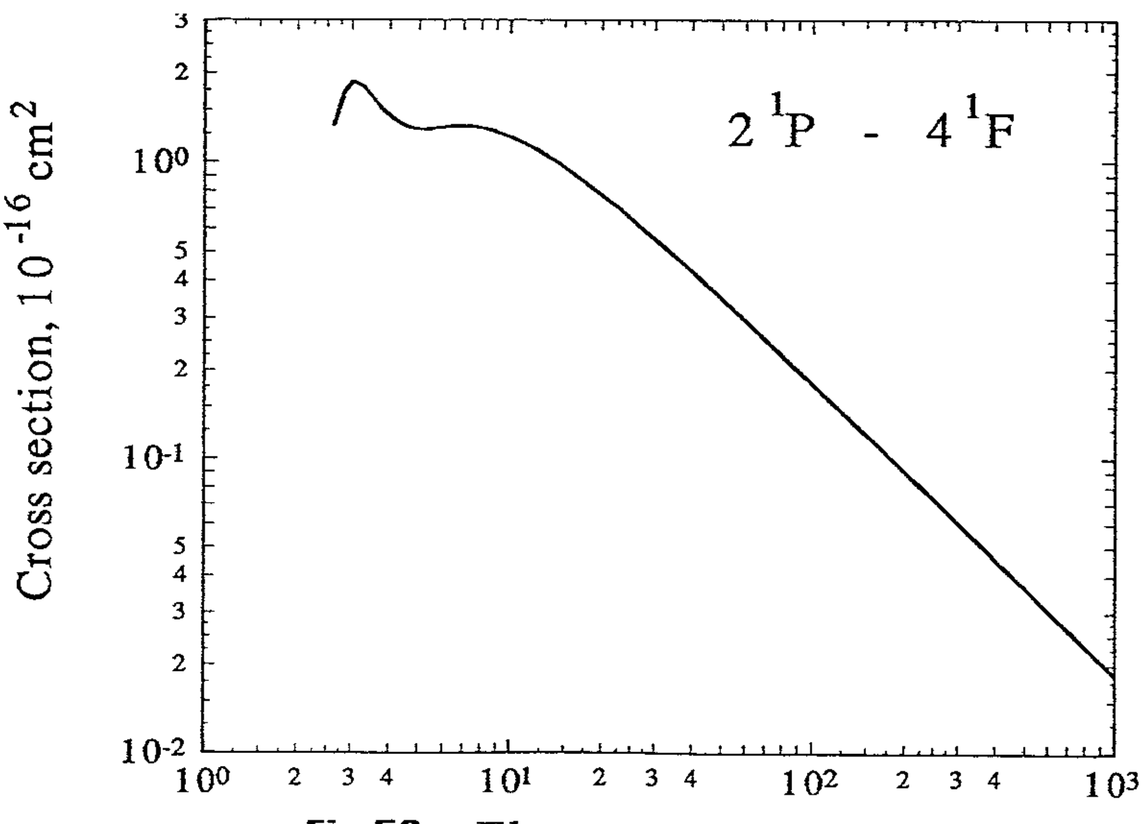

Cross section, 10^-16 cm^2
2 ¹P - 4 ¹F
Electron energy, eV

Fig.50

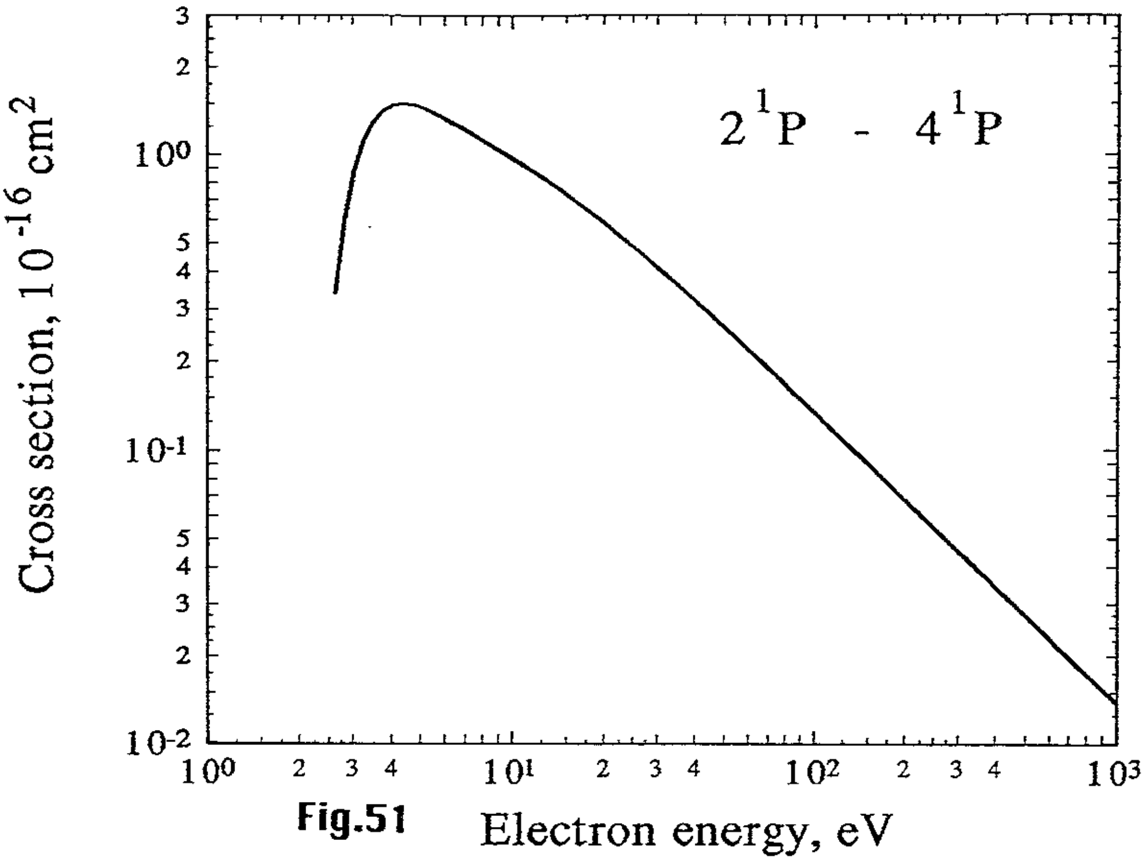

$2\,^1P$ - $4\,^1P$
Cross section, 10^{-16} cm^2
Electron energy, eV

Fig.51

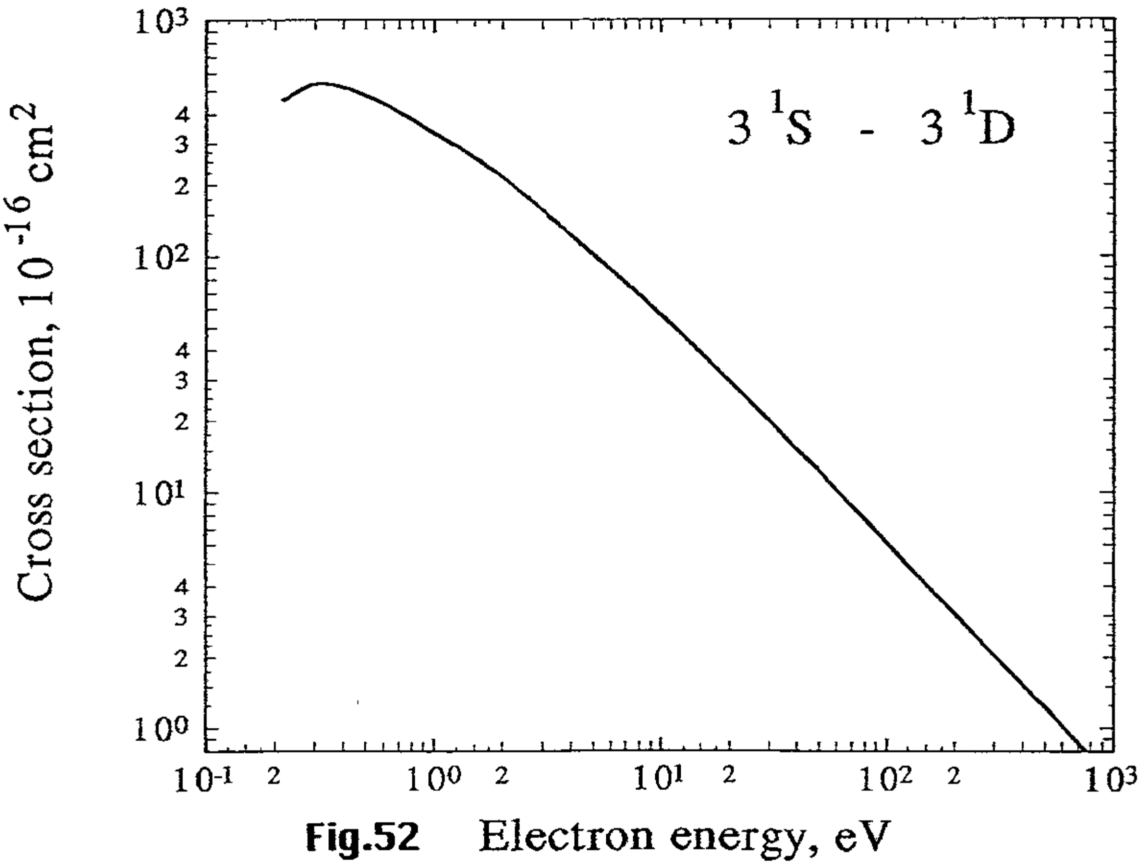

$3\,^1S$ - $3\,^1D$
Cross section, 10^{-16} cm^2
Electron energy, eV

Fig.52

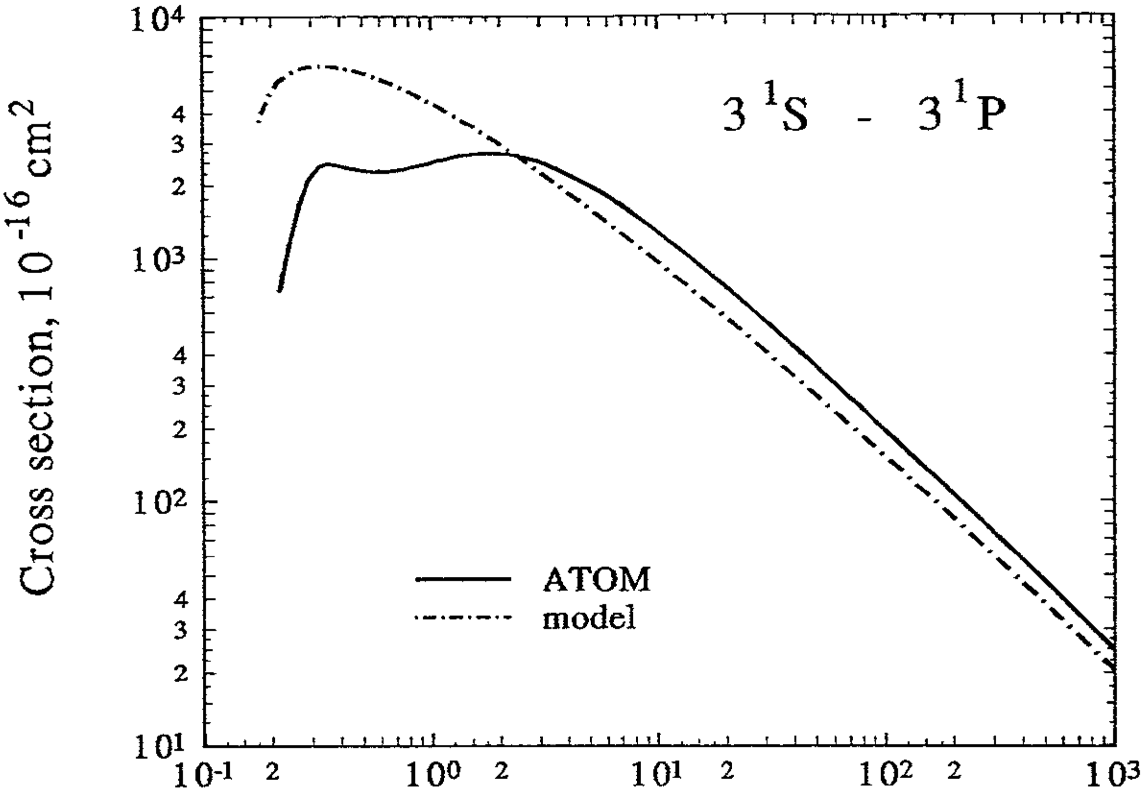

Fig.53 Electron energy, eV

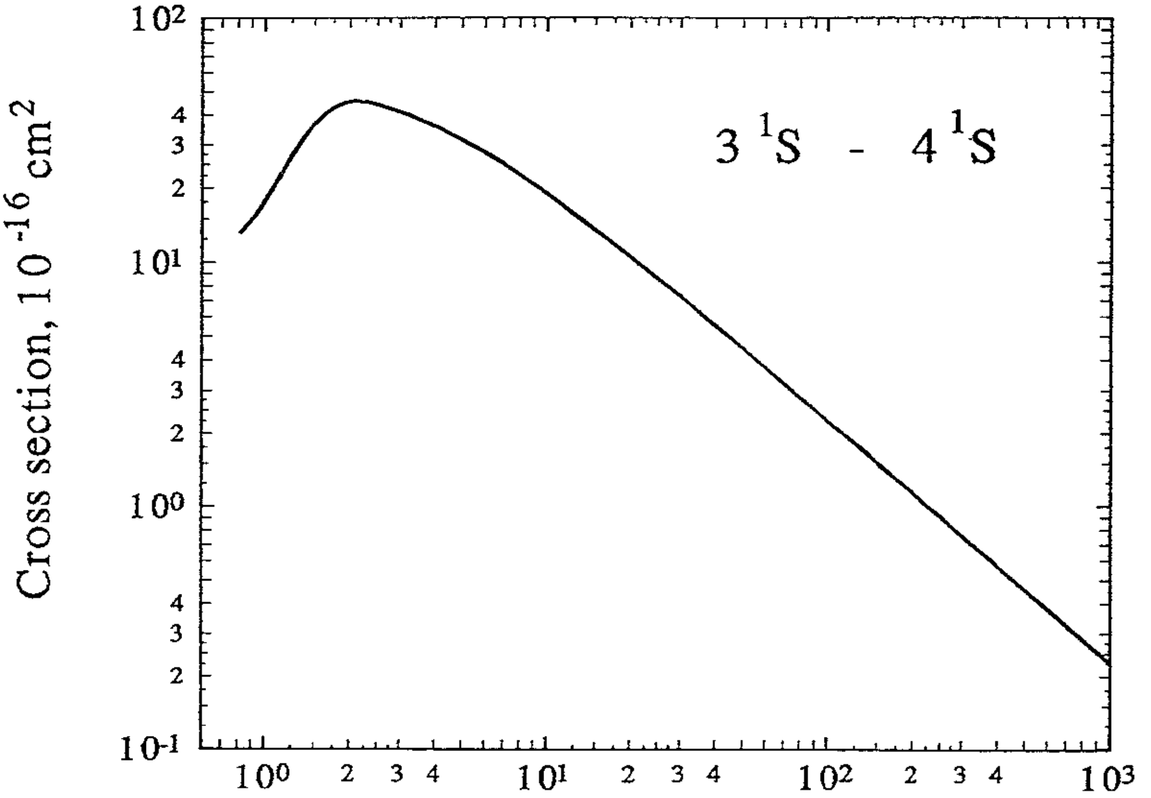

Fig.54 Electron energy, eV

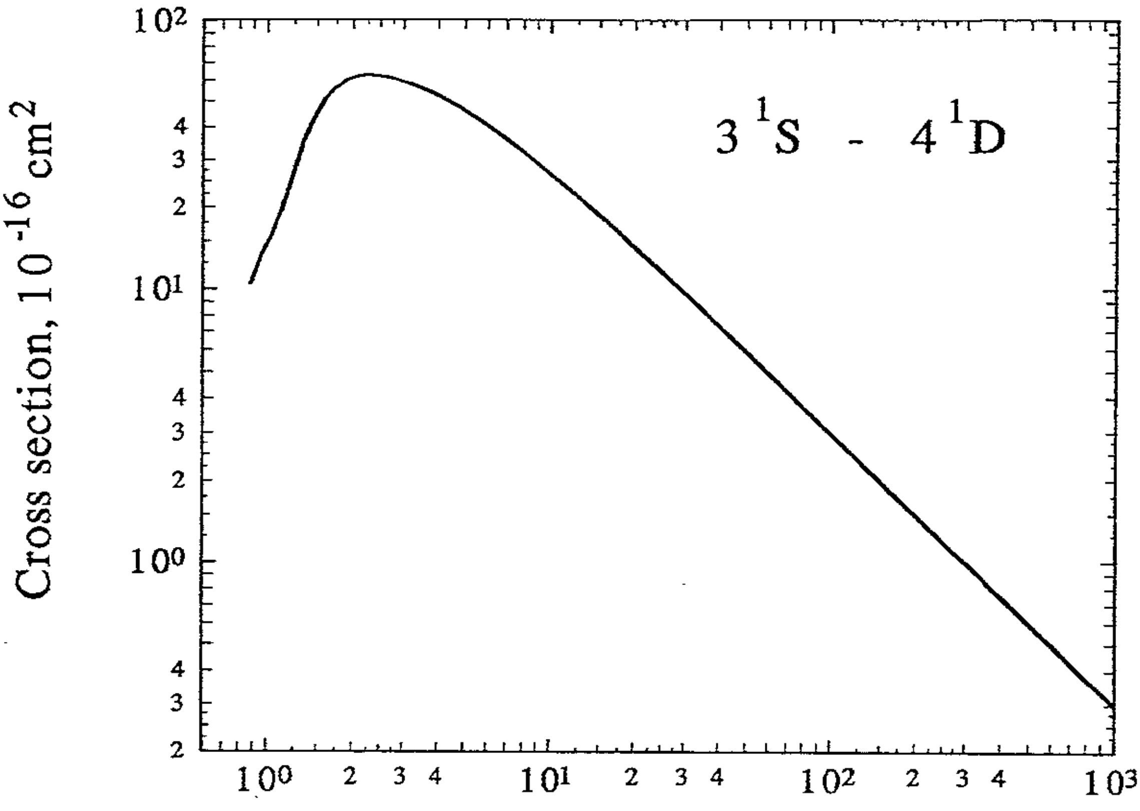

Fig.55 Electron energy, eV

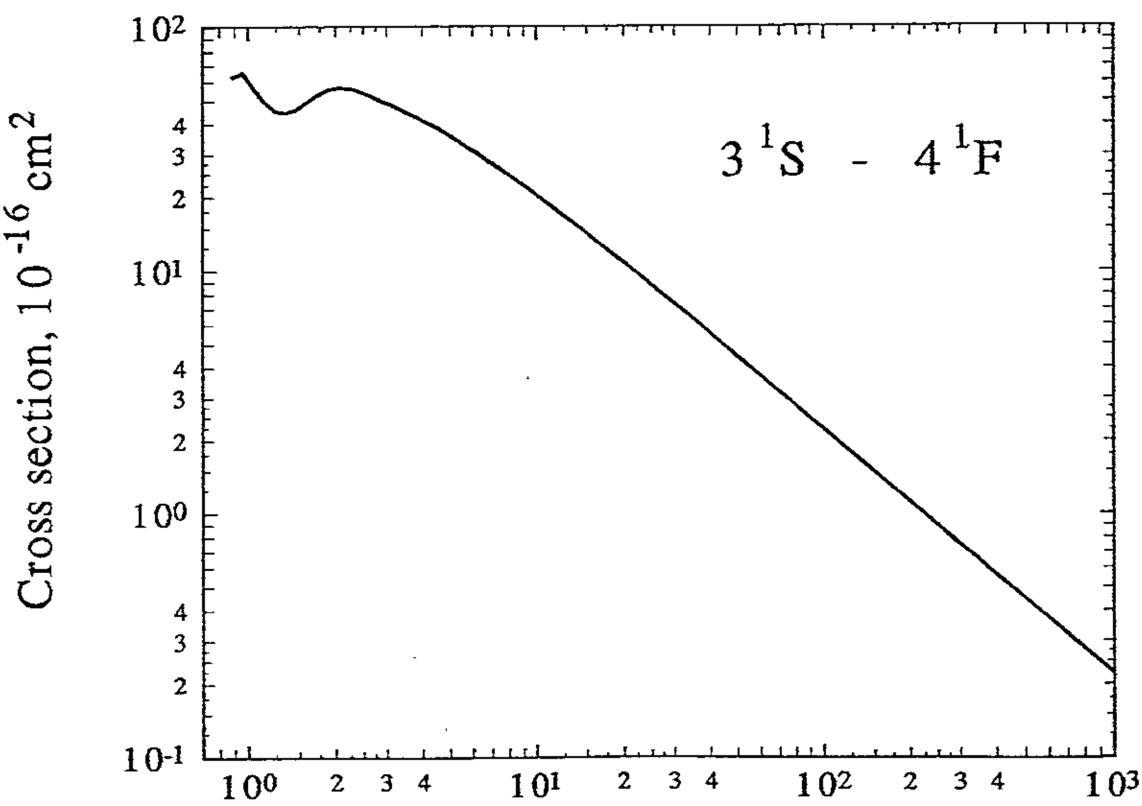

Fig.56 Electron energy, eV

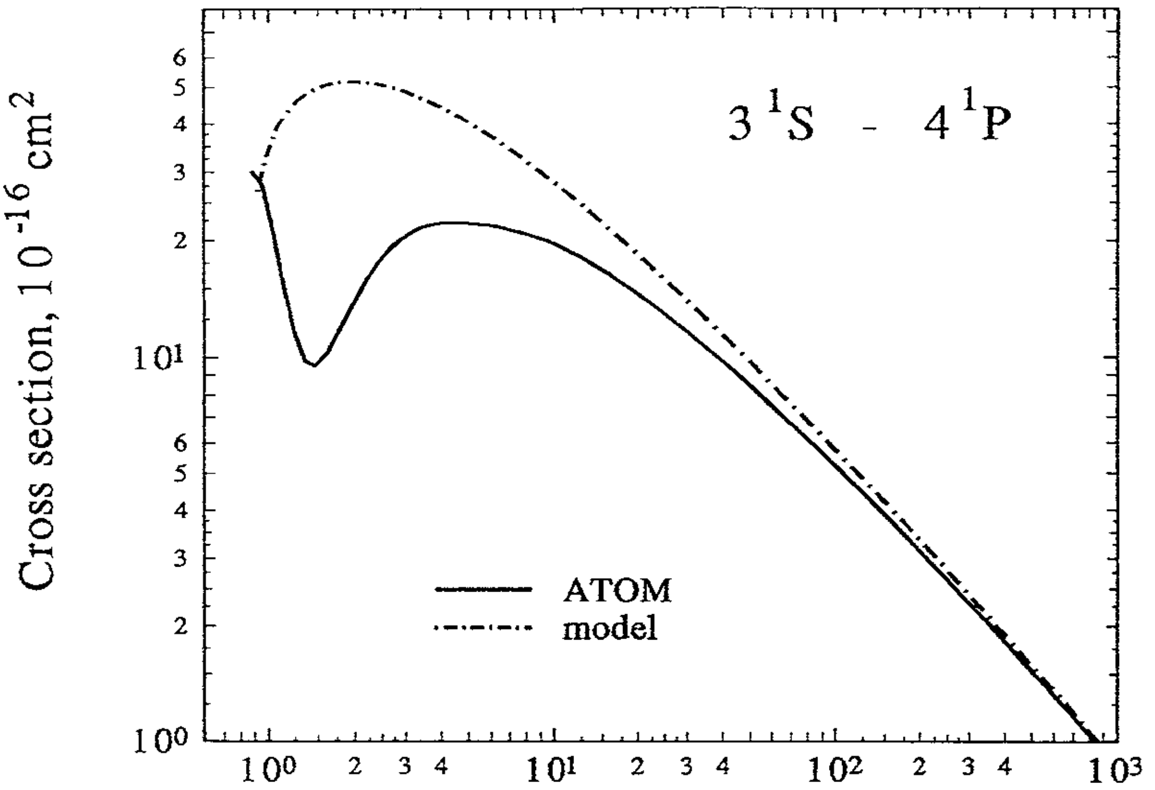
Cross section, 10 -16 cm2
3 1S - 4 1P
ATOM
model
10 0
10 1
10 0 2 3 4 10 1 2 3 4 10 2 2 3 4 10 3
Electron energy, eV

Fig.57

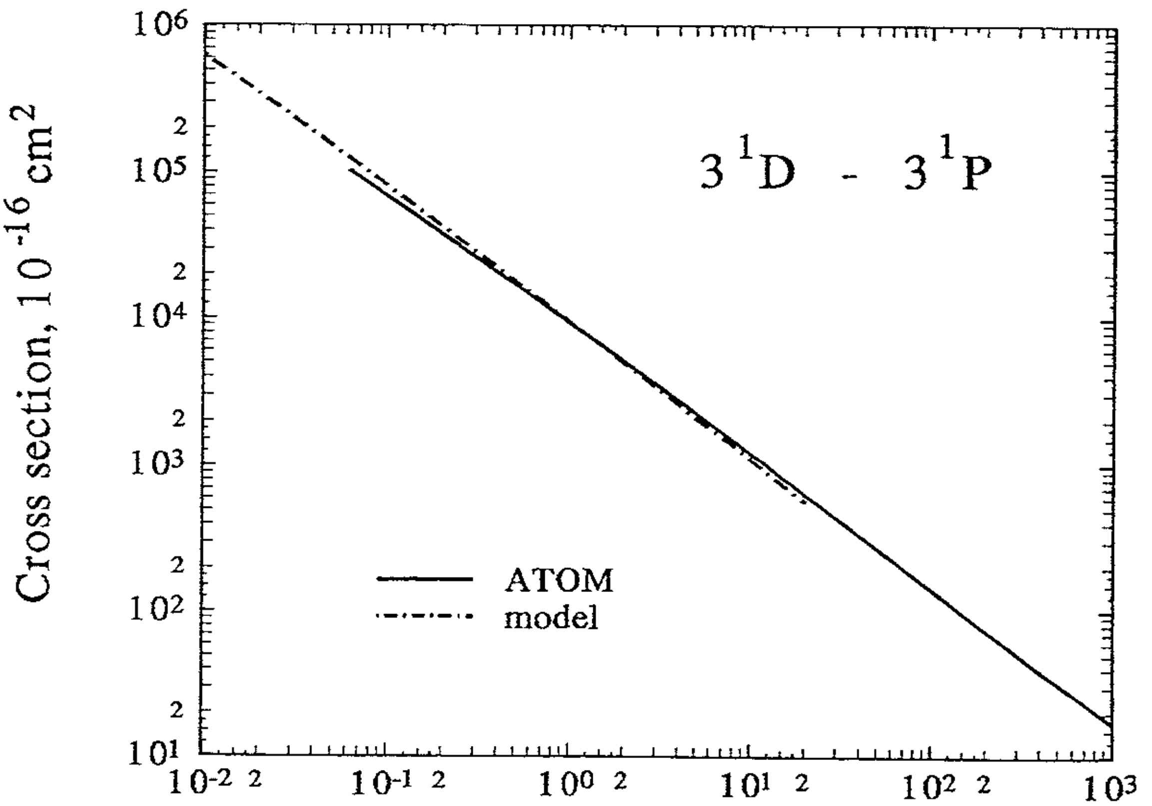
Cross section, 10 -16 cm2
3 1D - 3 1P
ATOM
model
10 1
10 2
10 3
10 4
10 5
10 6
10 -2 2 10 -1 2 10 0 2 10 1 2 10 2 2 10 3
Electron energy, eV

Fig.58

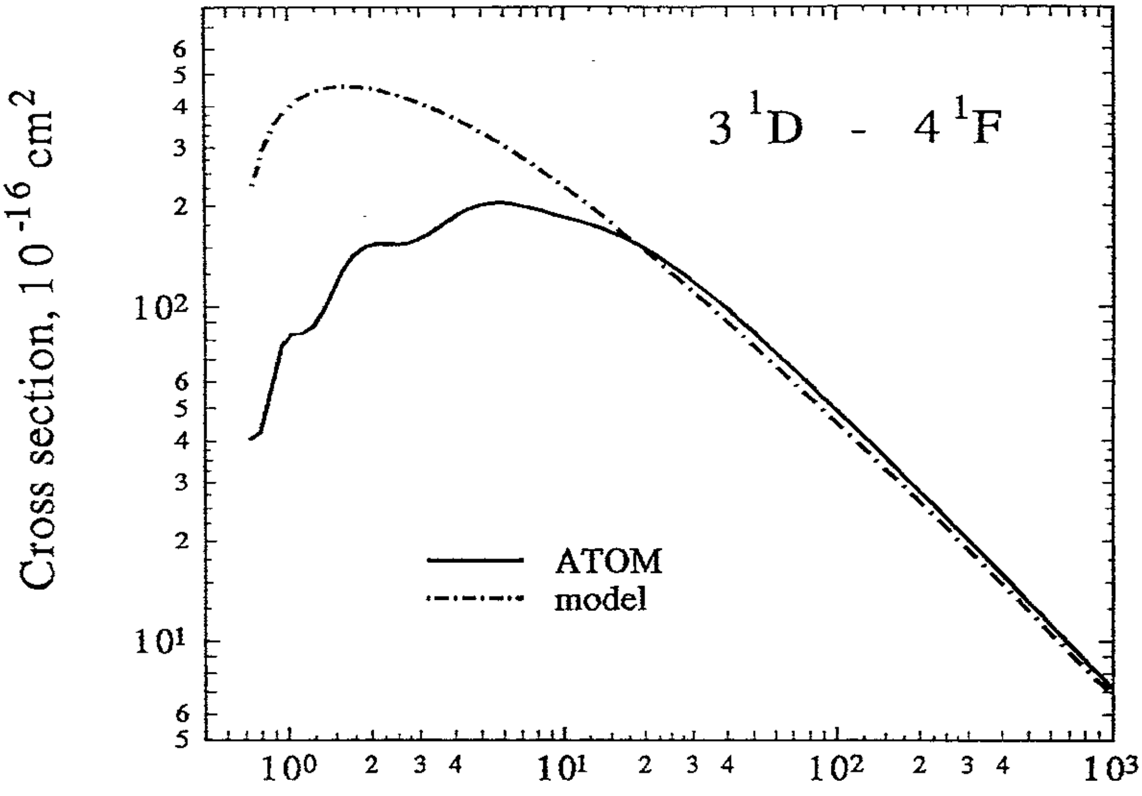

Fig.61 Electron energy, eV

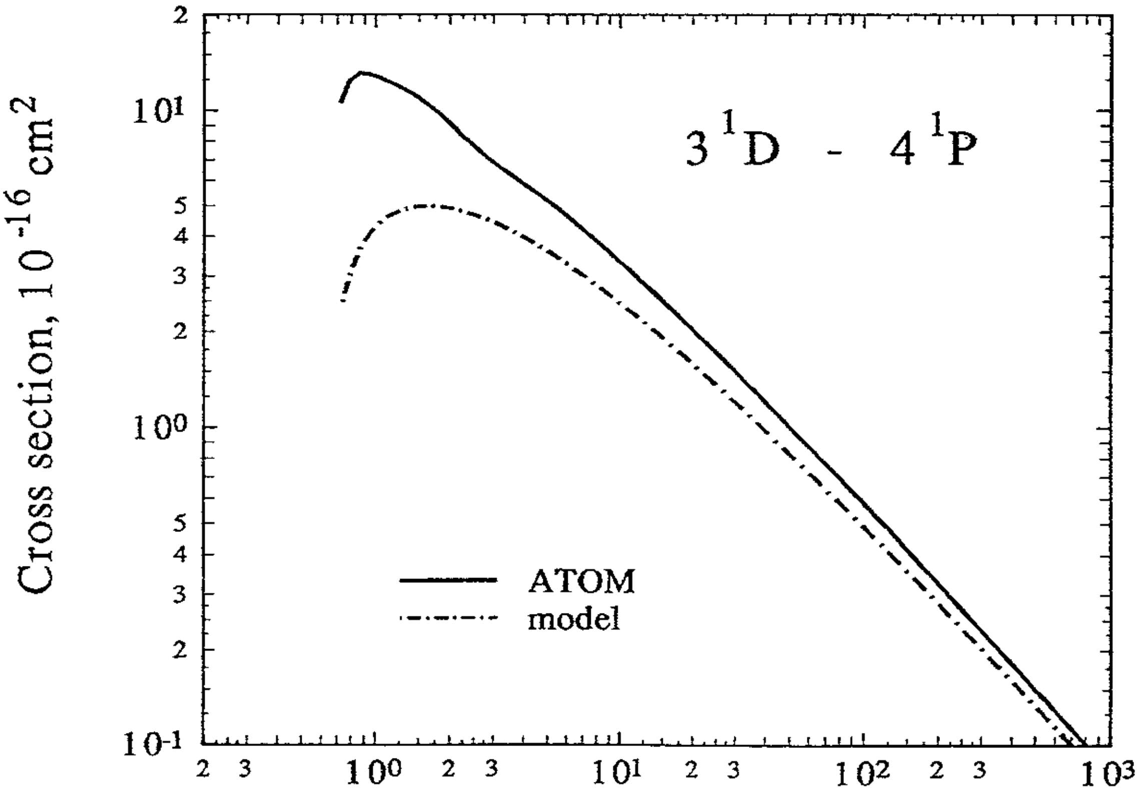

Fig.62 Electron energy, eV

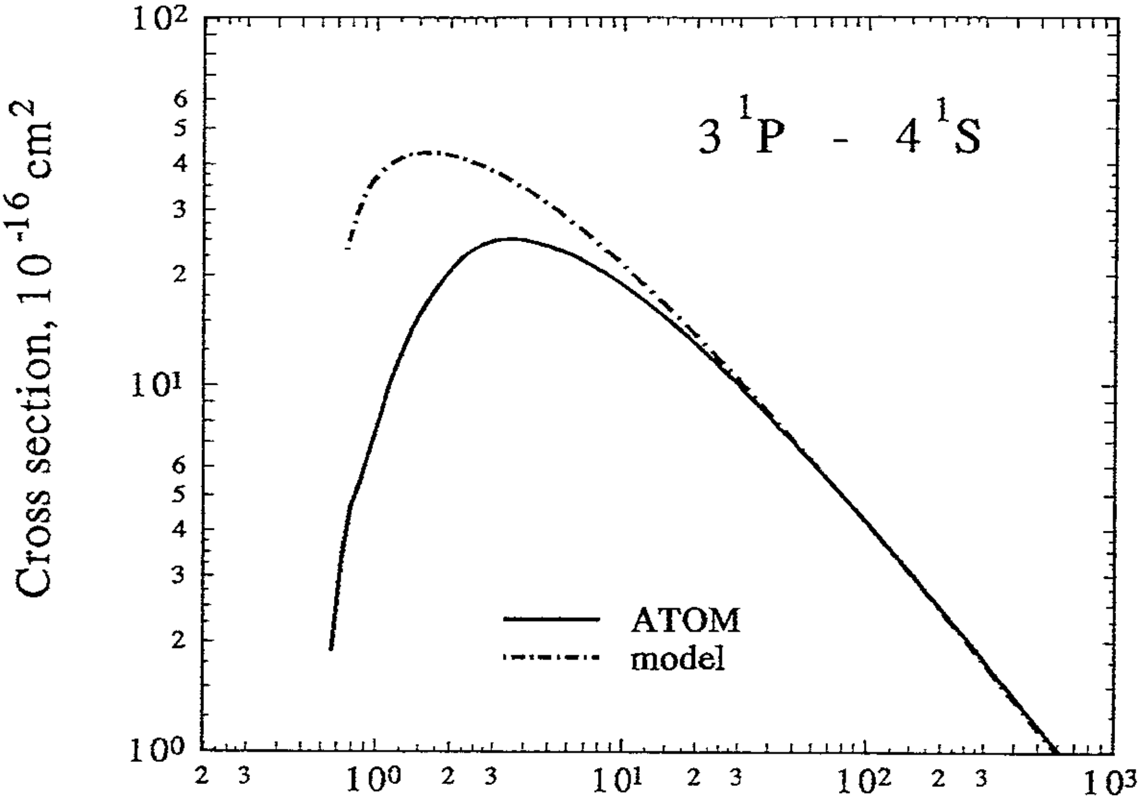

Fig.63 Electron energy, eV

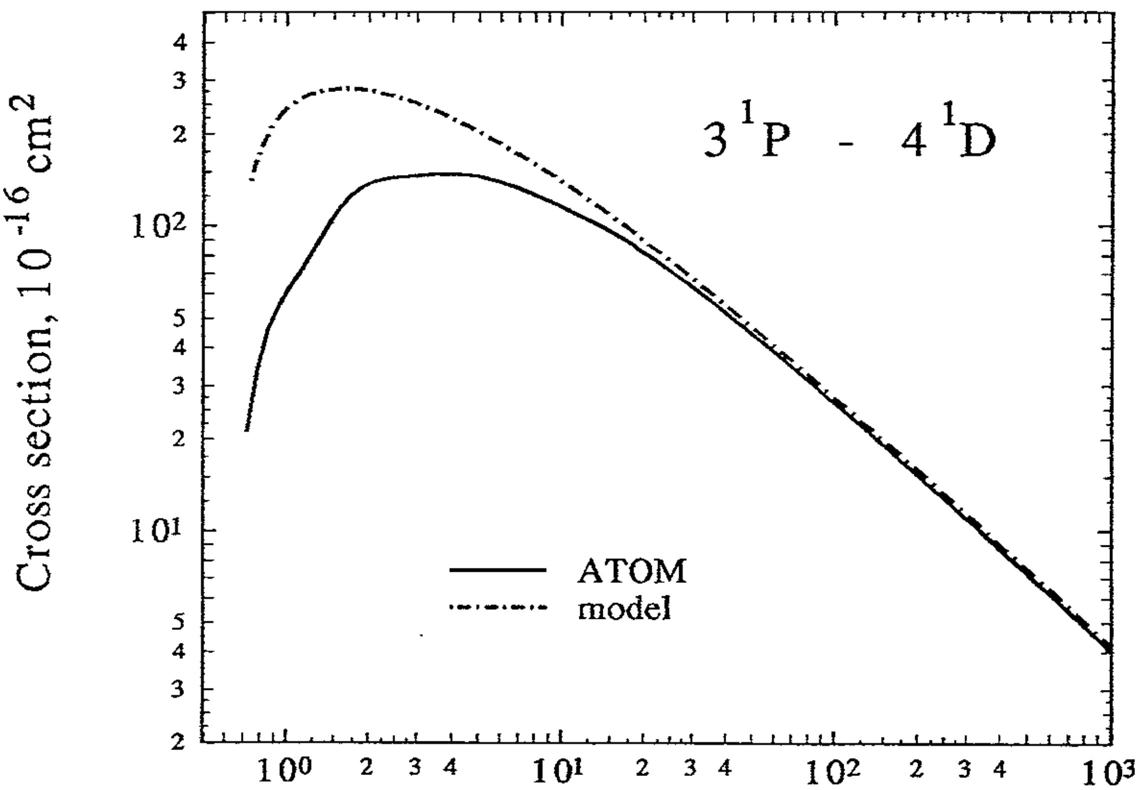

Fig.64 Electron energy, eV

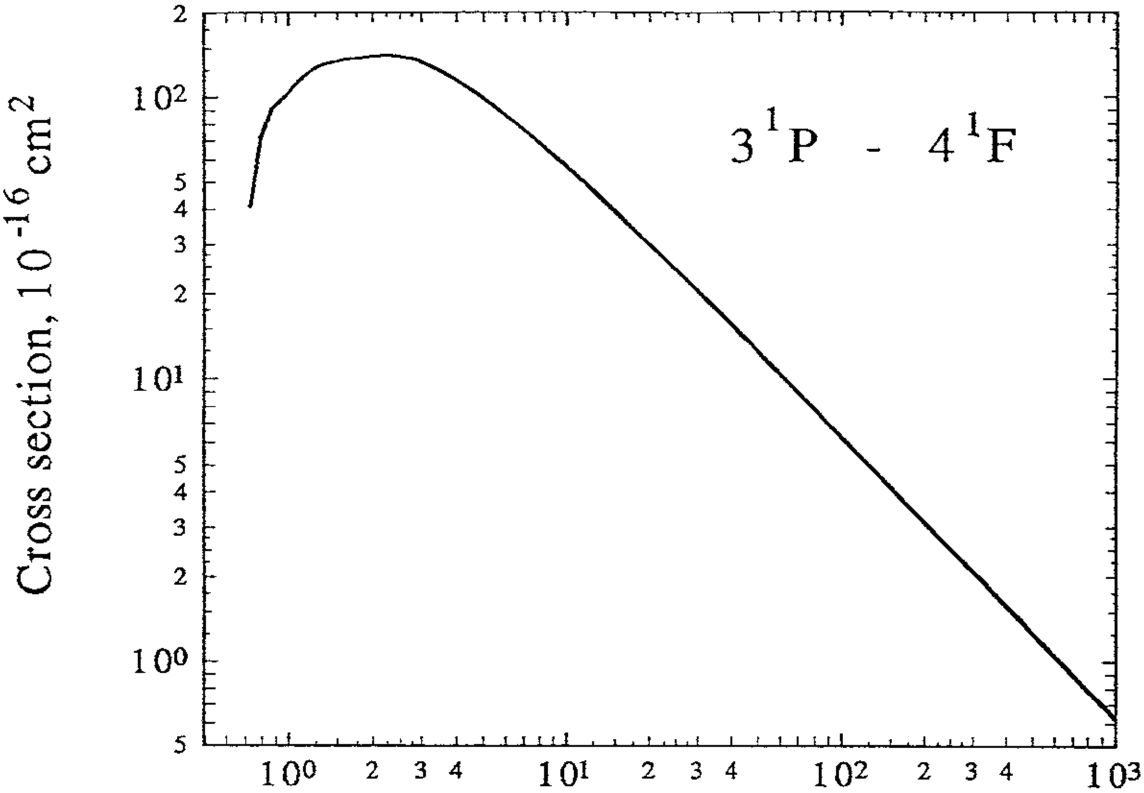

Fig.65 Electron energy, eV

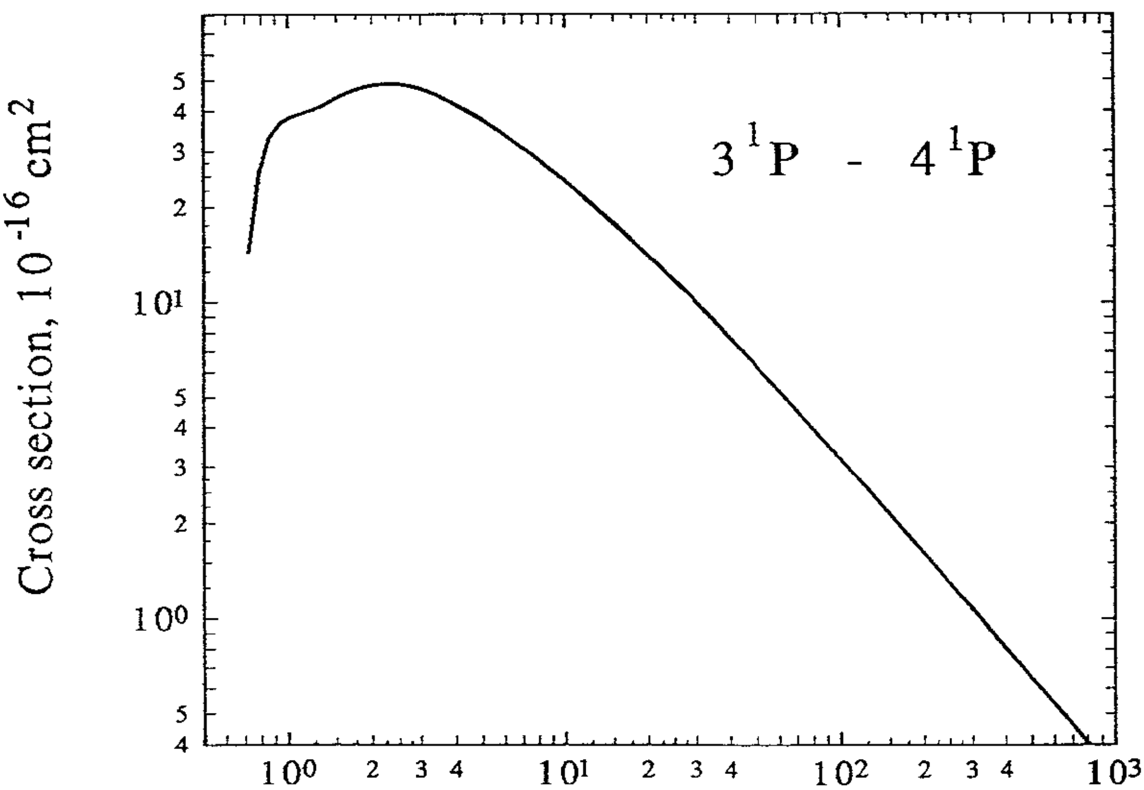

Fig.66 Electron energy, eV

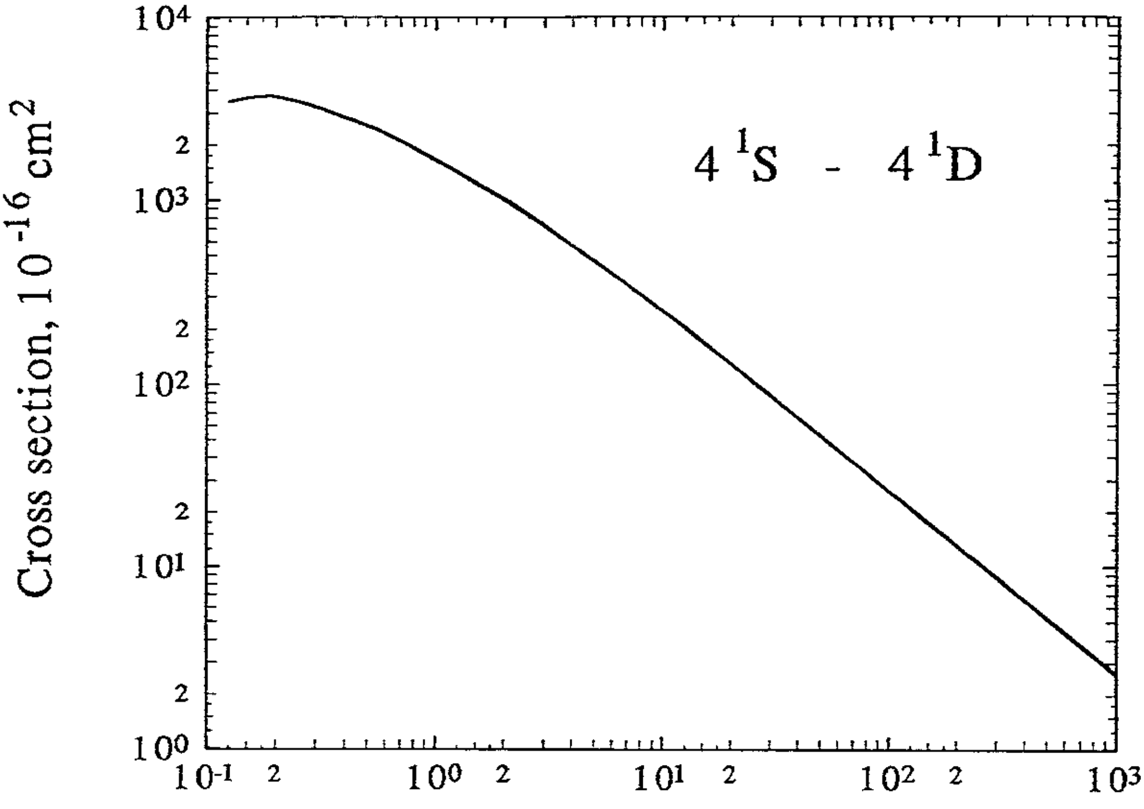

$4\,^1S - 4\,^1D$
Cross section, 10^{-16} cm^2
Electron energy, eV

Fig.67

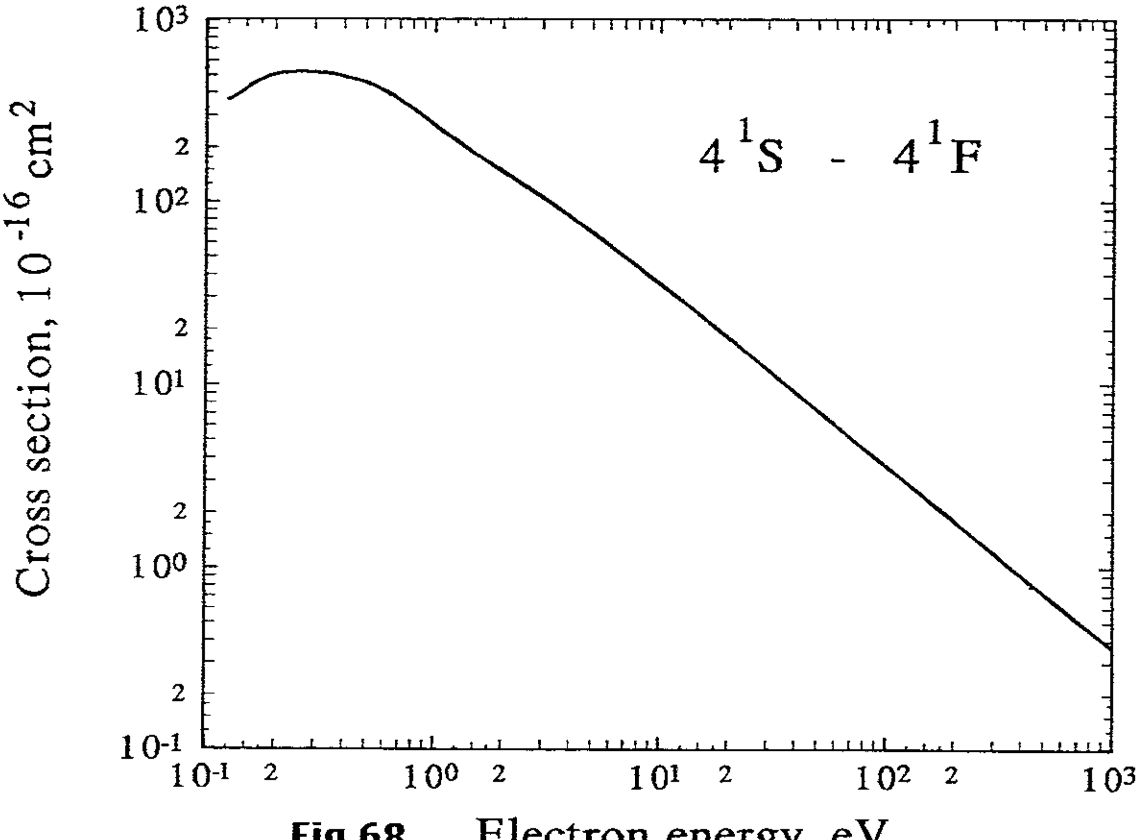

$4\,^1S - 4\,^1F$
Cross section, 10^{-16} cm^2
Electron energy, eV

Fig.68

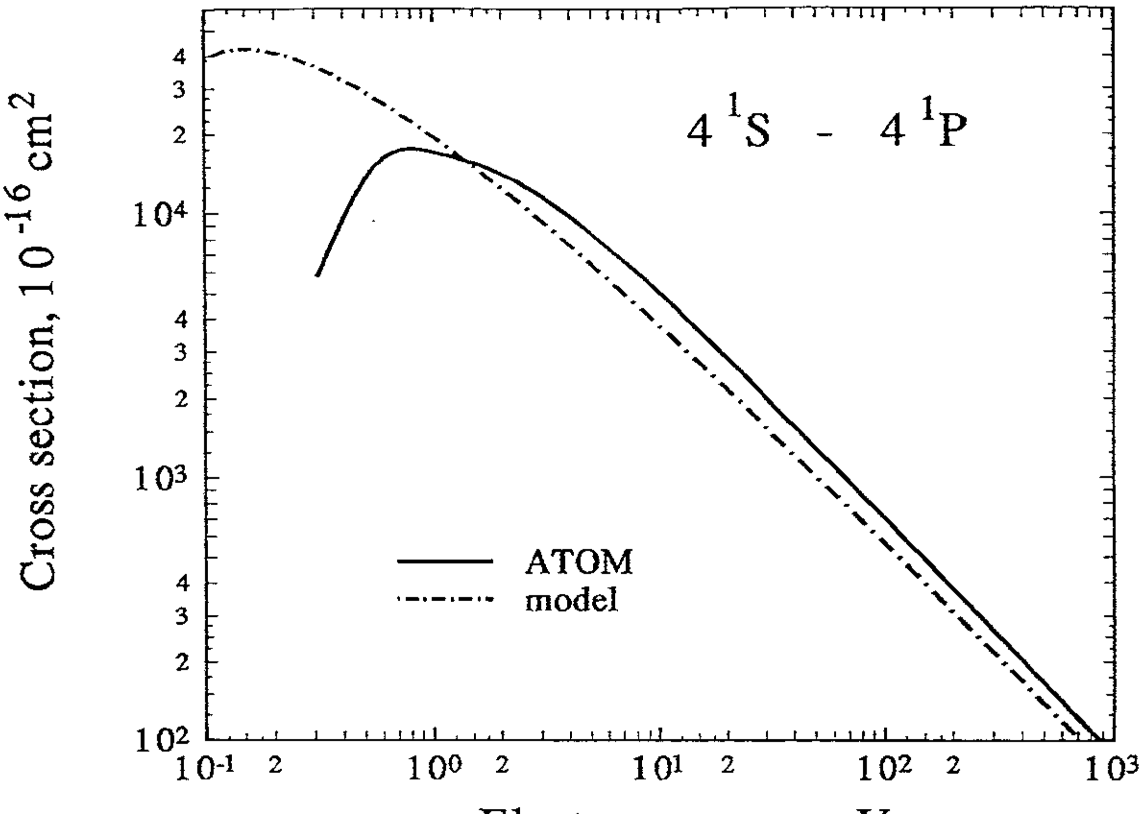

4 ¹S - 4 ¹P
ATOM
model
Cross section, 10⁻¹⁶ cm²
Electron energy, eV

Fig.69

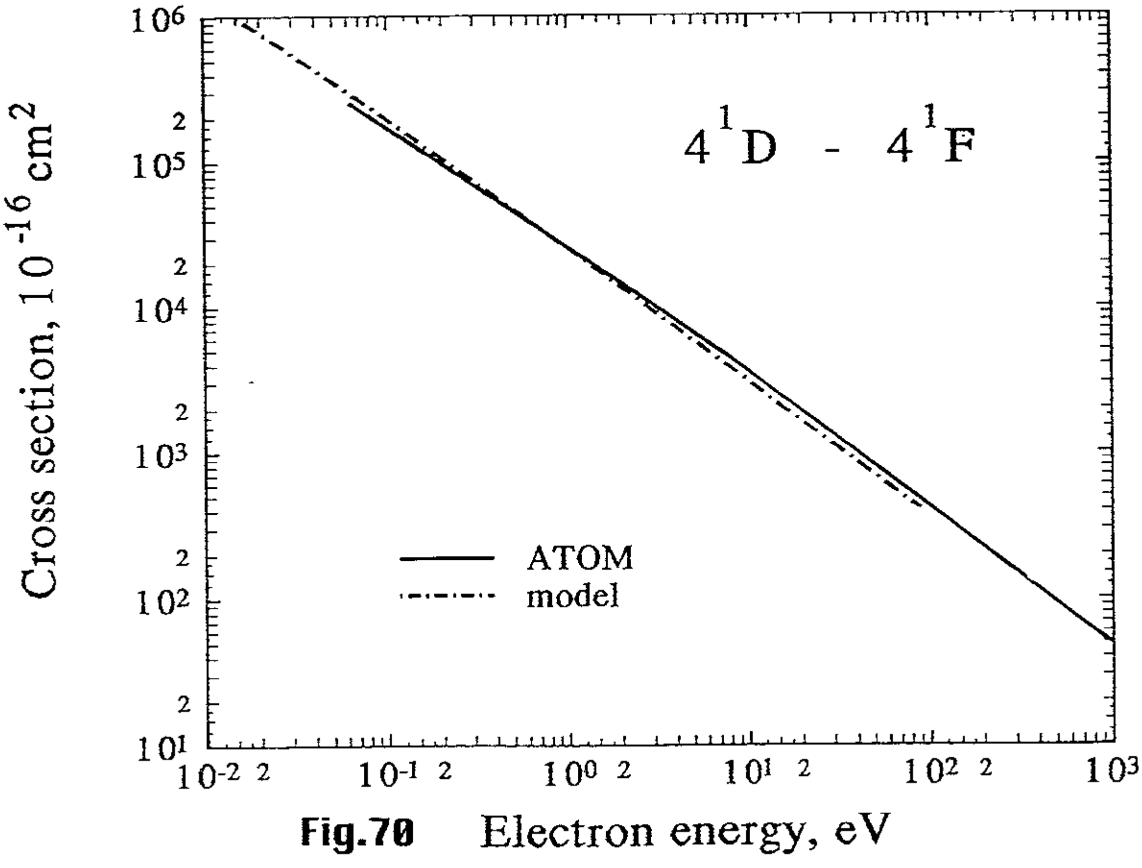

4 ¹D - 4 ¹F
ATOM
model
Cross section, 10⁻¹⁶ cm²
Electron energy, eV

Fig.70

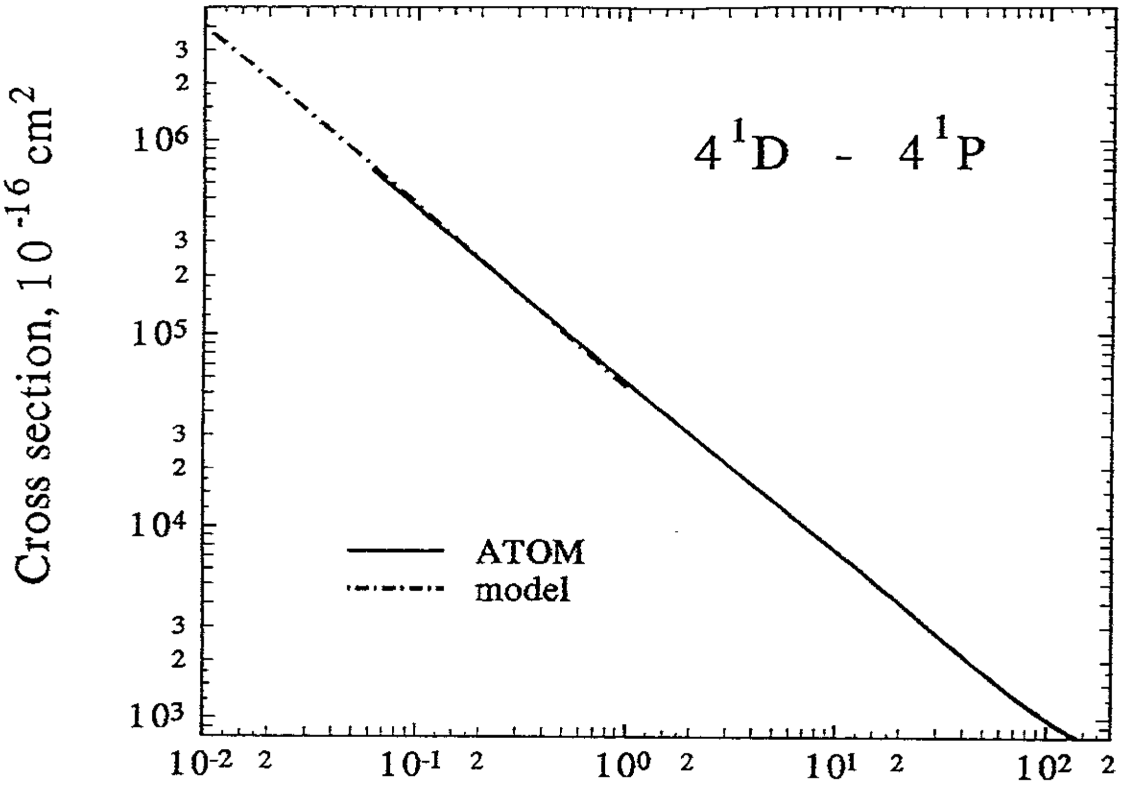

Fig.71 Electron energy, eV

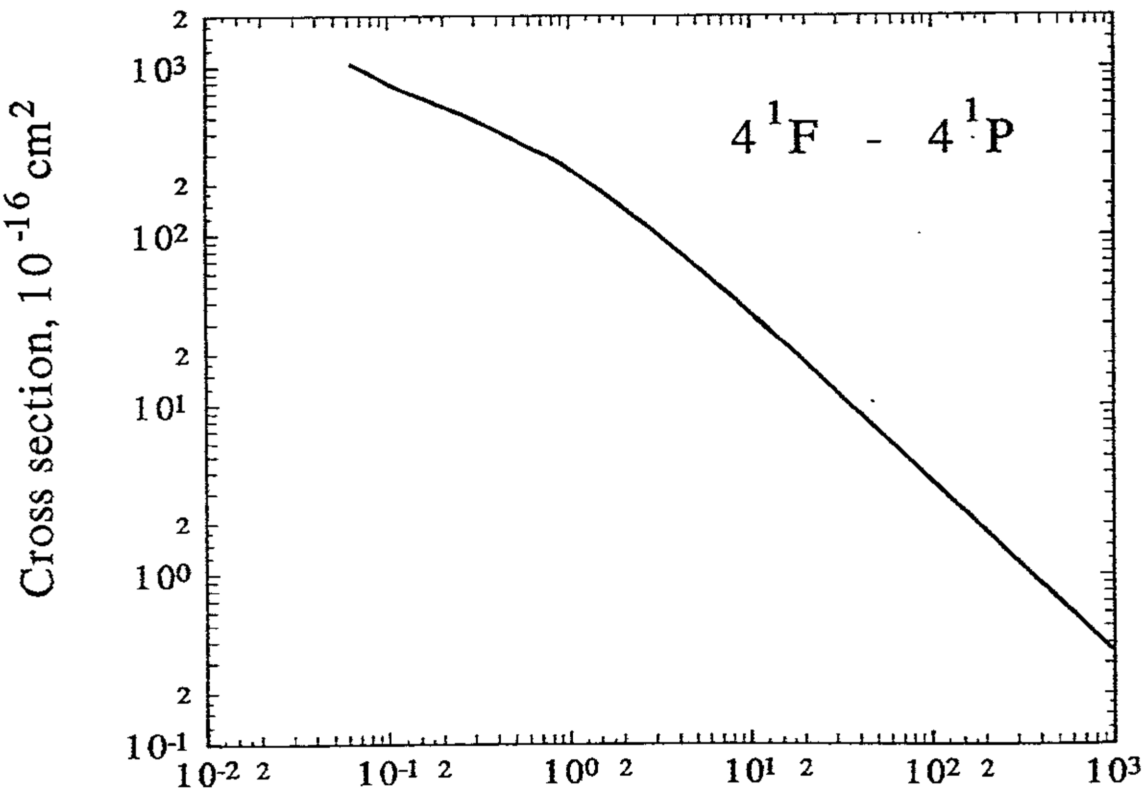

Fig.72 Electron energy, eV

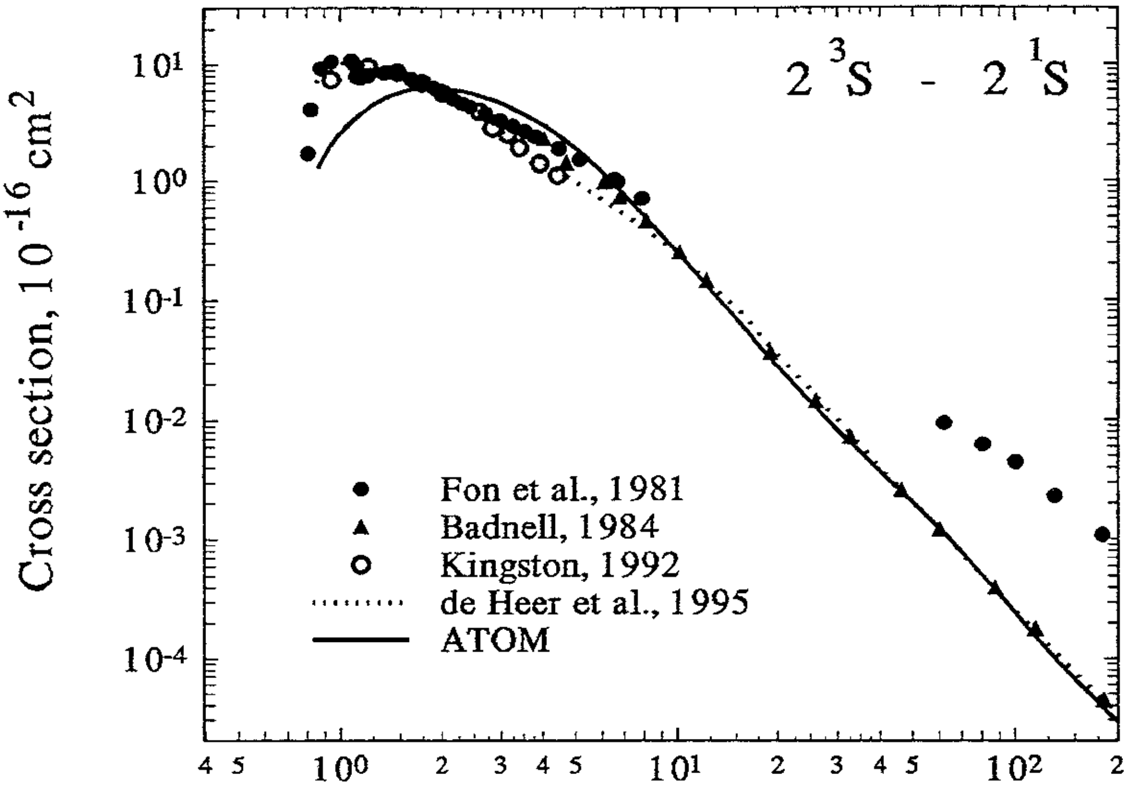

Fig.73 Electron energy, eV

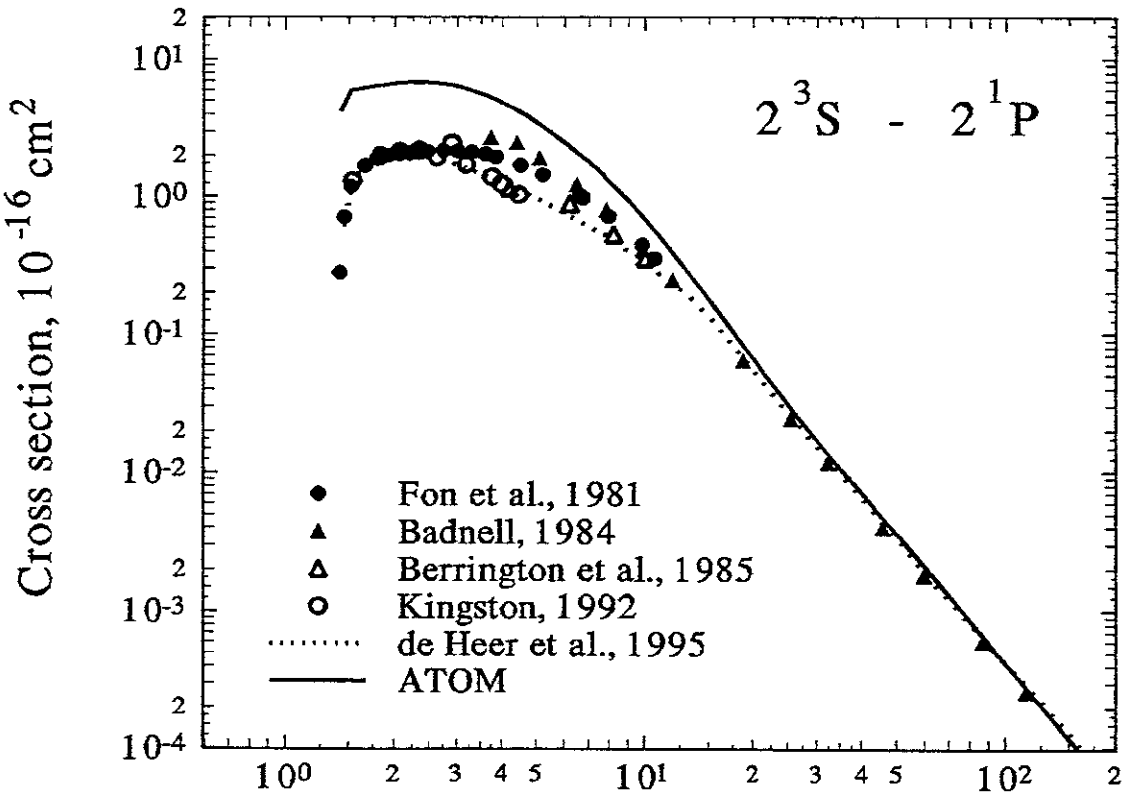

Fig.74 Electron energy, eV

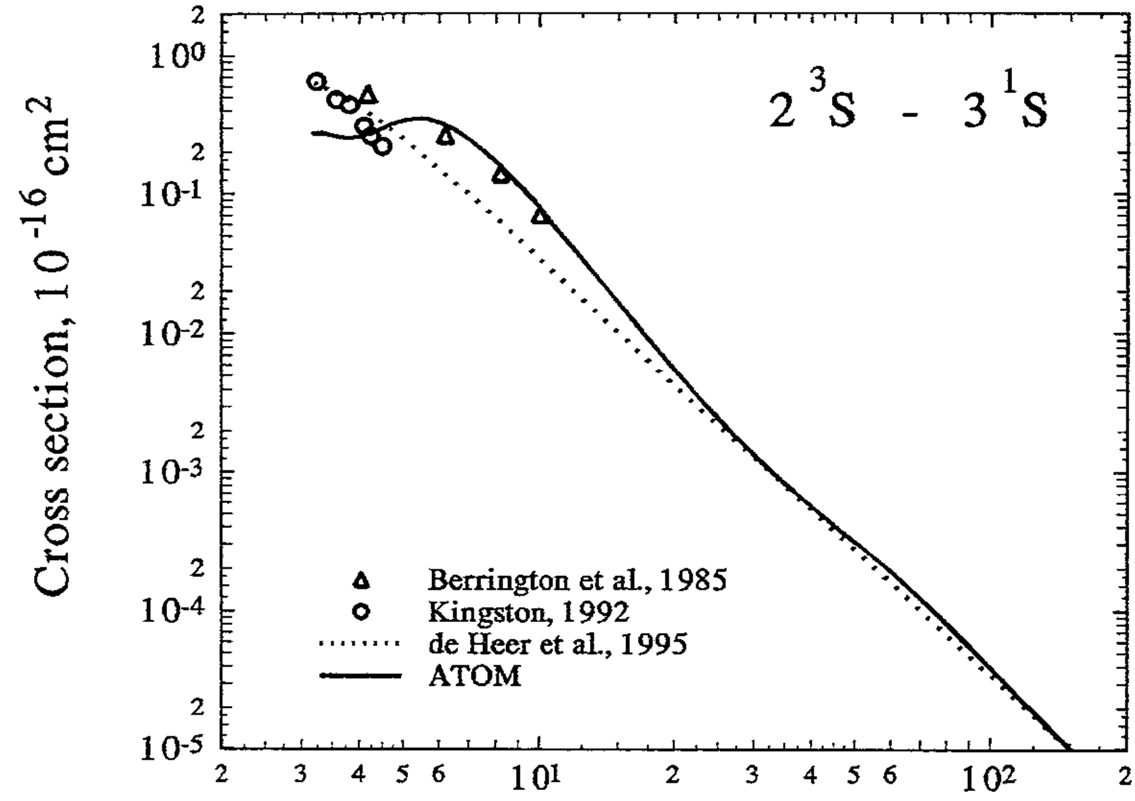
2 3S - 3 1S
Berrington et al., 1985
Kingston, 1992
de Heer et al., 1995
ATOM
Cross section, 10 -16 cm2
Electron energy, eV

Fig.75

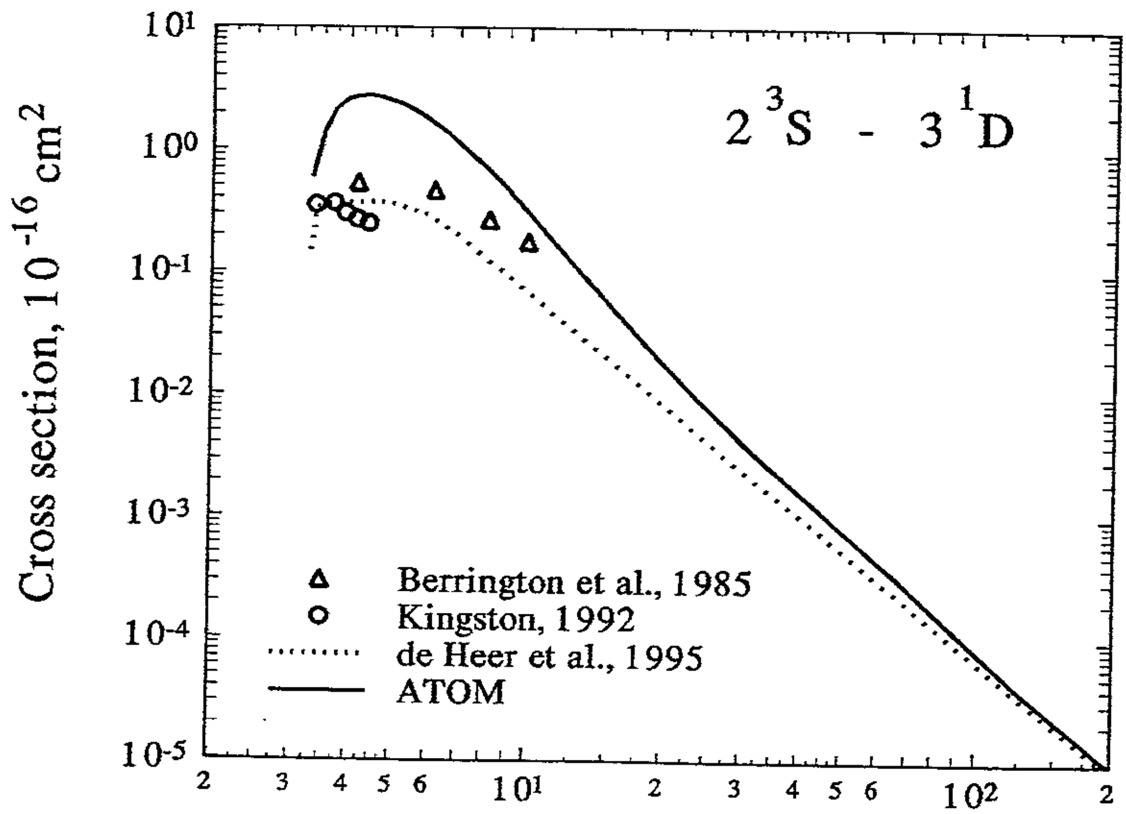
2 3S - 3 1D
Berrington et al., 1985
Kingston, 1992
de Heer et al., 1995
ATOM
Cross section, 10 -16 cm2
Electron energy, eV

Fig.76

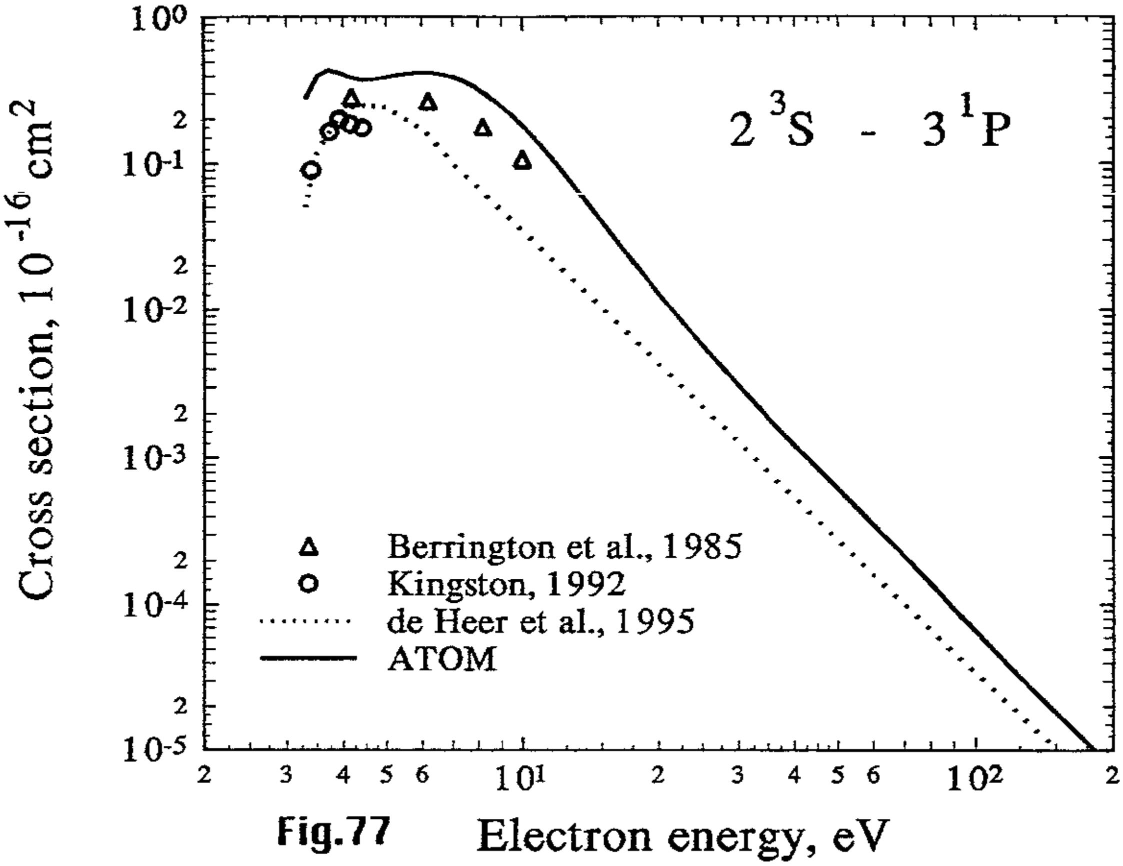

Cross section, 10^-16 cm^2
2 3S - 3 1P
Berrington et al., 1985
Kingston, 1992
de Heer et al., 1995
ATOM
Electron energy, eV

Fig.77

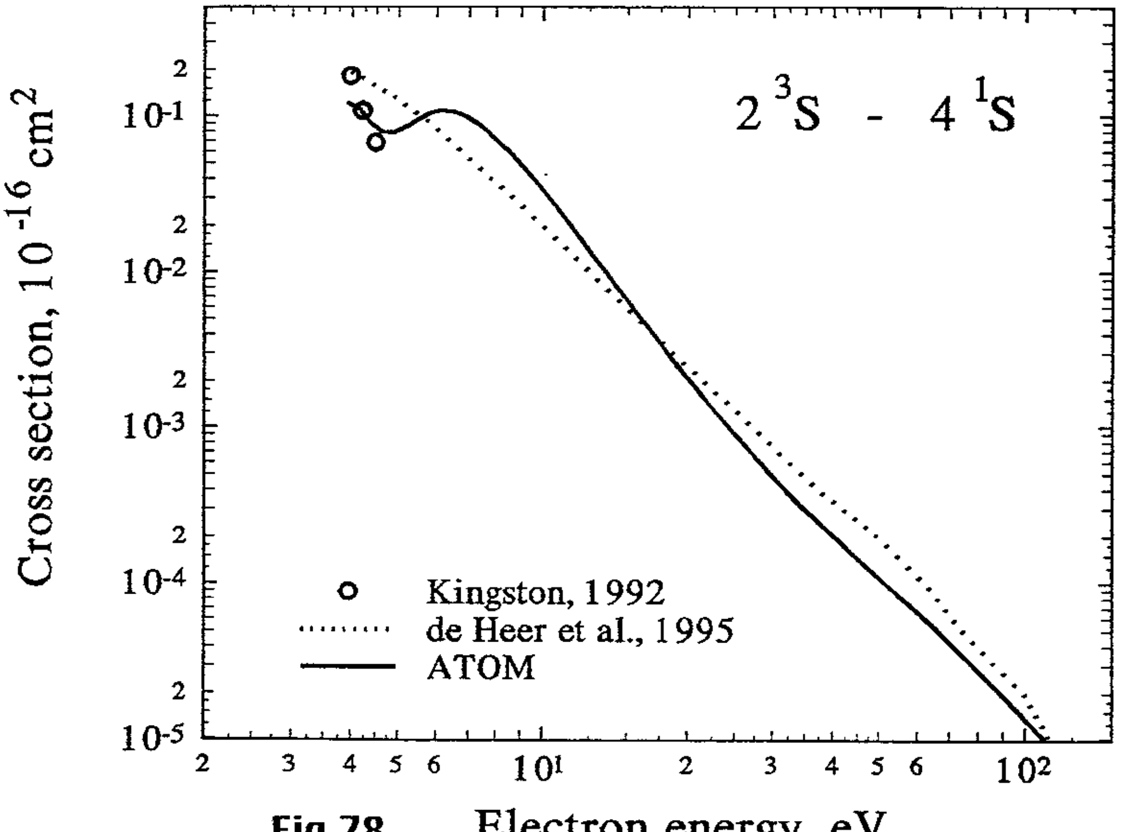

Cross section, 10^-16 cm^2
2 3S - 4 1S
Kingston, 1992
de Heer et al., 1995
ATOM
Electron energy, eV

Fig.78

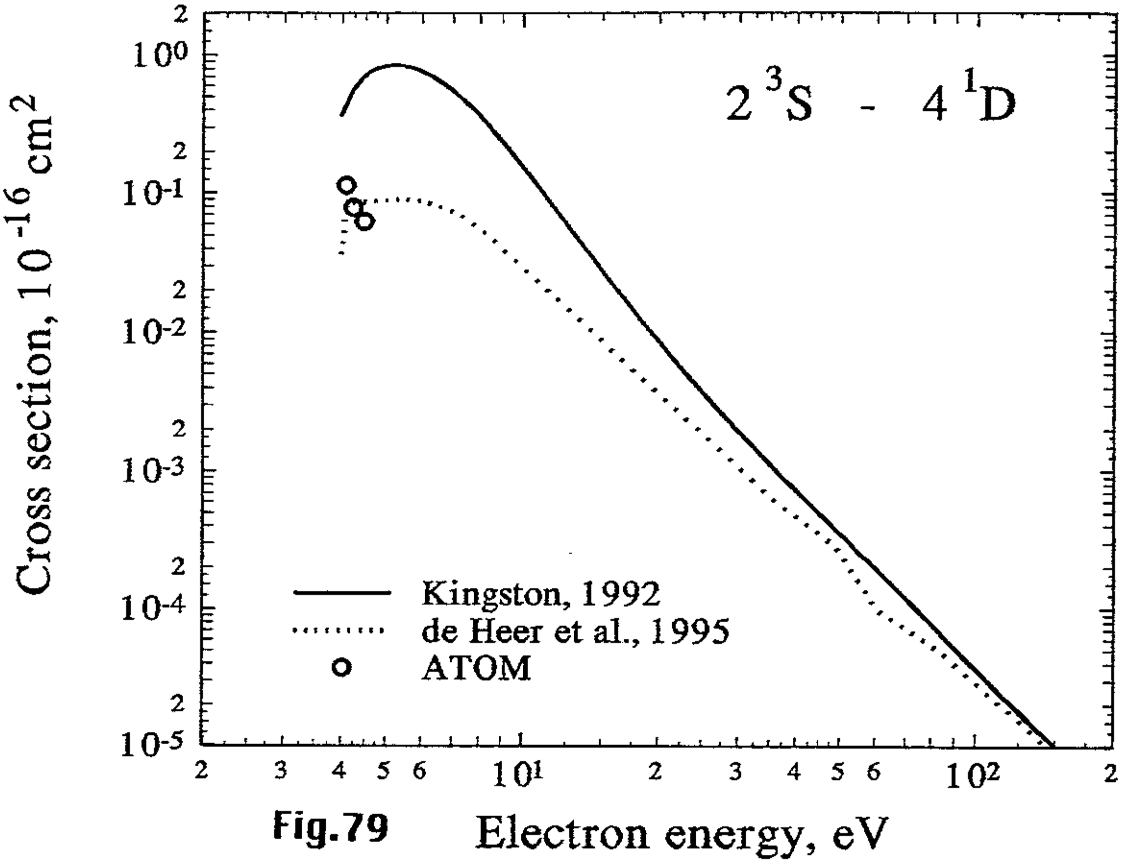

$2\,^3S\ -\ 4\,^1D$
Cross section, $10^{-16}\,cm^2$
Electron energy, eV
Kingston, 1992
de Heer et al., 1995
ATOM

Fig.79

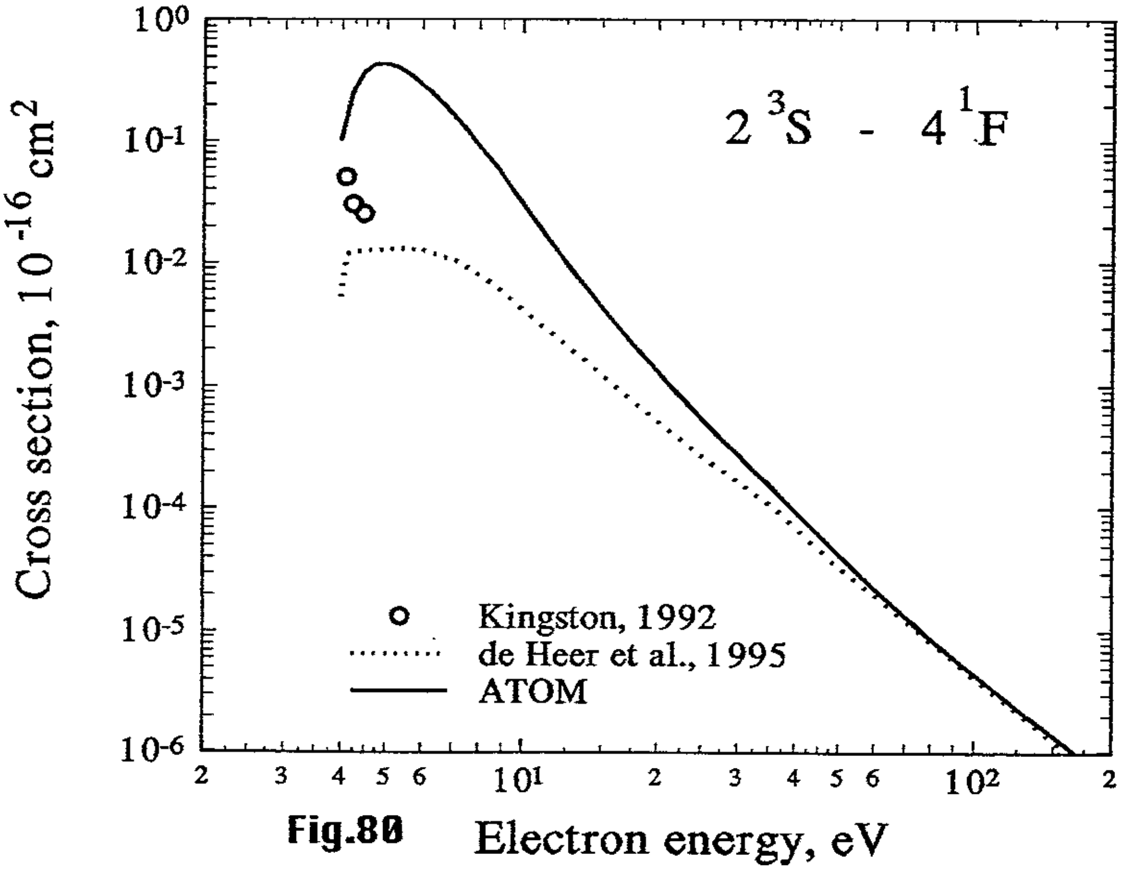

$2\,^3S\ -\ 4\,^1F$
Cross section, $10^{-16}\,cm^2$
Electron energy, eV
Kingston, 1992
de Heer et al., 1995
ATOM

Fig.80

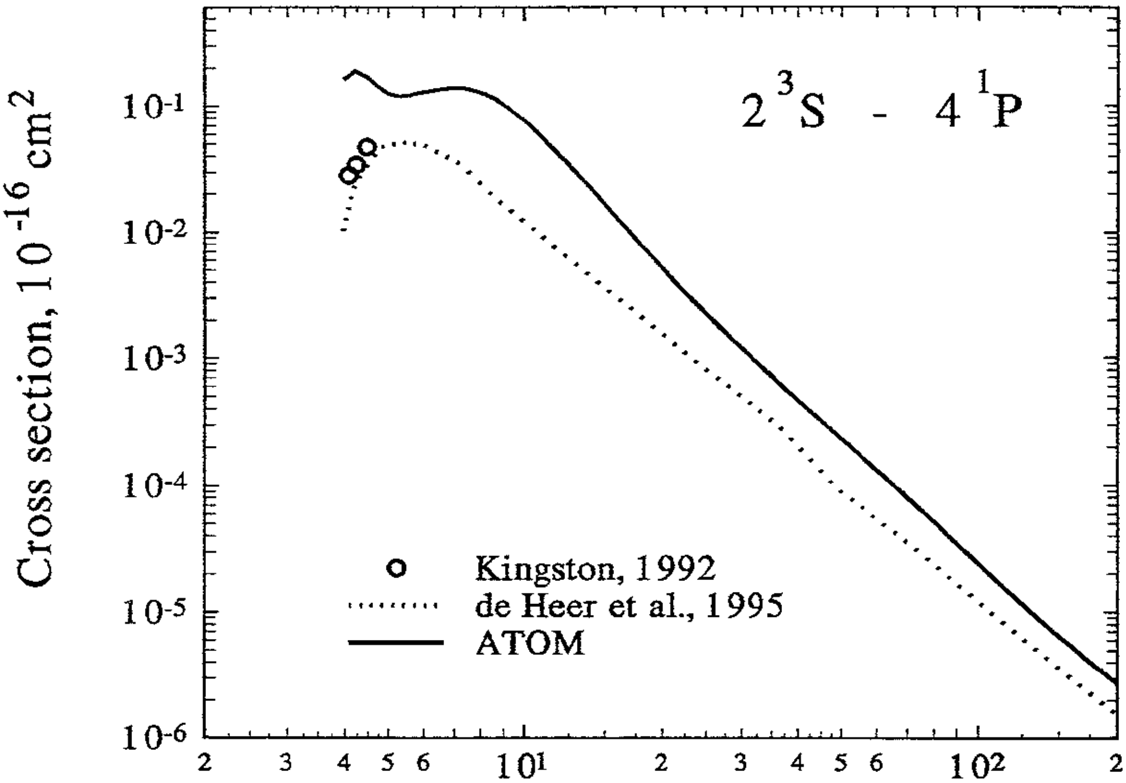

Fig.81 Electron energy, eV

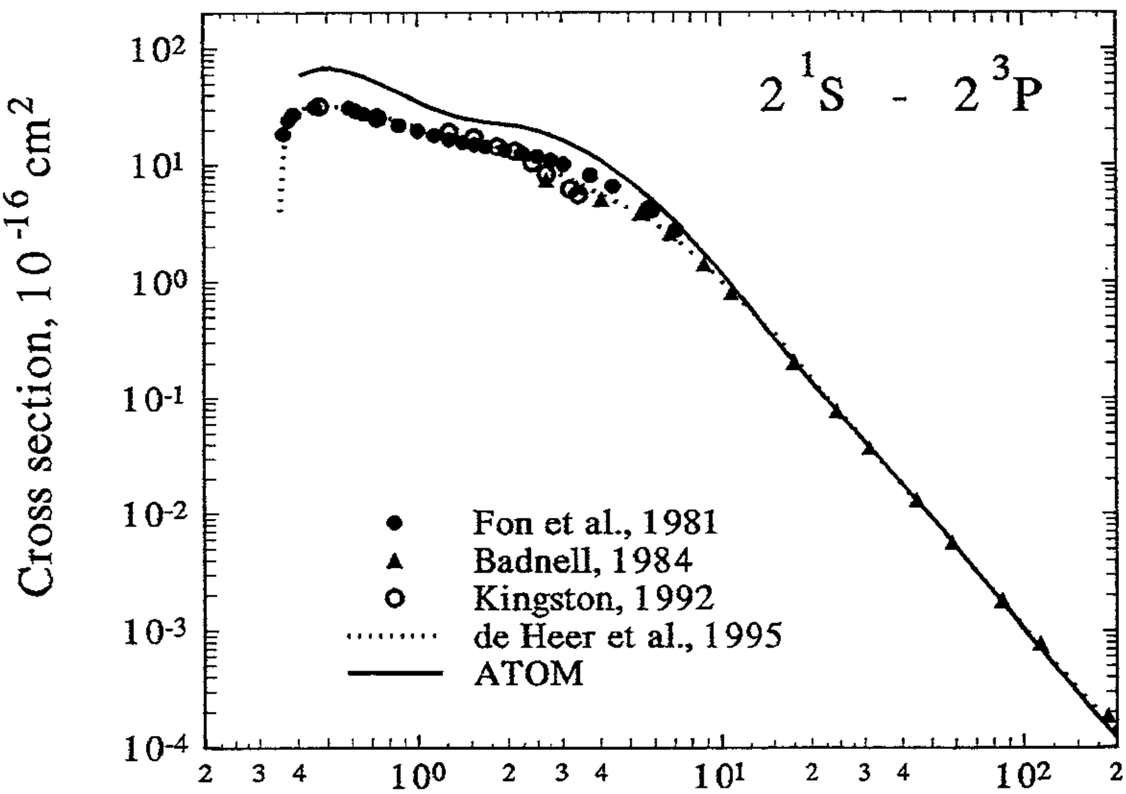

Fig.82 Electron energy, eV

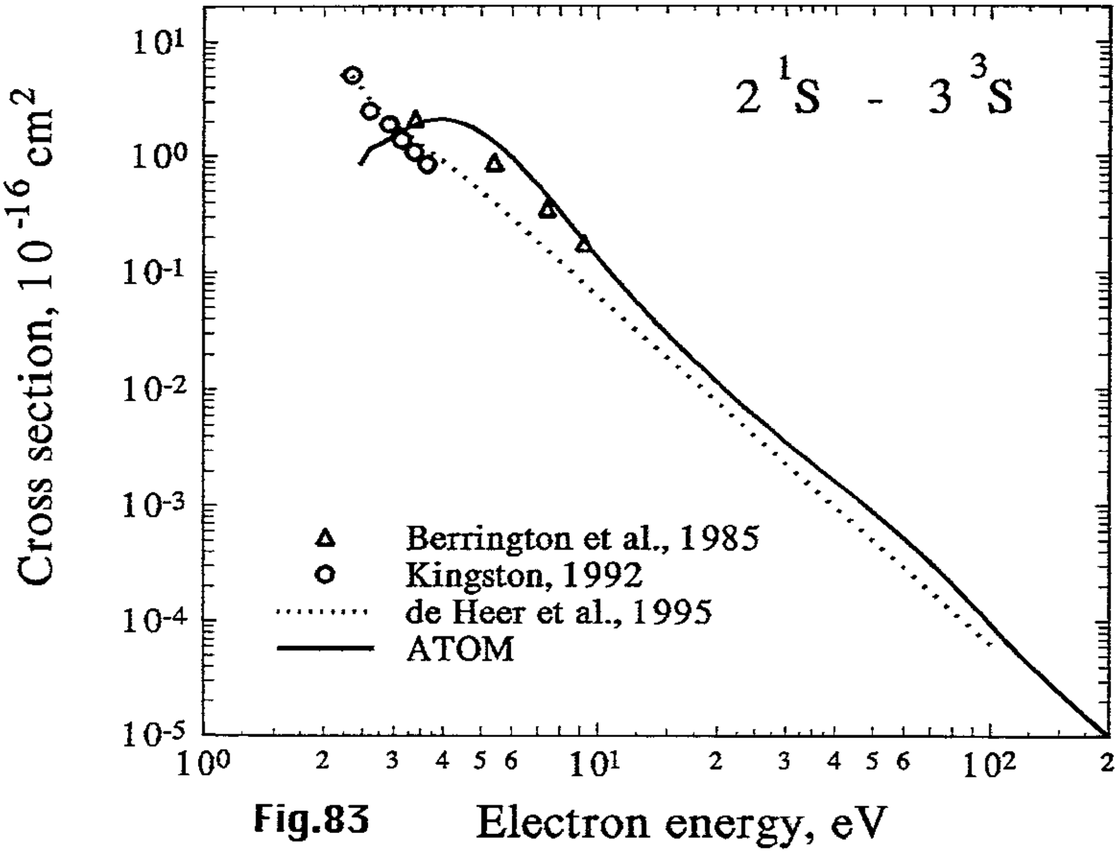

$2\,^1S - 3\,^3S$
Cross section, 10^{-16} cm^2
Electron energy, eV
Berrington et al., 1985
Kingston, 1992
de Heer et al., 1995
ATOM

Fig.83

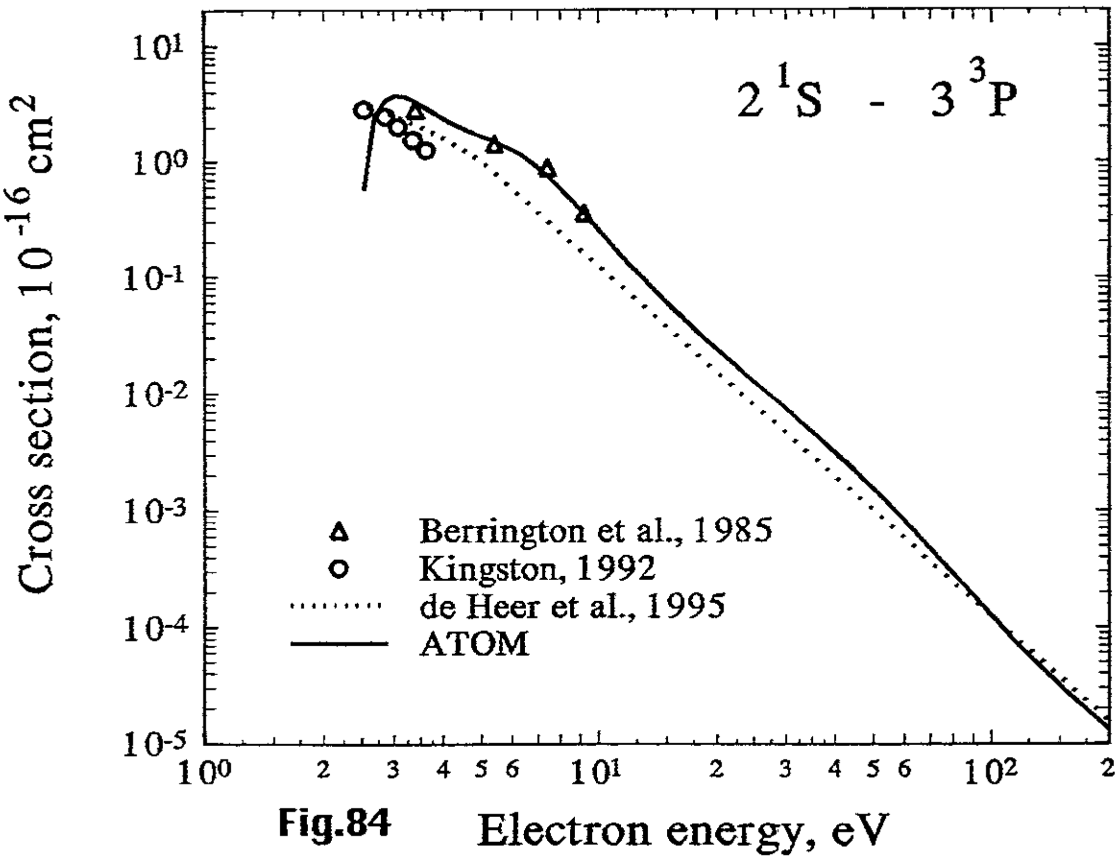

$2\,^1S - 3\,^3P$
Cross section, 10^{-16} cm^2
Electron energy, eV
Berrington et al., 1985
Kingston, 1992
de Heer et al., 1995
ATOM

Fig.84

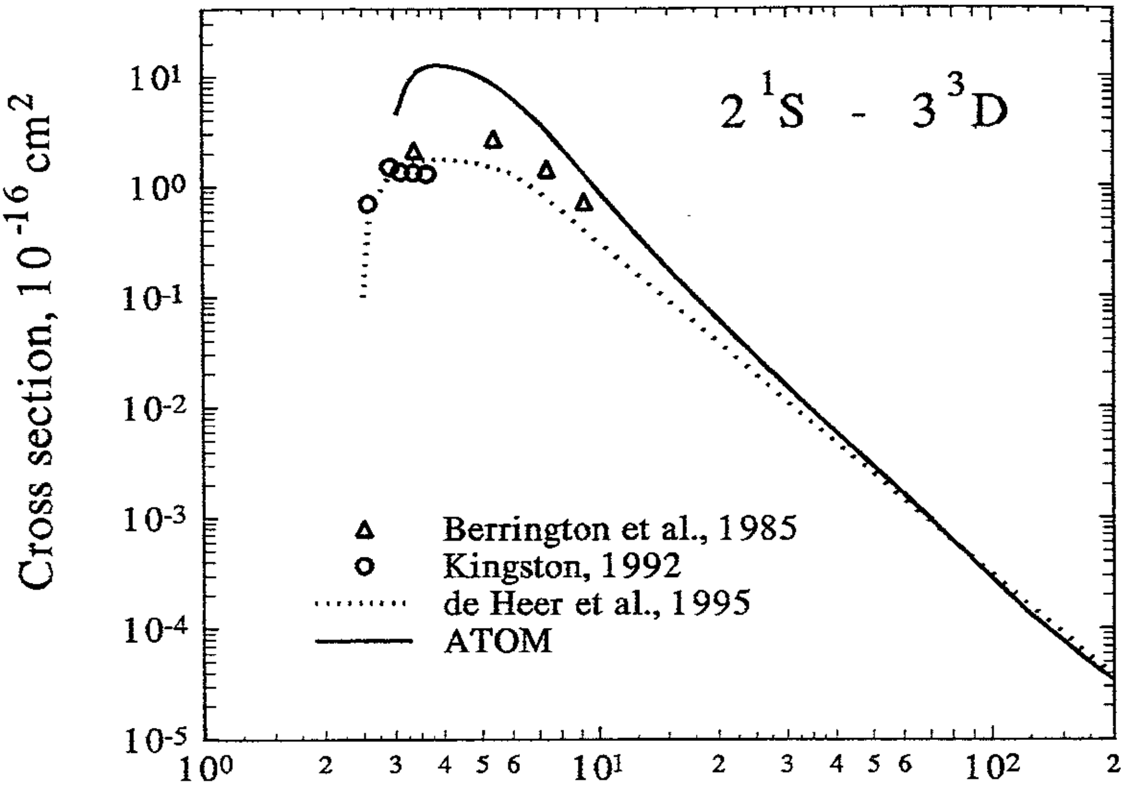

Fig.85 Electron energy, eV

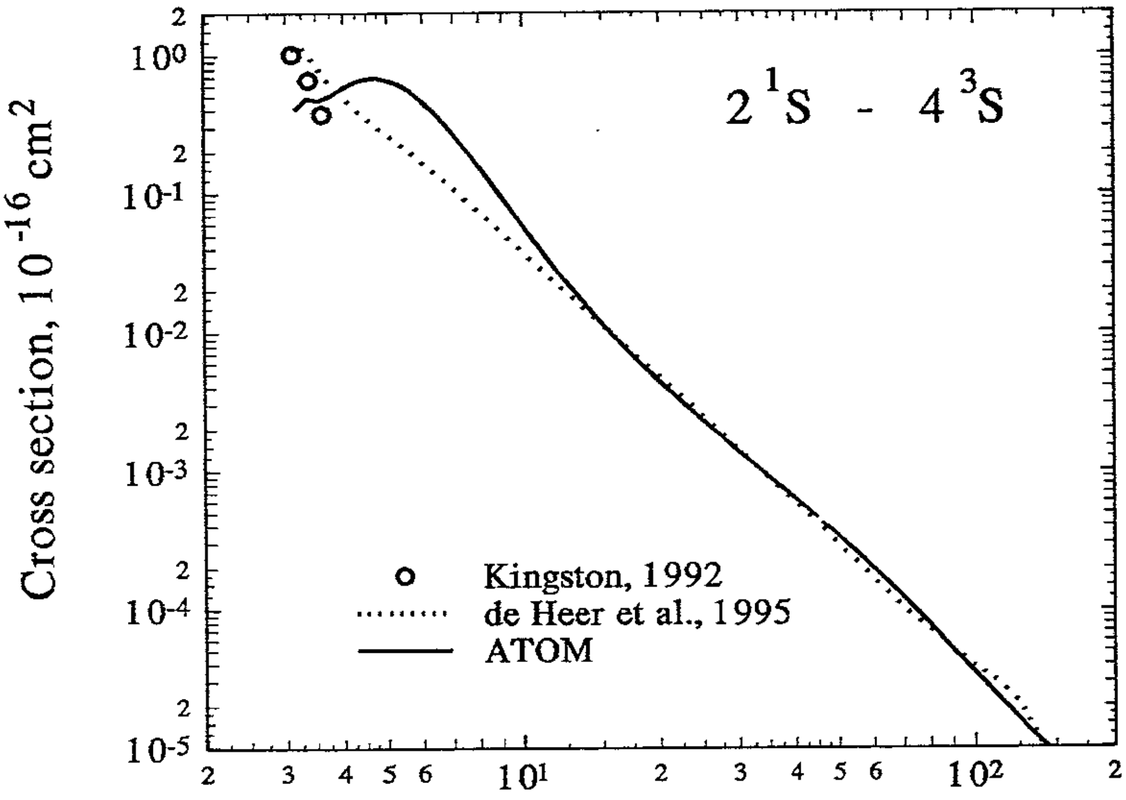

Fig.86 Electron energy, eV

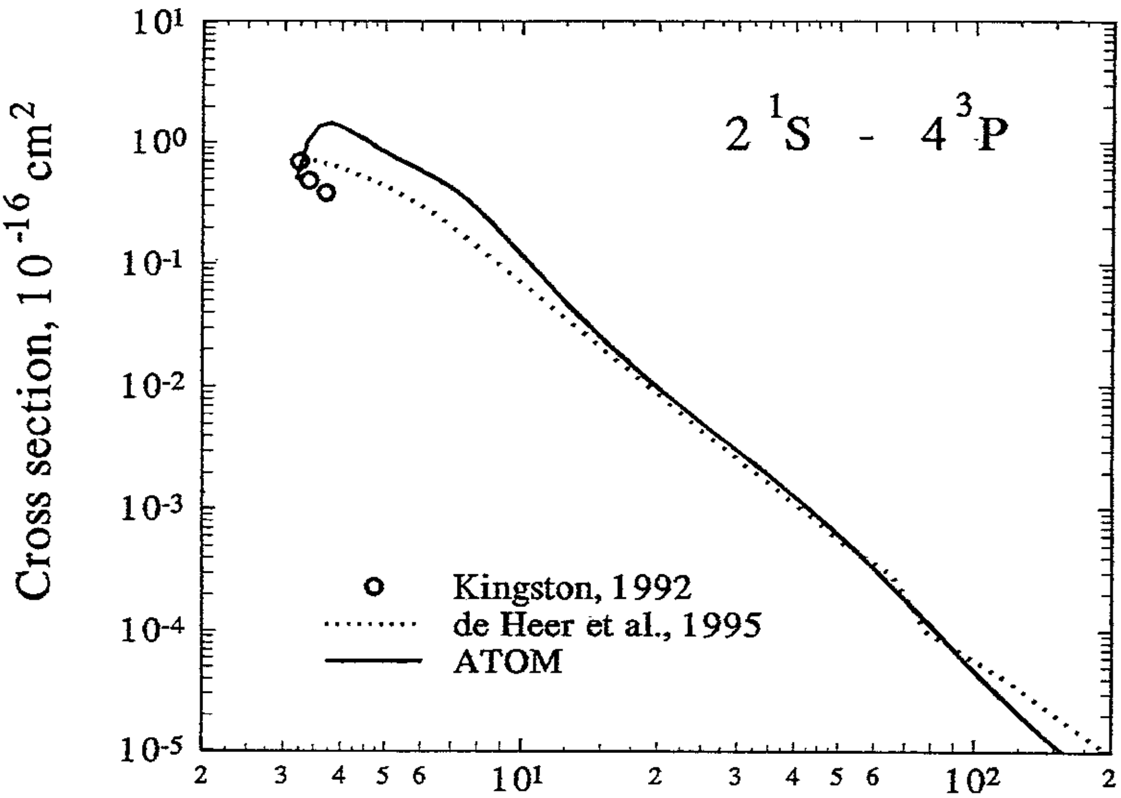

Fig.87 Electron energy, eV

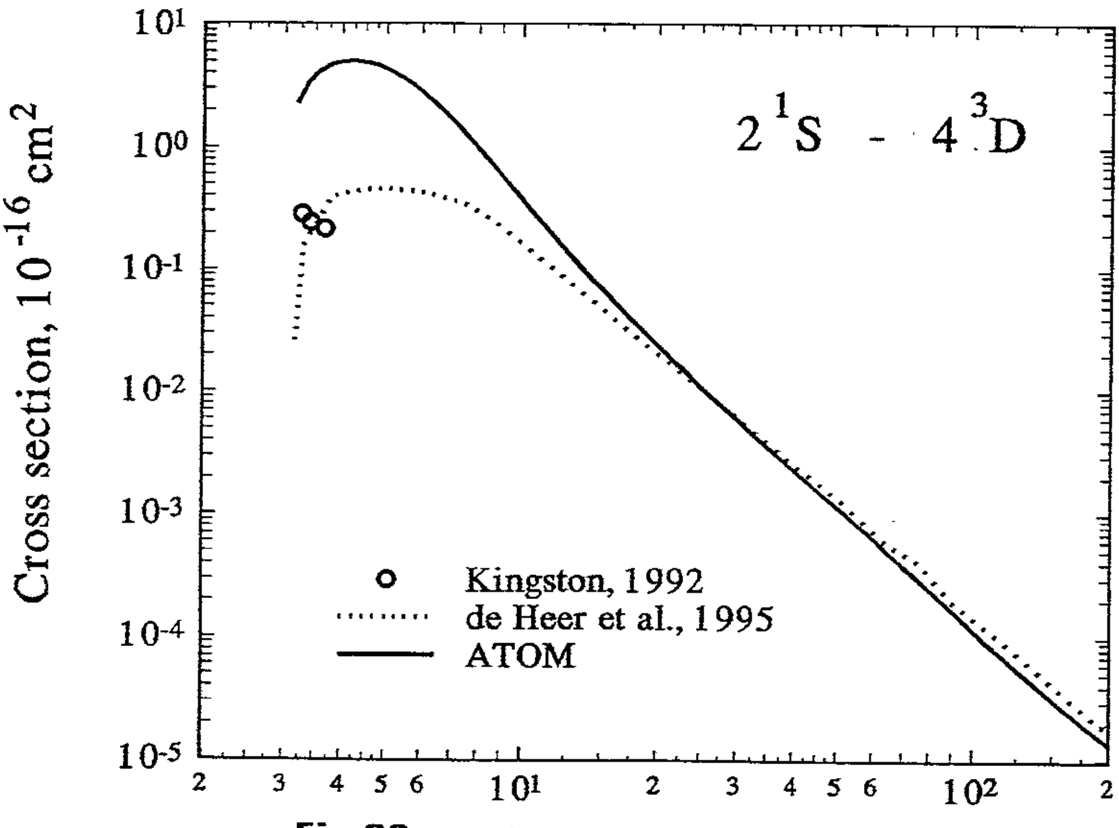

Fig.88 Electron energy, eV

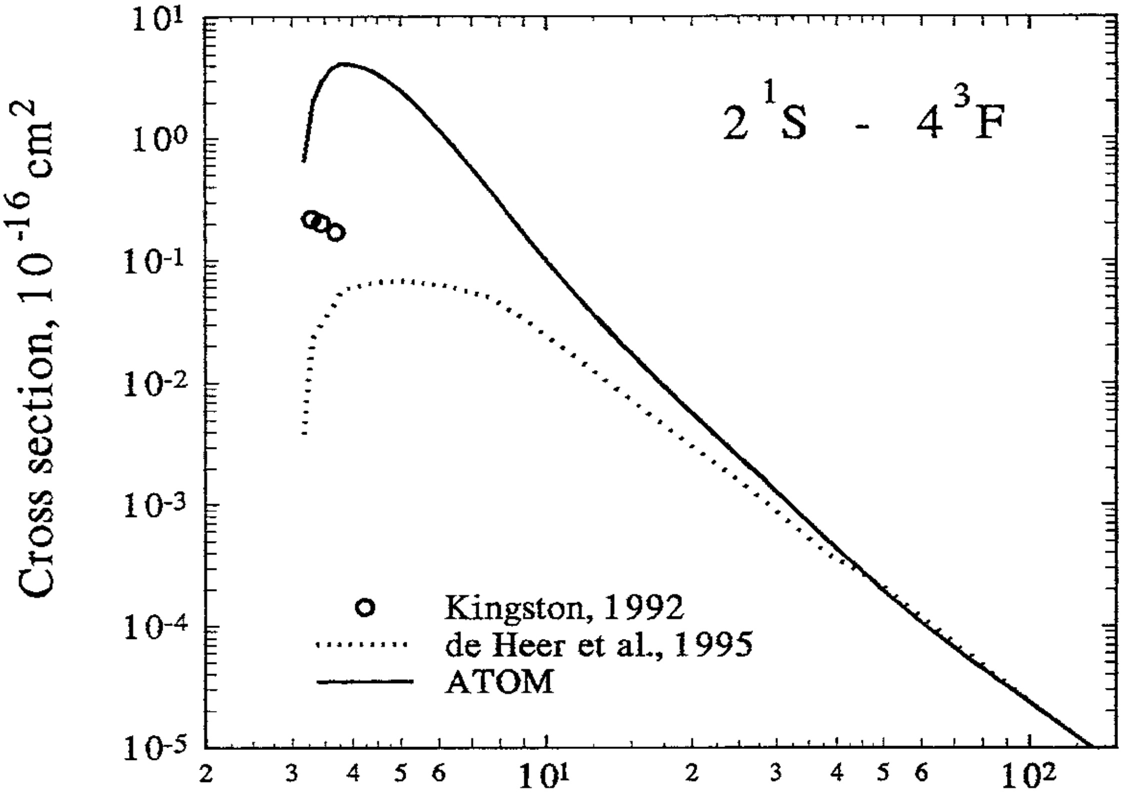

Fig.89 Electron energy, eV

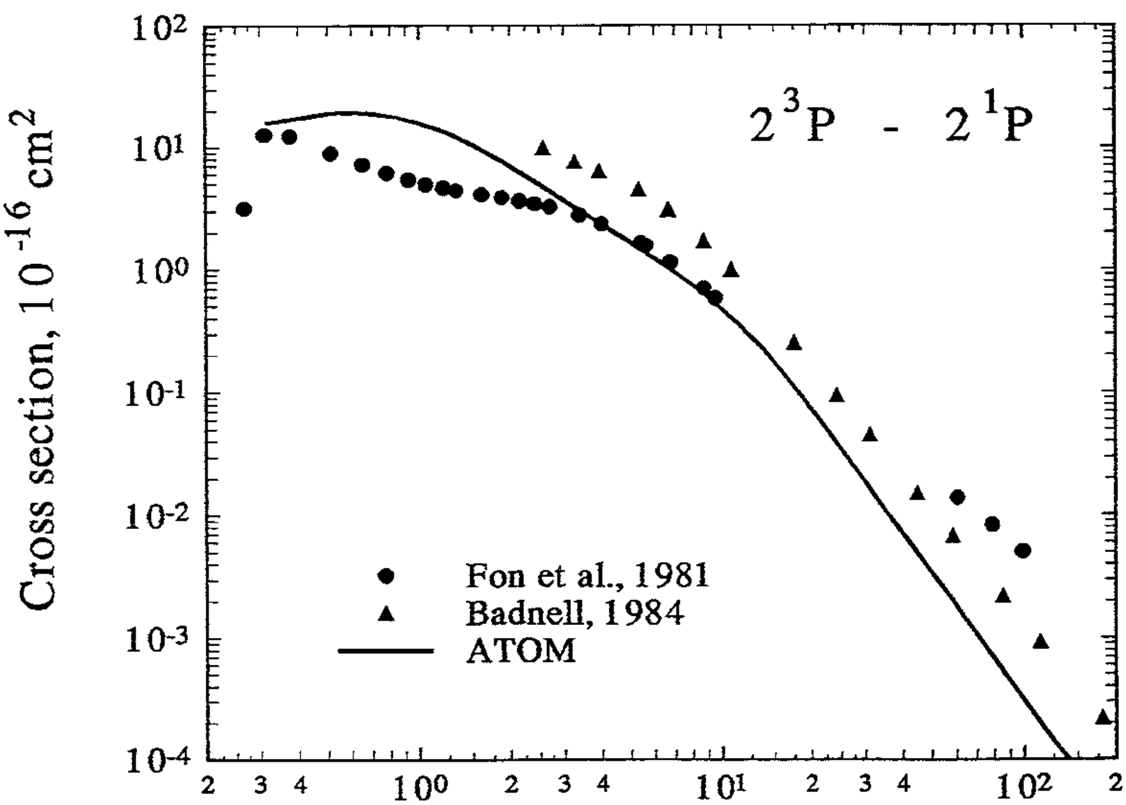

Fig.90 Electron energy, eV

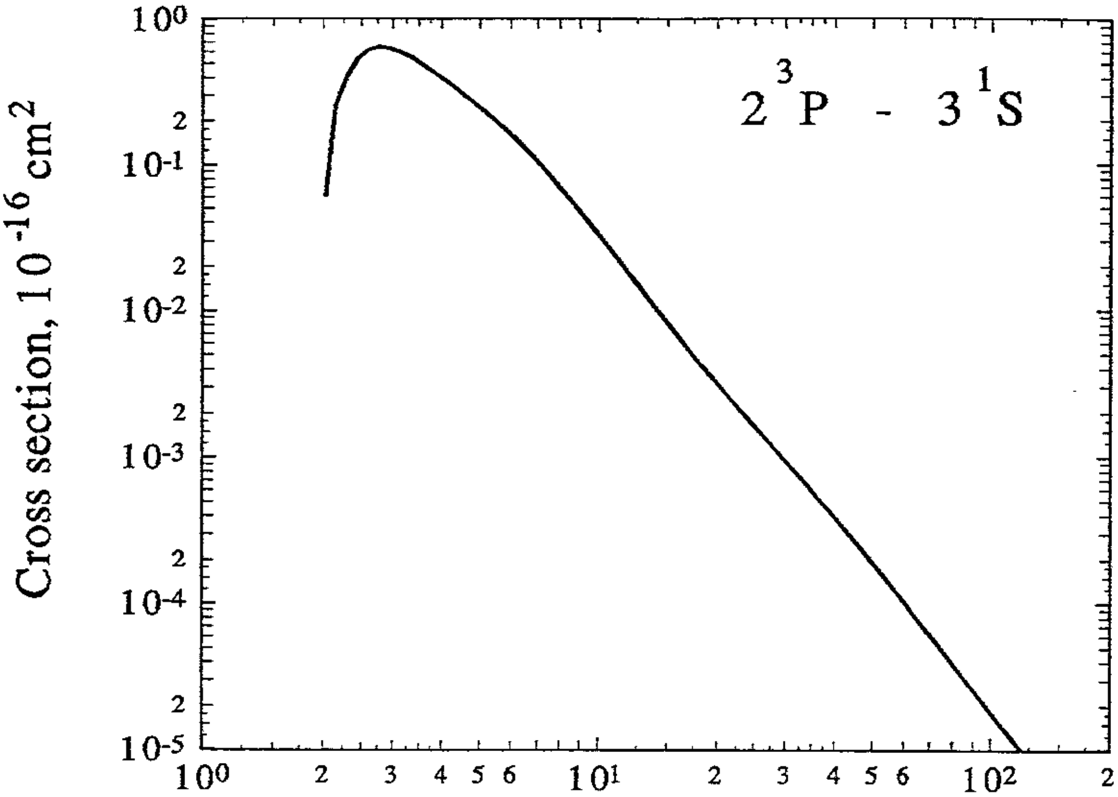
$2\,^3P - 3\,^1S$
Cross section, 10^{-16} cm^2
Electron energy, eV

Fig.91

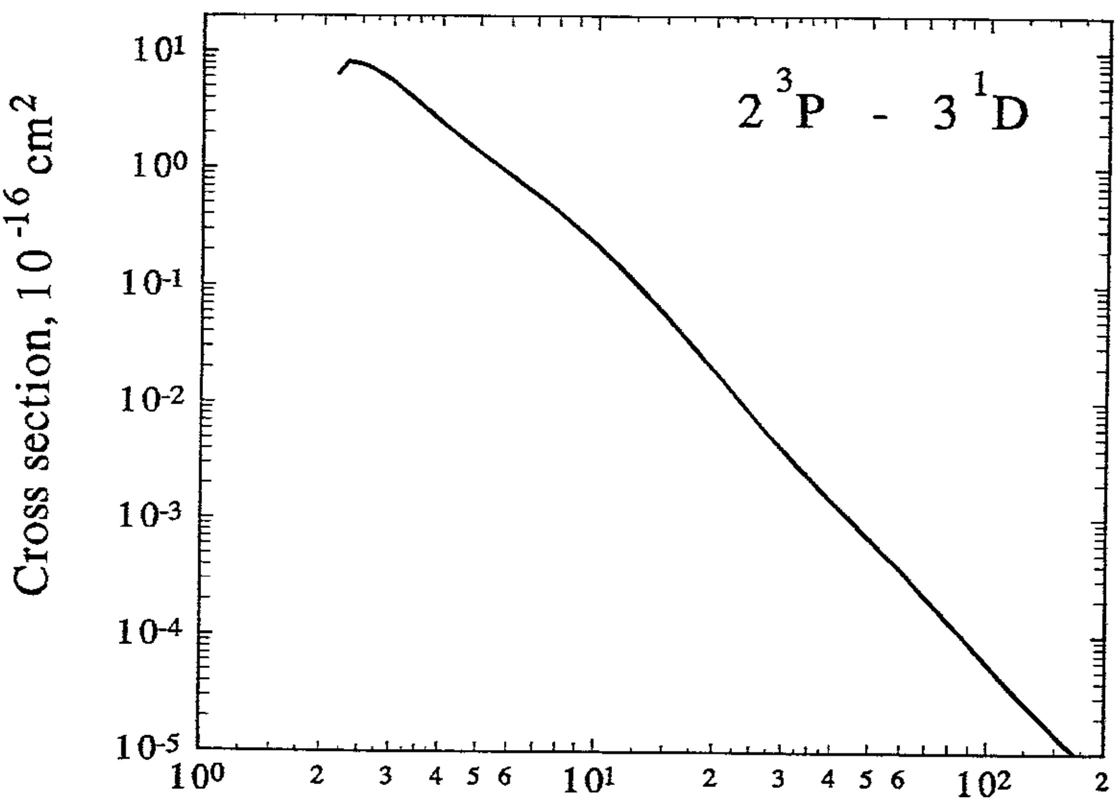
$2\,^3P - 3\,^1D$
Cross section, 10^{-16} cm^2
Electron energy, eV

Fig.92

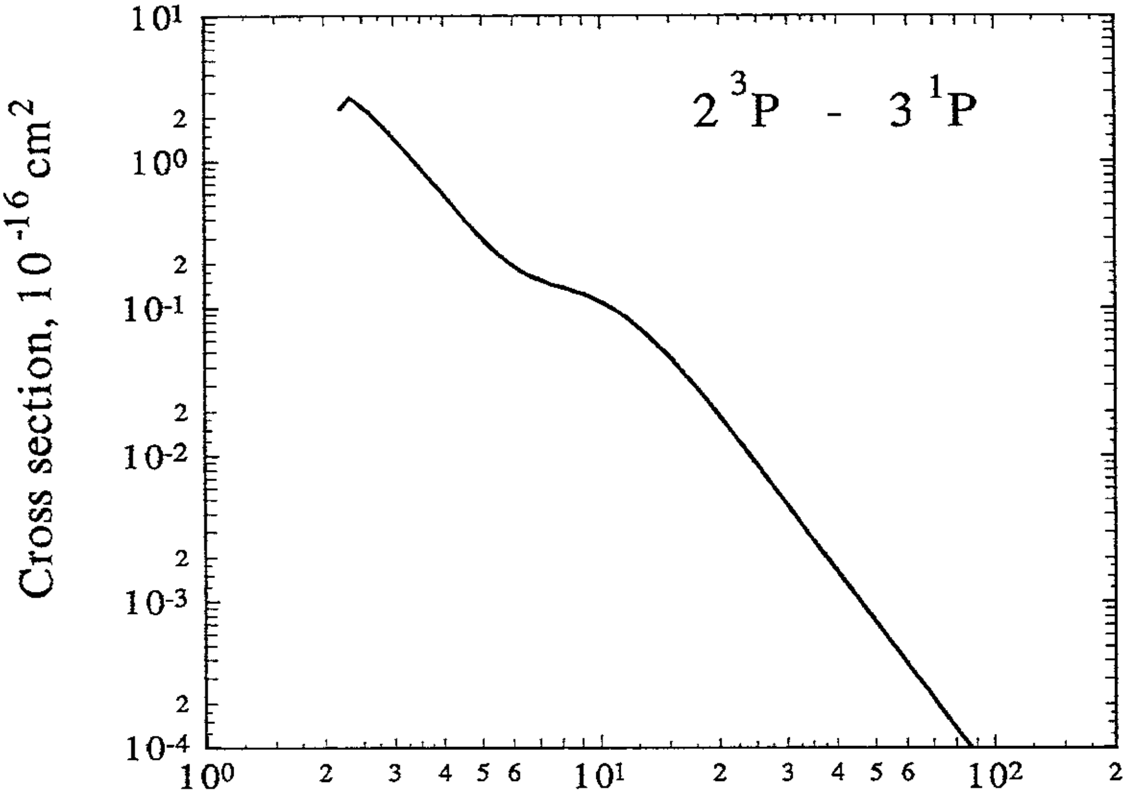

Fig.93 Electron energy, eV

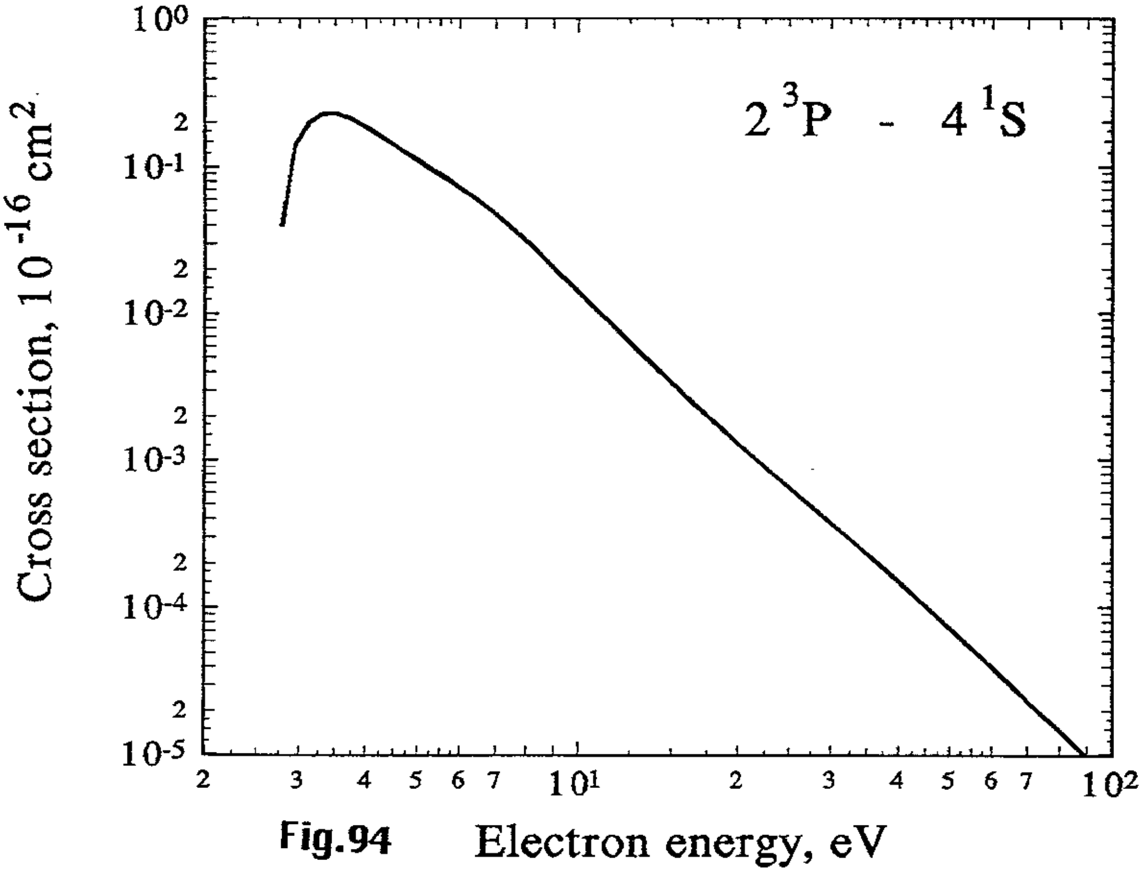

Fig.94 Electron energy, eV

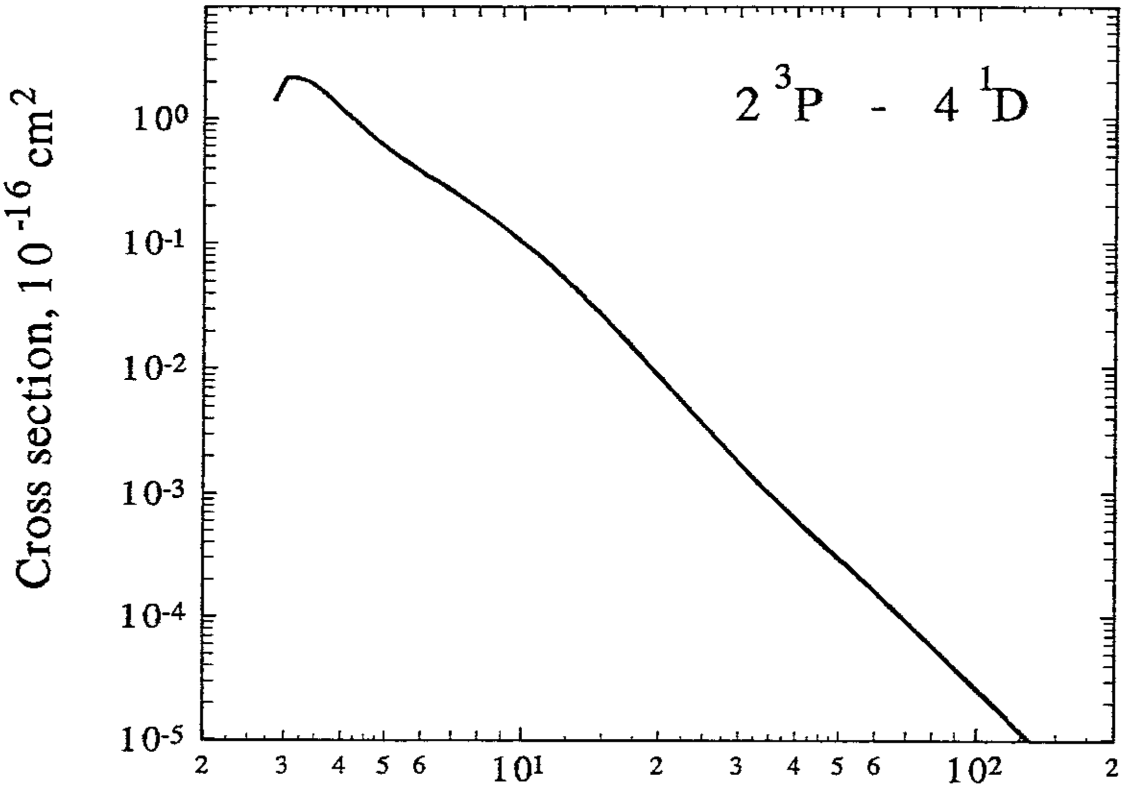

Fig.95 Electron energy, eV

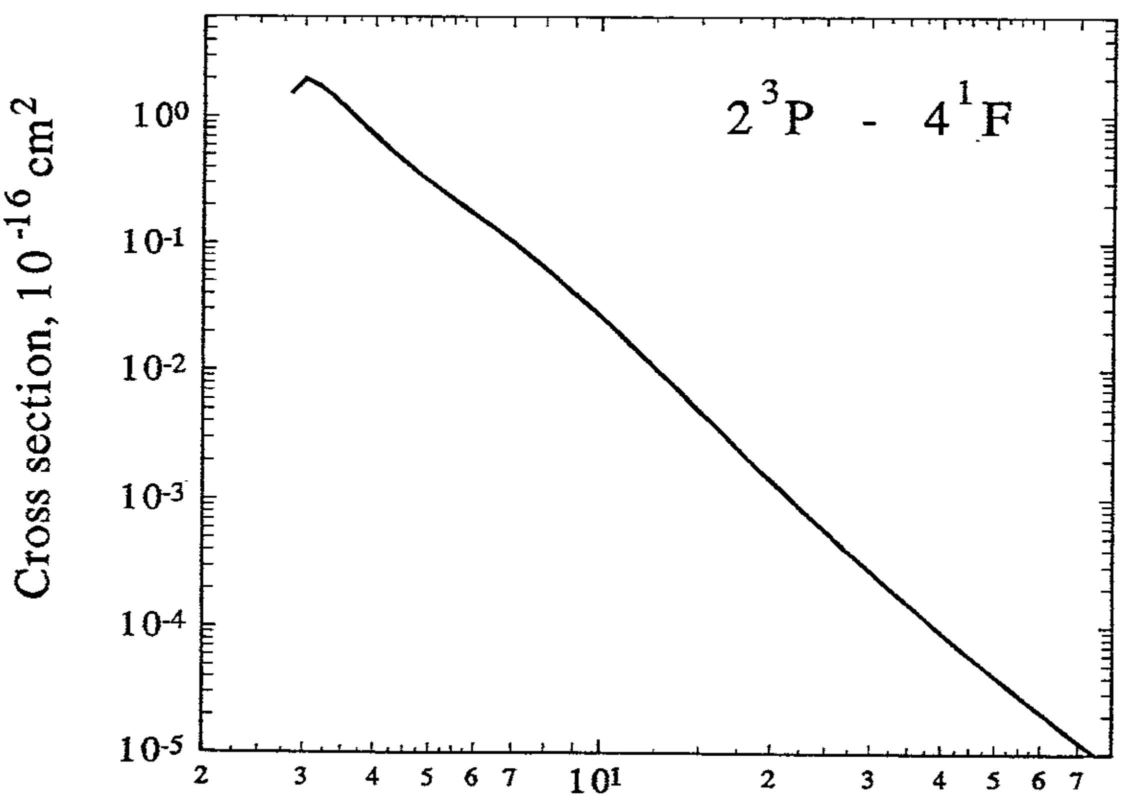

Fig.96 Electron energy, eV

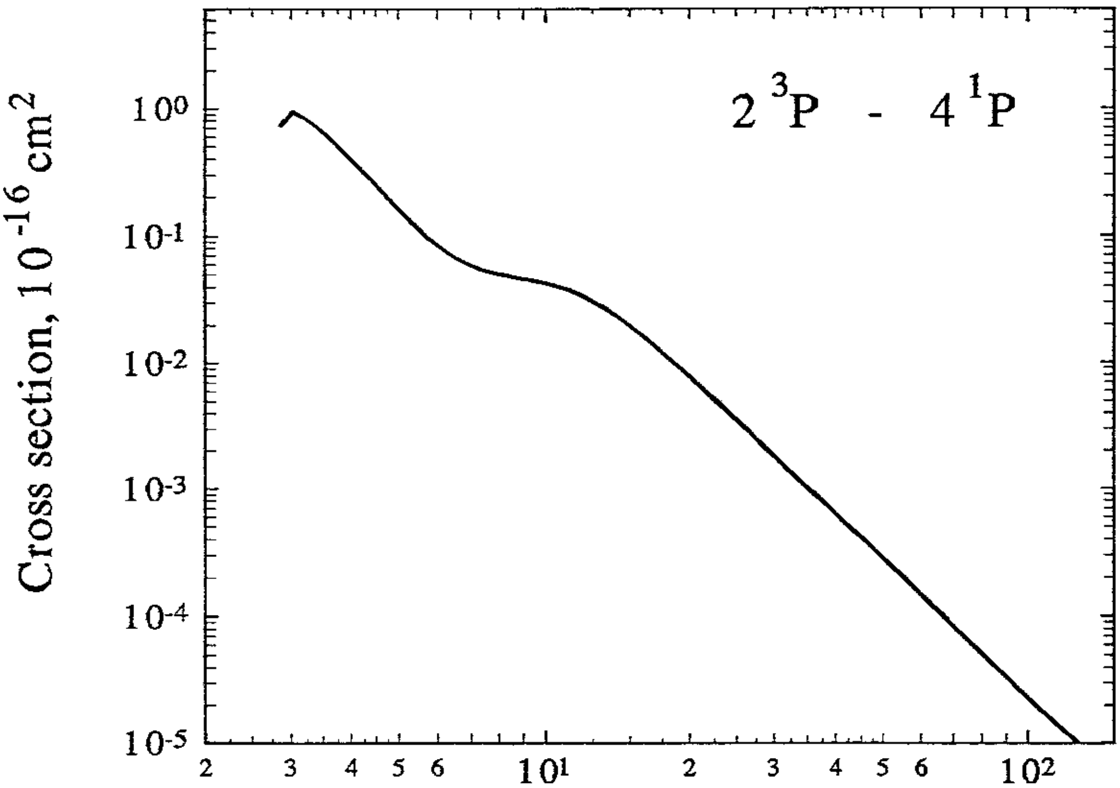

Fig.97 Electron energy, eV

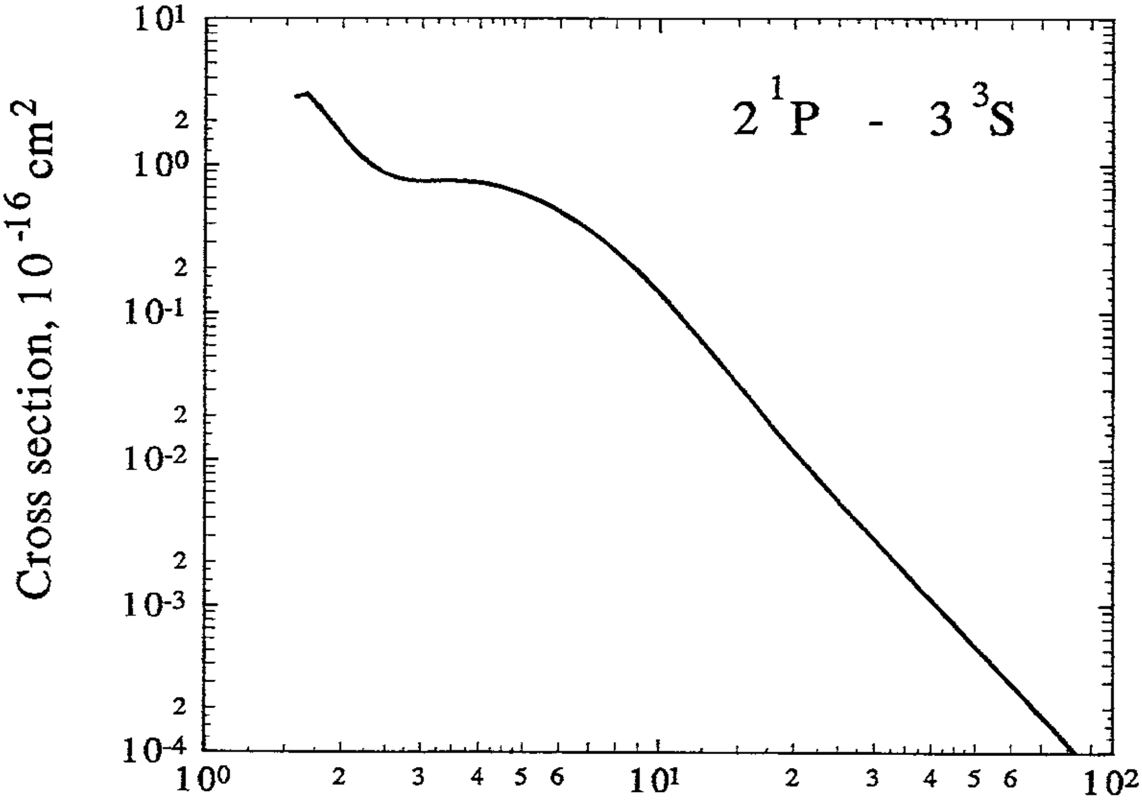

Fig.98 Electron energy, eV

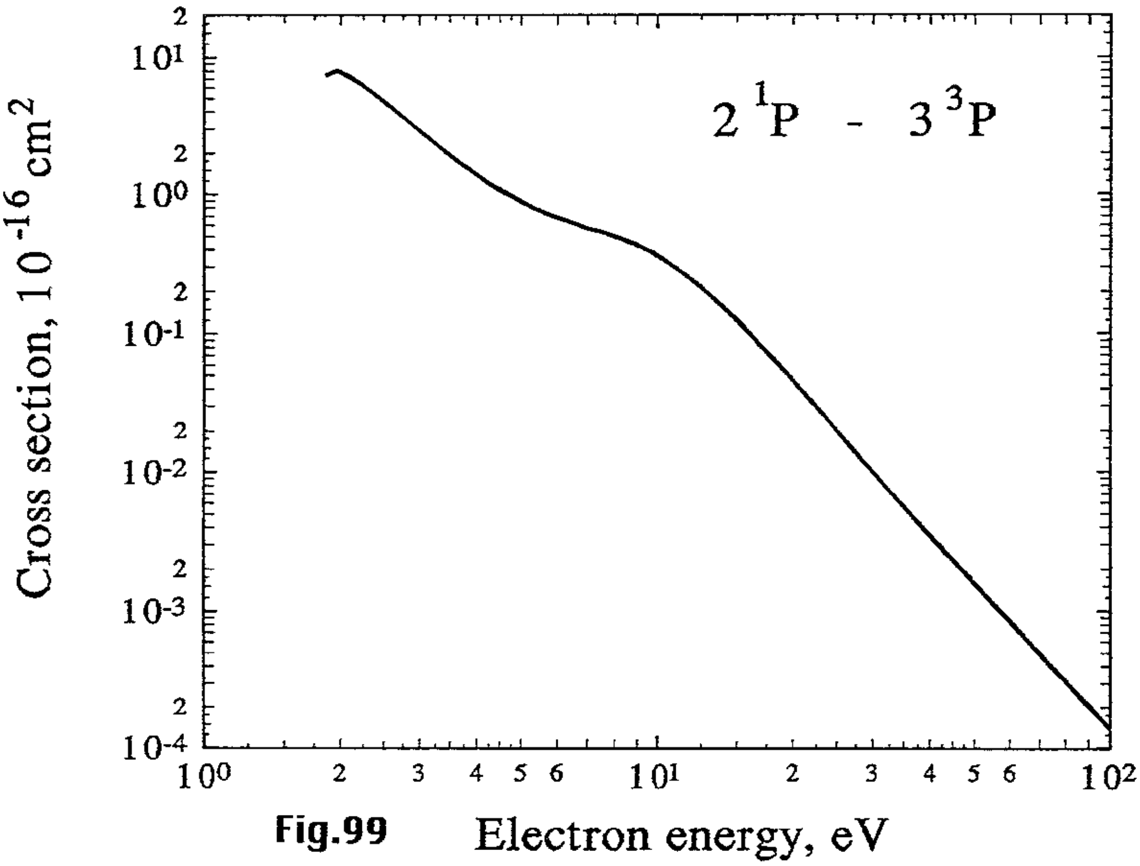

Fig.99

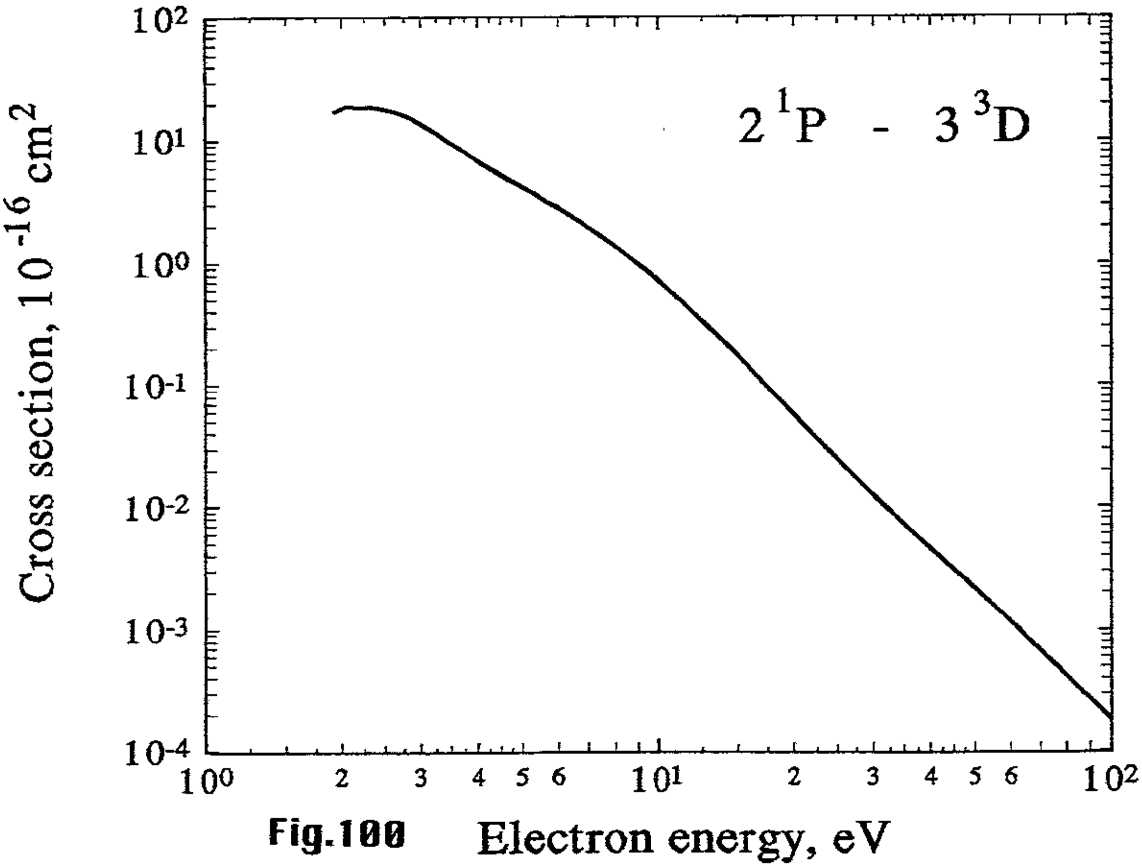

Fig.100

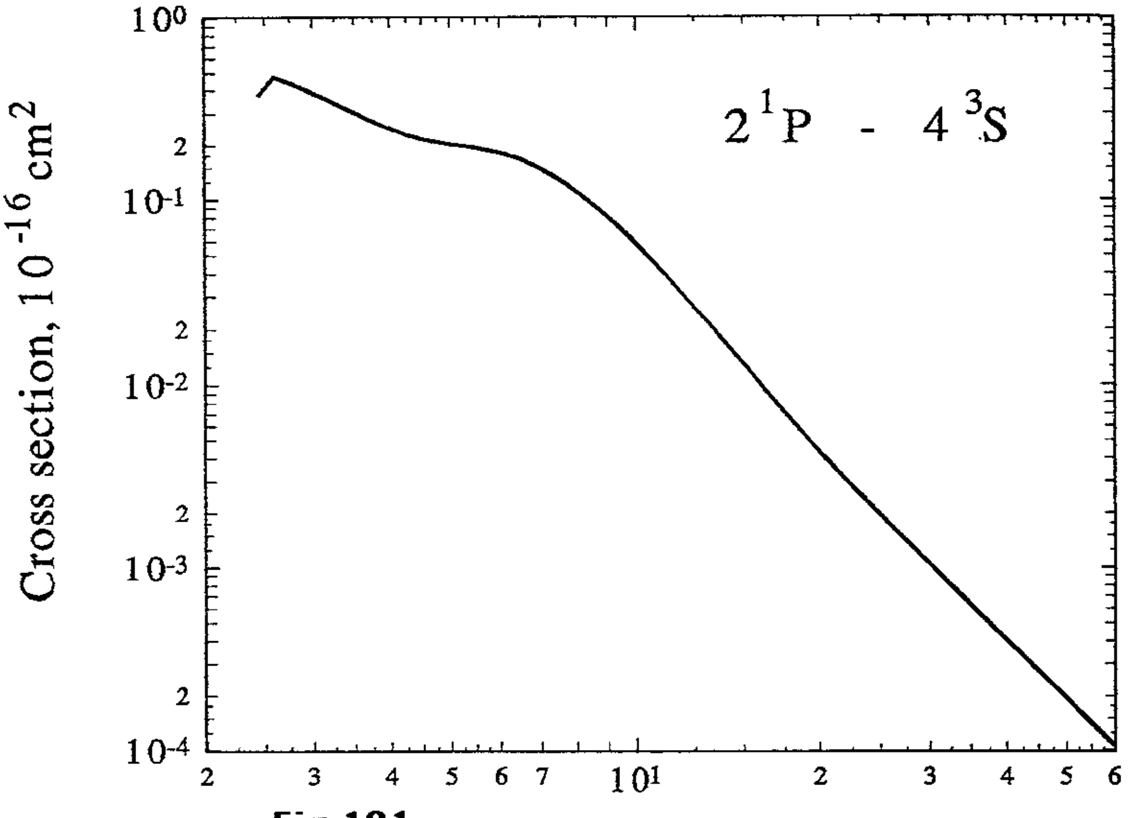

Fig.101 Electron energy, eV

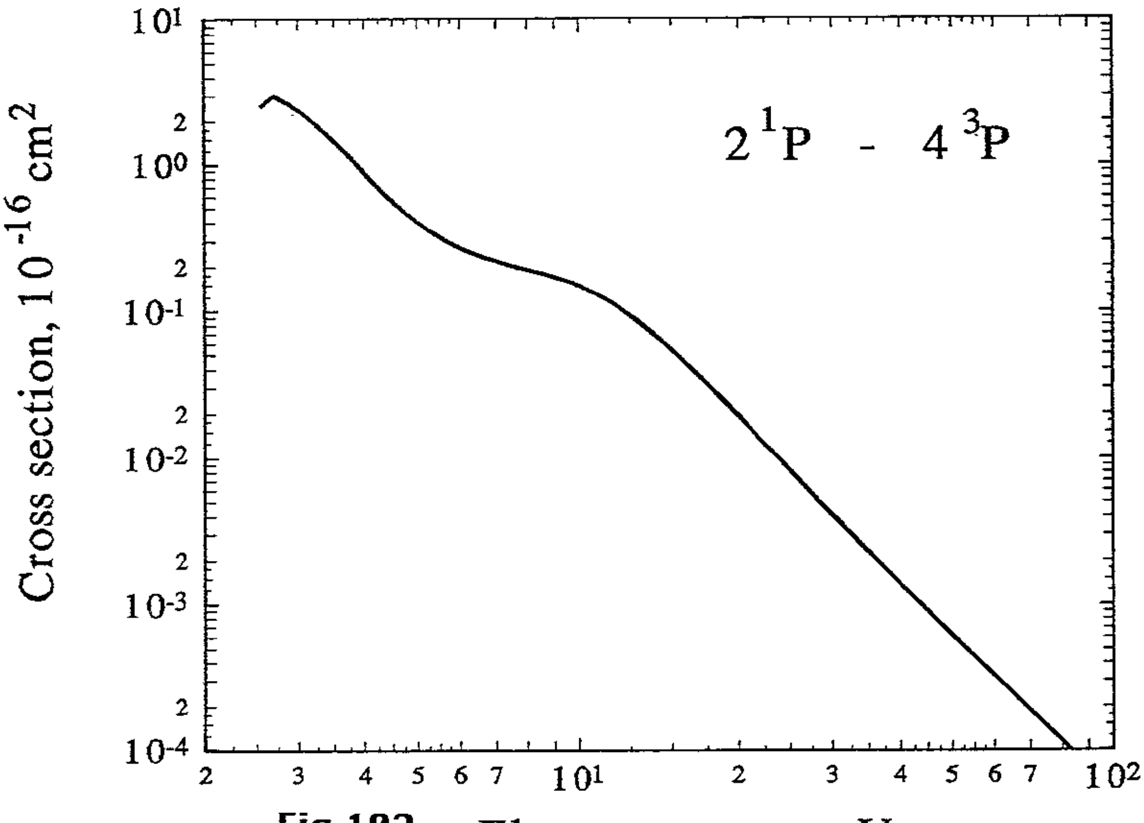

Fig.102 Electron energy, eV

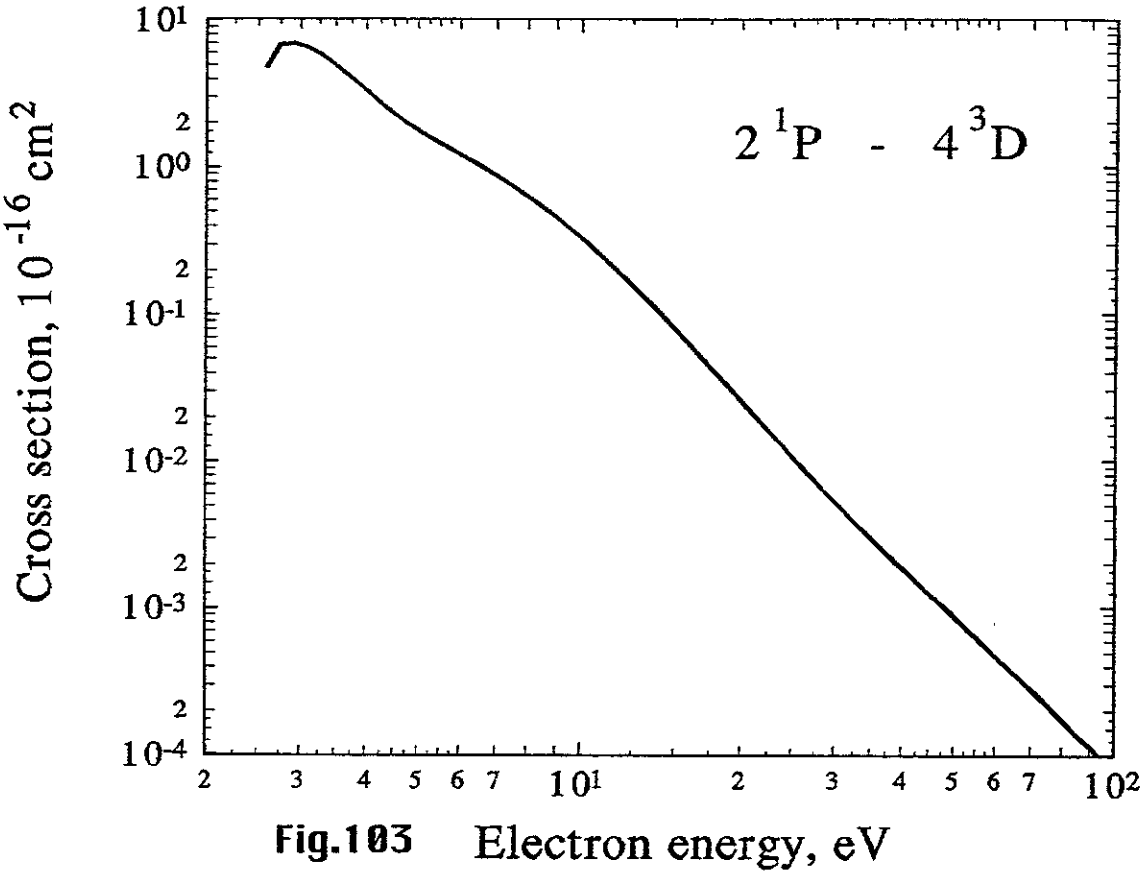

Fig.103

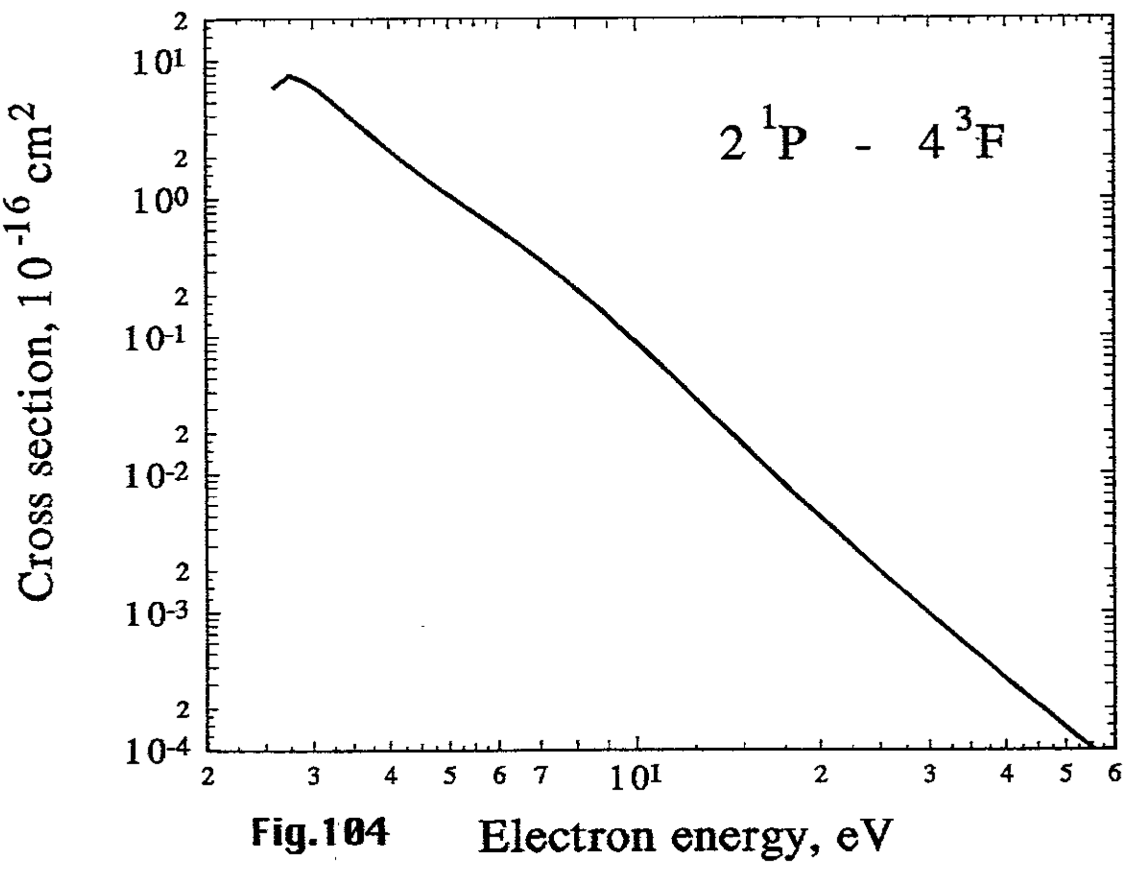

Fig.104

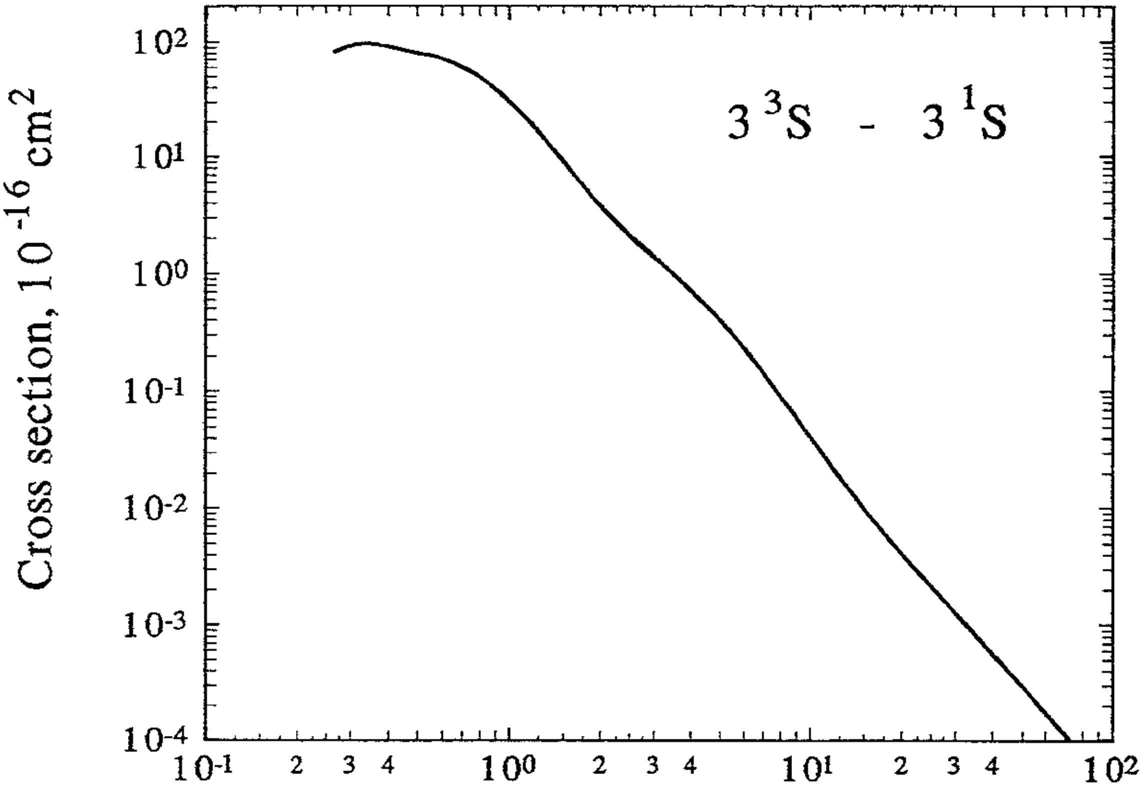

Fig.105 Electron energy, eV

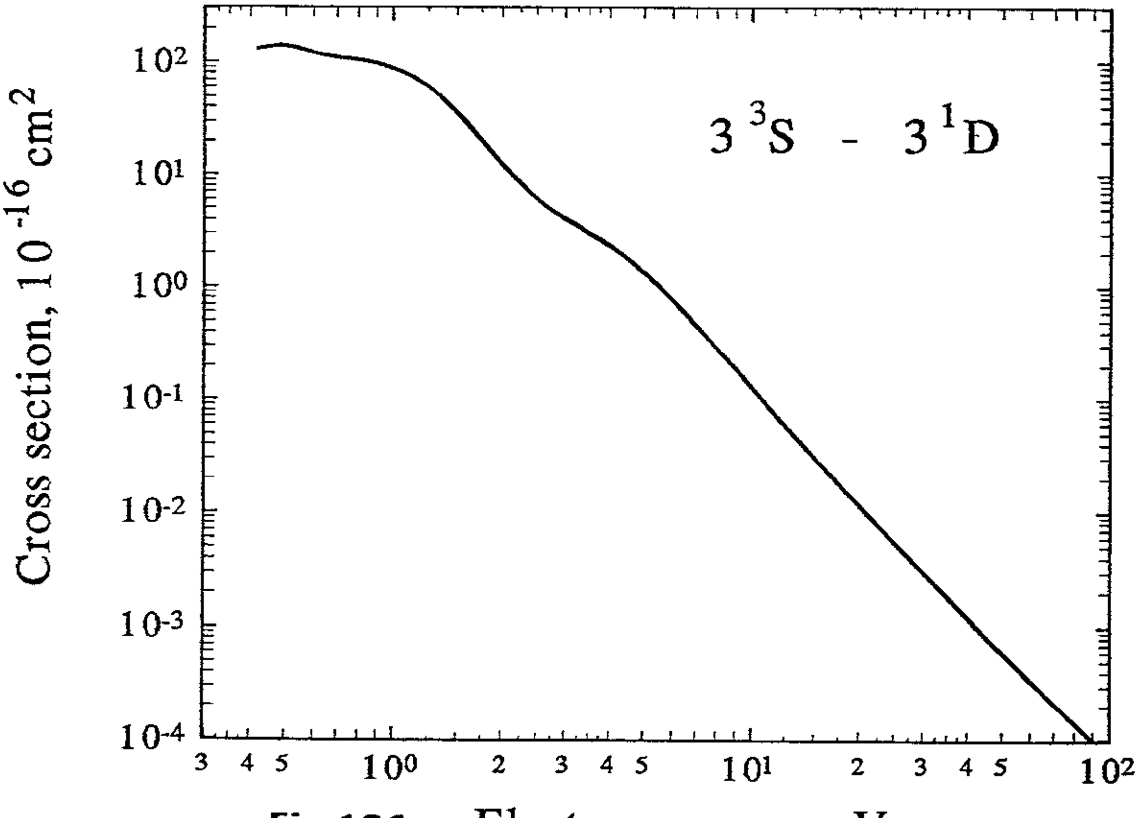

Fig.106 Electron energy, eV

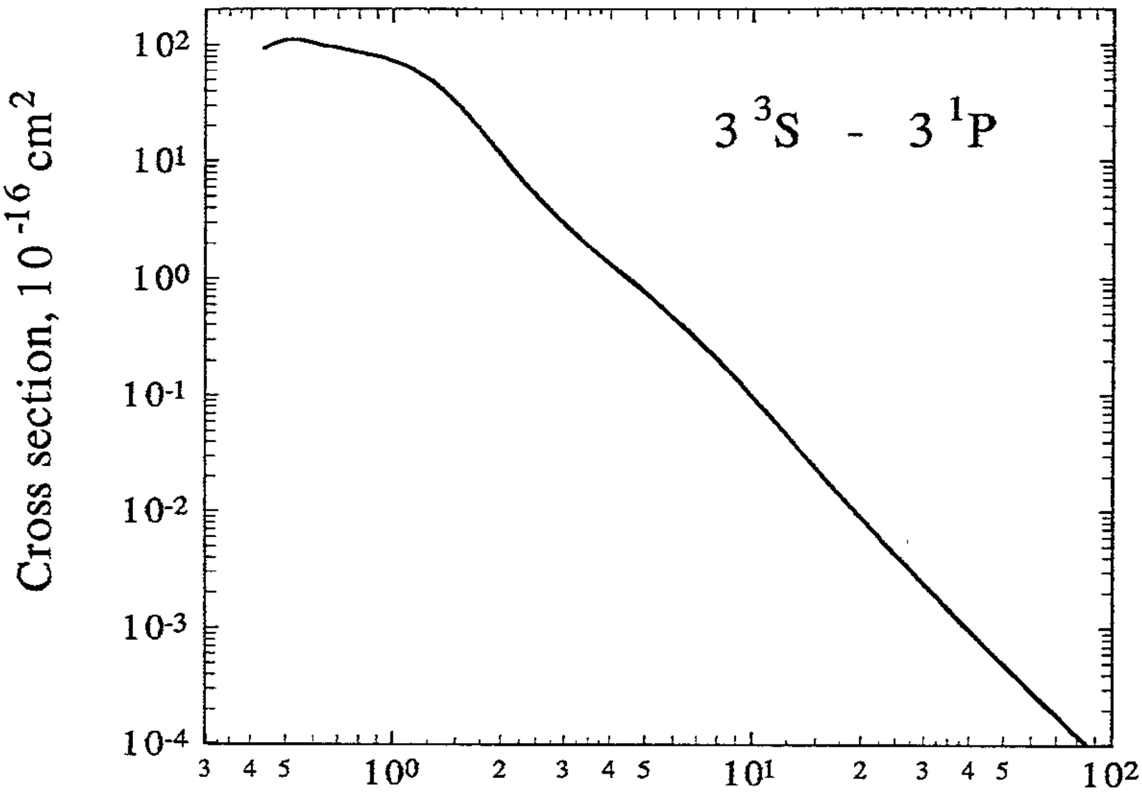

Fig.107 Electron energy, eV

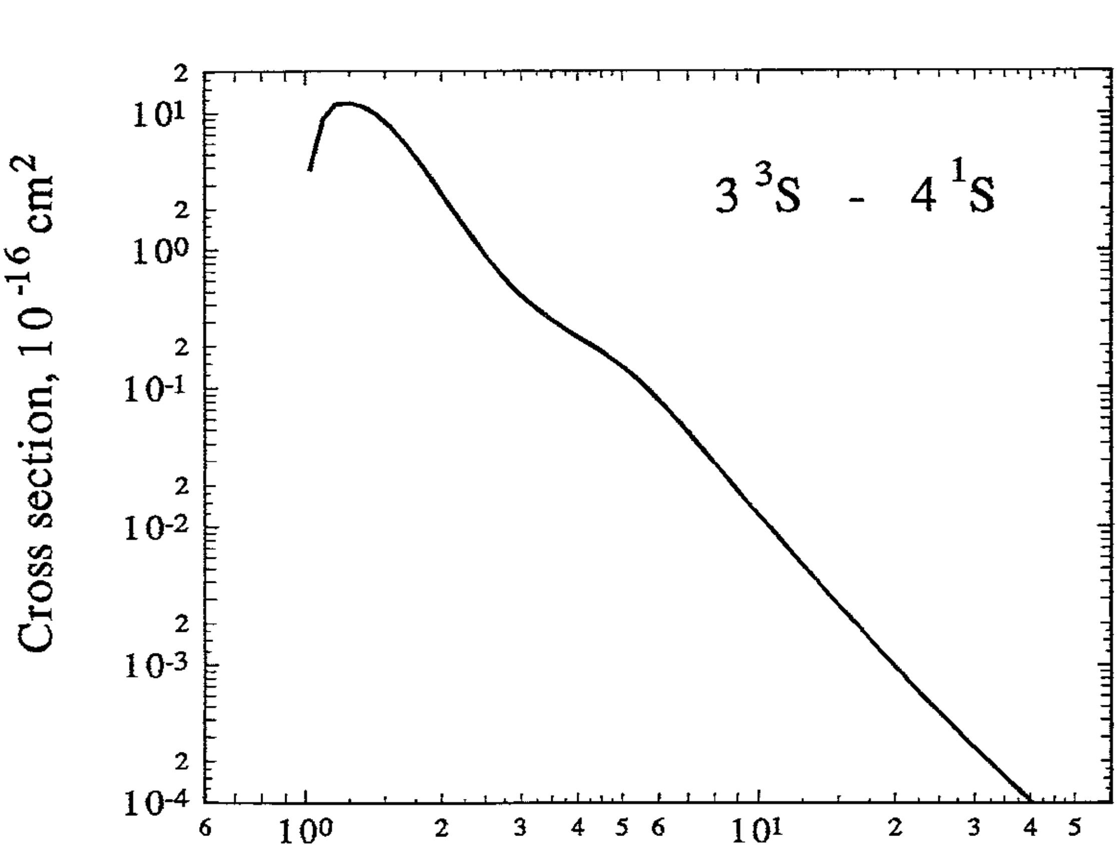

Fig.108 Electron energy, eV

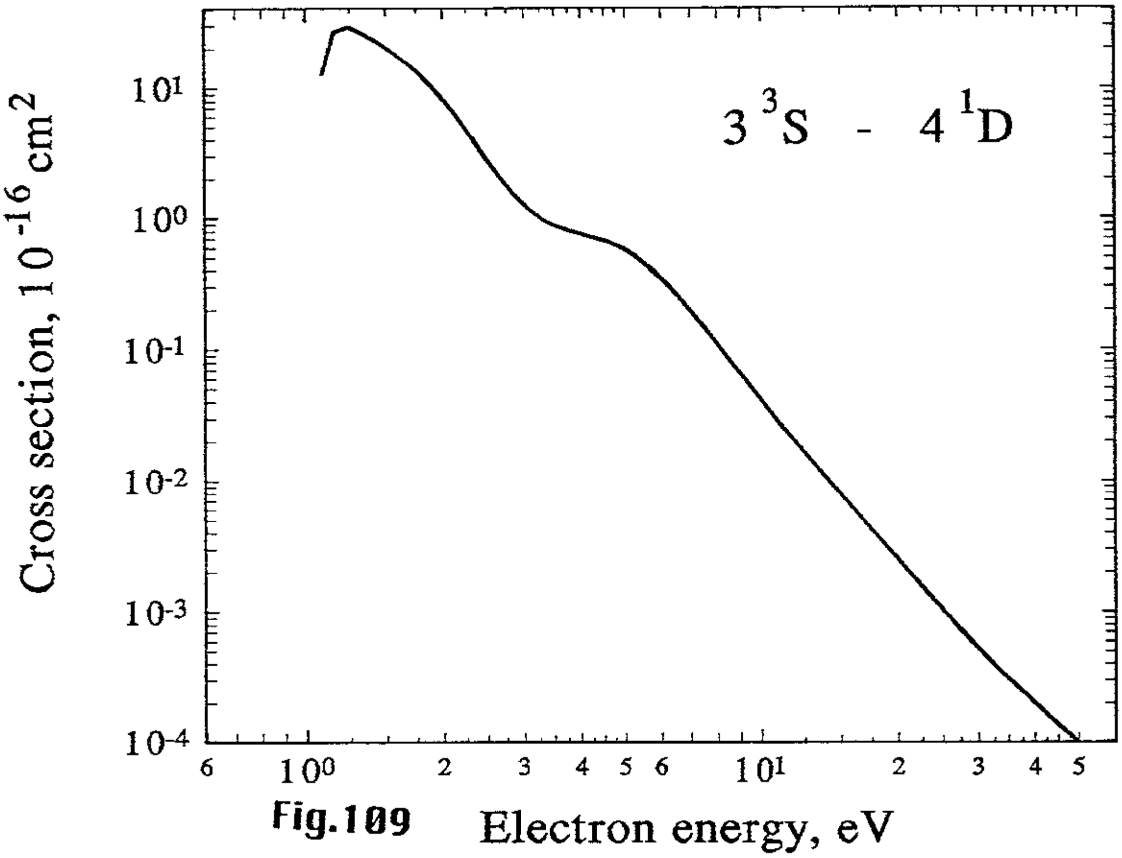

Fig.109

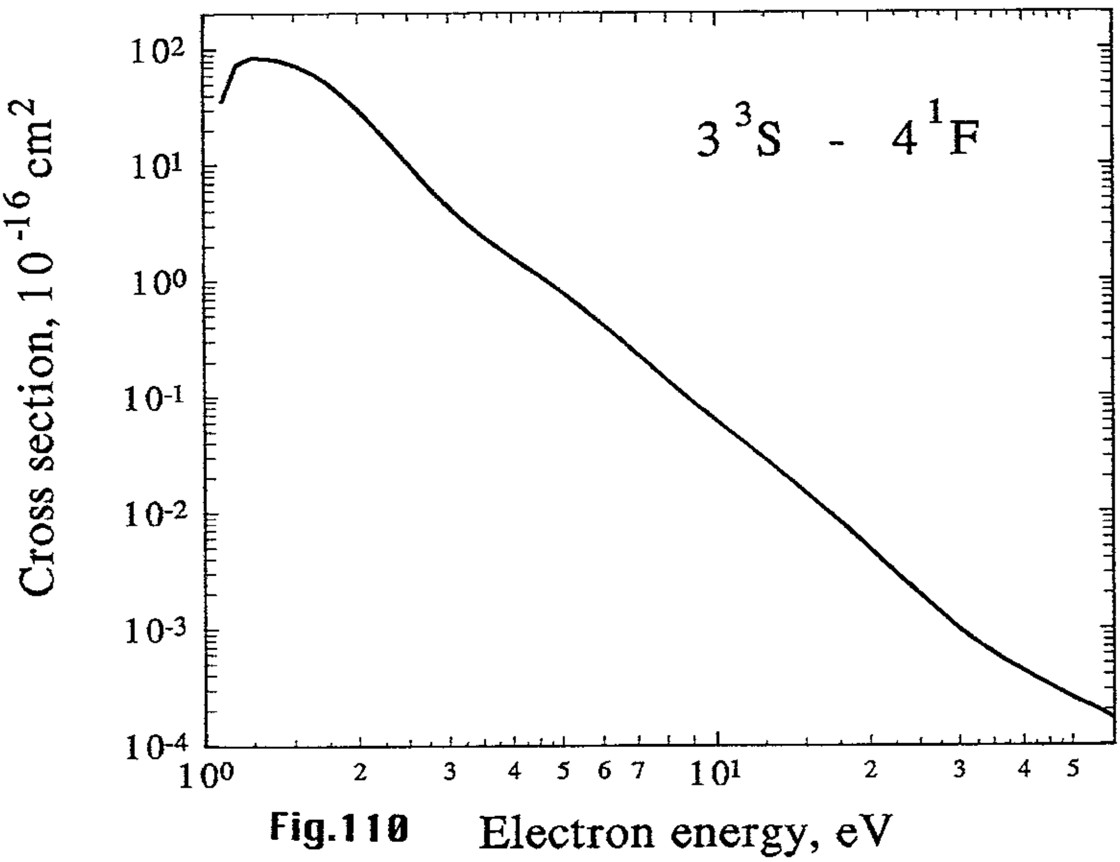

Fig.110

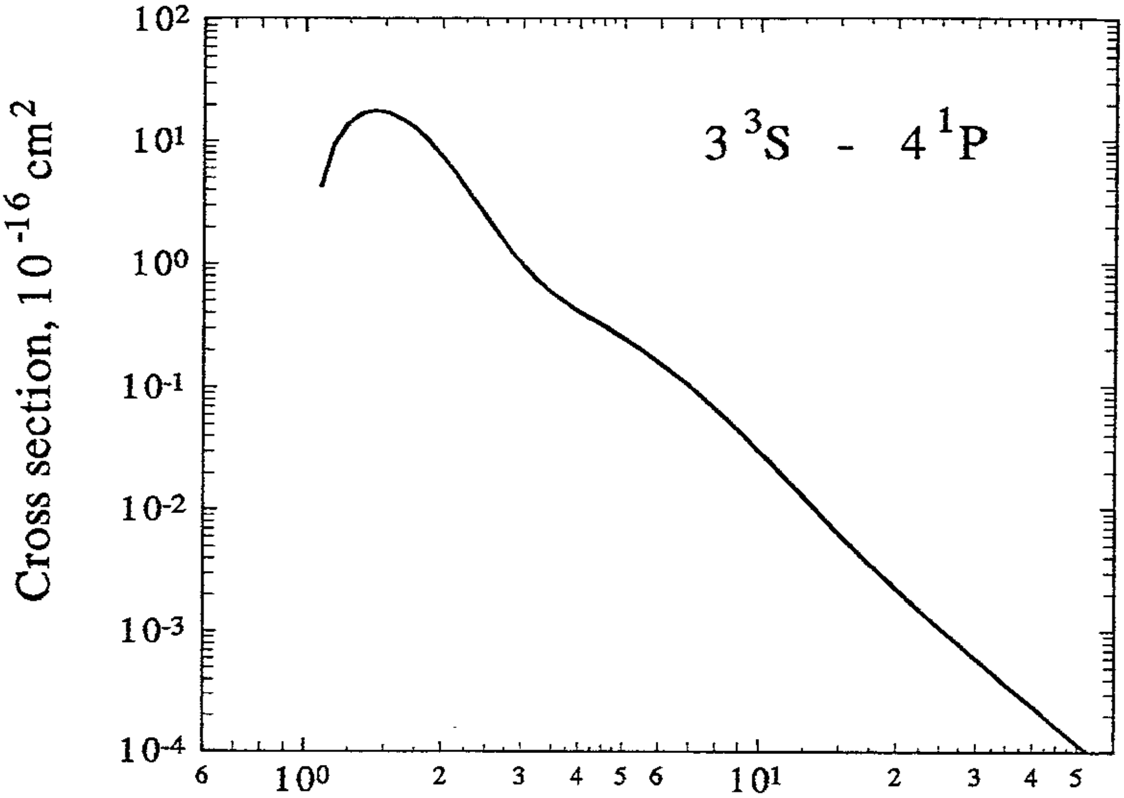

Fig.111 Electron energy, eV

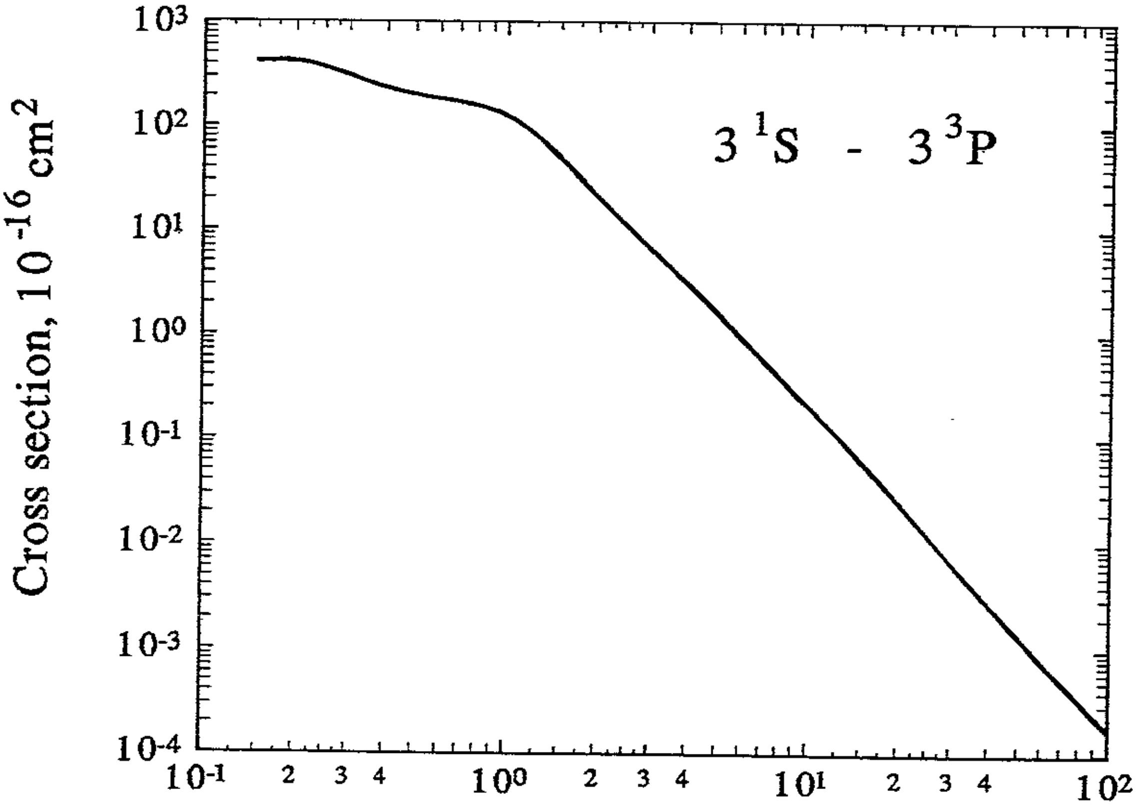

Fig.112 Electron energy, eV

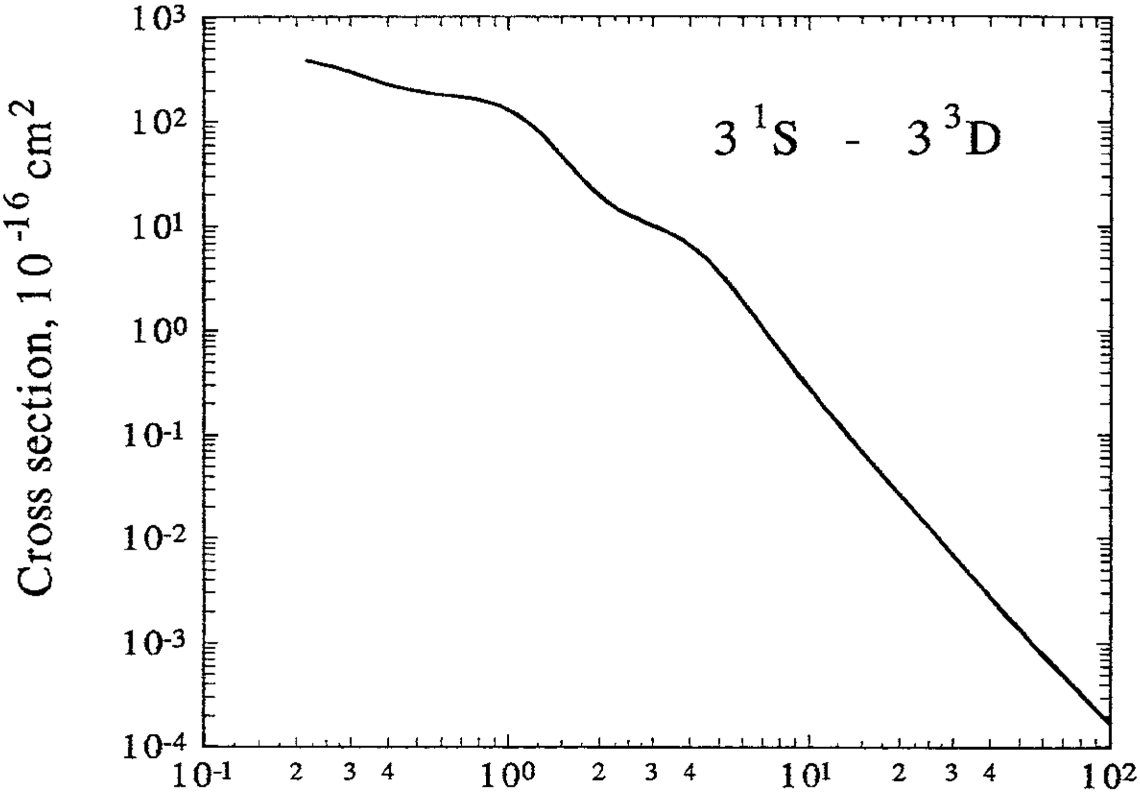

Fig.113 Electron energy, eV

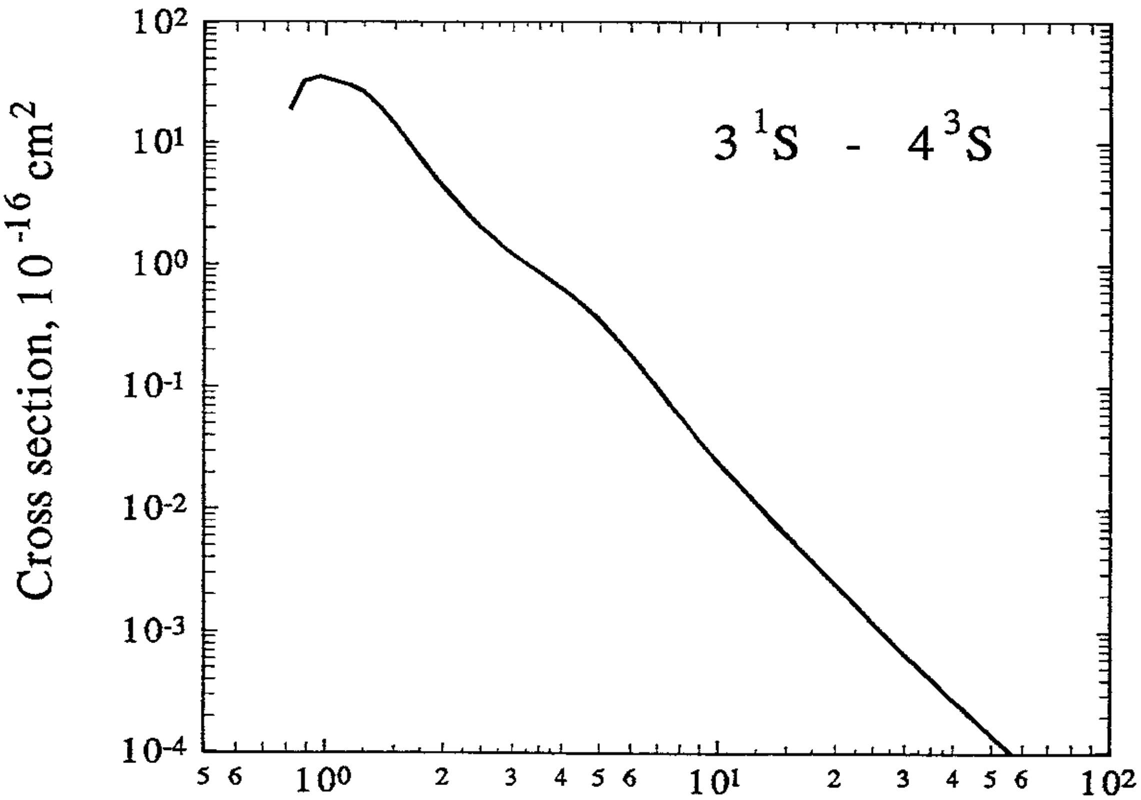

Fig.114 Electron energy, eV

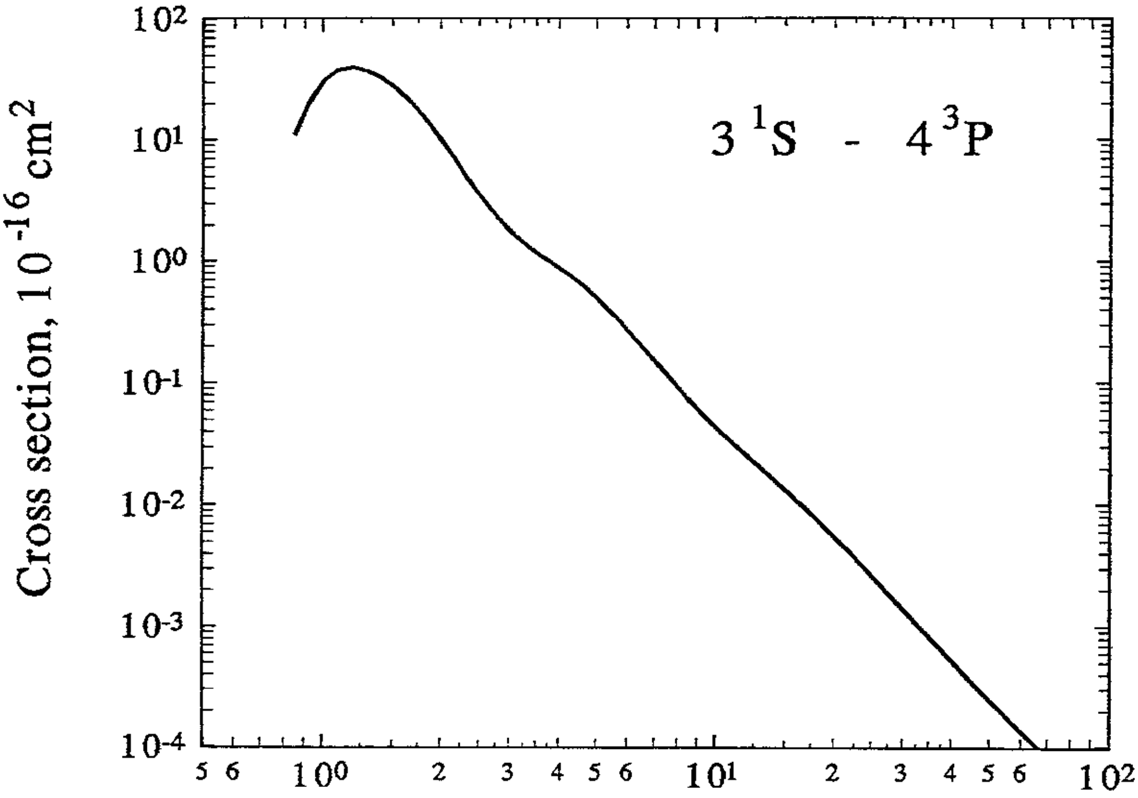

Fig.115 Electron energy, eV

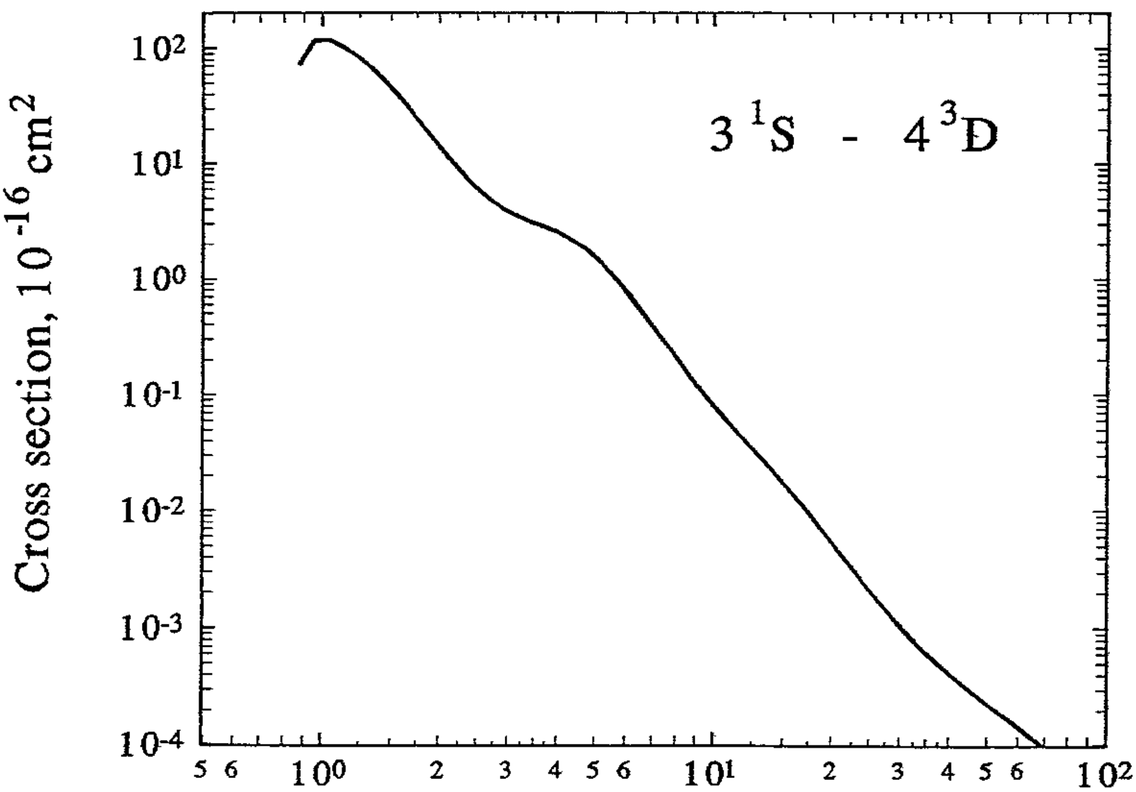

Fig.116 Electron energy, eV

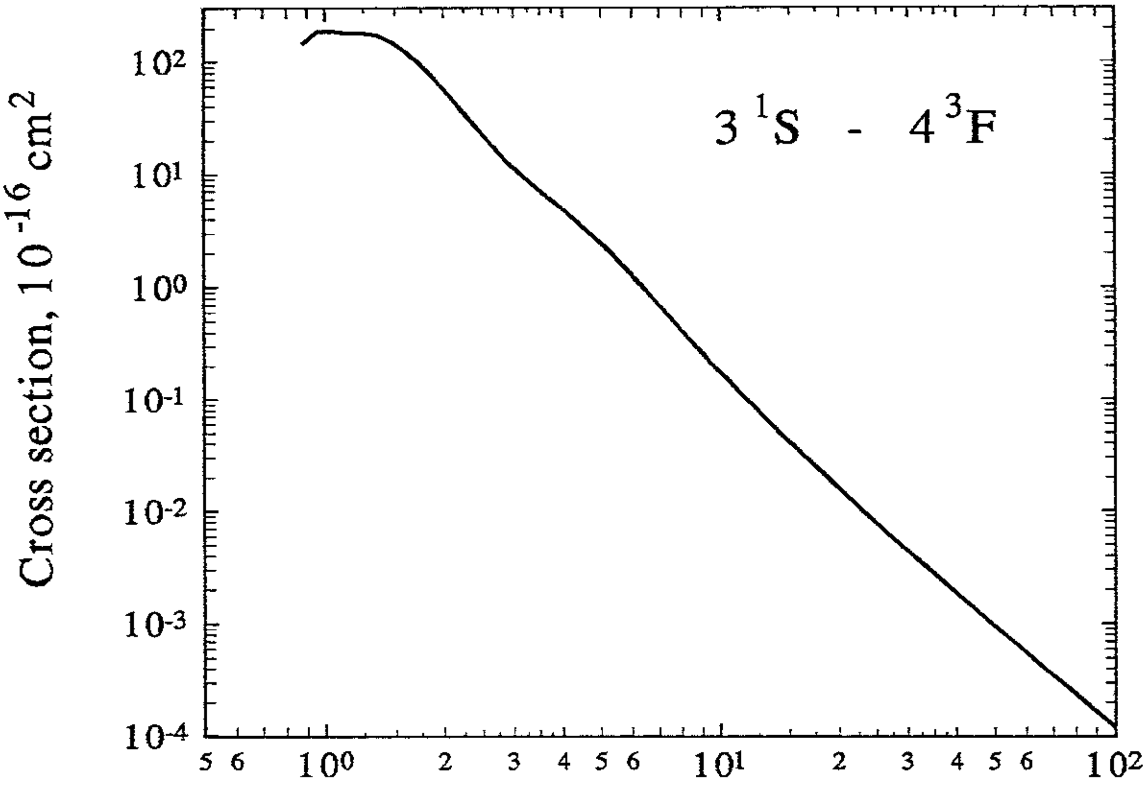

Fig.117 Electron energy, eV

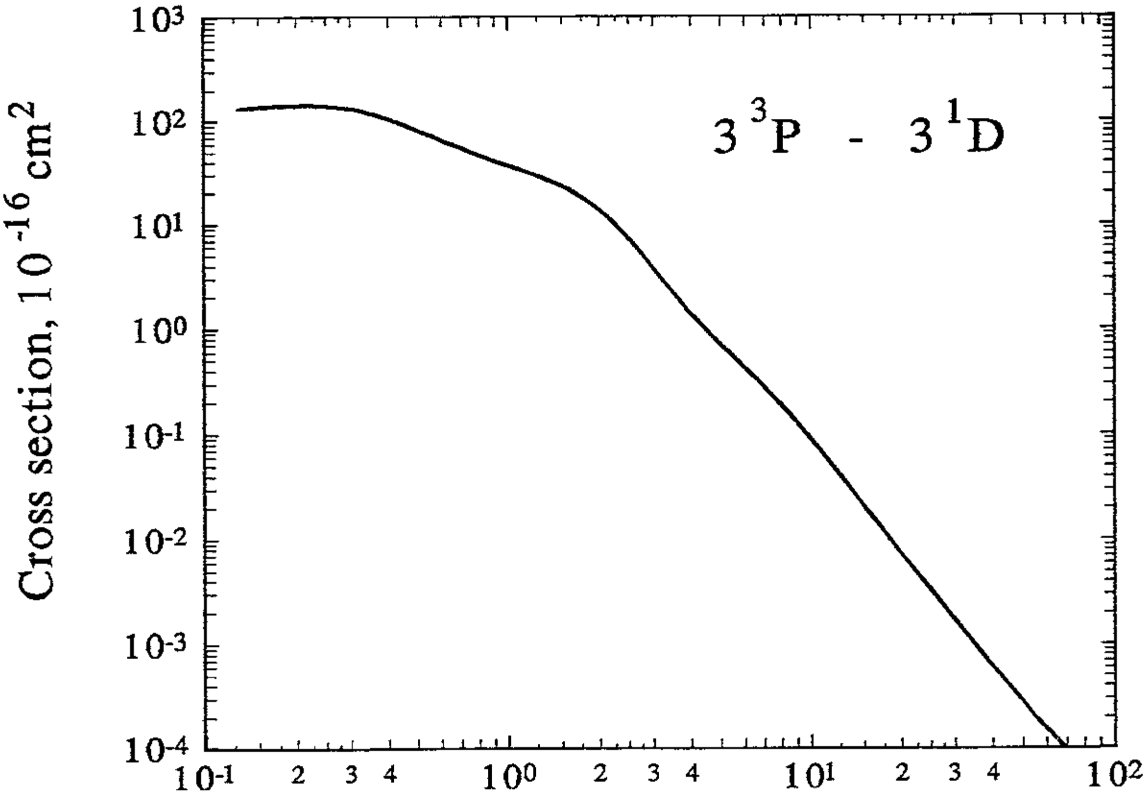

Fig.118 Electron energy, eV

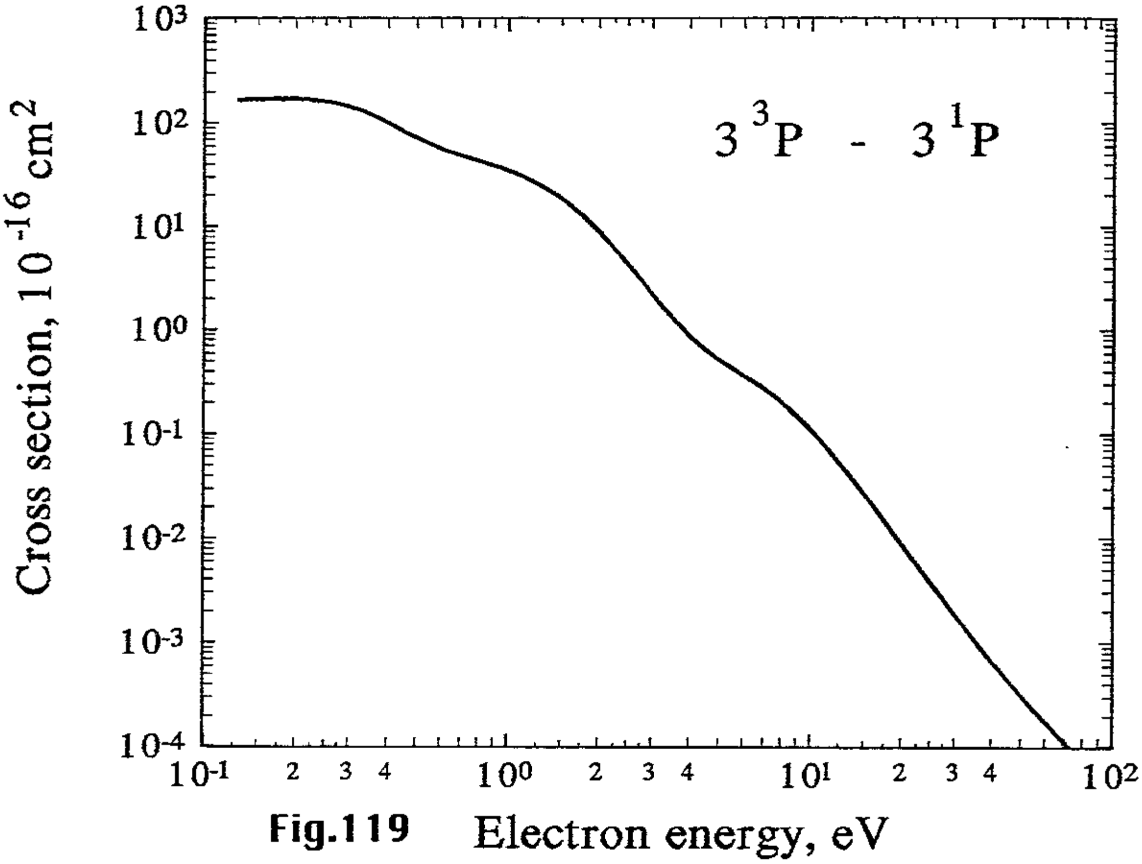

Fig.119

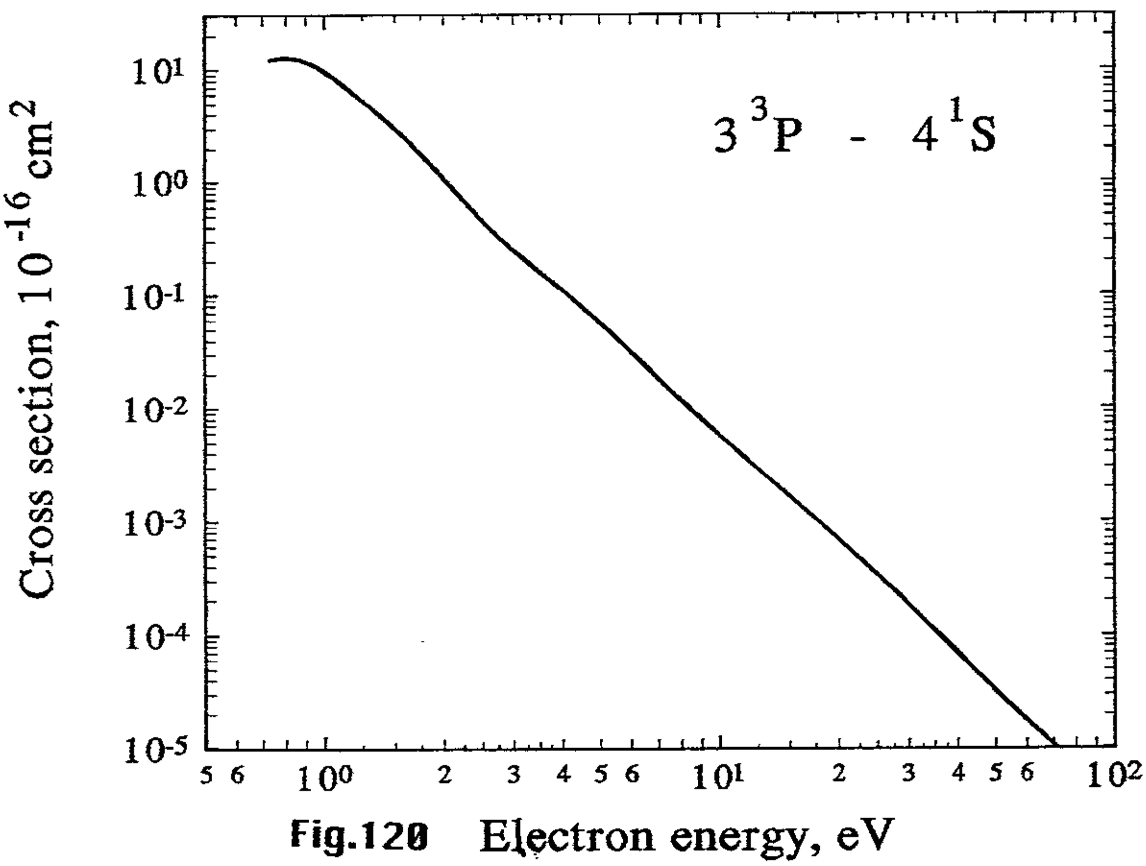

Fig.120

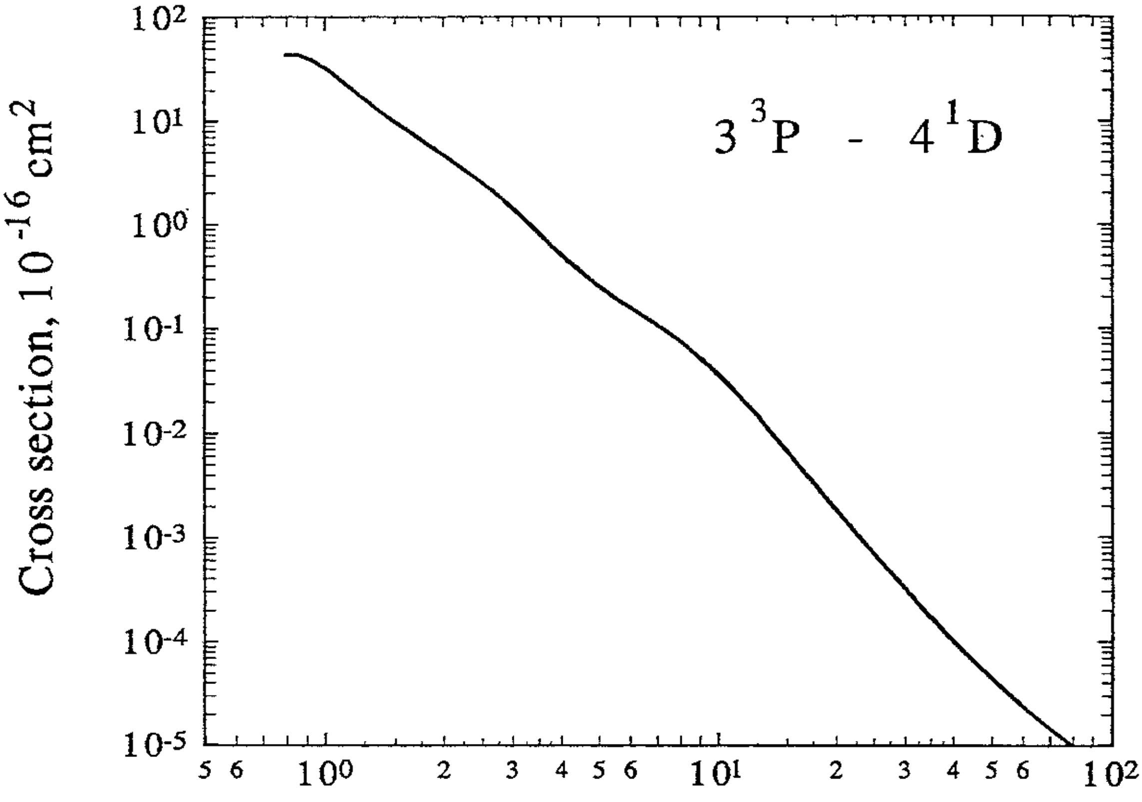

Fig.121 Electron energy, eV

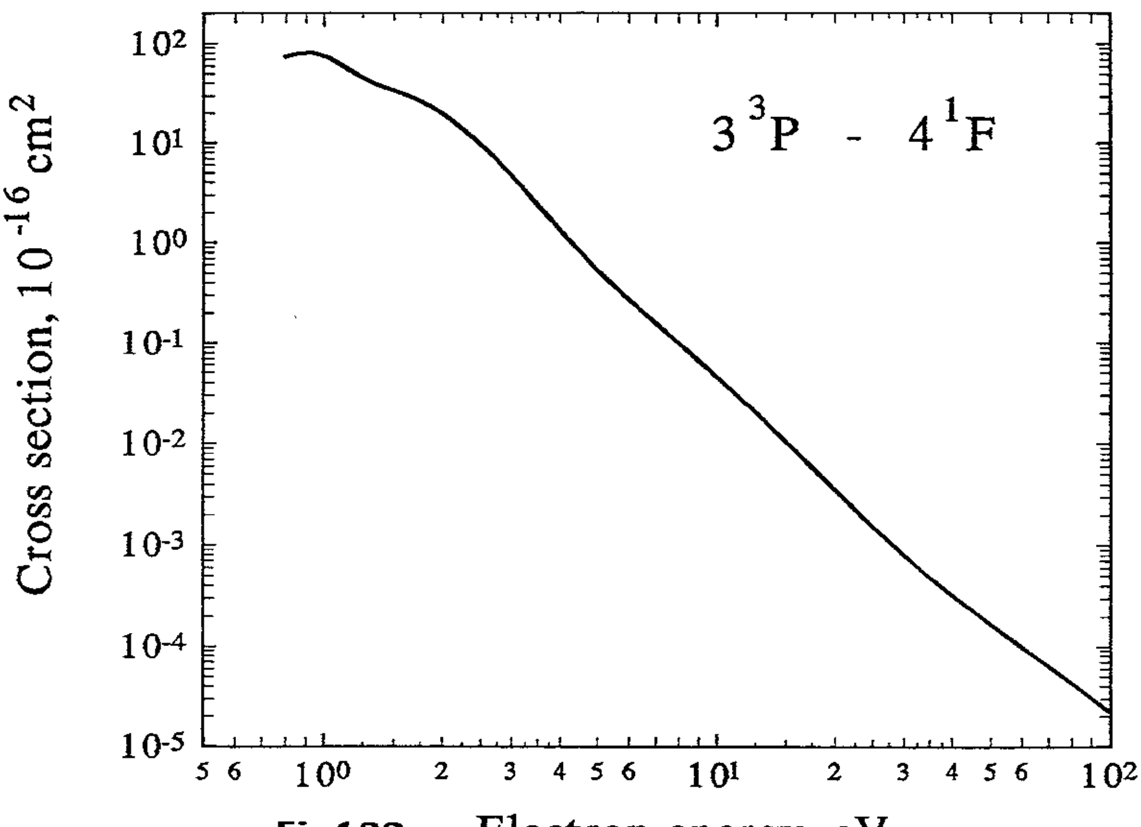

Fig122 Electron energy, eV

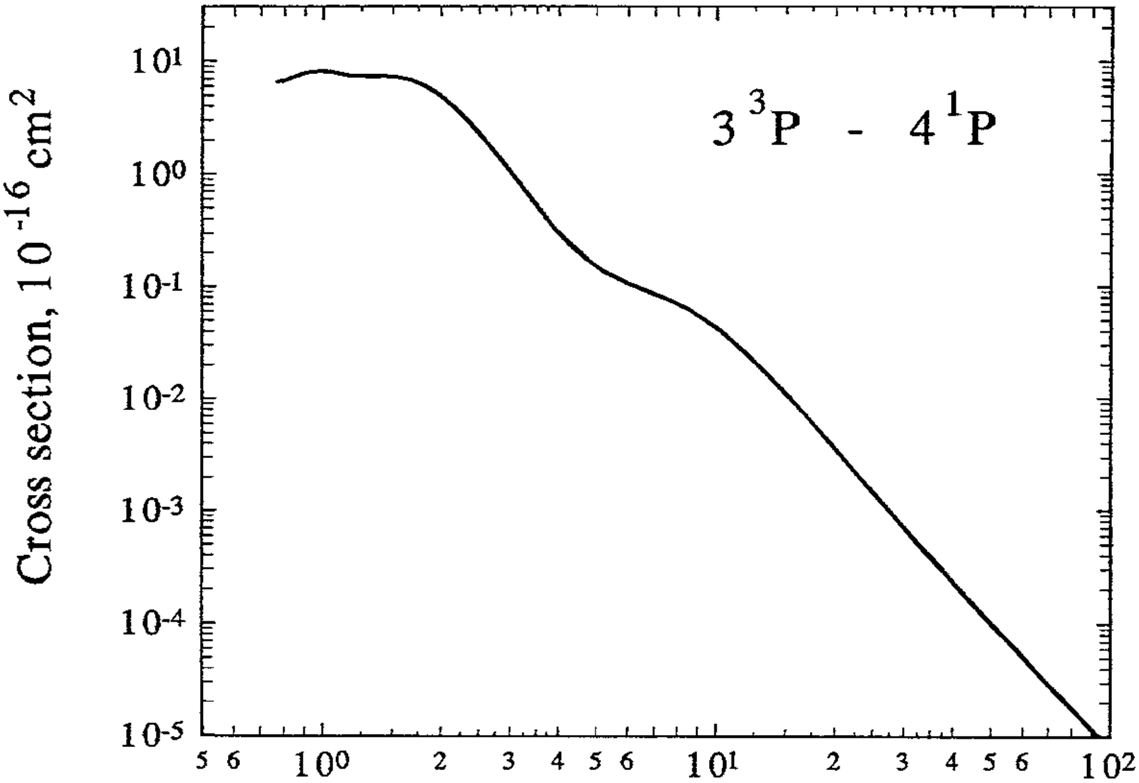

Fig.123 Electron energy, eV

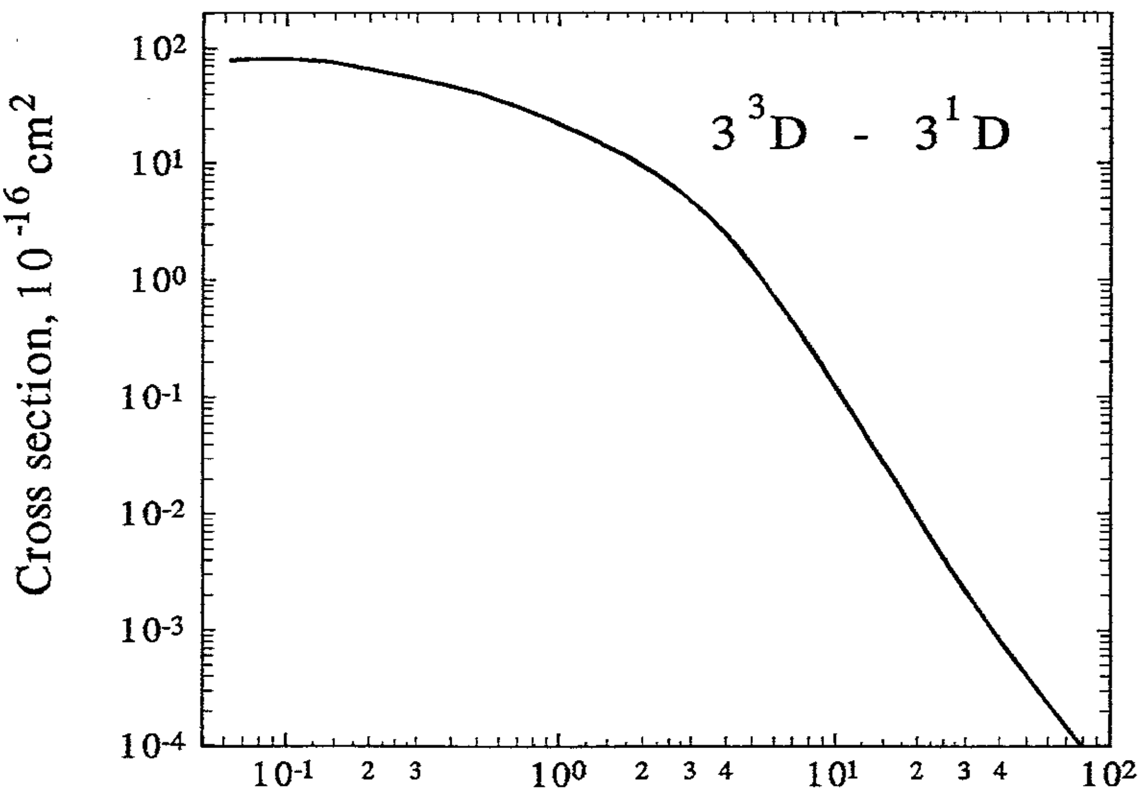

Fig.124 Electron energy, eV

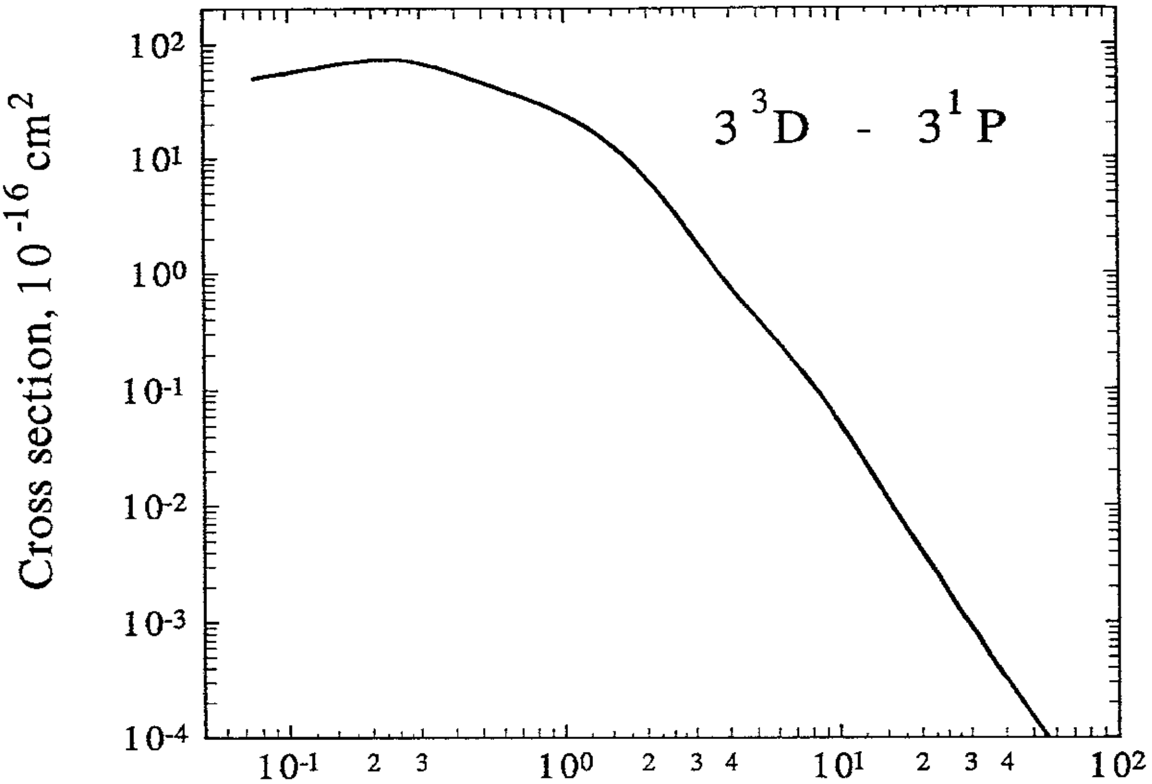

Fig.125 Electron energy, eV

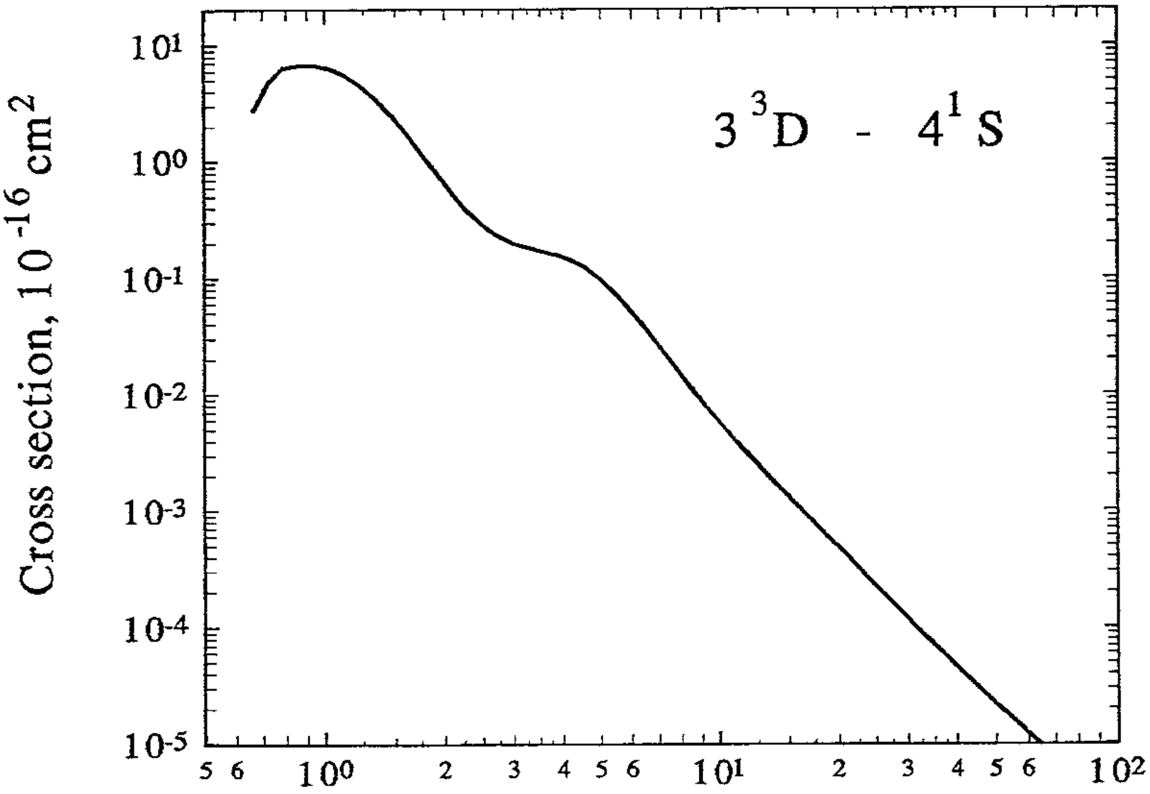

Fig.126 Electron energy, eV

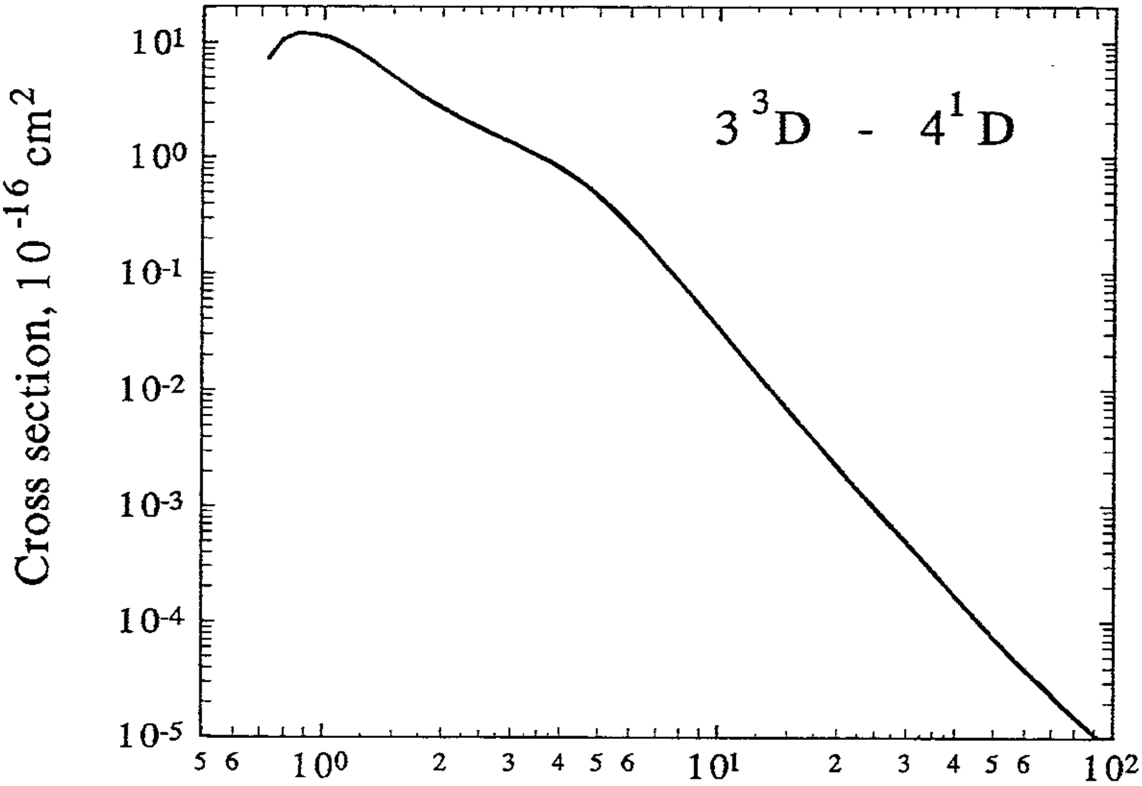

Fig.127 Electron energy, eV

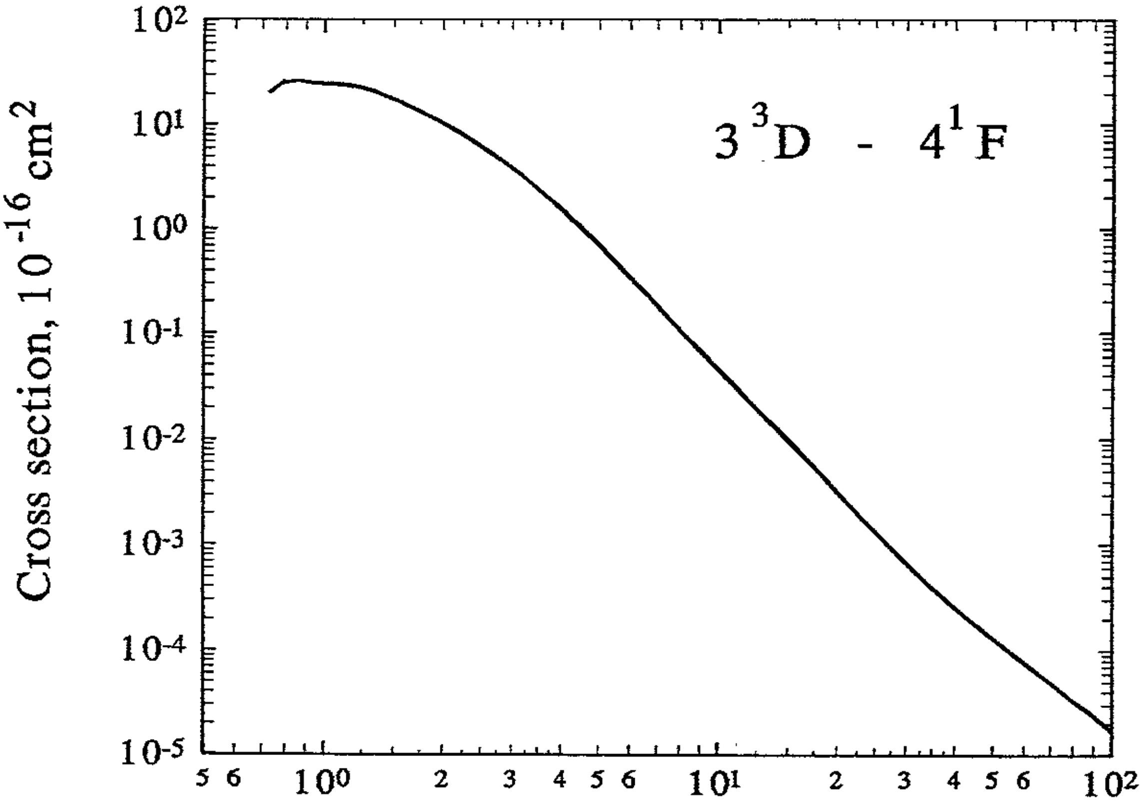

Fig.128 Electron energy, eV

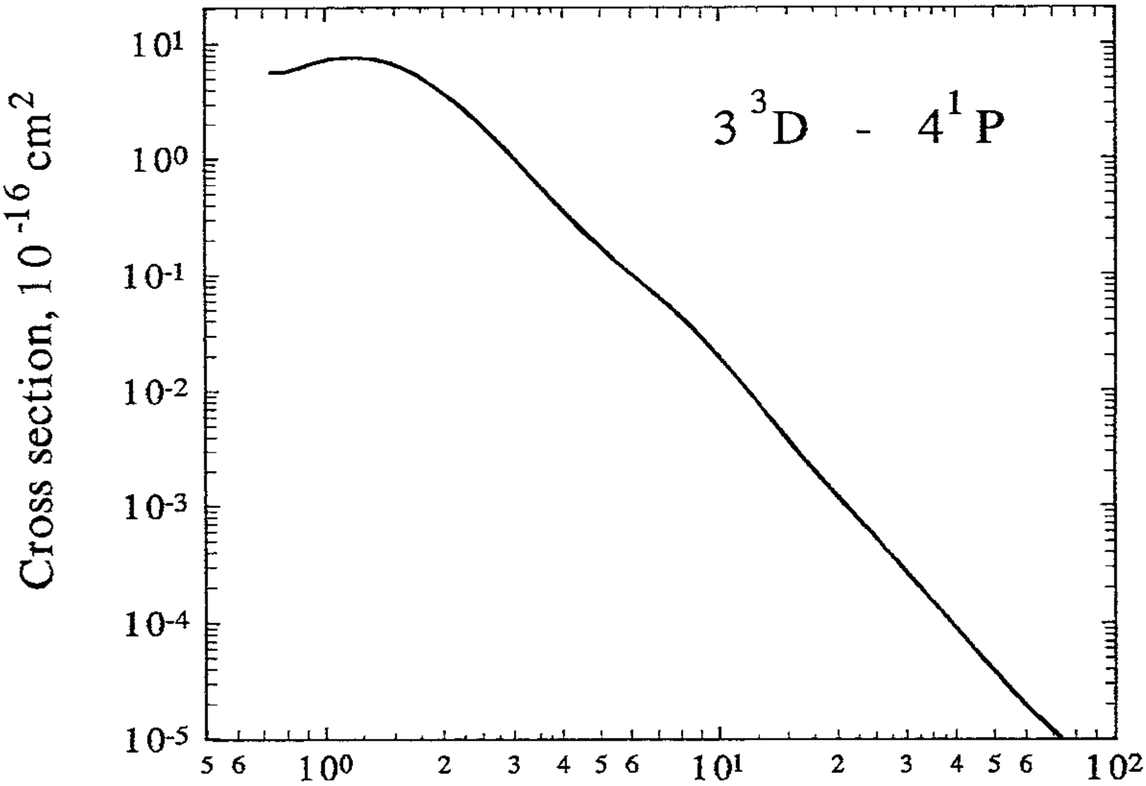

Fig.129 Electron energy, eV

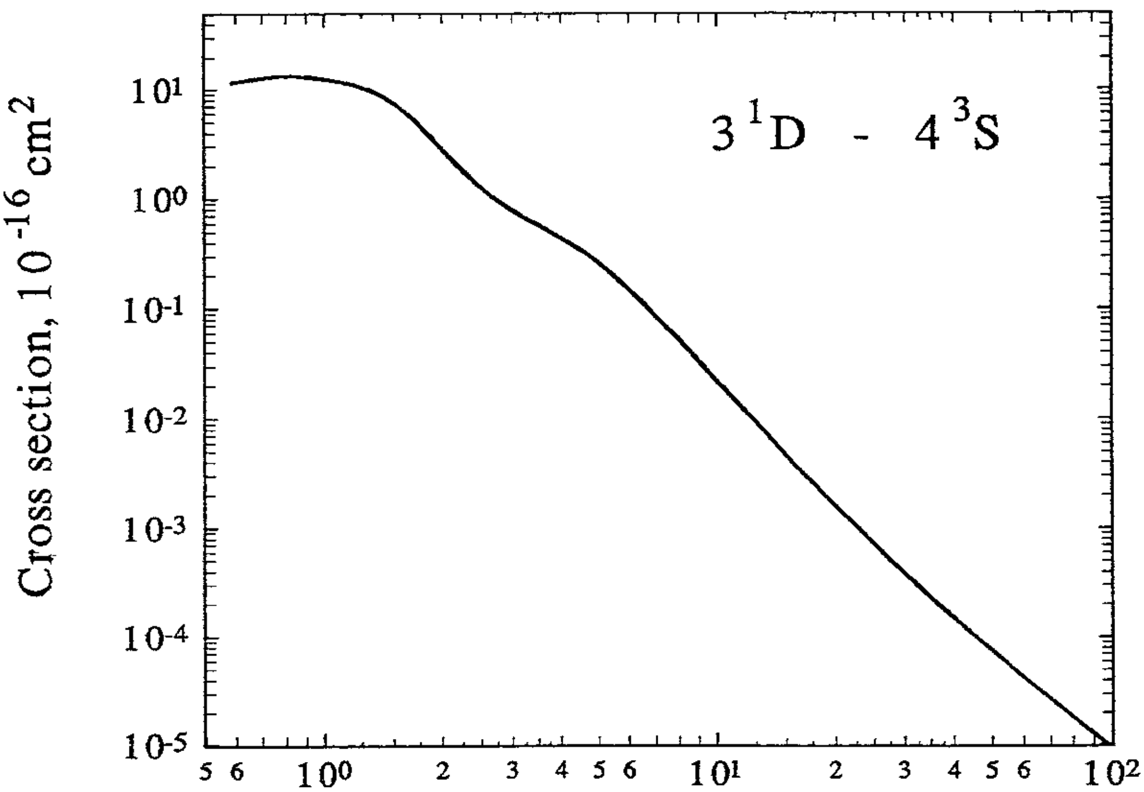

Fig.130 Electron energy, eV

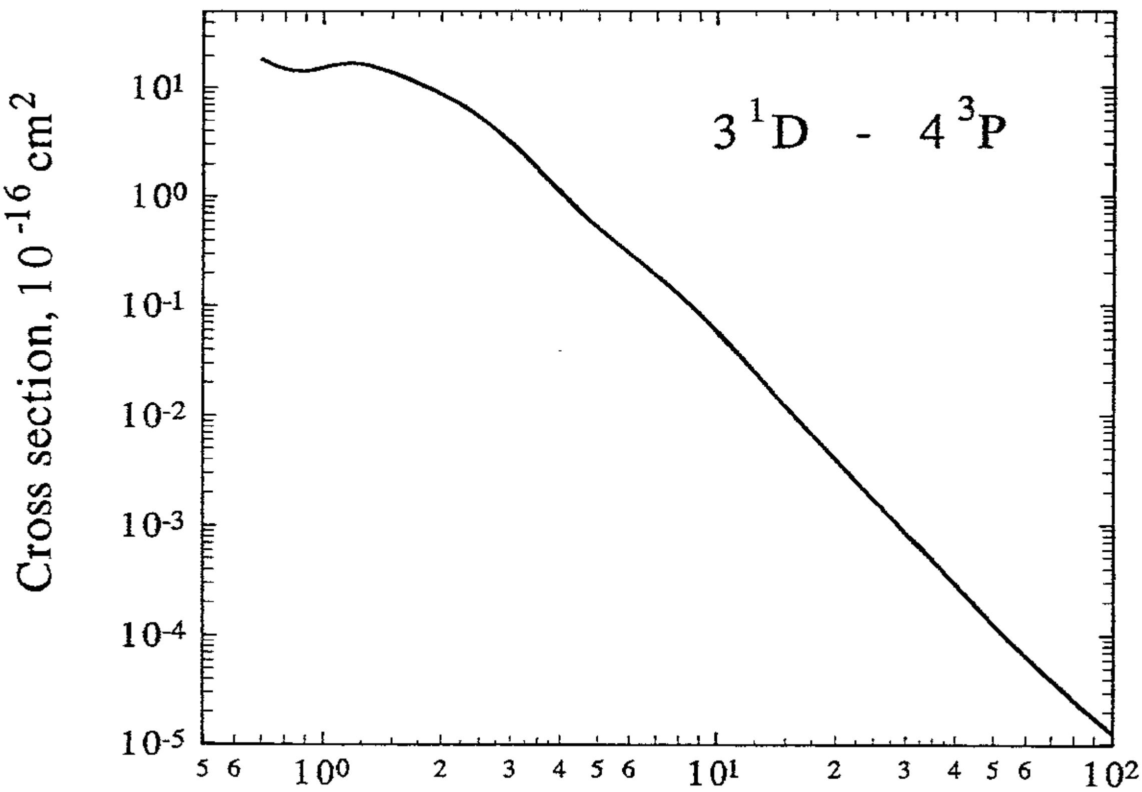

Fig.131 Electron energy, eV

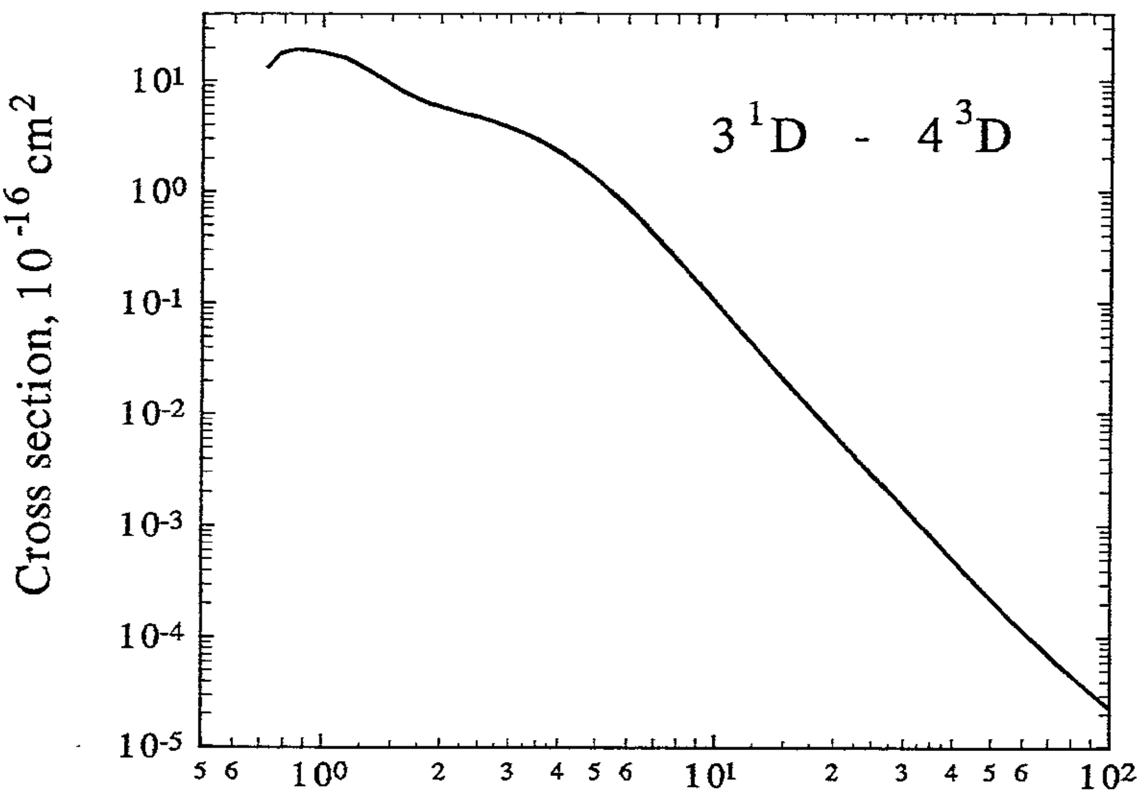

Fig.132 Electron energy, eV

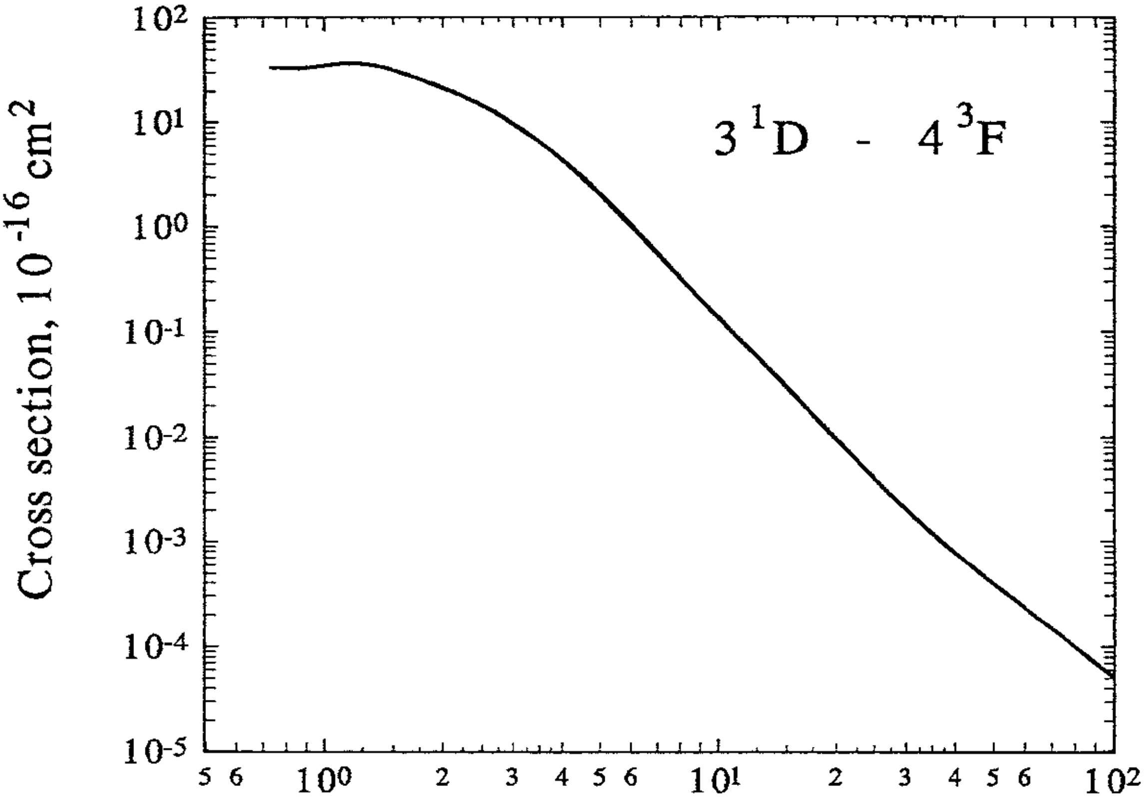

Fig.133 Electron energy, eV

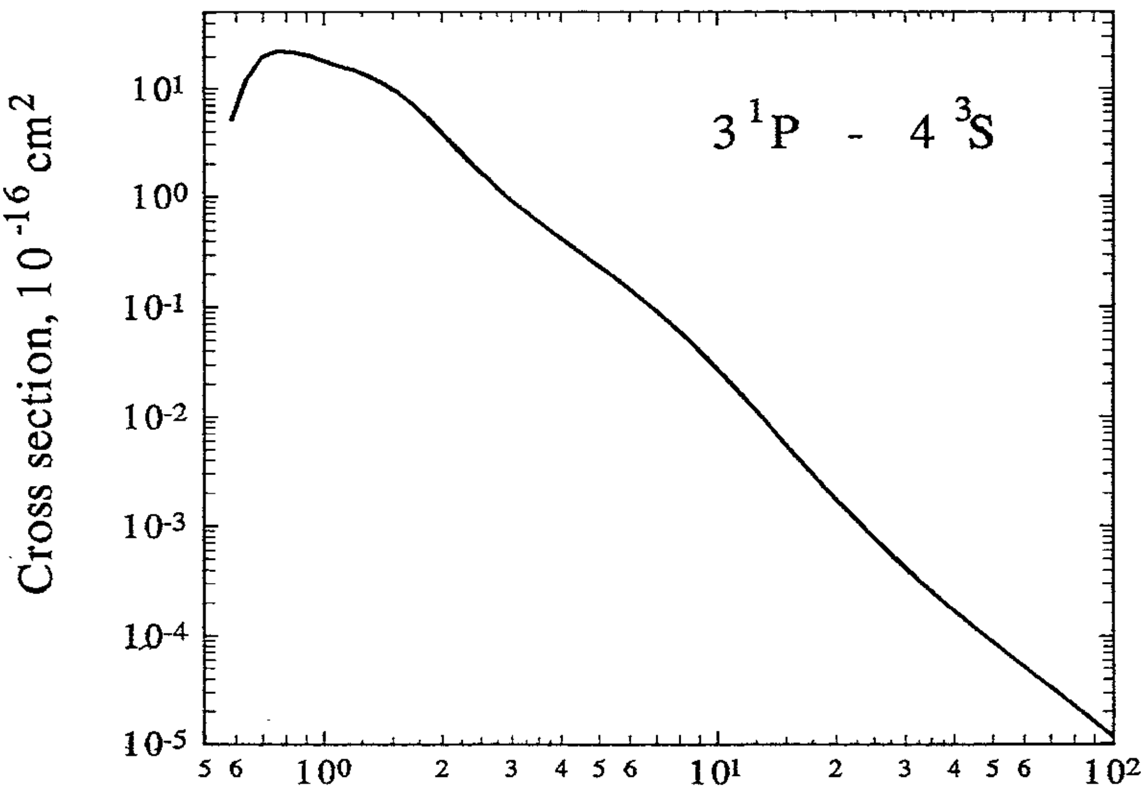

Fig.134 Electron energy, eV

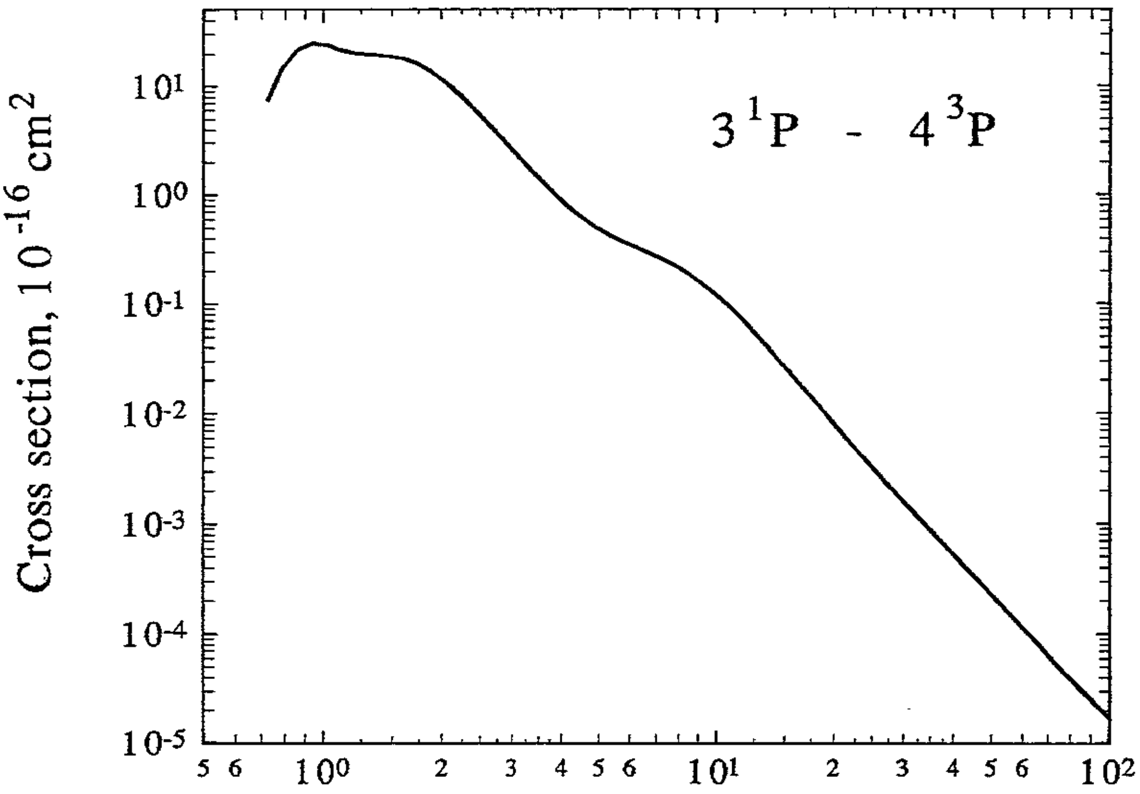

Fig135

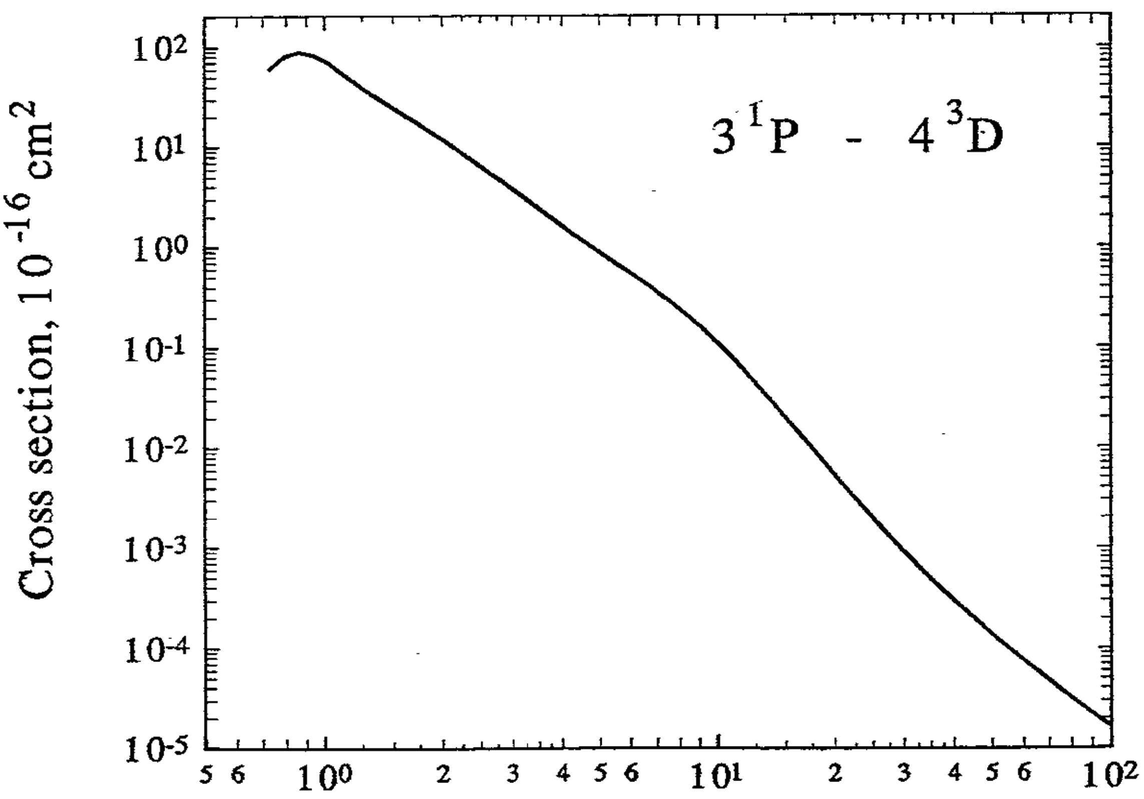

Fig.136

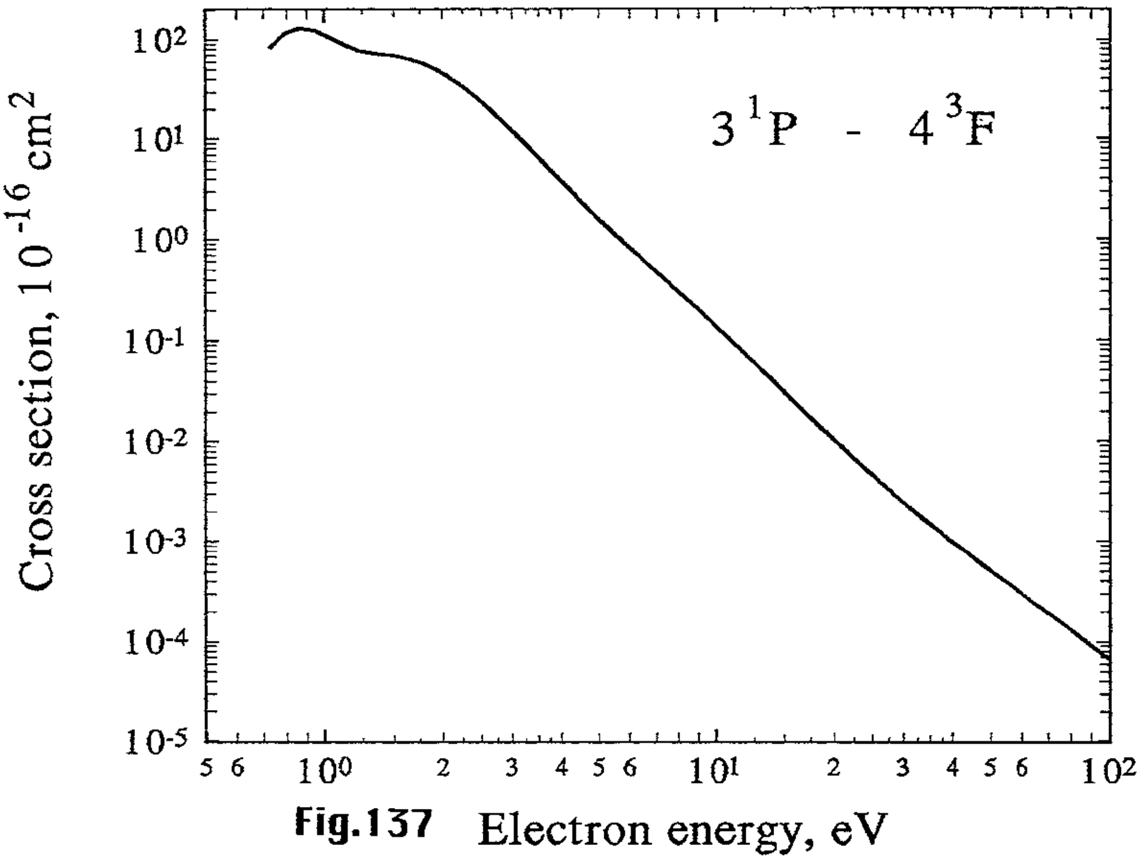

Fig.137

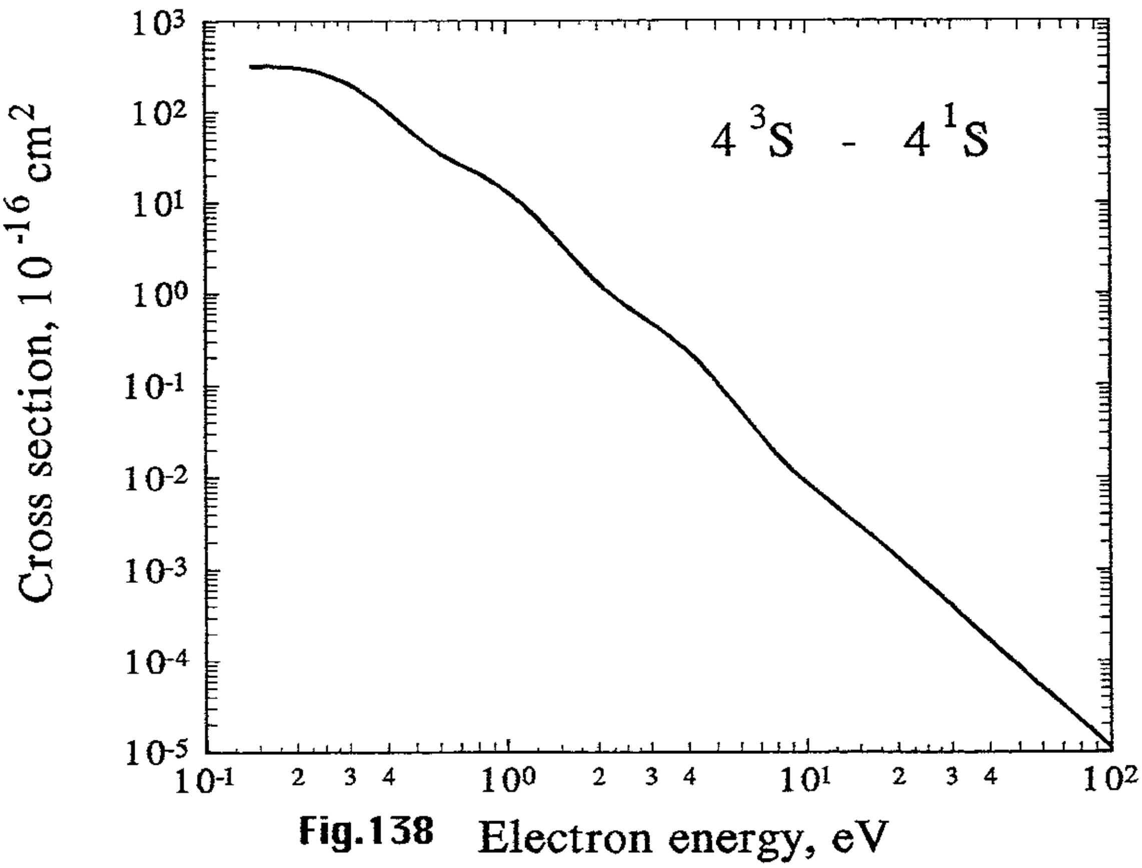

Fig.138

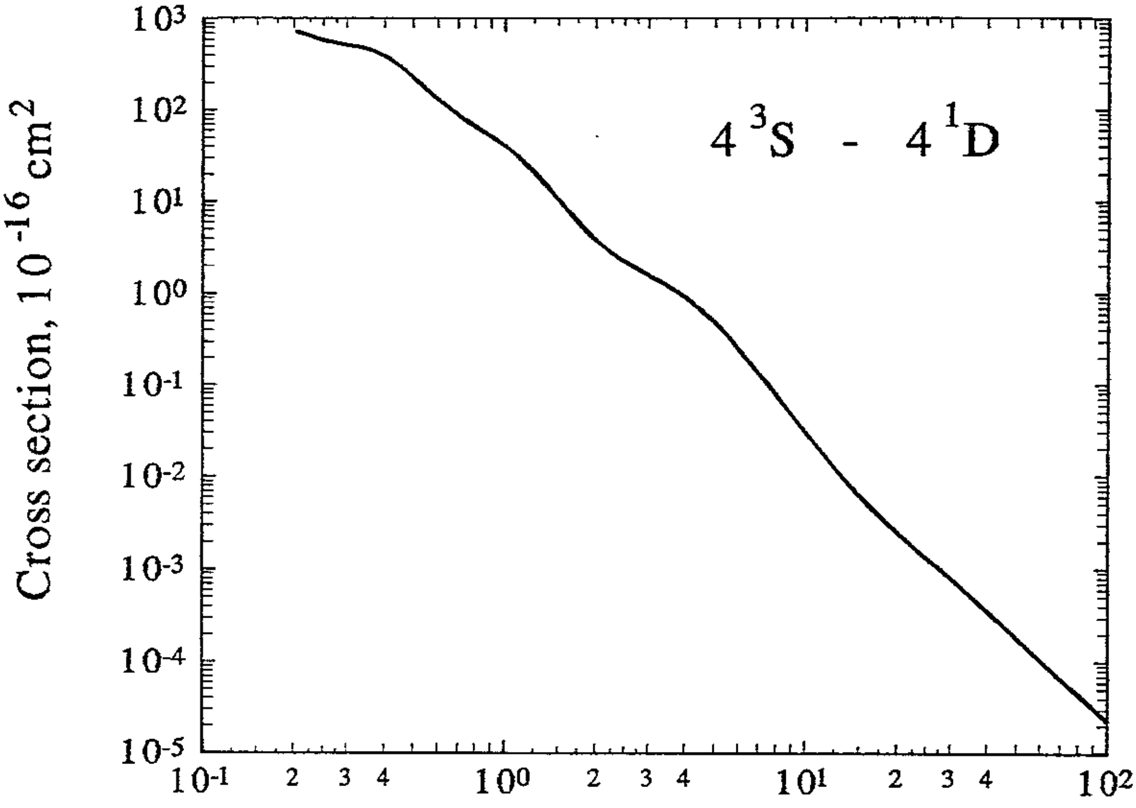

Fig.139 Electron energy, eV

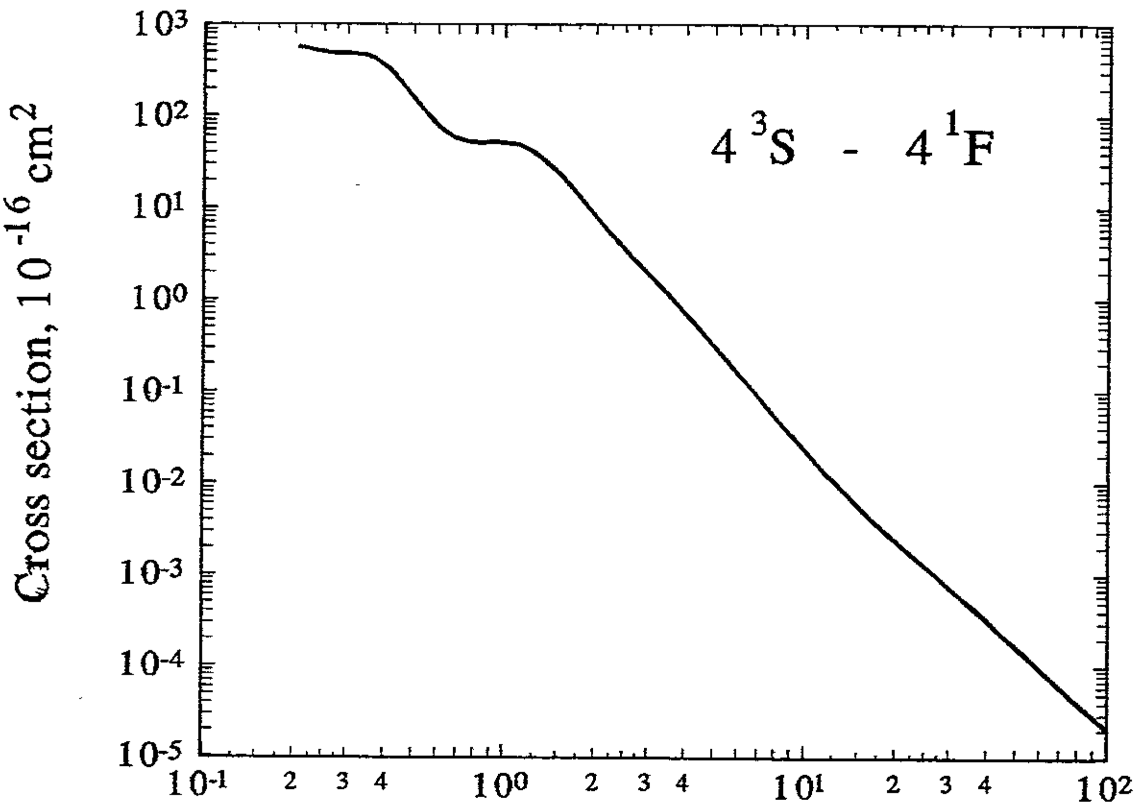

Fig.140 Electron energy, eV

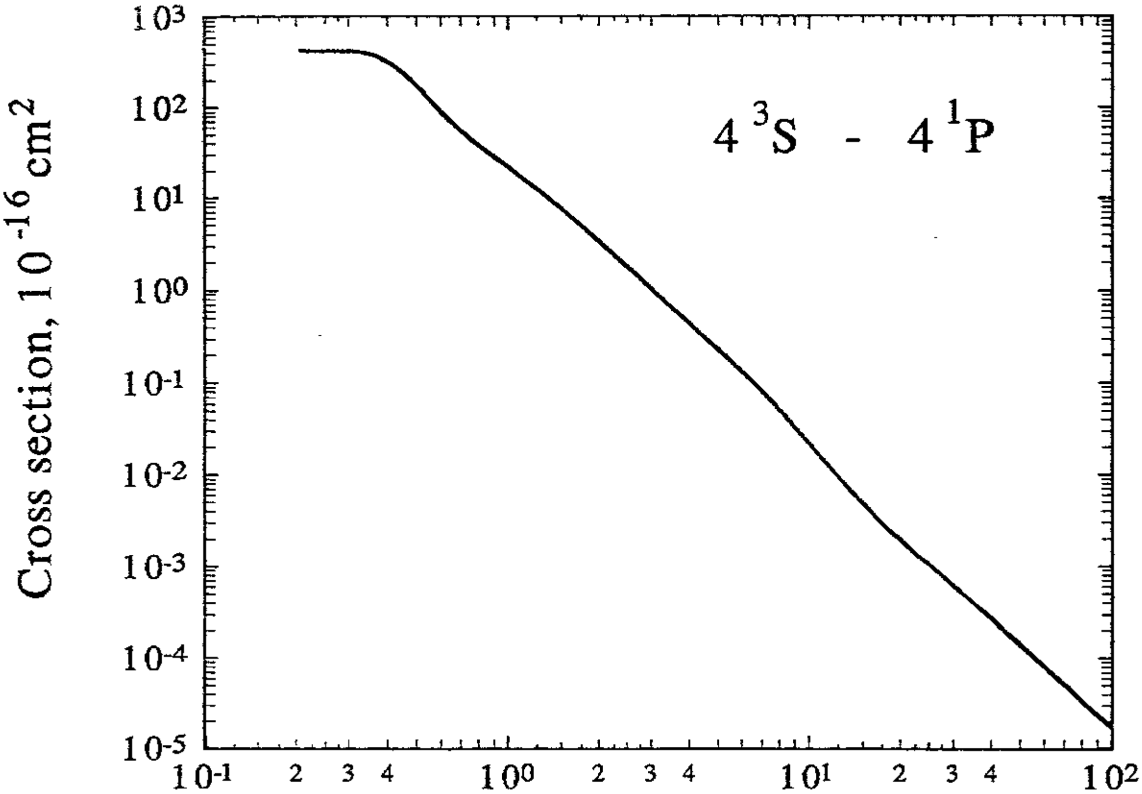

Fig.141 Electron energy, eV

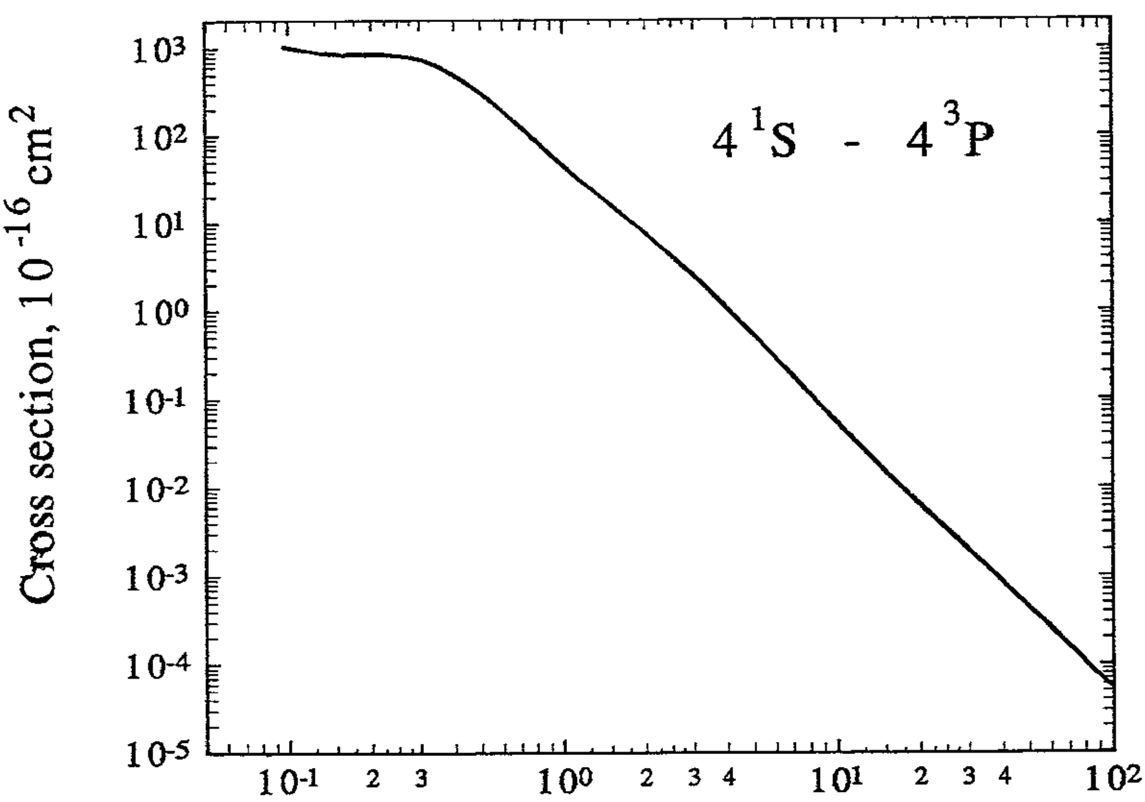

Fig.142 Electron energy, eV

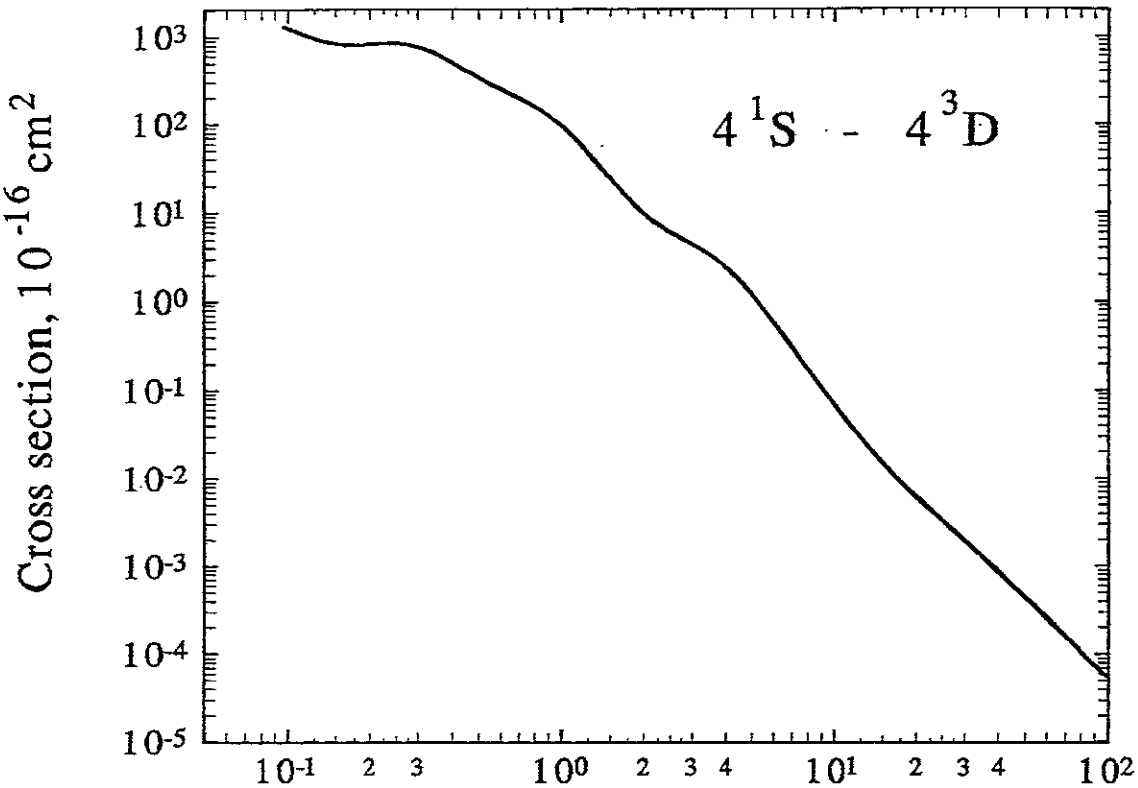

Fig.143 Electron energy, eV

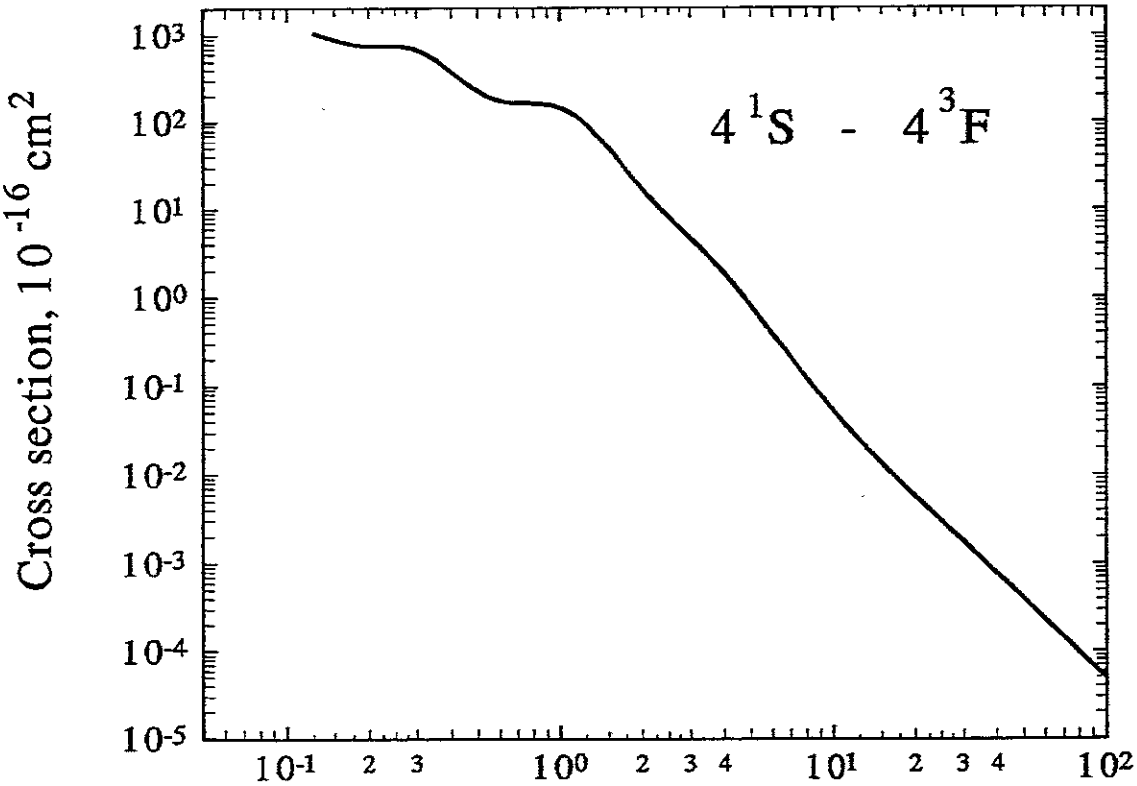

Fig.144 Electron energy, eV

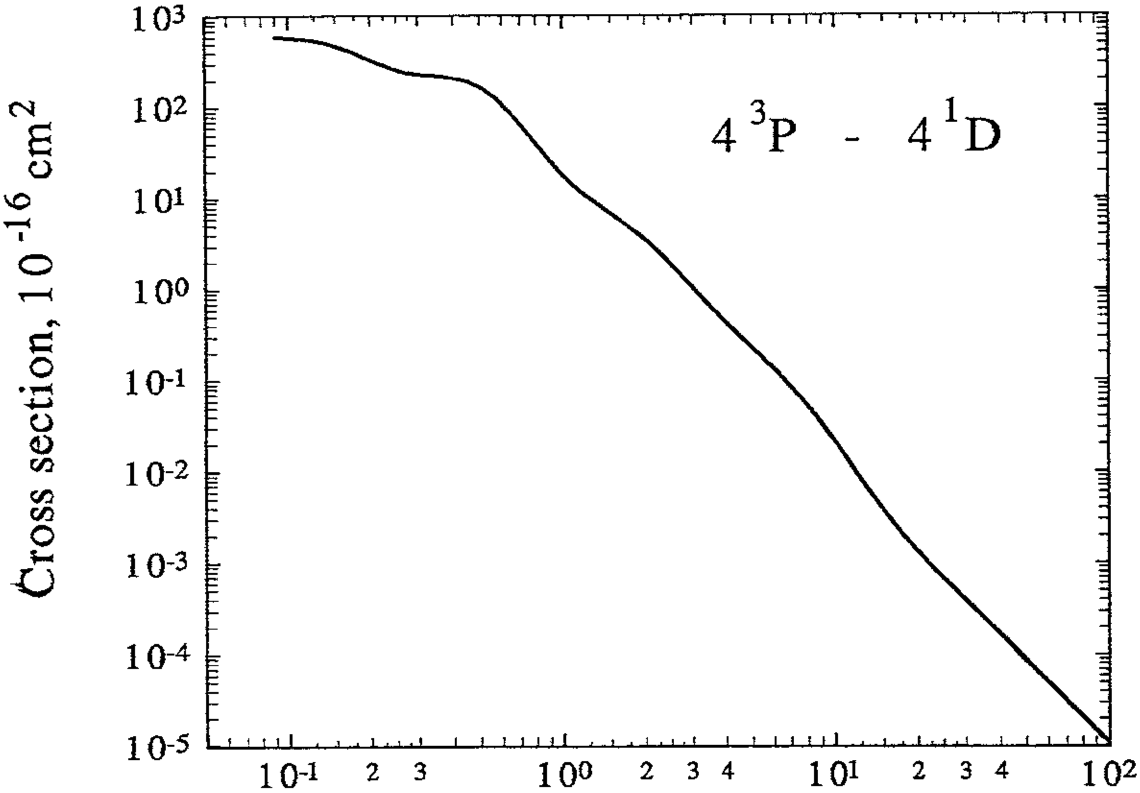

Fig.145 Electron energy, eV

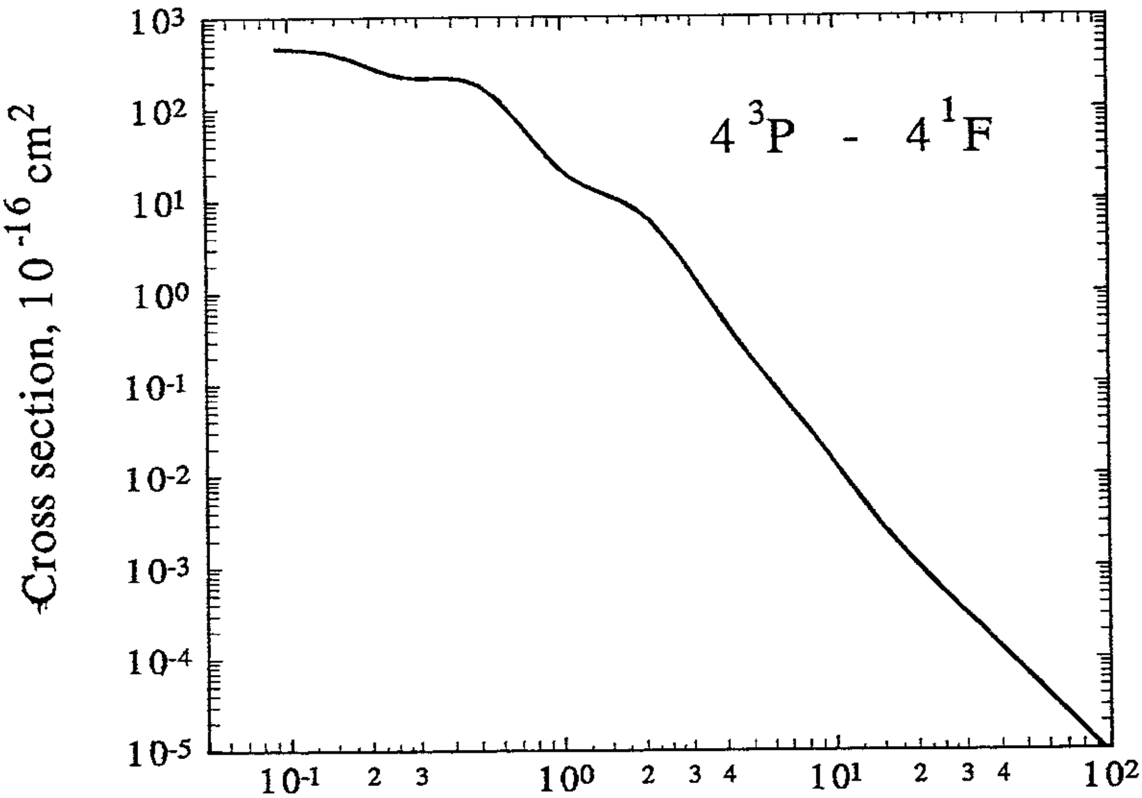

Fig.146 Electron energy, eV

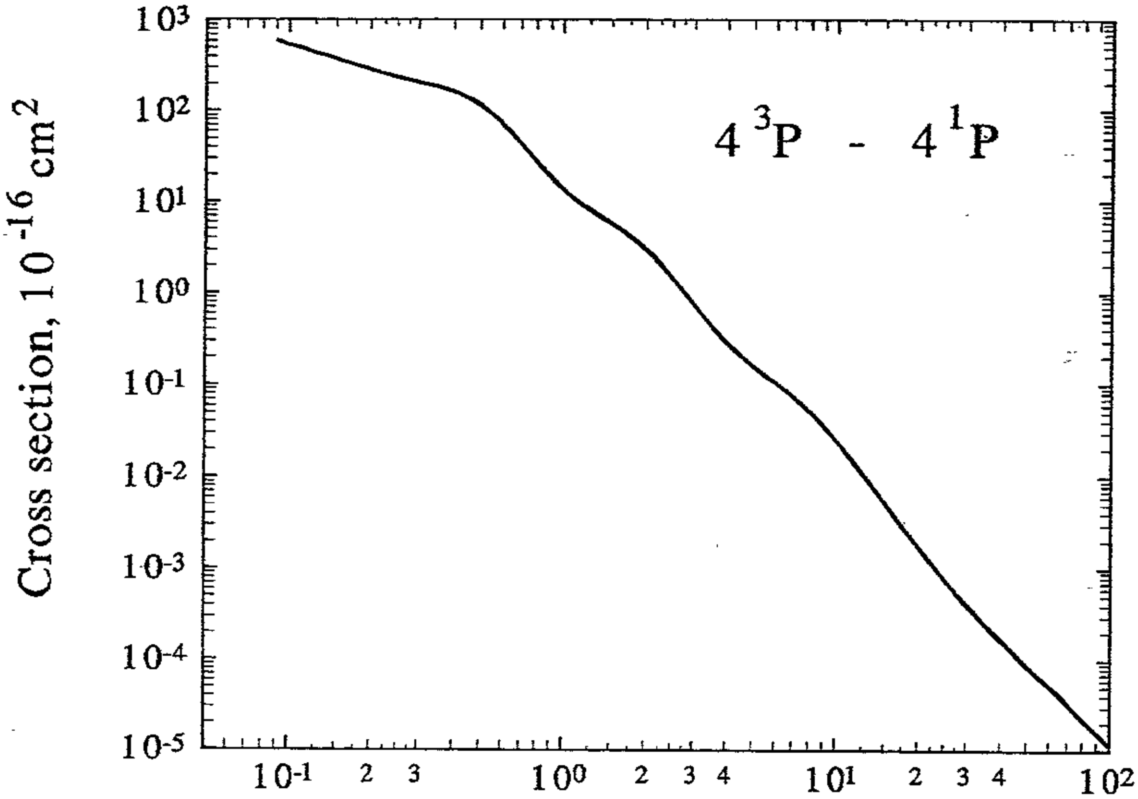

Fig.147 Electron energy, eV

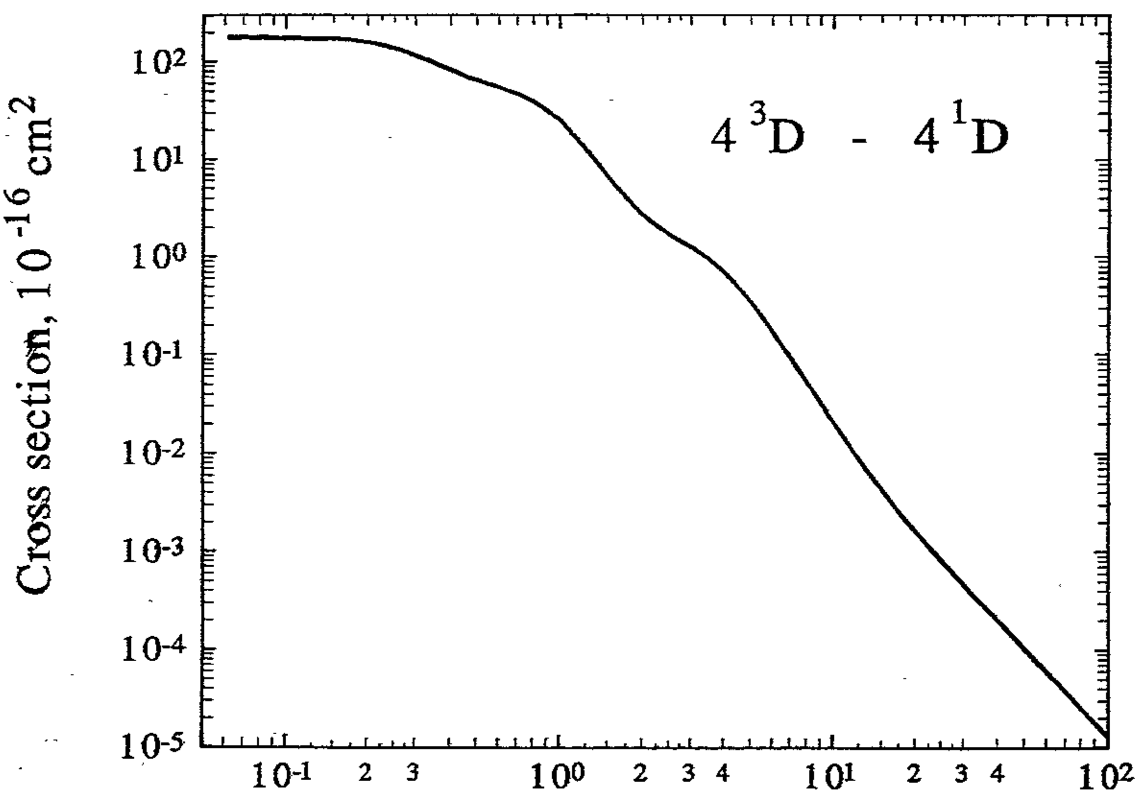

Fig.148 Electron energy, eV

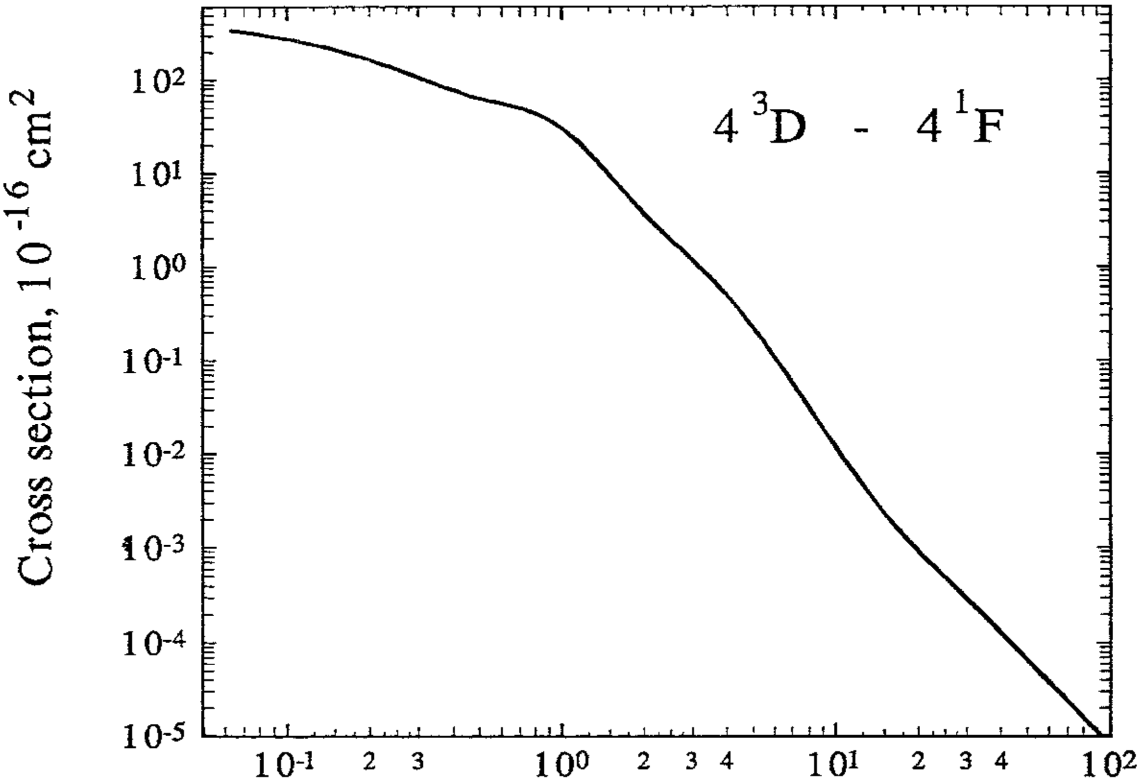

Fig.149 Electron energy, eV

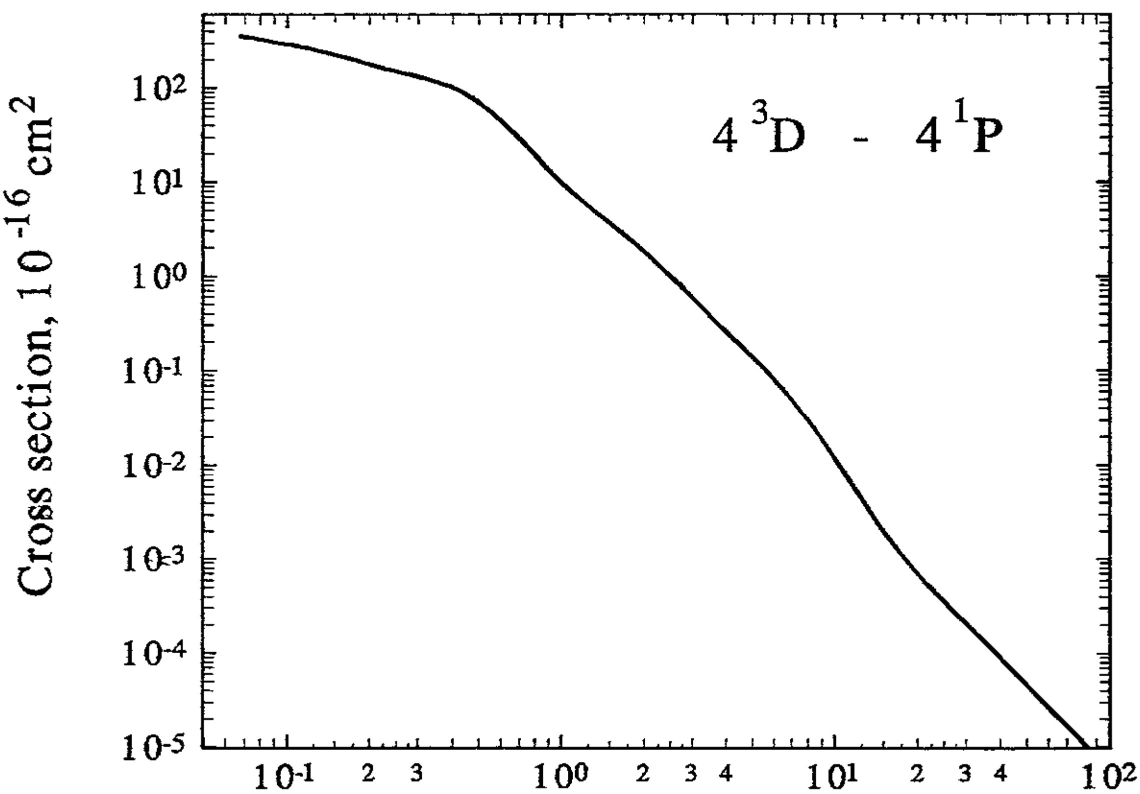

Fig.150 Electron energy, eV

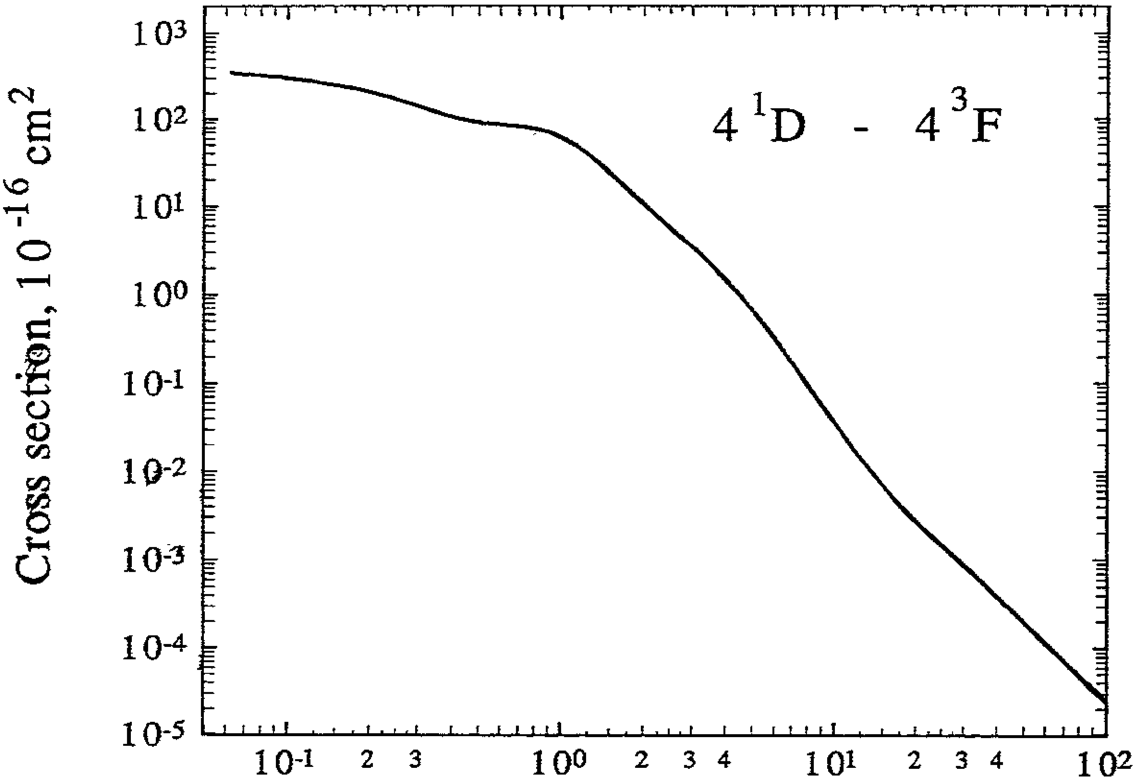

Fig.151 Electron energy, eV

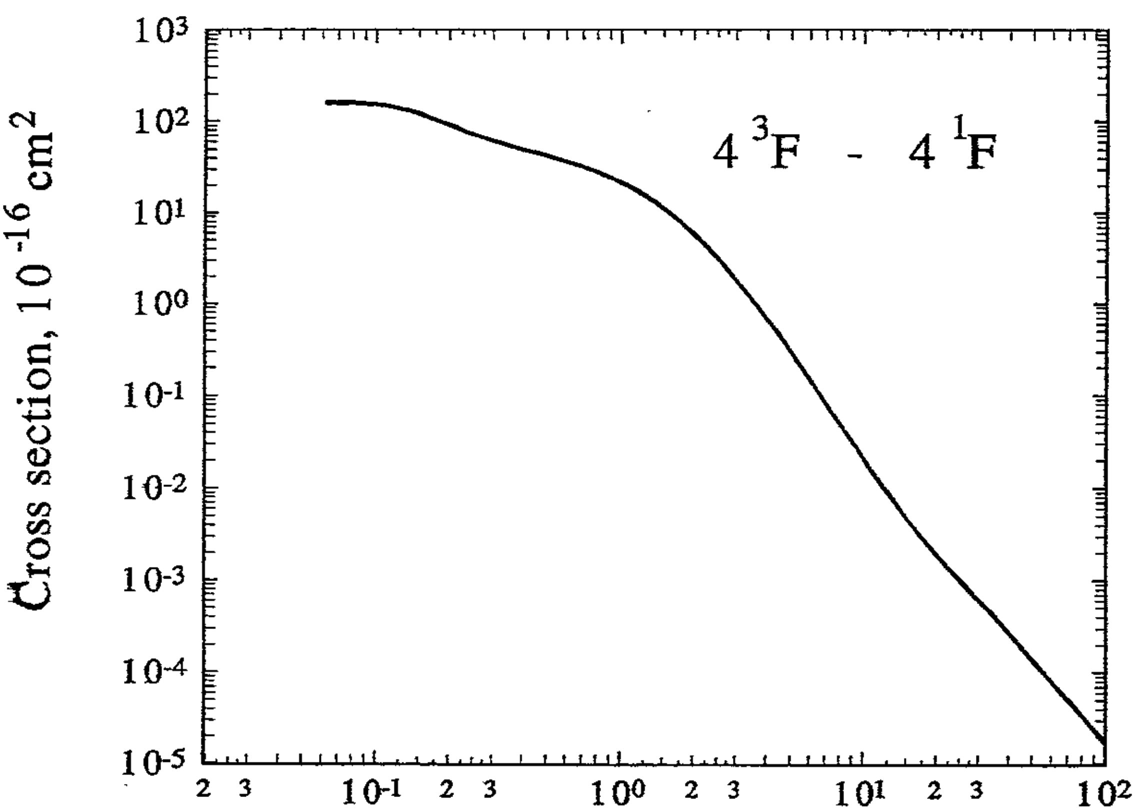

Fig.152 Electron energy, eV

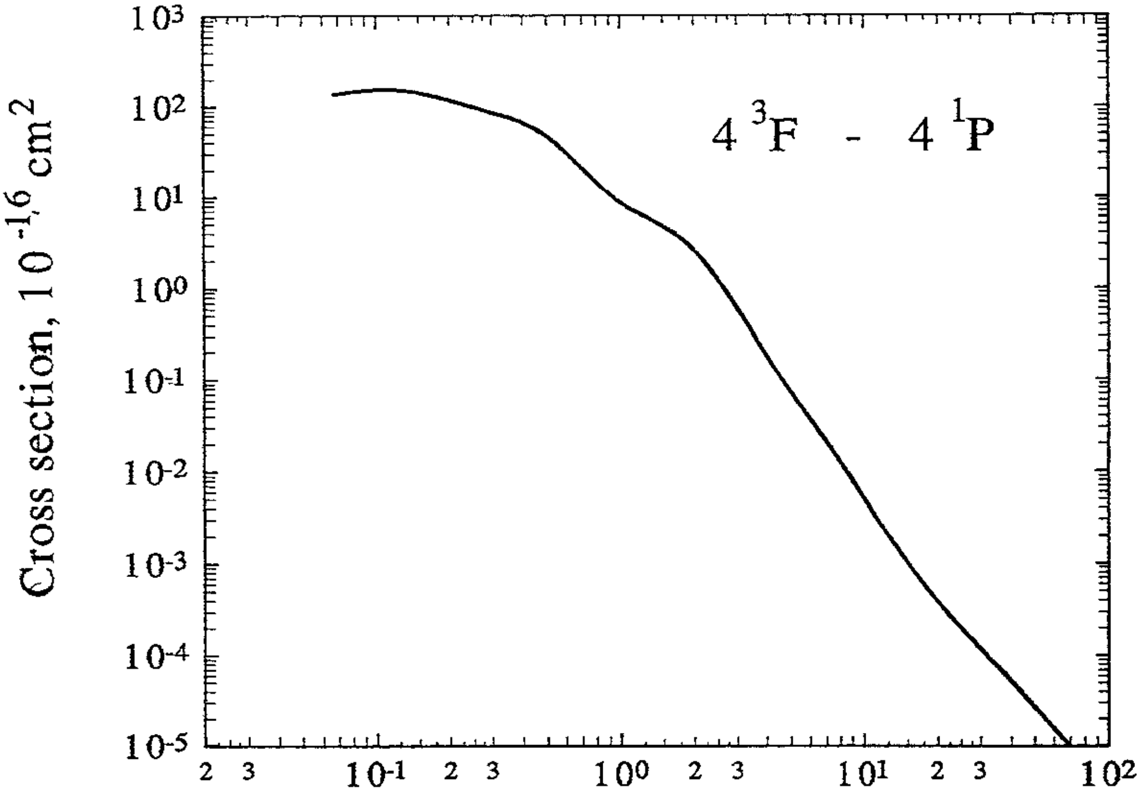

Fig.153 Electron energy, eV

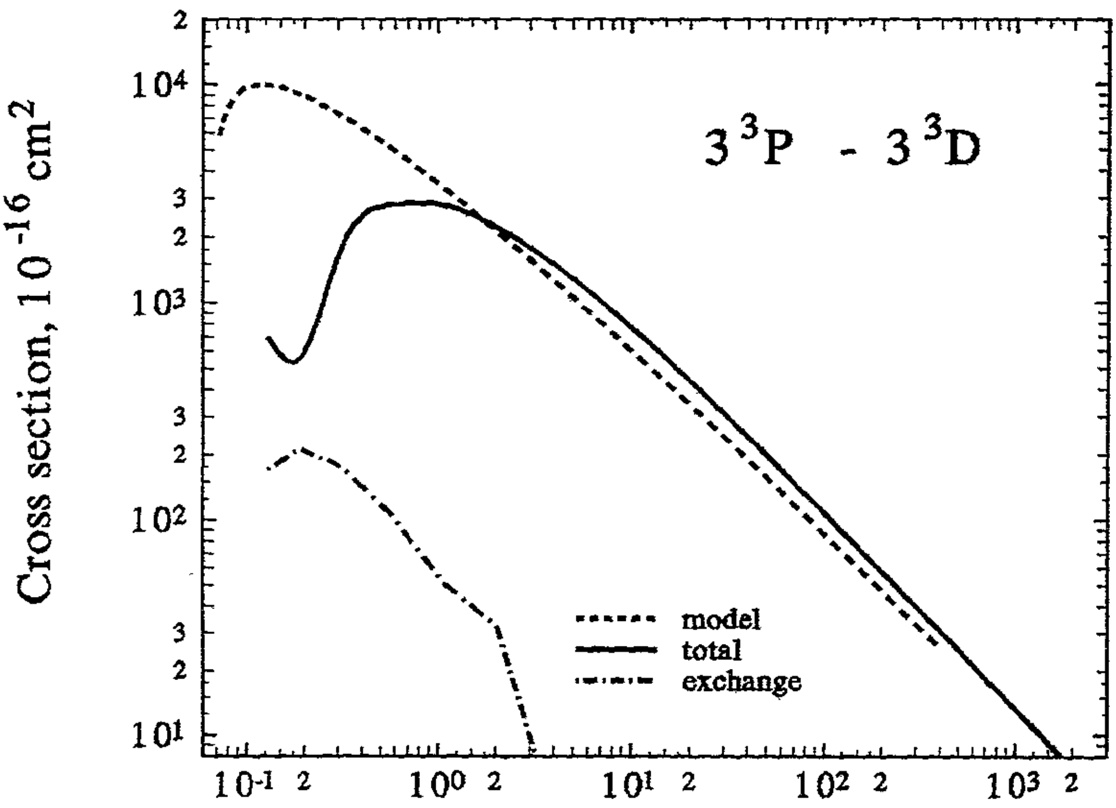

Fig.154 Electron energy, eV

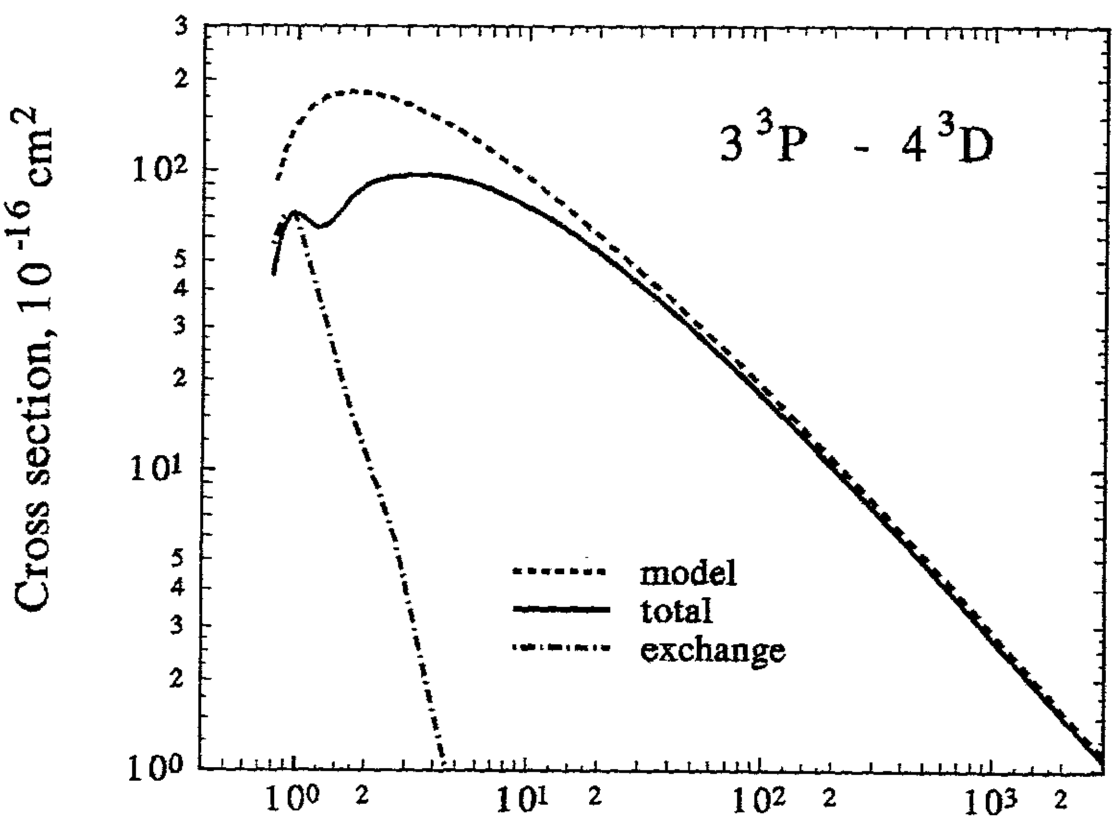

Fig.155 Electron energy, eV

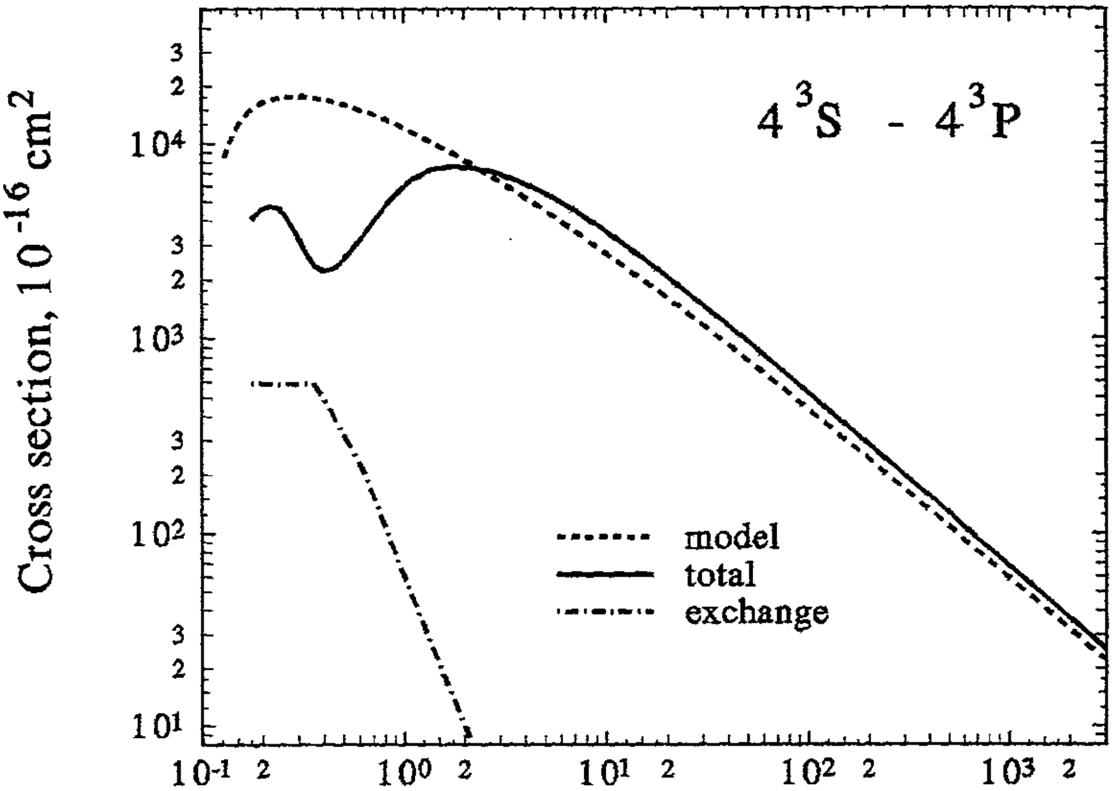

Fig.156 Electron energy, eV

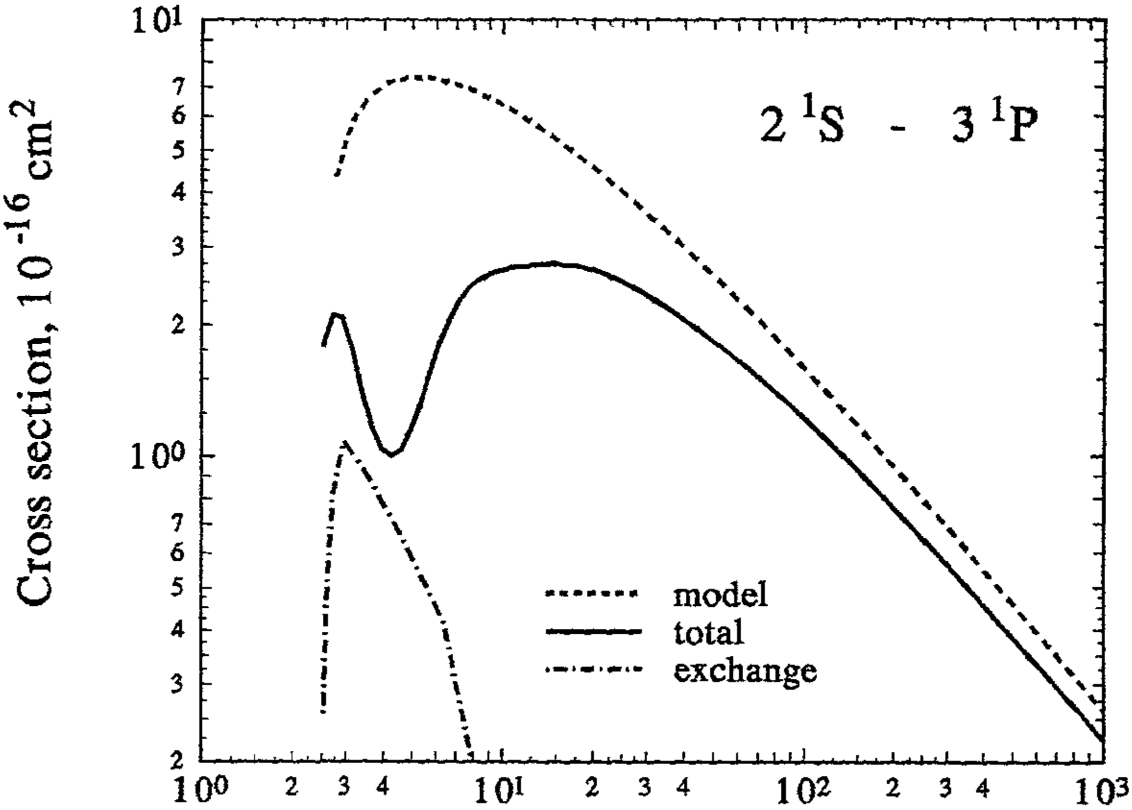

Fig.157 Electron energy, eV

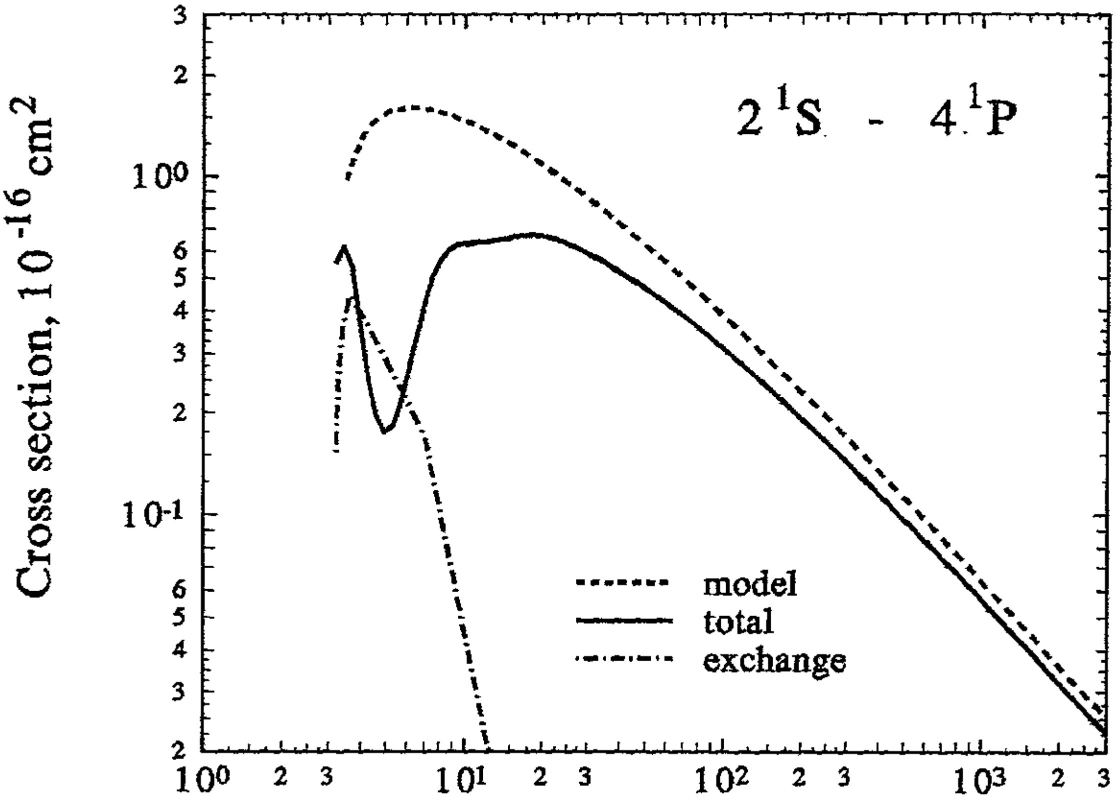

Fig.158

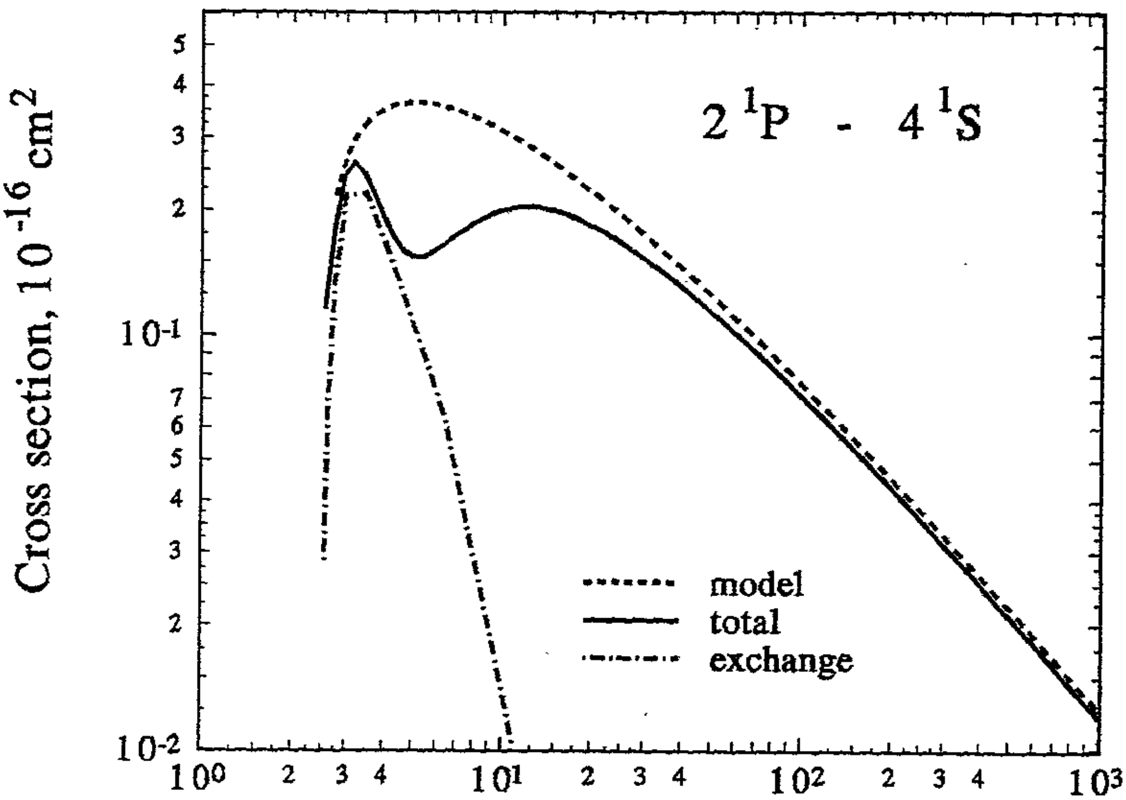

Fig.159

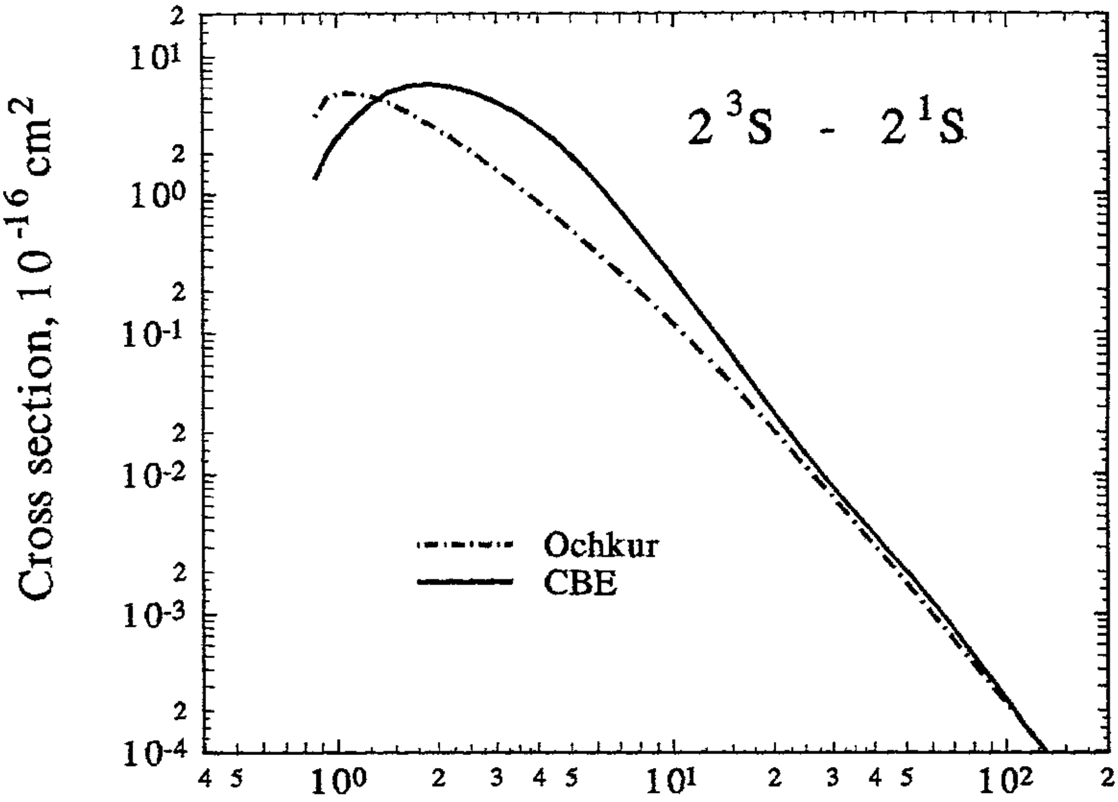

Fig.160 Electron energy, eV

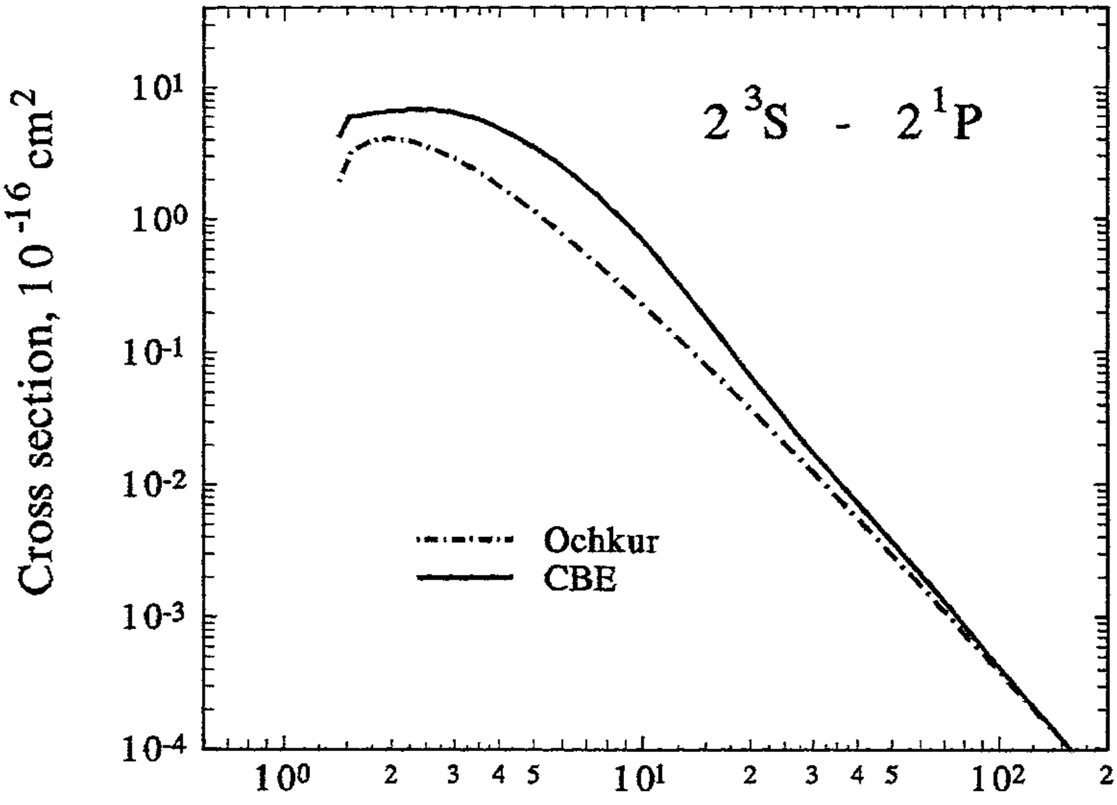

Fig.161 Electron energy, eV

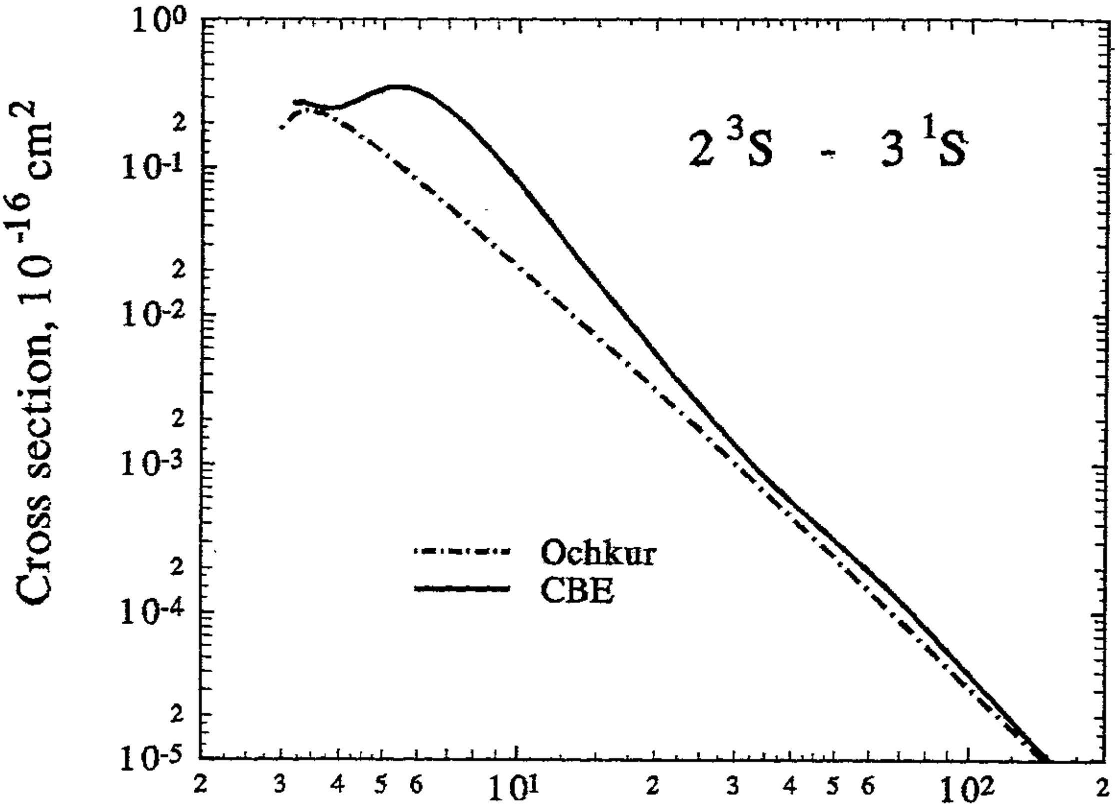

Fig162 Electron energy, eV

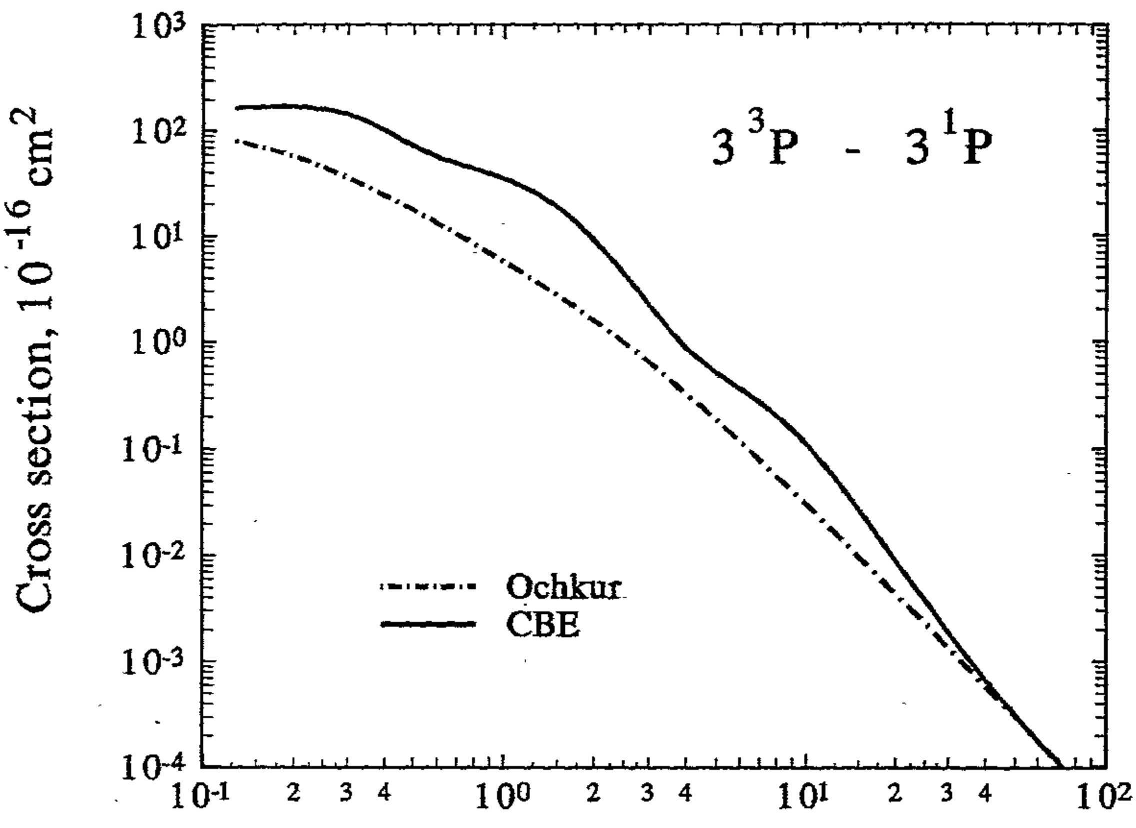

Fig.163 Electron energy, eV

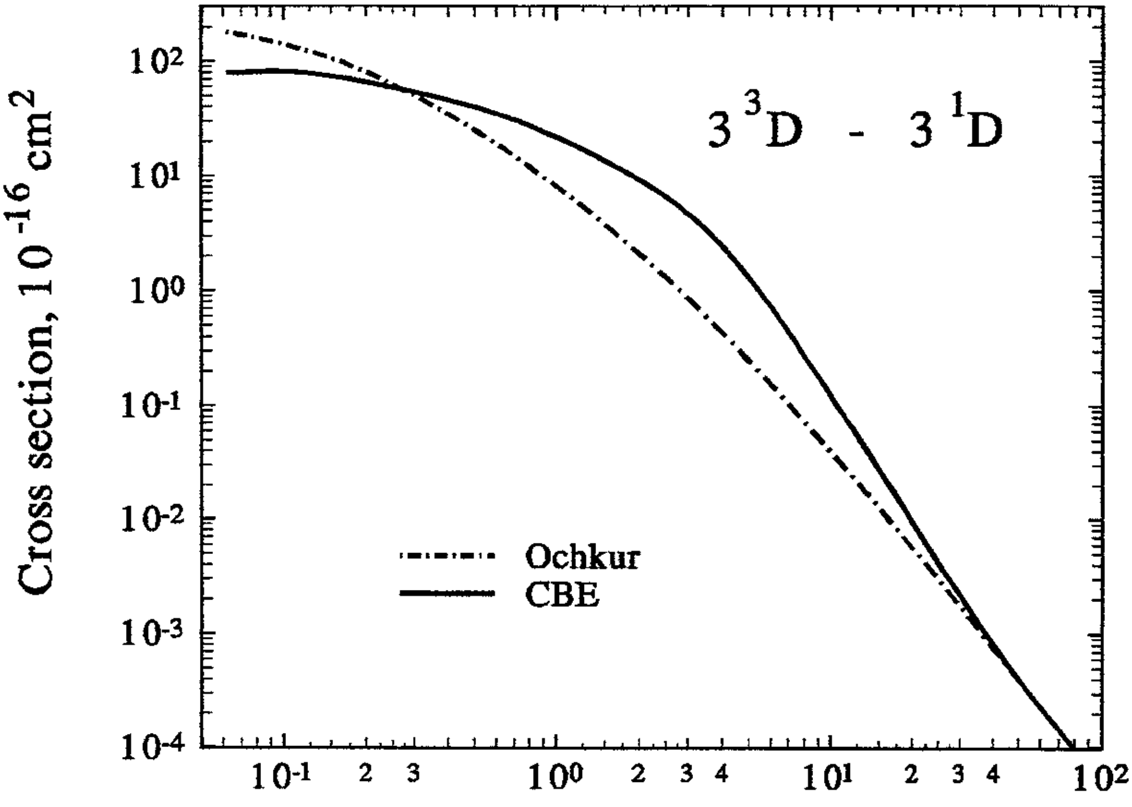

Fig.164 Electron energy, eV

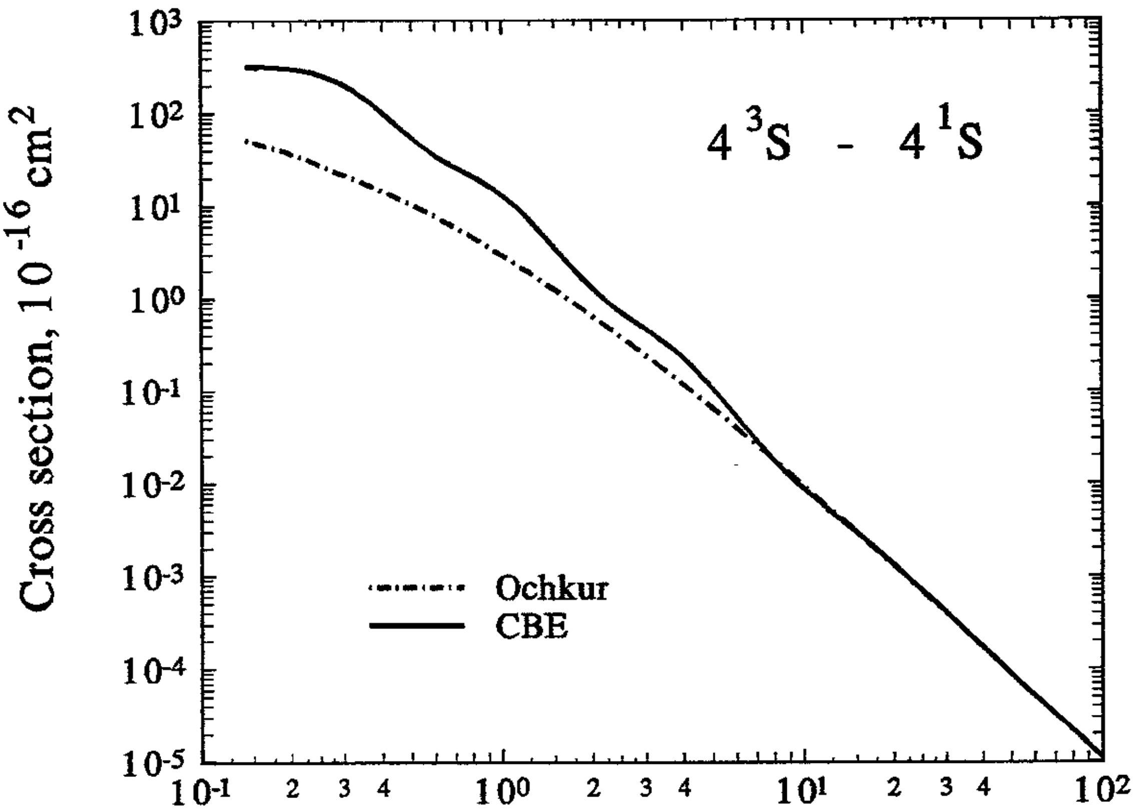

Fig.165 Electron energy, eV

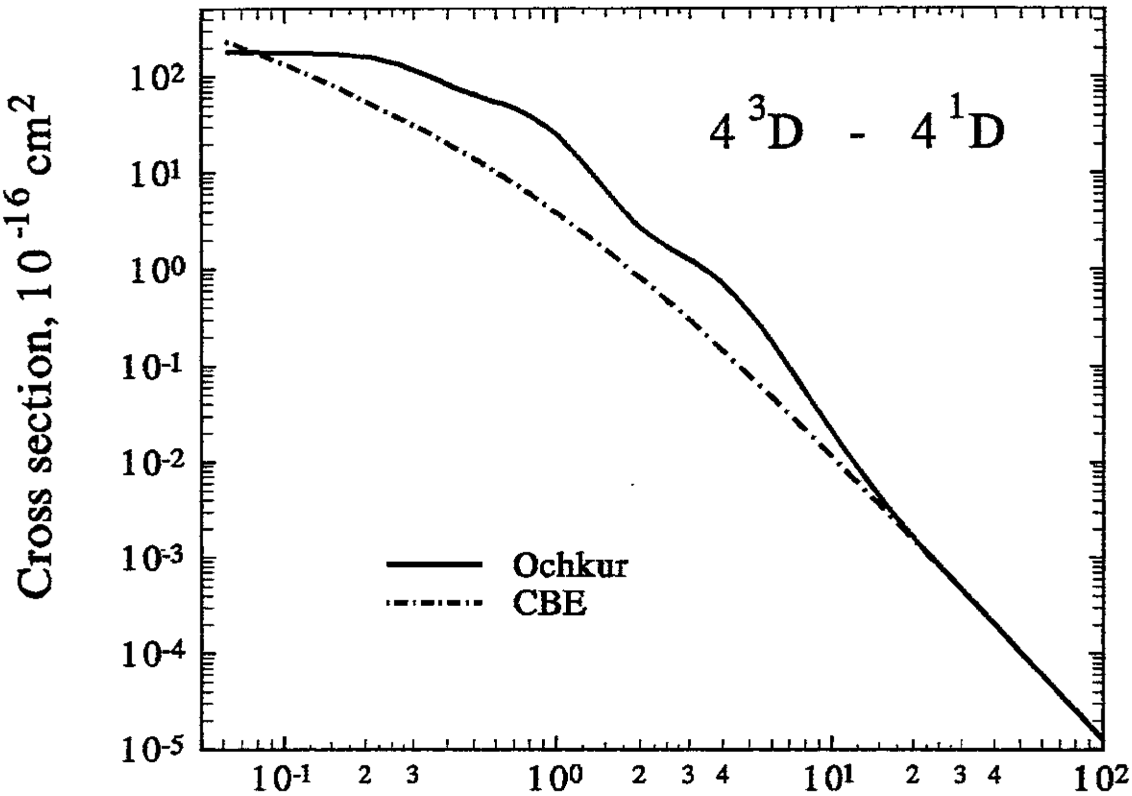

Fig.166 Electron energy, eV

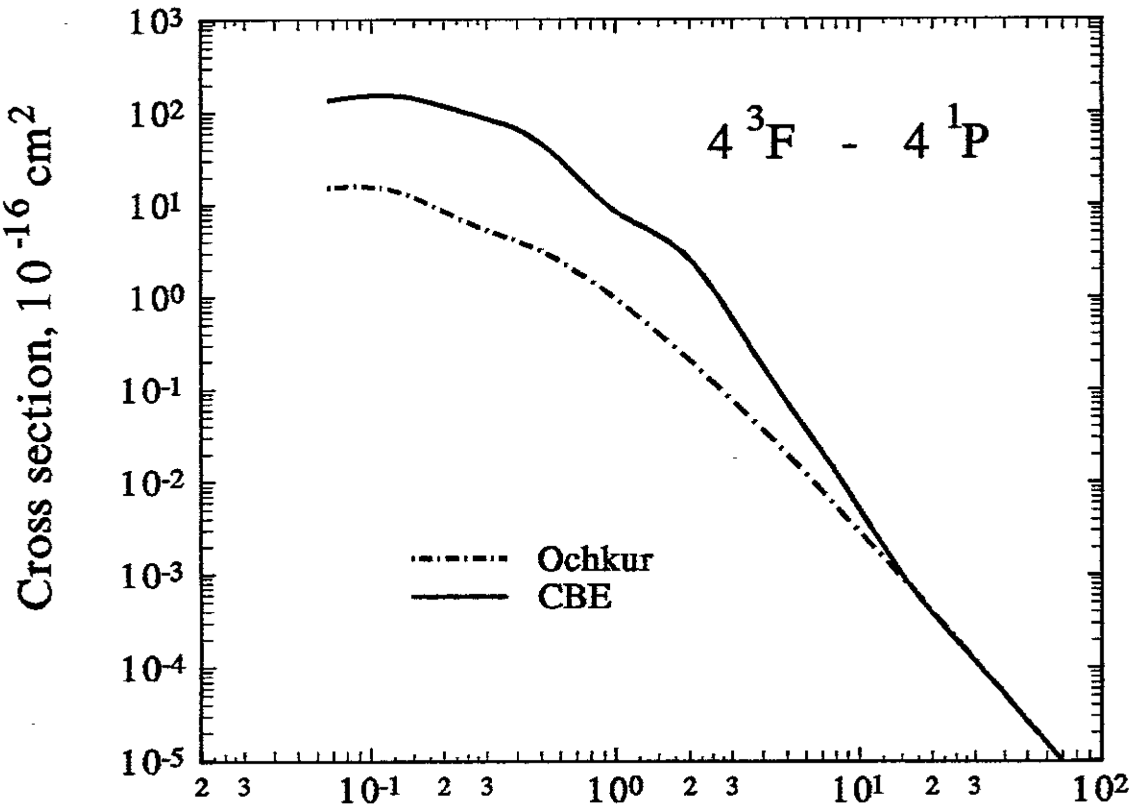

Fig.167 Electron energy, eV

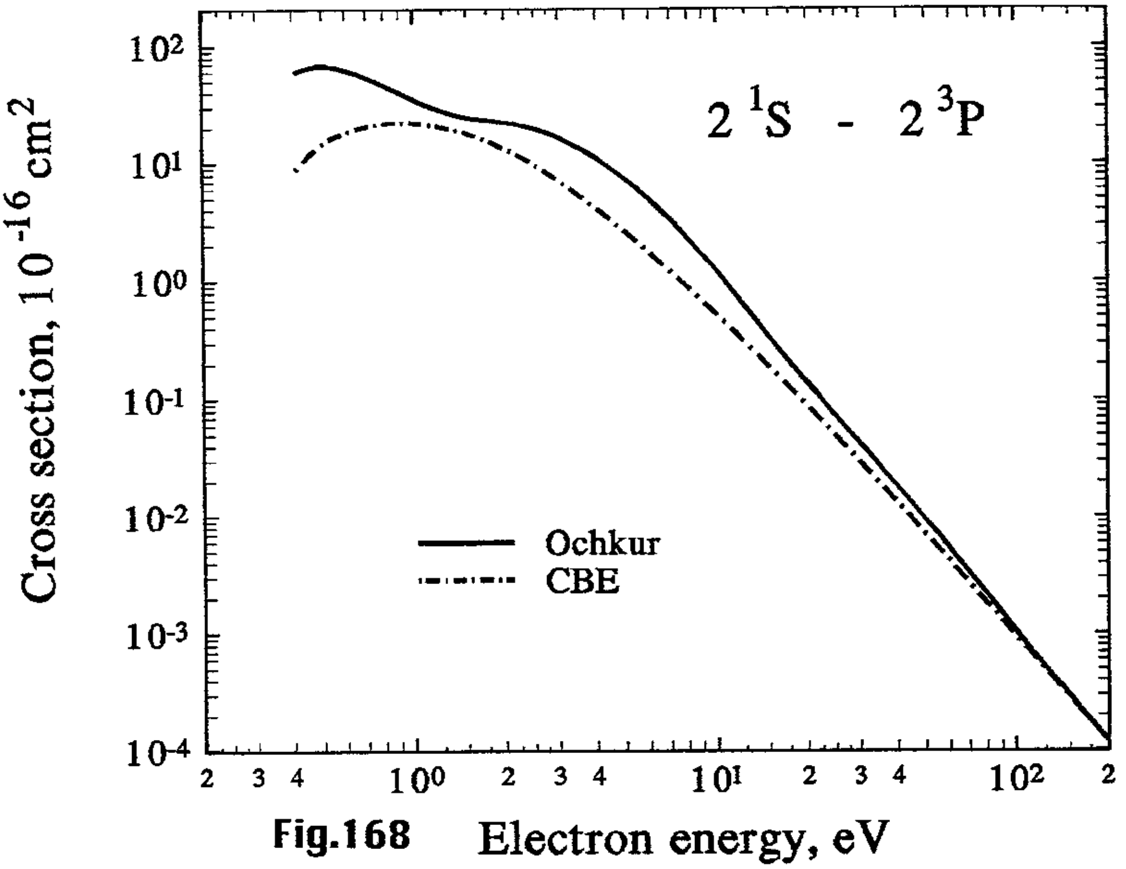

Fig.168

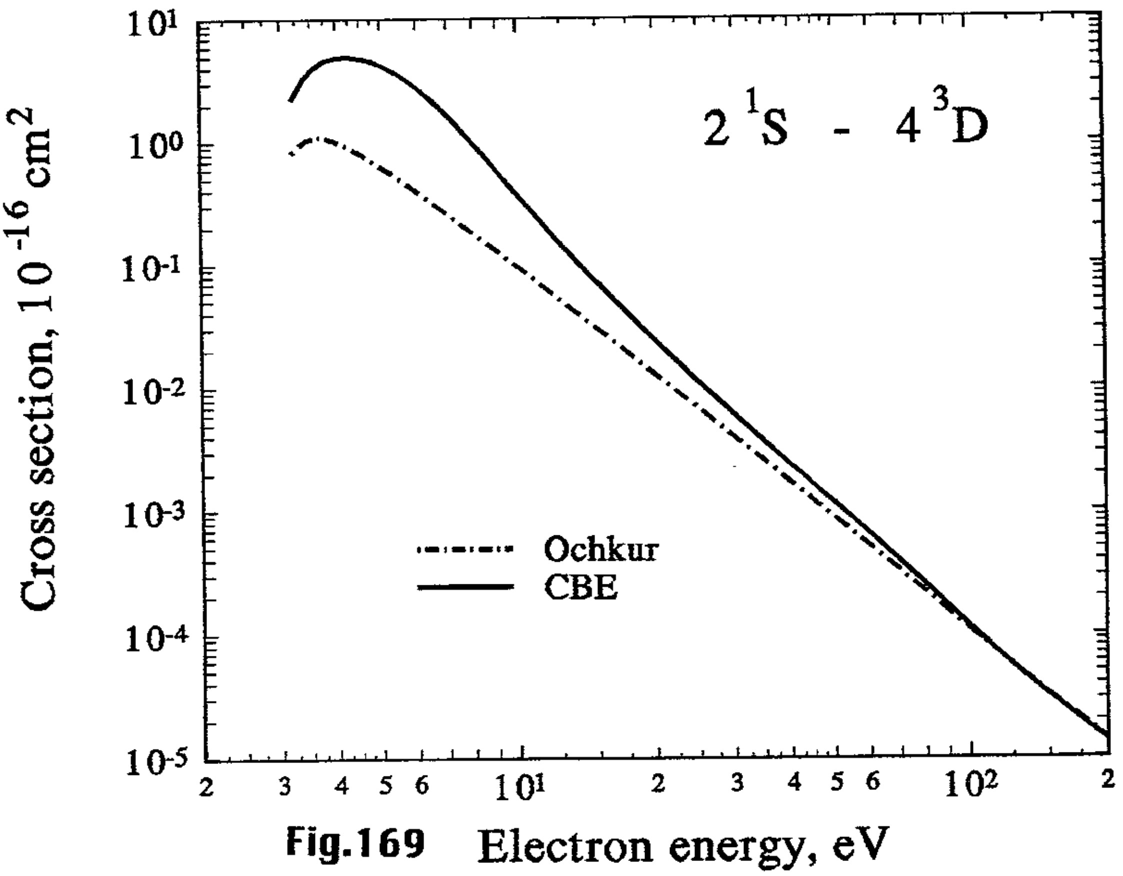

Fig.169

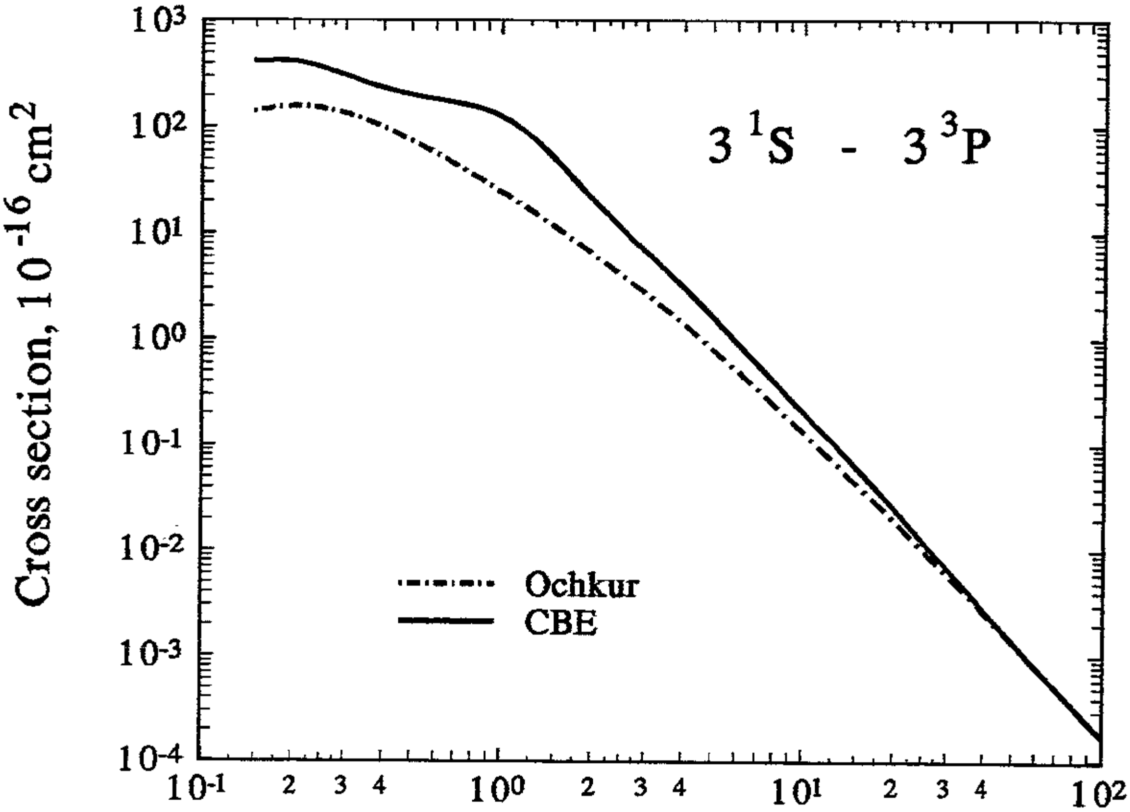

Fig.170 Electron energy, eV

Publication List of NIFS-DATA Series

NIFS-DATA-1 Y. Yamamura, T. Takiguchi and H. Tawara,
Data Compilation of Angular Distributions of Sputtered Atoms;
Jan. 1990

NIFS-DATA-2 T. Kato, J. Lang and K. E. Berrington,
Intensity Ratios of Emission Lines from OV Ions for Temperature and Density Diagnostics ; Mar. 1990 [At Data and Nucl Data Tables 44(1990)133]

NIFS-DATA-3 T. Kaneko,
Partial Electronic Straggling Cross Sections of Atoms for Protons
;Mar. 1990

NIFS-DATA-4 T. Fujimoto, K. Sawada and K. Takahata,
Cross Section for Production of Excited Hydrogen Atoms Following Dissociative Excitation of Molecular Hydrogen by Electron Impact ; Mar. 1990

NIFS-DATA-5 H. Tawara,
Some Electron Detachment Data for H^- Ions in Collisions with Electrons, Ions, Atoms and Molecules – an Alternative Approach to High Energy Neutral Beam Production for Plasma Heating– ;
Apr. 1990

NIFS-DATA-6 H. Tawara, Y. Itikawa, H. Nishimura, H. Tanaka and Y. Nakamura,
Collision Data Involving Hydro-Carbon Molecules ; July 1990
[Supplement to Nucl. Fusion 2(1992)25]

NIFS-DATA-7 H.Tawara,
Bibliography on Electron Transfer Processes in Ion-Ion/Atom/Molecule Collisions –Updated 1990–; Aug. 1990

NIFS-DATA-8 U.I.Safronova, T.Kato, K.Masai, L.A.Vainshtein and A.S.Shlyapzeva,
Excitation Collision Strengths, Cross Sections and Rate Coefficients for OV, SiXI, FeXXIII, MoXXXIX by Electron Impact ($1s^22s^2$-$1s^22s2p$-$1s^22p^2$ Transitions) Dec.1990

NIFS-DATA-9 T.Kaneko,
Partial and Total Electronic Stopping Cross Sections of Atoms and Solids for Protons; Dec. 1990

NIFS-DATA-10 K.Shima, N.Kuno, M.Yamanouchi and H.Tawara,
Equilibrium Charge Fraction of Ions of Z=4-92 (0.02-6 MeV/u) and Z=4-20 (Up to 40 MeV/u) Emerging from a Carbon Foil; Jan.1991
[AT.Data and Nucl. Data Tables 51(1992)173]

NIFS-DATA-11 T. Kaneko, T. Nishihara, T. Taguchi, K. Nakagawa, M. Murakami, M. Hosono, S. Matsushita, K. Hayase, M.Moriya, Y.Matsukuma, K.Miura and Hiro Tawara,
Partial and Total Electronic StoppingCross Sections of Atoms for a Singly Charged Helium Ion: Part I;Mar. 1991

NIFS-DATA-12 Hiro Tawara,
Total and Partial Cross Sections of Electron Transfer Processes for Be^{q+} *and* B^{q+} *Ions in Collisions with H,* H_2 *and He Gas Targets - Status in 1991-;* June 1991

NIFS-DATA-13 T. Kaneko, M. Nishikori, N. Yamato, T. Fukushima, T. Fujikawa, S. Fujita, K. Miki, Y. Mitsunobu, K. Yasuhara, H. Yoshida and Hiro Tawara,
Partial and Total Electronic Stopping Cross Sections of Atoms for a Singly Charged Helium Ion : Part II; Aug. 1991

NIFS-DATA-14 T. Kato, K. Masai and M. Arnaud,
Comparison of Ionization Rate Coefficients of Ions from Hydrogen through Nickel ; Sep. 1991

NIFS-DATA-15 T. Kato, Y. Itikawa and K. Sakimoto,
Compilation of Excitation Cross Sections for He Atoms by Electron Impact; Mar. 1992

NIFS-DATA-16 T. Fujimoto, F. Koike, K. Sakimoto, R. Okasaka, K. Kawasaki, K. Takiyama, T. Oda and T. Kato,
Atomic Processes Relevant to Polarization Plasma Spectroscopy ; Apr. 1992

NIFS-DATA-17 H. Tawara,
Electron Stripping Cross Sections for Light Impurity Ions in Colliding with Atomic Hydrogens Relevant to Fusion Research; Apr. 1992

NIFS-DATA-18 T. Kato,
Electron Impact Excitation Cross Sections and Effective Collision Strengths of N Atom and N-Like Ions -A Review of Available Data and Recommendations- ; Sep. 1992

NIFS-DATA-19 Hiro Tawara,
Atomic and Molecular Data for H_2O, *CO &* CO_2 *Relevant to Edge Plasma Impurities*, Oct. 1992

NIFS-DATA-20 Hiro. Tawara,
Bibliography on Electron Transfer Processes in Ion-Ion/Atom/Molecule Collisions -Updated 1993-; Apr. 1993

NIFS-DATA-21 J. Dubau and T. Kato,
Dielectronic Recombination Rate Coefficients to the Excited States of C I from C II; Aug. 1994

NIFS-DATA-22 T. Kawamura, T. Ono, Y. Yamamura,
Simulation Calculations of Physical Sputtering and Reflection Coefficient of Plasma-Irradiated Carbon Surface; Aug. 1994

NIFS-DATA-23 Y. Yamamura and H. Tawara,
Energy Dependence of Ion-Induced Sputtering Yields from Monoatomic Solids at Normal Incidence; Mar. 1995

NIFS-DATA-24 T. Kato, U. Safronova, A. Shlyaptseva, M. Cornille, J. Dubau,
Comparison of the Satellite Lines of H-like and He-like Spectra; Apr. 1995

NIFS-DATA-25 H. Tawara,
Roles of Atomic and Molecular Processes in Fusion Plasma Researches - from the cradle (plasma production) to the grave (after-burning) -; May 1995

NIFS-DATA-26 N. Toshima and H. Tawara
Excitation, Ionization, and Electron Capture Cross Sections of Atomic Hydrogen in Collisions with Multiply Charged Ions; July 1995

NIFS-DATA-27 V.P. Shevelko, H. Tawara and E.Salzborn,
Multiple-Ionization Cross Sections of Atoms and Positive Ions by Electron Impact; July 1995